Universitat Autònoma de Barcelona

Molecular regulation of carotenoid biosynthesis in tomato fruits. New biotechnological strategies

Lucio D'Andrea

MOLECULAR REGULATION *of* *carotenoid biosynthesis* IN TOMATO FRUIT

new biotechnological strategies

Lucio D'Andrea

2016

Universitat Autónoma de Barcelona

Facultat de Biociències

Doctorat de Biologia i Biotecnologia Vegetal

2016

Molecular regulation of carotenoid biosynthesis in tomato fruits

New biotechnological strategies

Memoria presentada por Lucio D'Andrea para optar al título de doctor por la Universitat Autónoma de Barcelona

Lucio D'Andrea

Candidato a doctor

Manuel Rodriguez-Concepción

Director

Briardo Llorente

Co-director

Joan Barceló Coll

Tutor

“Procuremos inventar pasiones nuevas, o reproducir las viejas con pareja intensidad”

Del libro *Rayuela* de Julio Cortázar

“Caminando en línea recta no puede uno llegar muy lejos”

Del libro *El Principito* de Antoine de Saint-Exupéry.

Esta tesis se la dedico

A mi abuela *Nelly* y a mi madre.

A la primera por las raíces y a la segunda por las alas.

Table of contents

Agradecimientos

Probablemente esta sea la parte que más me costó escribir. No porque no supiese a quién agradecer, sino más bien porque es tanta la gente, que es muy probable que la memoria me juegue una mala pasada. Por tanto, prefiero asumir que será inevitable dicho olvido y agradecer a todas aquellas personas que formaron parte de mi vida durante estos cuatro años.

Empiezo. Quiero agradecer:

Al Ministerio de Educación, Cultura y Deporte del Gobierno de España por haberme concedido la beca de Formación de Personal Universitario y con ello la posibilidad de realizar esta tesis doctoral.

A mi director, Manuel, porque esta tesis no habría sido posible sino fuese porque cuatro años atrás, cuando estaba a punto de dejar de intentarlo, me tendió su mano. Sin duda, uno de los momentos más gratos de mi vida fue leer aquel e-mail, diciendo que tendría mi segunda oportunidad para realizar la tesis doctoral. Agradecerle también por su dirección continua, por su predisposición, por el apoyo constante, por las discusiones científicas y, fundamentalmente, por enseñarme a pensar. Más aún, por la libertad y la confianza en el laboratorio. Y sobre todo, gracias por enseñarnos que es mejor ser líder que jefe.

A mi co-director y amigo, Briardo. Me considero un afortunado, por haber tenido al mejor ejemplo de amor a la ciencia, tenacidad y perseverancia. Gracias por el apoyo, tanto personal como científico durante estos años. Gracias por enseñarme que cuando se persigue, se consigue. Pero de lo que más agradecido estoy es de haber podido aprender de vos todos estos años; sin dudas sos y serás uno de mis pilares fundadores en esto de ser científico.

A la Dra Li, Li y al Dr. Theodore Thannhauser de la Universidad de Cornell, por haberme dado la oportunidad de conocer, no solo nuevas técnicas, sino también, nuevas maneras de hacer ciencia.

A mi familia. Que cuando hace 6 años dije que me venía a Europa todo fueron palabras de aliento. Porque siempre me brindaron todo el apoyo para que mis proyectos se cumplan. A mis padres, mis hermanas, mis cuñados, y en especial, a mis sobrinos, Emilia, Tiago y Juani, que sus sonrisas han hecho que esos días no tan buenos sean maravillosos.

Al 2.01 TODO. A los viejos, Águila, Jordi, David, Mike, Cata, Pablo, Esther; a los nuevos Neto, Vicky, Miguel, Sofía; y a las que estuvieron durante todos estos años Miriam y Rosa. Por las risas, por los llantos (pero sobre todo por las risas). Por todas las *fú*, por “las casas por la ventana”, “los

tenis” y los asados en Segur. Por aguantarme las locuras y dejarme aguantar las de todos ustedes. Sin dudas todo este tiempo ha hecho que seamos más que un laboratorio, una gran familia.

Al personal investigador del CRAG. Especialmente a mis compañeros (algunos ya viejas glorias). Esos con los que hemos andado juntos algunos años. Agradecerle especialmente a Mariana, Pat, Luis, Walter, Elena, Norma, Pep, Sil, Chiqui y Carmen.

A los servicios científicos y personal de administración del CRAG, por hacer todo lo posible para que las cosas nos sean fáciles y rápidas. Especialmente a Pilar, porque fueron varios años de luchar codo a codo, contra aún no tenemos muy claro qué; pero parece que le hemos ganado.

A las *troupe*s que me acogieron estos años en España. A los *argentos,* los *descarrilados* y los *madrileños.* Mariana, Briar, Tomás, Nadi, Eli, Rochi, Nina, Nico, Tommaso, María, Iria, David, Paco, Andre, Ruth, Marcos, Ana y Vir. A la *troupe argentina* que me vio partir hace varios años atrás y siguen estando, a Ale, Gi, Bele y Mati. A la *troupe* del “fantástico mundo”, a Marce y a Eli, porque ese verano en Ithaca es inolvidable.

Especialmente a Vir, porque la aventura “Europa” no habría sido lo mismo sin vos. Porque siempre estuviste y estás. Porque tu palabra es siempre de aliento. Por tu familia, que también es un poquito mía. A Marisa, porque esto de la ciencia me regaló una hermana, y estoy feliz de que seas vos.

A la persona que me acobijó y me escuchó en un momento más que importante de mi vida y ahora es responsable de la portada de esta tesis. A María.

A ese grupito de personas que me integraron como parte de su familia, y son grandes culpables que haya logrado sobrevivir al proceso de escritura de esta tesis. A Neal, Hernán, Marcos, Paulo y Xavi.

A Tomeu, porque has sido esencial en estos últimos meses de estrés y agobio. Y porque con vos aprendo todo eso que la tesis no me enseñó. Gracias por estar.

GRACIAS

Resumen

Los carotenoides son metabolitos isoprenoides de gran relevancia económica como pigmentos naturales y fitonutrientes. Flores y frutos han desarrollado un tipo de plasto especializado denominado cromoplasto, el cuál es capaz de acumular niveles elevados de carotenoides como β-caroteno (naranja) y licopeno (rojo). Por ejemplo, durante la maduración del fruto de tomate (*Solanum lycopersicum*) se pueden distinguir tres estadios según el color del fruto, que depende del número de días post-antesis (DPA): Verde Maduro (VM) (aprox. 36 DPA), Naranja (N) (47 DPA) y Rojo (R) (52 DPA). La transición de VM a N y por último a R, se caracteriza por una fuerte inducción en la acumulación de los niveles de carotenoides y, por ende, la diferenciación de cloroplastos en cromoplastos.

La acumulación global de carotenoides depende de la actividad de enzimas biosintéticas como DXS y PSY. Sin embargo, el aumento de la expresión de genes codificantes para estas enzimas no genera un aumento proporcional en la producción final de carotenoides en frutos de tomate. Una posible razón de esta falta de correlación puede deberse a la existencia de mecanismos de regulación post-traduccionales que operan controlando los niveles finales de dichas enzimas. Si bien existe un gran desconocimiento acerca de la identidad de dichos mecanismos en frutos de tomate, trabajos previos en *Arabidopsis thaliana* han demostrado que los niveles de proteína DXS son regulados por componentes del sistema plastidico de Control de Calidad de Proteinas (CCP), tal como el complejo de la Clp proteasa. Por tanto, en esta tesis hemos decidido explorar una nueva alternativa biotecnológica basada en manipular los niveles del complejo Clp proteasa para así aumentar los niveles de enzima DXS y por tanto, el flujo metabólico hacia la síntesis de carotenoides en frutos de tomate. Exitosamente, la disminución de dicha actividad proteolítica mediante silenciamiento génico, generó frutos transgénicos enriquecidos en β-caroteno (pro-vitamina A) y,otros isoprenoides plastídicos como los tocoferoles (vitamina E). Por otro lado, la caracterización de dichos frutos mediante técnica de microscopía electrónica sirvió como plataforma para establecer la importancia de dicho complejo proteolítico durante la diferenciación de cloroplastos en cromoplastos. Finalmente, estudios en el campo de la proteómica cuantitativa ayudaron a la elucidación de nuevas proteínas blanco de dicha proteasa, tal como enzima limitante en la biosíntesis de carotenoides, PSY1.

Por otro lado, durante esta tesis se participó en la caracterización de la regulación transcripcional del gen *PSY1* en frutos de tomate. En este marco, demostramos que de manera similar a Arabidopsis, *PSY1* es una diana directa de un factor de transcripción regulado por luz, denominado PIF1a. En concordancia, frutos de tomate con niveles reducidos de dicho represor mostraron una sobre-acumulación de *PSY1* y por tanto, una mayor acumulación de carotenoides. Finalmente, hemos establecido un mecanismo molecular basado en la regulación de la estabilidad por luz de PIF1a, que ayuda en la sincronización entre el proceso de maduración del fruto de tomate y la síntesis de carotenoides.

Summary

Carotenoids are isoprenoid metabolites of great economic importance as natural pigments and phytonutrients. Flowers and fruits have develop a type of specialized plastid called chromoplast able to accumulate high levels of carotenoids like lycopene (red) and β-carotene (orange). For example, during the ripening of the tomato fruit (*Solanum lycopersicum*) we can distinguish three different stages according to the color of the fruit, which depends on the number of days post-anthesis (DPA): Mature Green (MG) (36 DPA), Orange (O) (47 DPA) and Ripe (R) (52 DPA). The transition from MG to O, and finally to R, is characterized by a strong induction in the levels of carotenoids and therefore, the differentiation of chloroplasts into chromoplasts.

The global accumulation of carotenoids depends on the activity of biosynthetic enzymes such as DXS and PSY. However, the increase in the expression of genes coding for these enzymes does not generate a commensurate rise in the final production of carotenoids in tomato fruits. A possible reason for this lack of correlation it may be due to the existence of regulatory post-translational mechanisms that operate controlling the final levels of these enzymes. While there is a great lack of knowledge about the identity of these mechanisms in tomato fruits; previous work in *Arabidopsis thaliana* have shown that the levels of DXS protein are regulated by components of the plastidial Protein Quality Control (PQC) system, such as the Clp protease complex. Hence, in this thesis we have decided to explore a new biotechnological alternative based on the manipulation of chromoplastidial Clp protease complex to increase the levels of DXS protein and therefore the metabolic flux toward the synthesis of carotenoids in tomato fruits. Successfully using gene silencing approaches, the Clp proteolytic activity was decreased, generating transgenic fruits enriched in β-carotene (pro-vitamin A). In addition, the characterization of these fruits by TEM and Raman imaging helped us to establish the relevance of this proteolitic complex in carotenoid accumulation and chromoplastogenesis. Finally, quantitative proteomic studies serve to elucidate potential Clp protease targets in chromoplasts, such as the rate-limiting enzyme in carotenoid biosynthesis, PSY1.

Additionally, during this thesis it has been characterized and manipulated the transcriptional regulation of the *PSY1* gene in tomato fruits. In this context, it was demonstrated that similarly to Arabidopsis, *PSY1* gene is directly repressed by the light-regulated transcriptional factor PIF1a. In agreement, tomato fruits with reduced levels of this repressor show *PSY1* up-regulation and hence, an enhancement in the carotenoid levels. Finally, we have established a molecular mechanism based in the regulation of PIF1a photo-stability, that finally help in the orchestration between tomato fruit ripening and carotenoid biosynthesis.

Index of Figures

Introduction

Results

Chapter I

Discussion

Index of Tables

Introduction

Results

Chapter I

Chapter II

Materials and Methods

Introduction

Section I

The tomato fruit.

Solanum lycopersicum, commonly known as tomato, is a plant species that belongs to the S*olanaceae* family, together with other commercially relevant plants like *Nicotiana tabacum* (tobacco), *Capsicum annuum* (pepper) and *Solanum tuberosum* (potato). The commercial interest of these plants resides in their leaves (tobacco), tubers (potato) or fruits (pepper and tomato). Figure I1 shows the morphology of the tomato fruit. Tomato fruits are internally divided into sections called locular cavities. These cavities are separated by the funiculus and contain the placenta where seeds are located. The most external tissue of the tomato fruit is the pericarp. The pericarp includes (from outside to inside) the exocarp, the mesocarp and the endocarp.

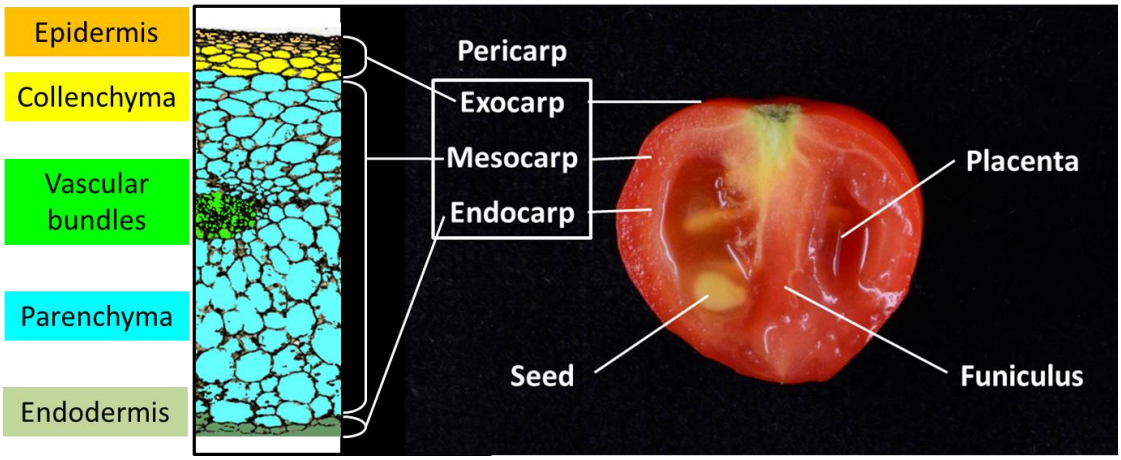

Figure I1. The tomato fruit anatomy. The picture shows a ripe tomato fruit of the MicroTom (MT) variety. Different parts of the tomato fruit are indicated. Pericarp layers and tissues are also indicated in the cartoon, corresponding to a cross section of the pericarp taken from the tomato eFP browser at bar.utoronto.ca.

In general terms, fruits can be classified into *non-climacteric* (e.g. cherry, grape and lemon) and *climacteric* (e.g. tomato, banana and apple) fruits, depending on the

absence or presence, respectively, of a sudden rise in the respiration rate and in ethylene production. The tomato fruit is classified as climacteric, and its development can be divided into two separate phases or systems: system I and system II (Figure I2) (Burg and Burg, 1965).

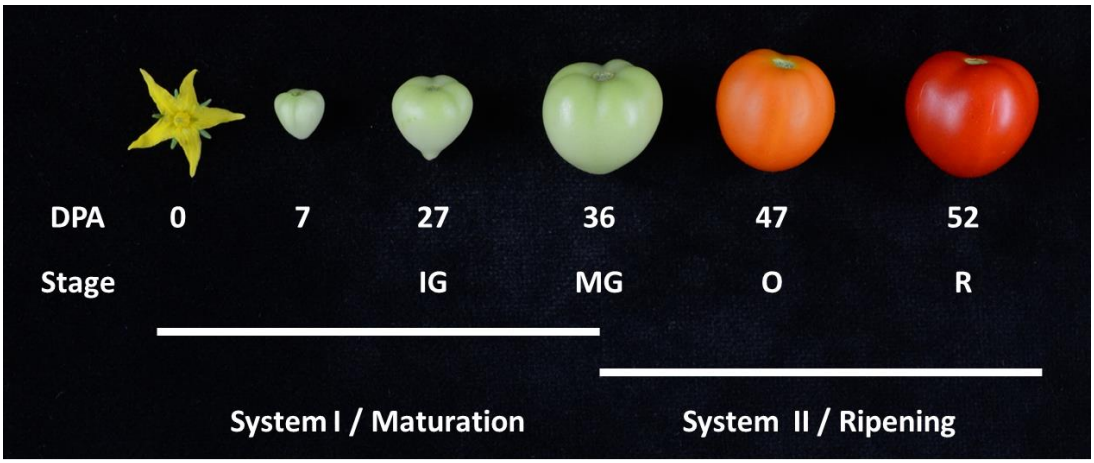

Figure I2. Tomato fruit development. Tomato fruit development could be divided en two phases or systems: System I/Maturation and System II/Ripening. System I compromises from the fertilization event (0 days post-anthesis or DPA) until the fruit gets its final size (aprox. 36 DPA in the MT variety). System II is characterized by profound changes in the organoleptic properties of the fruit. In the MT variety, fruits are typically ripe at 52 DPA. The main stages of the fruit used in this thesis are the following: Immature Green (IG); Mature Green (MG); Orange (O) and Ripe (R).

Stages of tomato fruit development

System I or Maturation

Right after fertilization triggers fruit set and development, a rapid cell division rate leads to a progressive increase in pericarp cell number. When tomato reaches the so-called *Immature Green* (IG) stage the cell division rate markedly goes down.

During a second stage, fruit growth relies on cell expansion that leads to a significant increase in weight. By the end of this stage, the fruit enters the *Mature Green* (MG) stage and attain its final size, which varies greatly among cultivar and environmental conditions. As shown in Figure I2, the fruits of the MicroTom (MT) variety reach the MG stage about 36 DPA (days post-anthesis).

System II or Ripening

About two days after reaching the MG stage, the tomato fruit undergoes an extensive metabolic reorganization, which marks the beginning of the fruit ripening process (Ho and Hewitt, 1986). Then, two main stages follow, which are referred to as the *Orange* (O) and the *Ripe* (R) stages. The first changes in color from green to yellow-orange due to chlorophyll degradation at the onset of ripening mark an intermediate stage name *Breaker*. However, this is a highly variable and subjective stage and we decided not to consider it for this work. When the green color is gone, the fruit acquires a rather homogeneous orange color that signals the O stage. The R phase is characterized by the accumulation of lycopene, a red carotenoid intermediate that is not normally accumulated in most plants, with a few exceptions like tomato, watermelon, or red cultivars of grapefruit and orange fruits.

The following sections will cover the main metabolic, biochemical and gene expression events that occur during ripening.

Metabolic changes during ripening

One of the main features that characterize tomato fruit ripening is the profound changes in the metabolome. However, not all the metabolic pathways are equally affected. While some of them do not vary during ripening (e.g. oxidative pentose phosphate pathway and many aspects of lipid metabolism), others differ greatly during this developmental process (Gapper et al., 2013).

The most visually evident changes are those impacting the color of the tomato fruit, that is, the breakdown of chlorophylls and the accumulation of carotenoids and their derivatives, which change the fruit color from green to orange and red when ripe. The green fruit has a chlorophyll and carotenoid profile that is typical of photosynthetic tissues such as leaves. During ripening, chlorophylls are degraded and carotenoid biosynthesis is boosted. In particular, the fruit mainly accumulates the orange carotenoid β-carotene (the main precursor of vitamin A) and the red carotenoid lycopene (a powerful anticancer agent) (Yuan et al., 2015; Klee and Giovannoni, 2011). At the beginning of ripening, β-carotene and lycopene start to over-accumulate, being the ratio between them so that the overall fruit color is orange (O stage). When the

ripening proceeds, lycopene accumulates more and the β-carotene-to-lycopene ratio decreases, finally changing the overall fruit color to red (R stage).

Flavonoids are another group of important fruit pigments. They are synthesized from the phenylpropanoid pathway in the epidermal cells of the fruit and transported into the cuticle of the fruit as it ripens (Mintz-oron et al., 2008). Naringenin, naringenin chalcone, quercetin (rutin) and kaempferol are the most abundant flavonoids in the tomato fruit cuticle (Laguna et al., 1999). These metabolites provide pigmentation to the peel of the fruit, as illustrated by the characteristic pink color displayed by fruits of the tomato *colorless epidermis (y/y)* mutant, which does not produce naringenin chalcone (Adato et al., 2009; Ballester et al., 2010). However, the yellow colors provided by these flavonoids are normally masked by the fruit carotenoids and they are only observable when carotenoid biosynthesis is blocked (Figure I3). For example, the yellow color of the ripe fruit in the tomato *yellow flesh* (*r*) mutant, which is unable to synthesize carotenoids during ripening, is due to the accumulation of flavonoids (Fray and Grierson, 1993).

Figure I3. The *r mutation blocks* carotenoid accumulation in tomato fruit, allowing to see the yellow color provided by flavonoids. Wild type (WT) and *yellow flesh* (*r*) ripe (52 DPA) tomato fruits are shown. The*r* mutant harbors a mutation in the fruit-specific isoform of phytoene synthase (PSY1) imparing carotenoid accumulation during tomato fruit ripening. Yellow color is due to naringenin chalcone pigments present in the fruit cuticle.

In addition to the enhancement in the levels of pigments, tomato fruits also increase the production of volatiles which are molecules that contribute to its final aroma and flavor. Volatile molecules derive mainly from branch-chain (isoleucine and leucine) and aromatic (phenylalanine) amino acids, fatty acids (linolenic acid), and

carotenoids (lycopene and β-carotene) (Rambla et al., 2014). While it is well established that the production of volatiles derived from fatty acids strongly depends on ethylene, it is not so clear in the case of carotenoid-derived volatiles (Chen et al., 2004; Kovàcs et al., 2009). Carotenoids are enzymatically processed due to the activity of carotenoid cleavage dioxygenases (CCDs) and 9-cis-epoxycarotenoid dioxygenases (NCEDs) (Auldridge et al., 2006; Vogel et al., 2008; Huang et al., 2009). In tomato, the isoforms CCD1B and CCD1A contribute to the production of the vast majority of tomato volatiles derived from carotenoids (Ilg et al., 2014; Simkin et al., 2004), including β-ionone and geranyl acetone, which positively contribute to the flavor of ripe fruits (Tieman et al., 2012). The fact that carotenoids are major contributors of both the color and aroma of ripe tomato fruits reflects the huge economic and biological relevance of these metabolites (McQuinn et al., 2015; Rambla et al., 2014).

Finally, sugar metabolism suffers profound changes during tomato fruit development. In this regards, the transient starch that accumulates in green fruits decreases when tomato starts to ripe, being metabolized into glucose and fructose that finally contribute to the sweetness of the ripe fruit. As ripe fruits are not photosynthetically active, they act as a sink organ that imports photoassimilates from green tissues (leaves). Although the precise mechanism regulating this process is not known, some tomato sucrose transporters have been found to be important in sugar transport from leaves to fruits by phloem (Osorio et al., 2014).

The chloroplast to chromoplast transition

When tomato fruits ripe chlorophylls are degraded and there is a 10-14 fold enrichment in carotenoid levels (Fraser et al., 1994). This enhancement in carotenoid production promotes deep changes in plastid ultrastructure in order to accommodate the increasing levels of these lipophilic metabolites. As a consequence, carotenoid accumulation during ripening is paralleled by the differentiation of pre-existing chloroplasts in MG fruits into specialized carotenoid-accumulating plastids named chromoplasts. During this conversion, an intermediate plastid type called chloro-chromoplast has been observed in O fruits (Egea et al. 2011). Interestingly, based on the differential spectral properties of chlorophylls and carotenoids, Egea et al (2011) showed that the chloroplast to chromoplast transition is synchronous for all plastids of

a single cell. In other plant systems, chromoplasts can also differentiate from non-green plastids such as proplastids, leucoplasts or amyloplasts. For example, during carrot root development white proplastids differentiate into chromoplasts that accumulate high levels of β-carotene (Li and Yuan, 2013).

In addition and oppositely to chloroplasts, once tomato fruit chromoplasts develop their total number remains fairly constant during the ripening process (Cookson et al., 2003). In agreement, it has been observed that the levels of proteins involved in plastid division such as Filamenting Temperature-Sensitive Z 2 (FtsZ2) and Accumulation and Replication of Chloroplasts 6 (ARC6) decrease during the tomato fruit chloroplast-to-chromoplast transition (Barsan et al., 2012).

A profound re-organization of the plastidial membrane system takes place when chloroplasts are transformed into chromoplasts. The most visible alterations in the plastid architecture are the disintegration of the thylakoid grana and the biogenesis of carotenoid-containing bodies. In addition, stromules (stroma-filled tubules), which are dynamic extensions of the plastid envelope allowing communication between plastids and other cell compartments like the nucleus, are also affected during chromoplast biogenesis (Pyke and Howells, 2002). As a larger number of long stromules can be found in mature chromoplasts compared with chloroplasts, it is assumed that the potential exchange of metabolites and other components is increased in chromoplasts. Associated with all these structural changes at the membrane level, a marked re-organization of the protein transport complex occurs. For instance, the TOC/TIC transmembrane transport machinery is disintegrated, becoming other transport systems, such as the non-canonical signal peptide and the intracellular vesicles, the most active (Barsan et al., 2012).

Chromoplasts can actually be classified into five different categories depending on the main carotenoid sequestering substructure: globular, crystalline, membranous, fibrillary and reticulo-tubular. Furthermore, one particular chromoplast type can have more than one storage structure. For instance, tomato fruit chromoplasts are considered crystalline due to the large abundance of lycopene crystals. However, they also develop plastoglubules (PGs) that characterize globular chromoplasts (Jeffery et al., 2012; Egea et al., 2011). PGs arise from a blistering of the stroma-side leaflet of the thylakoid membrane, being physically attached to it (Austin et al., 2006). PGs were

shown to provide a lipophilic environment where carotenoids and other lipophilic molecules, like tocopherols, can accumulate (Barsan et al., 2012). Accordingly with their nature, a large increase in size and number of PGs is observed during chloroplast-to-chromoplast transition. Interestingly, it has been demonstrated that PGs are actively participating in those metabolic pathways that synthesize carotenoids and tocopherols. For instance, PGs harbor a tocopherol cyclase, an enzyme involved in the production of γ-tocopherol. In addition, some enzymes of the carotenoid biosynthetic pathway (ζ-carotene desaturase, lycopene β-cyclase and two β-carotene hydroxylases) were found in PGs (Ytterberg et al., 2006).

Ethylene production and perception

As tomato is a climacteric fruit, its ripening progression strongly depends on the ethylene burst. Due to the central role of ethylene in tomato fruit development, its production and perception have been extensively studied.

Ethylene biosynthesis involves the coordinated action of two enzymes. Firstly, S-adenosylmethione is converted into 1-aminocyclopropane-1-carboxylate (ACC) by ACC synthase (ACS). Then, ACC is subsequently transformed to ethylene by ACC oxidase (ACO). Both enzymes, ACS and ACO, are encoded by a multi-gene family in the nuclear genome of tomato. However, not all gene members are essential during tomato fruit ripening. For instance, only *ACS2* and *ACS4* genes are significantly up-regulated during fruit ripening, indicating a particular role of these two isoforms in ripening-associated ethylene production (Rottmann et al, 1991). Despite ACO enzymes are also up-regulated during ripening; ACO activity is not rate-limiting in this process (Barry et al., 1996). The characteristic burst in ethylene production is achieved mainly by the auto-catalytic nature of ACS2 and ACS4 enzymes. This means that the ethylene synthetized by ACS2 and ACS4 can act as a positive modulator of their own activity. In addition, ethylene can trigger the up-regulation of genes involved in its own production. For instance, the *E8* gene, which encodes a dioxygenase enzyme related to ACO, is induced by ethylene at the beginning of fruit ripening (Lincoln et al., 1987; Penarrubia et al., 1992).

Once produced, ethylene is perceived by a specific battery of Ethylene Receptors (ETRs) phylogenetically related to the bateria two-component histidine

kinases (Bleecker, 1999). ETRs localize in the endoplasmic reticulum and act as negative regulators of ethylene signaling. The current model proposes that ETRs are in a functionally "on" state in the absence of ethylene, repressing ethylene response. Upon ethylene binding, ETRs become de-activated and the ethylene response begins (Cherian et al., 2014; Klee and Giovannoni, 2011; Seymour et al., 2013a). In tomato, ETRs are encoded by a gene family with seven members that display differential expression patterns (Tieman et al., 2000). In particular, *ETR4*, *ETR6* and *ETR3/Nr* genes were shown to be up-regulated specifically during ripening (Kevany et al., 2007). In fact, a single amino acid change in ETR3 blocks ripening progression, giving rise to a fruit ripening mutant called *Never ripe* (*Nr*) (Lanahan et al., 1994). In addition, Kevany et al (2007) demonstrated that although *ETR* genes are transcriptionally regulated during ripening, they can be also regulated at the protein level, as in the presence of ethylene they are targeted for degradation by the proteasome. Altogether these findings lead to the actual model that proposed that ETRs regulate the onset of ripening by cumulatively measuring ethylene exposure (Gapper et al., 2013).

Despite ethylene is the major hormone regulating ripening in climacteric fruits, other hormones also plays important roles. Tomato mutants with an altered abscisic acid (ABA) pathway show a dramatic impact in carotenoids accumulation and/or ripening. For instance, *high pigment 3* (*hp3*), a mutant in an enzyme involved in carotenoid and ABA biogenesis (zeaxanthin epoxidase (ZEP)), has enlarged plastids that allow a higher carotenoid storage capacity (Galpaz et al., 2008).

Transcriptional regulators of tomato ripening.

During the last decades, reverse genetics studies have contributed to decipher the transcriptional network behind tomato ripening. Mutants able to develop to the MG stage but unable to ripe were screened to identify genes involved in the transcriptional regulation of ripening. They include *ripening-inhibitor* (*rin*) (Vrebalov et al., 2002), *Never ripe* (*Nr*), *non-ripening* (*nor*) and *Colorless non-ripening* (*Cnr*) (Manning et al., 2006).

The *rin mutation* impacts almost all ripening pathways, which supports its role as a master regulator of the ripening process (Martel et al., 2011). The *rin* phenotype results from a spontaneous deletion that removes part of the 3' coding region of the

RIN gene. The *RIN* locus encodes a MADS-box transcription factor termed RIN-MADS (Vrebalov et al., 2002). RIN-MADS is involved in switching from system I to system II through the induction of *ACS2*. Moreover, this transcription factor is able to directly control the expression of a wide range of other ripening-related genes, including some encoding carotenoid biosynthetic enzymes (Seymour et al. 2013b). So, RIN-MADS controls the on-set of ripening via both ethylene-dependent and ethylene-independent pathways.

Nr encodes an ethylene receptor (Wilkinson et al., 1995). *Nr* tomato mutants are known to be unable to ripe due to a single amino acid change (i.e. Pro^{36} to Leu) in the sensor domain of the ethylene receptor ETR3 that confers ethylene insensitivity. Thus, the *Nr* gene is involved in the ethylene-dependent pathway in the tomato fruit ripening.

The *nor* mutants have a phenotype similar to that of *rin*, but due to a mutation in a member of the NAC-domain family of transcription factors (Giovannoni, 2007). NOR was proved to act upstream of ethylene in the tomato fruit ripening cascade and determine the competency of fruit ripening.

The *Cnr* mutant not only fails to ripe, but also shows a loss of cell-to-cell adhesion (Thompson et al., 1999; Eriksson et al., 2004). Manning et al (2006) found that the *Cnr* phenotype is due to an epigenetic mutation in a gene encoding a member of the SQUAMOSA Promoter Binding (SPB-box) Protein-like (SPL) family of transcription factors. It is assumed that hypermethylation of the *SPL-CNR* gene causes its silencing and finally the *Cnr* phenotype. It is worth to mention that uncovering the molecular basis of the *Cnr* mutation not only unveiled a new ripening player, but it also suggested that regulation of the epigenome dynamics could play an important role during tomato fruit ripening. The tomato fruit epigenome is very dynamic, being especially important in controlling transcription factor binding during ripening. Trying to integrate this new regulatory layer, Zhong et al (2013) proposed a three-component model for the control of fruit ripening in which, through interacting mechanisms that remain unclear, the ripening hormone ethylene and fruit-specific transcription factors, together with epigenome reprogramming, transition the fruit to a ripening-competent state when seeds become viable.

On the other hand, analysis of the fruit transcriptome uncovered a new set of

genes that play an important role during ripening. Moreover, chromatin immunoprecipitation followed by sequencing (ChIP-seq) helped to get more information about the transcriptional network controlling tomato fruit ripening. For instance, *TAG1* and *TAGL1* (Pan et al., 2010), two genes that belong to the AGAMOUS clade of MADS-box genes, were proposed to act as positive ripening regulators in a redundant manner. However, the exact molecular mechanism by which these transcription factors act remains elusive. Not only positive ripening regulators have been identified. AP2a, a MADS-box transcription factor that belongs to the APETALA family, negatively regulates ripening progression as its silencing results in accelerated ripening, elevated ethylene production and altered carotenoid accumulation (Chung et al., 2010). Dong et al, (2013) proposed that MADS1, another MADS-box family member, could also be a ripening repressor by sequestering RIN. Tomato fruits with reduced levels of *MADS1* exhibit enhanced levels of ripening-related transcripts (Dong et al., 2013). The R2-R3 MYB transcription factor AN2 seems to also work as a ripening repressor, although its specific role in the ripening network is still unclear. Tomato fruits that overexpress *AN2* have reduced carotenoid accumulation and an altered ethylene emission profile (Meng et al., 2015).

Section II

Carotenoid biosynthesis.

Carotenoids are a group of isoprenoid molecules synthesized by all photosynthetic organisms (including plants) and some non-photosynthetic bacteria and fungi. Plant carotenoids are tetraterpenes derived from geranylgeranyl diphosphate (GGPP) and produced in plastids. Depending on their chemical nature, carotenoids can be grouped in two major classes (Figure I5): carotenes (hydrocarbons that can be cyclized at one or both ends of the molecule) and xanthophylls (oxygenated derivatives of carotenes).

Like all isoprenoids, carotenoids are synthesized from the 5-C units isopentenyl diphosphate (IPP) and its double-bond isomer dimethylallyl diphosphate (DMAPP). Two independent and compartmentalized pathways exist in plant cells for the production of these precursors. While in the cytosol isoprenoids are synthesized through the mevalonate (MVA) pathway, in plastids they are generated by the methylerythritol 4-phosphate (MEP) pathway. Although there is evidence that isoprenoid precursors can be exchanged between subcellular compartments, this transport must be limited as MVA-derived precursors cannot rescue plants with a blocked MEP pathway and vice versa (Bick and Lange, 2003; Laule et al., 2003; Flores-Perez et al., 2008; Rodríguez-Concepción, 2010). As a consequence of this limited exchange of metabolites, each pathway generates precursors to mainly (but no exclusively) produce a particular set of isoprenoid compounds. In particular, plant carotenoids are mainly produced from precursors synthesized by the MEP pathway, which also provides most precursors for the production of other plastidial isoprenoids such as the side chain of chlorophylls, tocopherols, phylloquinones, and plastoquinones (Rodríguez-Concepción, 2010) (Figure I4).

The MEP pathway

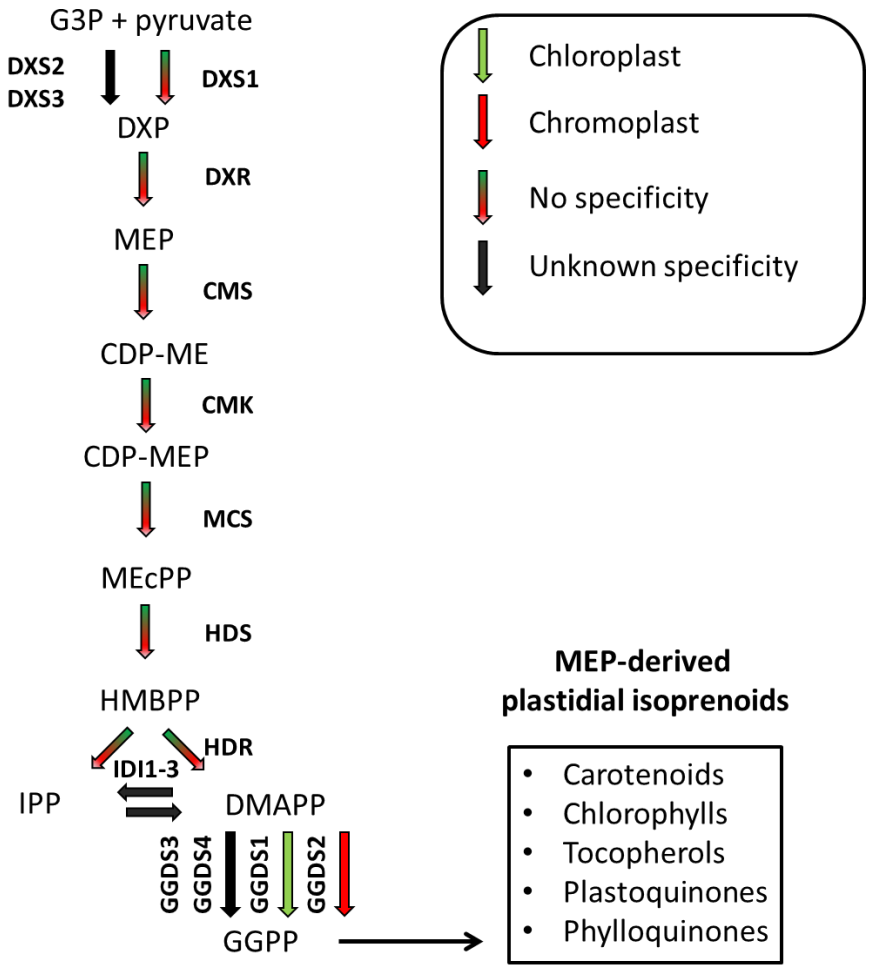

Figure I4. The MEP pathway in tomato fruit. Acronyms for intermediates and enzymes are indicated in the text. Arrows color indicates where the enzyme isoforms accumulate mostly. Green arrows indicate chloroplast containing tissues (green tissue), red arrows indicate chromoplast containing tissue, green-red arrows indicate non-tissue specificity and black arrows indicate unknown specificity.

Since the elucidation of the MEP pathway in microorganisms, a lot of research efforts have been put forward to identify and characterize all the enzymatic steps in plants, mostly using Arabidopsis as a model (Ruiz-Sola and Rodriguez-Concepción, 2012). In Arabidopsis, all the MEP pathway enzymes are encoded by nuclear genes and targeted to the stroma of plastids (Ruiz-Sola and Rodriguez-Concepción, 2012). The first reaction of the MEP pathway is the condensation of a molecule of glyceraldehyde-3-

phosphate (G3P) with (hydroxyethyl) thiamine derived from pyruvate. This irreversible reaction produces deoxyxylulose 5-phosphate (DXP) and CO_2, and it is catalyzed by DXP synthase (DXS). The next step transforms DXP into MEP by a reaction catalyzed by DXP reductoisomerase (DXR). MEP is afterwards converted via cytidine diphosphomethylerythritol (CDP-ME) and CDP-ME 2-phosphate (CDP-MEP) into methylerythritol 2,4-cyclodiphosphate (MEcPP) by the enzymes MEP cytidylyltransferase (CMS), CDP-ME kinase (CMK) and MEcPP synthase (MCS), respectively. In the last two steps of the pathway, the enzyme hydroxymethylbutenyl diphosphate (HMBPP) synthase (HDS) transforms MEcPP into HMBPP, whereas HMBPP reductase (HDR) converts HMBPP into a ca. 5:1 mixture of IPP and DMAPP. Both 5-C metabolites can be interconverted in a reversible reaction catalyzed by the enzyme IPP isomerase (IDI), which maintains a proper IPP:DMAPP ratio. Addition of 3 IPP molecules to 1 DMAPP acceptor catalyzed by GGPP synthase (GGDS) then produces the starting precursors for the production not only of carotenoids but also of other groups of plastidial isoprenoid metabolites (Figure I4). The Arabidopsis and tomato homologues of these enzymes and their accessions are listed in Table I1.

Table I1. Tomato and Arabidopsis MEP pathway homologues

	Arabidopsis	Tomato	
Enzyme	**Accession**	**Accession**	**Isoform name**
DXS	At4g15560	Solyc01g067890	DXS1
		Solyc11g010850	DXS2
		Solyc01g028900	DXS3
DXR	At5g62790	Solyc03g114340	DXR
CMS	AT2G02500	Solyc01g102820	MCT
CMK	AT2G26930	Solyc01g009010	CMK
MCS	AT1G63970	Solyc08g081570	MDS
HDS	AT5G60600	Solyc11g069380	HDS
HDR	AT4G34350	Solyc01g109300	HDR
IDI	AT5G16440	Solyc08g075390	IDI1
	AT3G02780	Solyc05g055760	IDI2
		Solyc04g056390	IDI3
GGDS	At2g18620	Solyc02g085700	GGDS1
	At3g29430	Solyc04g079960	GGDS2

	At3g32040	Solyc11g011240	GGDS3
	At4g36810	Solyc02g085710	GGDS4

Several studies suggest that the control of the metabolic flux through the MEP pathway is shared among several enzymes, with a major contribution of DXS and, to a lower extent, DXR and HDR (Ruiz-Sola and Rodriguez-Concepción, 2012). These studies were mostly based on analyzing the impact of overexpressing individual genes of the pathway on the levels of plastidial isoprenoid end products, including carotenoids. More recently, metabolic control analysis (MCA) calculations confirmed that DXS is the enzyme with the highest flux control coefficient, that is, the major rate-limiting enzyme of the pathway (Wright et al., 2014). Most plants appear to have small gene families encoding functionally specialized DXS isoforms of at least three classes (Walter et al., 2002; Cordoba et al., 2011; Paetzold et al., 2010; Saladie et al., 2014). Although DXS isozymes belonging to all three classes have been found to participate in carotenoid biosynthesis, their differential expression during development and in specific organs suggests non-redundant function (Cordoba et al., 2011; Krushkal et al., 2003). For instance, type I DXS genes (including tomato DXS1; Table I1) are typically expressed in green tissues and are thought to supply the precursors for housekeeping and photosynthetic metabolites such as carotenoids and chlorophylls. Tomato DXS1, however, also provides the precursors for carotenoid biosynthesis during fruit ripening (Lois et al. 2000; Walter et al. 2000; Paetzold et al. 2010). Type II DXS genes are usually expressed in specialized contexts like apocarotenoid-accumulating roots colonized by mycorrhizas (Walter et al., 2000). In tomato, the role of DXS2 appears to be most relevant in trichomes (Paetzold et al. 2010). A third clade of DXS-like sequences (type III) has been proposed, but DXS activity for this group has not been conclusively demonstrated (Vallabhaneni and Wurtzel, 2009). In contrast to DXS, single genes encode the core enzymes of the MEP pathway (including DXR and HDR) in tomato (Table I1). However, small gene families encode IDI and GGDS, like in most other plants. By *in-silico* analysis, we found that the tomato genome harbors at least 4 GGDS homologues (Table I1), two of them being previously identified. While *GGDS1* is predominantly expressed in leaves, *GGDS2* appears to mainly act in chromoplasts-containing flowers and fruits (Ament et al., 2006).

Carotenoid Biosynthesis

The structural pathway for carotenoid biosynthesis has been well established in plants (Ruiz-Sola & Rodriguez-Concepcion 2012). A schematic representation including some of the available mutants in biosynthetic enzymes is shown in Figure I5. While the core carotenoid pathway is fairly conserved among plants, changes in particular steps in particular organisms eventually generate an astonishing diversity of carotenoids in plants and beyond (Maresca et al. 2008).

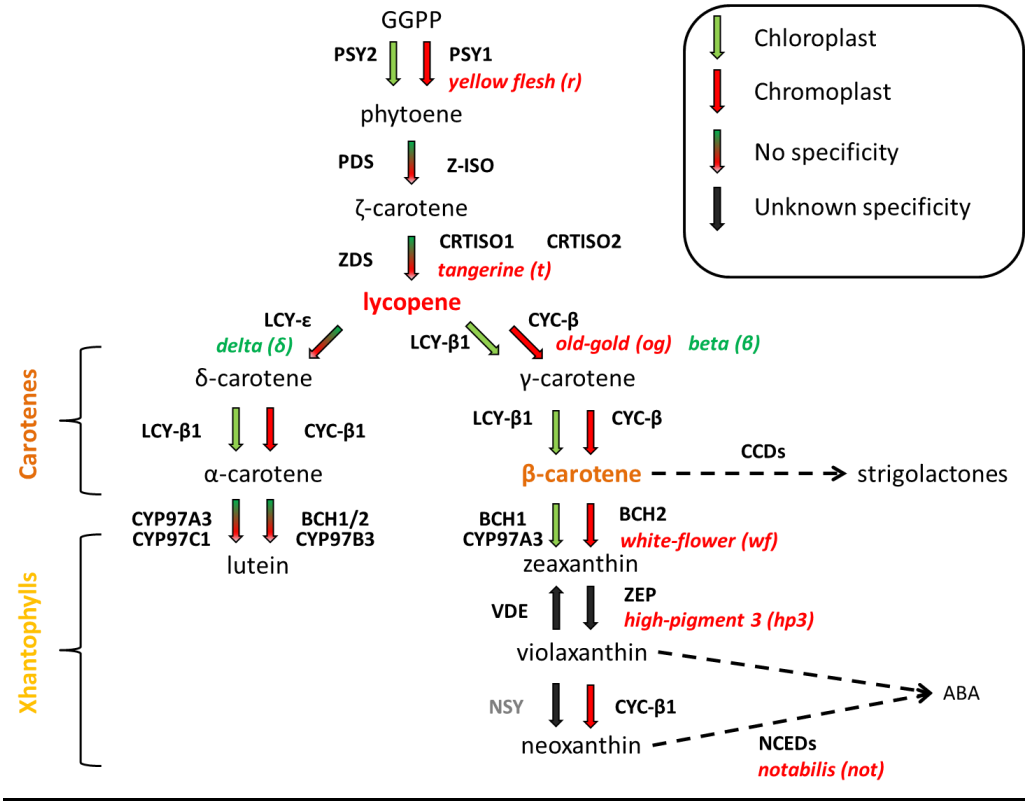

Figure I5. Carotenoid pathway in tomato fruit. Arrows color indicates where the enzyme isoforms accumulate mostly. Green arrows indicate chloroplast containing tissues (green tissue), red arrows indicate chromoplast containing tissue, green-red arrows indicate non-tissue specificity and black arrows indicate unknown specificity. Loss-of-function mutants are indicated in red next to the mutated enzyme. Similarly, gain-of-function mutants are indicated in green.

GGPP to phytoene: phytoene synthase (PSY)

The first committed step in plant carotenoid biosynthesis is catalyzed by PSY (Dogbo et al., 1988) and it involves the head-to-head condensation of two molecules of GGPP to form phytoene (7,8,11,12,7',8,',11',12'-octahydro-ψ,ψ-carotene).

PSY enzymes from land plants, algae and cyanobacteria are similar to the

bacterial and fungal enzymes (named crtB) and share amino acid sequence similarity with GGDS and other prenyltransferases (Cunningham and Gantt, 1998; Bouvier et al., 2005). While only one *PSY* gene is present in Arabidopsis (Table I2), small gene families appear to encode PSY in most plants (Ruiz-Sola and Rodriguez-Concepción, 2012). The tomato nuclear genome contains sequences encoding three PSY enzymes, named PSY1, PSY2 and PSY3 (Table I2). These three enzymes are mainly involved in the synthesis of carotenoids in ripening fruit, green tissue, and roots, respectively (Bartley and Scolnik, 1993; Fraser et al., 1994, 1999; Fantini et al., 2013; Walter et al., 2015). The presence of three PSY genes in tomato is consistent with the proposed genome triplication that occurred during its evolution, which added new gene family members that mediate important fruit-specific functions such as lycopene biosynthesis (The tomato Genome Consortium, 2012).

Table I2. Tomato and Arabidopsis carotenoid pathway homologues

	Arabidopsis	Tomato	
Enzyme	Accession	Accession	Isoform
PSY	At5g17230	Solyc03g031860	PSY1
		Solyc02g081330	PSY2
		Solyc01g005940	PSY3
PDS	At4g14210	Solyc03g123760	PDS
ZDS	At3g04870	Solyc01g097810	ZDS
Z-ISO	At1g10830	Solyc12g098710	Z-ISO
CRTISO	At1g06820	Solyc10g081650	CRTISO1
	At1g57770	Solyc05g010180	CRTISO2
LCY-B	At3g10230	Solyc04g040190	LCY-β1
		Solyc10g079480	LCY-β2 (CYC-β)
LCY-E	At5g57030	Solyc12g008980	LCY-ε
BCH	At4g25700	Solyc06g036260	BCH1
	At5g52570	Solyc03g007960	BCH2
CYP97	At1g31800	Solyc04g051190	CYP97A3
	At4g15110	Solyc05g016330	CYP97B3
	At3g53130	Solyc10g083790	CYP97C1
ZEP	At5g67030	Solyc06g060880	ZEP1
		Solyc02g090890	ZEP2
VDE	At1g08550	Solyc04g050930	VDE

NSY	At1g67080	Solyc02g089050	NSY1
		Solyc02g063170	NSY2
		Solyc03g034240	NSY3

One important source of evidence about the specialization of tomato PSY isoforms is the phenotype of the *yellow flesh (r)* mutant (Figure I3). The *r* mutant harbors a mutated version of the *PSY1* gene leading to a yellow flower corolla, pale-yellow fruit flesh, and more intensely yellow-colored fruit skin. This phenotype is explained by a complete lack of carotenoids only in chromoplasts of flowers and fruits (Fray and Grierson, 1993).

From phytoene to lycopene

In the following steps of the carotenoid pathway, phytoene, an uncolored carotene, is converted into all-*trans*-lycopene, a pink/red-colored carotenoid. This transformation is achieved by a series of desaturation (dehydrogenation) and isomerization reactions that increase the number of conjugated double bonds in the initial structure. Algae, land plants, cyanobacteria and green sulfur bacteria require at least four enzymes to carry out these reactions (Moise et al. 2014; Frigaard et al. 2004), i.e. phytoene desaturase (PDS), zeta-carotene desaturase (ZDS), zeta-carotene isomerase (Z-ISO), and carotenoid isomerase (CRTISO) (Figure I5 and Table I2). All other carotenogenic organisms studied to date catalyze the entire process with just a single phytoene desaturase enzyme, crtI (Moise et al. 2014).

Of the four plant enzymes required to transform phytoene into all-*trans* lycopene, only CRTISO is normally encoded by several genes (Table I2). Virus-Induced Gene Silencing (VIGS) experiments have shown that the two genes that encode CRTISO in tomato are active in fruits (Fantini et al., 2013). One of these genes, CRTISO1, was discovered after the map-based cloning of the *tangerine (t)* mutation, which generates orange fruits, yellowish young leaves and pale flowers due to the accumulation of *cis* isomers of lycopene (pro-lycopene) instead of all-*trans* lycopene (Isaacson et al., 2002) (Figure I5).

From lycopene to cyclic carotenes

The cyclization of the C-40 chain of lycopene is a central branch point in the

carotenoid biosynthetic pathway (Figure I5). One of the branches leads to carotenoids with two β rings (β-carotene and derived ββ-xanthophylls such as zeaxanthin, violaxanthin, and neoxanthin), whereas the other leads to carotenoids with one β ring and one ε ring (α-carotene and derived βε-xanthophylls such as lutein). The only difference between these two ring types is the position of the double bond in the cyclohexene moiety. Lycopene fate is therefore determined by the action of two types of cyclases: lycopene β-cyclase (LCY-β) that catalyzes the formation of β-rings and lycopene ε-cyclase (LCY- ε) that catalyzes the formation of ε-rings. The LCY-β enzyme catalyzes a two-step reaction that creates one β ring at each end of the lycopene (ψ,ψ-carotene) molecule to produce the bicyclic β-carotene (ββ-carotene) via the monocyclic γ-carotene (ψ,b-carotene). On the other branch of the pathway, LCY-ε adds only one ε ring to lycopene, forming the monocyclic δ-carotene (ψ,e-carotene). Then, δ-carotene is transformed into α-carotene (βε-carotene) by LCY-β. The proportion of ββ/βε-carotenoids seems to be mainly determined by the relative amounts and/or activities of LCY-β and LCY-ε (Pogson et al., 1996; Ronen et al., 1999, 2000; Harjes et al., 2007; Bai et al., 2009). Interestingly, it has been shown that while β rings are ubiquitously found in all carotenoid synthesizing organisms, ε rings are restricted to land plants, algae, and cyanobacteria (Kim and DellaPenna, 2006). In fact, evolutionary studies strongly suggest that plant cyclases that generate ε rings arose by gene duplication of an ancient cyclase that generated β rings (Klassen, 2010). As prokaryotic cyclases like crtY (from non-photosinthetic bacteria) and crtL (from cyanobacteria), plant cyclases are flavoenzymes that require the reduced form of the FAD (flavin adenine dinucleotide) cofactor. Genome survey of different plant species has shown that while LCY-ε is typically encoded by a unique gene in most plants, including Arabidopsis and tomato, LCY-β is encoded by a single gene in some plants, like Arabidopsis, or by small gene families in others (Cunningham et al., 1996). For instance, there are two LCY-β isoforms in the tomato genome (Table I2): LCY-β1 (also known as CRTL-β), which is most active in green tissues and flowers, and LCY-β2 (also known as CYC-β), which is chromoplast-specific (Ronen et al., 2000) (Figure I5). The tomato *β (beta)* mutant accumulates high levels of β-carotene due to an activation of the endogenous gene encoding CYC-β (Ronen et al., 2000). In addition, a null mutation of this gene results in abolished β-carotene production but increased lycopene content in

fruits of the *old-gold (og)* mutant (Ronen et al., 2000). On the other hand, an enhancement in *LCY-ε* transcript levels in the *delta* tomato mutant generates orange-colored fruits that contain elevated levels of the monocyclic δ-carotene (Ronen et al., 1999) (Figure I5).

Biosynthesis of xanthophylls

Once the bicyclic β-carotene (ββ-carotene) or α-carotene (βε-carotene) are synthesized, they can be modified by hydroxylation to generate xanthophylls, a generic name for the oxygenated derivatives of carotenes (Figure I5). While the hydroxylation of α-carotene finally produces lutein, the same reaction from β-carotene gives rise to zeaxanthin (via β-cryptoxanthin) and downstream xanthophylls such as violaxanthin and neoxanthin (Figure I5). Two different types of carotenoid hydroxylases (CHYs) have been found in plants: (1) non-heme di-iron enzymes (BCH type), which are similar to the bacteria crtZ and cyanobacteria crtR-B enzymes that catalyze the hydroxylation of β rings, and (2) cytochrome P450 enzymes (CYP97 type) that catalyze the hydroxylation of both β and ε rings. In Arabidopsis, two CHY enzymes belong to the BCH family (BCH1 and BCH2) and three belong to the CYP97 family: CYP97A3, CYP97B3 and CYP97C1 (Table I2). Similar to other gene families, genes encoding for these hydroxylases show an organ-specific expression pattern, suggesting that the synthesis of ββ- and βε-xanthophylls operate independently (Ruiz-Sola and Rodriguez-Concepción, 2012).

In tomato, genetic and phylogenetic analyses have also led to the identification of CHYs belonging to both BCH and CYP97 families (Table I2). The genetic mapping of the gene responsible for the tomato *white flower (wf)* mutant phenotype allowed the identification of the first chromoplast-specific BCH, named *CrtR-b2* (or BCH2). Its homolog *CrtR-b1* (or BCH1), is mainly expressed in chloroplasts (Galpaz et al., 2006). Similarly, two tomato enzymes that belong to the CYP97 family, named CYP97A29 and CYP97C11, have carotene hydroxylase activity. The corresponding genes were found to be expressed at the same rate in most tissues, with the only exception of roots and chromoplast-containing fruits, where CYP97A29 accumulates at higher levels (Stigliani et al., 2011).

Xanthophyll cycle enzymes

As mentioned before, the hydroxylation of β-carotene gives rise to zeaxanthin, which can be then converted into violaxanthin. It is well described that zeaxanthin and violaxanthin levels accumulate differentially depending on light conditions; a process known as the xanthophyll cycle. Under normal light conditions, the enzyme zeaxanthin epoxidase (ZEP) converts zeaxanthin into violaxanthin, thus maintaining violaxanthin levels high. When light intensity becomes too high, however, the photosynthetic reactions change the pH in the lumen, leading to an increase in the activity of the enzyme violaxanthin de-epoxidase (VDE), which catalyzes the de-epoxidation of violaxanthin back to zeaxanthin. In this way, the plant maintains high levels of zeaxanthin, which is a better quencher to dissipate the excess of light energy as well as a scavenger for photosynthesis-derived ROS, during the day (Demmig-Adams et al., 1996; Cunningham and Gantt, 1998).

ZEP is a multi-component FAD-containing monooxygenase (Büch et al., 1995; Marin et al., 1996). The fact that Arabidopsis mutants defective in ZEP (named *aba1*) produce significantly lower ABA levels than wild type plants (Rock and Zeevaart, 1991), illustrates the relevance of this enzyme in controlling the ββ-branch flux for the production of this hormone. A similar situation occurs in the tomato *hp3* mutant (Galpaz et al. 2008). In contrast to ZEP, which is encoded by small gene families in some plants, including tomato (Table I2), VDE is usually encoded by a single gene. Tomato plants overexpressing VDE have been shown to alleviate the photoinhibition of photosystems under high light conditions due to increased activity of the xanthophyll cycle (Han et al., 2010).

Neoxanthin synthase

The last step of the ββ branch of the carotenoid pathway in plants is the conversion of violaxanthin into neoxanthin by neoxanthin synthase (NSY). Neoxanthin is a xanthophyll molecule that together with violaxanthin, can be converted into the phytohormone ABA. Enzymes claimed to display NSY activity include the tomato CYC-β isoform (Ronen et al., 2000) and the ABA4 protein that North et al (2007) found in Arabidopsis. A BLAST analysis using Arabidopsis ABA4 showed that tomato harbors 3 putative homologues in its genome (Table I2). However, evidence supporting the role

of these proteins as true NSY enzymes is still missing.

Biosynthesis of apocarotenoids

Besides their role as pigments and photoprotective metabolites, carotenoids act as precursors to biosynthesize plant hormones and other carotenoid-derived products called apocarotenoids. Apocarotenoids can be formed non-enzymatically or produced by enzymatic cleavage of carotenoids (Yanishlieva et al., 1998). Carotenoids can be cleaved by two kind of enzymes, carotenoid cleavage dioxygenases (CCDs) and 9-cis-epoxycarotenoid dioxygenases (NCEDs) (Nambara and Marion-Poll, 2010; Ruyter-Spira et al., 2013; Lewinsohn et al., 2005). While NCDEs are specific for the synthesis of ABA and degrade particular 9-cis-epoxycarotenoids (9-cis-neoxanthin and 9-cis-violaxanthin), CCDs are very promiscuous, cleaving carotenoids at certain positions. In particular, cleavage of 9-cis-β-carotene by the consecutive action of the enzymes CCD7, CCD8 and a cytochrome P450 enzyme produces strigolactones, a family of apocarotenoid hormones with roles in plant development and interaction with the environment (Alder et al., 2012). Recent reports have demonstrated that unidentified products of linear carotenoids participate in developmental processes in the leaves (Avendaño-Vázquez et al., 2014) and the root in Arabidopsis(Van Norman et al., 2014). Similarly, it was proposed the existence of a potential apocarotenoid signal derived from the first intermediates of the pathway (perhaps neurosporene or prolycopene) that would be able to modify the flux through the carotenoid pathway during tomato fruit ripening (Kachanovsky et al., 2012).

Section III

Molecular Regulation of Carotenoid Biosynthesis

Despite the relevance of carotenoids for plant life and their impact in human health (see Chapter IV below), the current understanding of how plant cells regulate their accumulation in plastids is still relatively poor. Nevertheless, it is becoming clearer that the regulation of carotenoids biosynthesis is linked with that of related pathways and cellular processes in which these isoprenoid pigments participate. Because of the tight interconnection between the MEP pathway and the carotenoid pathway, the regulatory mechanisms of these two pathways will be covered in this section.

The coordination between the MEP and carotenoid pathways

Several lines of evidence, both from Arabidopsis and from tomato, indicate that carotenoids are synthesized mainly from MEP-derived isoprenoid precursors. For instance, transgenic Arabidopsis plants and tomato fruits that overproduce MEP pathway enzymes, such as DXS, DXR or HDR have enhanced levels of carotenoids (Estévez et al., 2001; Enfissi et al., 2005; Botella-Pavía et al., 2004). In agreement with a relevant role for DXS1, but also for HDR, in the production of isoprenoid precursors for carotenoids biosynthesis in tomato fruit, the levels of transcripts encoding these enzymes are known to be upregulated during tomato fruit ripening (Lois et al., 2000; Botella-Pavía et al., 2004). By contrast, *DXR* transcript levels do not change (Rodríguez-Concepción et al., 2001). In addition, pharmacological experiments have shown that specific inhibition of MEP or carotenoid pathway enzymes in the fruit has a similar negative impact in the carotenoid content (Rodríguez-Concepción, 2010). On the contrary, when the cytosolic MVA-pathway is blocked, the production of carotenoids is not affected in the fruit (Figure I6).

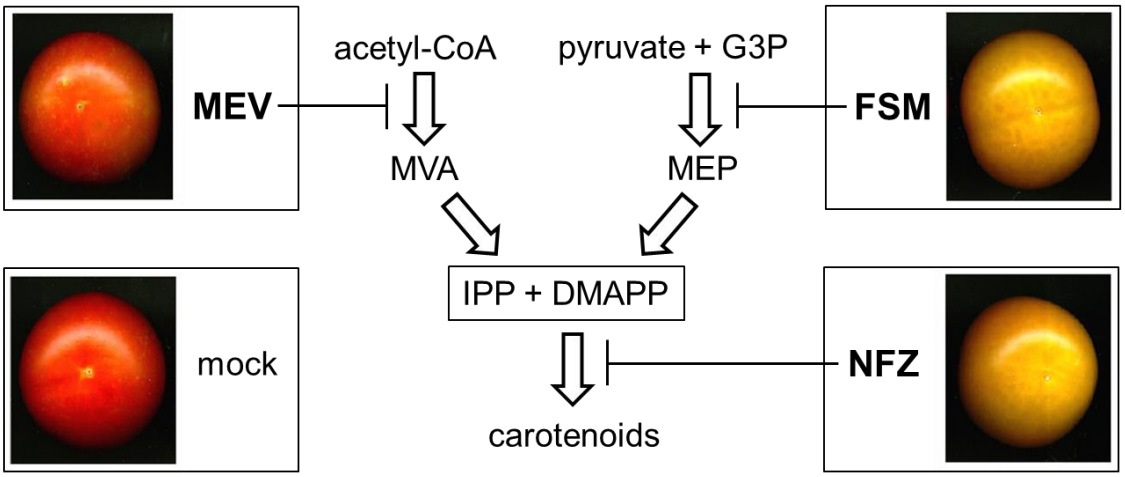

Figure I6. Pigmentation of tomato ripe fruit after treatment with inhibitors. Pictures show representative fruit injected at the MG stage with the indicated inhibitors or a mock solution and collected two weeks later, at the R stage. MEV, mevinolin (an inhibitor of the first committed enzyme of the MVA pathway); FSM, fosmidomycin (an inhibitor of DXR); NFZ, norflurazon (an inhibitor of PDS). The step blocked by each inhibitor is indicated. Adapted from Rodriguez-Concepcion, 2010.

The fact that the availability of MEP-derived precursors limits carotenoid production fueled the idea that an active crosstalk between the two pathways could be operating to ensure the correct supply of prenyl diphosphate precursors required for carotenoid biosynthesis when necessary (Giuliano et al., 2008; Sauret-Güeto et al., 2006; Cazzonelli and Pogson, 2010). This crosstalk appears to be mainly reliant on a tight coordination between the levels and activity of DXS and PSY, the main rate-limiting enzymes of the MEP and carotenoid pathways respectively. Although experiments corroborating this hypothesis were done in several plant species, the case of the tomato fruit is maybe one of the most explanatory. During ripening there is a boost in the production of carotenoids thanks to a coordinated induction of genes encoding the fruit rate-limiting enzymes DXS1 and PSY1 (Lois et al., 2000; Botella-Pavía et al., 2004; Fanciullino et al., 2008). Supplying the product of DXS activity was shown to trigger an upregulation of *PSY1* expression levels (Lois et al., 2000). Furthermore, while genetically modified tomato fruits with altered levels of PSY1 show negatively correlated changes in *DXS1* expression, the levels of proteins and enzyme activities follow the same trend (Lois et al., 2000; Fraser et al., 2007). Thus, higher PSY activity in the fruit results in lower *DXS1* transcripts but promotes DXS activity (Fraser et al. 2007). This lack of correlation between the behavior of transcripts and protein activity

could rely in post-transcriptional mechanisms like those reported in Arabidopsis (see below).

Transcriptional regulation

During the last decades, a huge effort has been done to understand how carotenoid accumulation is transcriptionally regulated during tomato fruit ripening. In particular, the characterization and genetic analysis of mutants impaired in the progression of ripening have led to the identification of a set of transcription factors that regulate most of the ripening-associated processes.

Developmental regulation

As was previously explained, as tomato fruit ripening proceeds, big changes in the carotenoid profile occurs. Different studies have shown that the carotenoid accumulation pattern in ripe fruits is mainly determined by a differential expression of genes encoding carotenoid biosynthetic enzymes (reviewed in Hirschberg, 2001). In detail, when ripening starts, the color changes from green to orange due to an accumulation of lycopene and β-carotene, which takes place due to a transcriptional up-regulation of those genes that encodes for carotenoid biosynthetic enzymes, like PSY1, PDS and CYC-β and down-regulation of *LCY-ε* and *LCY-β1*. Moreover, during the transition from O to ripe, the mRNA levels of *CYC-β*, which is involved in lycopene cyclization in chromoplasts, decreased. Hence, the enhanced flux to carotene is arrested at lycopene, which finally gives the characteristic red color to the ripe fruit (Hirschberg, 2001; Ronen et al., 2000).

*A*ll these regulatory events are known to be tightly coordinated with the developmental program associated with fruit ripening. The correct orchestration of these processes depends on a group of factors known as *ripening master regulators*. Maybe one of the best characterized master regulators is RIN, one of the earliest acting ripening regulators required for a normal ripening progression. Different transcriptomic approaches using tomato fruit *rin* mutant served to identify target genes, including some encoding enzymes involved in carotenoid production (Fujisawa et al. 2011; Fujisawa et al. 2012). RIN positively regulates the transcription of *CMK*, *PSY1*, *Z-ISO* and *CRTISO* by directly binding to unknown *cis*-elements in their promoter region, and of

DXS1, *GGDS2* and *ZDS* in an indirect manner. RIN can also negatively regulate the expression of genes involved in the MEP pathway such as *DXS2* and *IDI2*, and in lycopene cyclization, like *LCY-ε* and *CYC-β*. Thus, the up and down-regulation triggered by the RIN transcription factor is expected to channel biosynthetic pathways to the production of lycopene during the ripening process (Fujisawa et al., 2013). *PSY1* is also known to be up-regulated by ethylene (Fray and Grierson, 1993). This activation is indirectly promoted by RIN, as it up-regulates NOR and CNR transcription factors, which induce genes involved in the synthesis and signaling of this hormone (e.g. *ACS2* and *ACS4)* (Martel et al., 2011; Zhou et al., 2012; Ito et al., 2008; Fujisawa et al., 2011, 2012; Qin et al., 2012).

In addition to RIN, two other MADS box transcription factors, *FRUITFULL1* (*FUL1*; formerly named *TDR4*) and *FUL2,* are able to directly alter the expression of carotenoid biosynthetic genes during tomato fruit ripening (Itkin et al., 2009; Vrebalov et al., 2009; Giménez et al., 2010; Pan et al., 2010; Bemer et al., 2012; Shima et al., 2014). In accordance, FUL1/2 suppression results in ripening-defective phenotypes partly similar to the phenotype of the *rin* mutant. Transcriptomic data from tomato fruits with altered levels of these transcription factors revealed that many, but not all, of the RIN target genes are also regulated by FUL1, by binding to the same genomic region. Whereas genes involved in carotene production such as *PSY1*, *Z-ISO*, *CRTISO* and *CYC-β* were found to be common targets of RIN and FUL1, genes involved in carotene conversion, such as *BCH* and *NCED,* are targeted only by FUL1. Consistent with the idea that RIN and FUL1 share binding regions and target genes, it was demonstrated that in those cases FUL1 and RIN can act together as heterodimers (Leseberg et al., 2008; Bemer et al., 2012; Shima et al., 2013). Interestingly, plants that harbor a mutation in another MADS box gene named *AGAMOUS-LIKE1* (*TAGL1*) were found to have similar phenotype to *FUL1/2* suppression lines. Moreover, yeast-two-hybrid and gel retardation assays showed that RIN also interacts with *TAGL1* (Leseberg et al., 2008; Martel et al., 2011; Bemer et al., 2012; Shima et al., 2013). Although speculative at the moment, it is assumed that RIN, TAGL1 and FUL1 can regulate different target genes depending on the nature of the complex (FUL1/2-RIN, TAGL1-RIN or RIN-RIN) (Fujisawa et al., 2014).

In parallel to the transcriptional regulation, epigenomic studies have unveiled that changes in the methylation status of the tomato genome occur during ripening.

Genomic DNA methylation is known to be an important mechanism that influences gene expression, as methylation of promoters is known to inhibit gene transcription. In agreement, a detailed characterization uncovered that most of the methylation changes in the epigenome are located at the promoter region of ripening-associated genes. Particularly, DNA regions associated with RIN binding sites were found to be preferentially regulated at the methylation level. For instance, at the MG stage the promoter of the RIN target gene *PSY1* is mostly methylated, hence presumably impairing RIN binding. When ripening starts, *PSY1* promoter is demethylated (possibly by DEMETER-like DNA demethylase 2 (DML2)) so that RIN can now bind and enhance *PSY1* expression (Zhong et al., 2013; Liu et al., 2015).

Light signaling

Carotenoid production can be modulated by different environmental signals, including light. It has been shown that genes encoding carotenoid biosynthetic enzymes in Arabidopsis and tomato, including those of the MEP pathway, can be upregulated by light signals (Meier et al., 2011; Ruiz-Sola and Rodriguez-Concepción, 2012; Ghassemian et al., 2006).

Light is perceived through specialized photoreceptors. There are at least five types of plant sensory photoreceptors, each one able to detect specific regions of the electromagnetic spectrum (Galvao and Fankhauser, 2015). Cryptochromes (CRYs), phototropins and Zeitlupe family members function in the blue (390-500 nm) and ultraviolet-A (320-390 nm) wavelengths, while the photoreceptor UVR-8 operates in the ultraviolet-B (280-315 nm) region. Phytochromes (PHYs), which are probably the best studied photoreceptors, are receptors of red (R) and far-red (FR) light. Activation of fruit-localized phytochromes with R light treatments promotes carotenoid biosynthesis in tomato, while subsequent phytochrome inactivation by irradiation with FR light reverts it (Alba et al., 2000; Schofield and Paliyath, 2005). Furthermore, triple *phyA phyB1 phyB2* mutant plants produce white fruits completely devoid of pigments (Weller et al., 2000) similar to those obtained by preventing light exposure from the very early stages of fruit set and development results in white fruits (Cheung et al., 1993). In addition to regulating carotenoid levels in tomato fruits, PHYs appear to regulate the timing of stage transitions during ripening (Gupta et al., 2014).

PHYs exist in equilibrium between two photoconvertible isoforms: the R-light absorbing isoform Pr and the FR-light absorbing isoform Pfr (Neff et al., 2000; Azari et al., 2010). In land plants, darkness or low R/FR ratios typically associated with the proximity of other plants whose green tissues absorb red light (i.e. shade), shift the equilibrium to the inactive Pr form of PHYs, which accumulates in the cytoplasm. When this happens specific transcription factors, such as the phytochrome-interacting transcription factors (PIFs), are able to accumulate in the nucleus and thus bind to their genomic regulatory elements tuning the expression of numerous genes (Casal et al., 2013; Leivar and Monte, 2014). When the R/FR ratio increases (i.e. under sunlight), the photoequilibirum moves PHYs to the active Pfr form, which is then translocated to the nucleus to promote the inactivation of PIFs (mainly by proteasome-mediated degradation) and hence change the transcription of PIF target genes (Bae and Choi, 2008; Leivar and Monte, 2014).

PIFs are helix-loop-helix transcription factors that mediate a variety of light-related responses, including carotenoid biosynthesis. Previous work in our lab has shown that PIF1 can directly bind the promoter of the Arabidopsis *PSY* gene to repress its expression and hence inhibit the production of carotenoids in the dark and under shade conditions (Toledo-Ortiz et al., 2010, 2014; Bou-Torrent et al., 2015) but it appears to have no role in the regulation of *PSY* expression and carotenoid biosynthesis in response to other stimuli such as ABA treatment or salt stress (Ruiz-Sola et al., 2014).

Multiple lines of evidence have exposed that light also modulates the genetic programs associated to tomato fruit development and ripening (Azari et al., 2010). As described before, among many light-signaling mutants displaying altered fruit phenotypes, the tomato *high pigment* (*hp*) mutants, *hp1* and *hp2* are two of the best characterized. These mutants were shown to harbor mutations in genes that encode for light signaling transduction components. While *hp1* has deficient levels of the DAMAGED DNA BINDING PROTEIN 1 (DDB1), *hp2* is defected in the DETIOLATED1 (DET1) protein (Levin et al., 2003; Mustilli et al., 1999; Schroeder et al., 2002). Other components that participate in the same light-signaling pathway also impact tomato fruit metabolism. For instance, silencing the tomato E3 ubiquitin-ligase CUL4, which directly interacts with DDB1, also produces highly pigmented fruits (Wang et al., 2008). Lastly, two highly conserved light signaling proteins like COP1 and HY5 are also present

in the tomato genome. Similar to Arabidopsis, COP1 specifically promotes the degradation of the light-signaling effector HY5 in tomato fruit (Schwechheimer and Deng, 2000). In agreement with the demonstrated role of these components regulating *PSY* expression and carotenoid biosynthesis in Arabidopsis (Rodríguez-Villalón et al., 2009b, 2009a; Toledo-Ortiz et al., 2010), transgenic tomato plants with downregulated transcripts of COP1 and HY5 produce tomato fruits with increased and reduced levels of carotenoids, respectively (Liu et al., 2004).

Post-transcriptional regulation

In order to ensure the proper levels of active proteins, cells have developed different layers of regulation that can be divided in two types: transcriptional and post-transcriptional. In this section, post-transcriptional regulation mechanisms controlling carotenoid contents will be reviewed. They can impact biochemical processes grouped into four major areas: (i) modulation of levels and activities of biosynthetic enzymes, (ii) metabolite channeling by multi-enzyme complexes, (iii) sequestration and storage capacity of carotenoids, and (iv) carotenoid turnover. As the last two mechanisms were covered before when referring to plastid ultrastructure (iii) and apocarotenoid synthesis (iv), this section will cover the modulation of enzyme levels and activities, and metabolite channeling by multi-enzyme complexes.

Modulation of enzyme levels and activities

In Arabidopsis plants, a fine control of the activity of MEP pathway enzymes, and presumably also carotenoid biosynthesis enzymes, can be achieved by modulating their folding and degradation rate. In this regard, it has been shown that specific components of the plastidial Protein Quality Control (PQC) system (i.e. plastidial chaperones and proteases) plays a major role in the maintenance of active rate-limiting enzymes such as DXS and DXR (Flores-Perez et al., 2008; Pulido et al., 2013, 2016). In the case of DXS, it has been shown that a J-domain co-chaperone (or J-protein) named J20 can specifically recognize misfolded or aggregated DXS proteins. J20 transfers the inactive DXS enzymes to plastidial Hsp70 chaperones, which then can deliver the client protein to Hsp100 proteins such as ClpB3 or ClpC1. Interaction with ClpB3 promotes the disaggregation and hence reactivation of DXS, whereas interaction with ClpC1

unfolds the protein for degradation via the stromal Clp protease complex (Pulido et al., 2013, 2016). In addition to DXS, Clp defective plants over-accumulate other MEP pathway enzymes such as DXR, HDS and HDR (Flores-Perez et al., 2008; Kim et al., 2009; Nishimura and van Wijk, 2015; Zybailov et al., 2009), suggesting that this protease complex might be involved in their degradation. However, the specific proteins involved in recognizing and delivering the damaged enzyme to the Clp protease complex for degradation appear not to be conserved. For instance, previous results in our lab have shown that, in the case of DXR, protein stability is influenced by Cpn60, another chaperone complex (unpublished data), and that enzyme turnover might occur by pathways other than Clp-mediated degradation (Perello et al., 2016).

The main rate-limiting enzyme for carotenoids synthesis, PSY, is also regulated by the plastidial PQC mechanisms. In this case, the Dna-J-like protein Orange (Or) is required to stabilize PSY, probably by protecting it from degradation by the Clp protease (Zhou et al., 2015; Li Li, personal communication). Because Or is the only protein reported to trigger chromoplastogenesis to date, these results highlight an intriguing connection between carotenoid biosynthesis and chromoplast differentiation. The possibility that the main rate-limiting enzymes controlling the carotenoid pathway flux (DXS and PSY) might be regulated by the same protease complex (Clp protease) further suggests that PQC mechanisms might coordinate both the supply of MEP-derived precursors and their channeling to the biosynthesis of carotenoids at the post-transcriptional levels, similarly to that observed at the transcriptional level.

The role of PQC in the regulation of carotenoids production in tomato remains little unexplored. It is known, however, that PSY1 is inhibited by direct interaction with STAY-GREEN 1 (SGR1), a nuclear-encoded chloroplast protein involved in chlorophyll degradation during fruit ripening. In fact, it has been shown that one single amino acid substitution in SGR1 is responsible for the *green-flesh* (*gf*) mutation of tomato that results in ripe fruits harboring both carotenoid-rich chromoplasts and chlorophyll-containing chloroplasts (Barry et al., 2008). Genetic and metabolic analyses of tomato fruits with silenced *SGR1* demonstrated that SGR1 interacts with PSY1 to coordinate the production of carotenoids with chlorophyll degradation during ripening (Hörtensteiner, 2009; Luo et al., 2013).

Another important layer of post-transcriptional regulation in the MEP and carotenoid pathways is the control of the enzyme redox status. For instance, the MEP pathway enzymes DXR, HDS and HDR appear to be targets of thioredoxin (Balmer et al., 2003; Lemaire et al., 2004), a member of the ferredoxin/thioredoxin system that is chemically reduced in photosynthetically-active chloroplasts to up-regulate the activity of its target proteins through the reduction of specific disulfide groups (Schürmann, 2003).

In the case of the carotenoid desaturases PDS and ZDS, they use plastoquinone as hydrogen acceptor and therefore their enzymatic activity is directly connected with the photosynthetic electron transport chain (Carol and Kuntz, 2001). In addition, the presence of a FAD-binding conserved domain in a set of carotenoid biosynthetic enzymes (including PDS, ZDS, CRTISO, LCY-β, LCY-ε, and ZEP), suggests the involvement of redox balance in their corresponding enzymatic reactions (Marin et al., 1996; Schnurr et al., 1996; Isaacson et al., 2002; Mialoundama et al., 2010). In agreement, an imbalance in the plastidial redox status due to a mutation in a NADH-dehydrogenase subunit (*Orr* mutant) lead to yellow-orange fruits, due to a substantial decreased in the levels of β-carotene and lutein. It is proposed that these changes in the carotenoid levels are caused by a reduction in the activity of those FAD-containing carotenoid enzymes (Nashilevitz et al., 2010).

Metabolite channeling by multi-enzyme complexes

A major determinant of the activity of carotenoid biosynthetic enzymes is membrane association, as many enzymes of the pathway (including PSY) function in a membrane context (Ruiz-Sola and Rodriguez-Concepción, 2012). Moreover, carotenoid enzymes seem to be associated in multi-enzyme complexes (metabolons), which could be a useful way to improve metabolic flux kinetics. Carotenoids are insoluble in aqueous environments, so direct transfer of carotenoid intermediates between physically interacting enzymes (from the one that produces it to the one that consumes it) might be advantageous. In particular, the existence of different chloroplast multi-enzyme complexes containing enzymes to channel phytoene to synthesize cyclic carotenes (Cunningham and Gantt, 1998; Bai et al., 2009) and of lycopene to synthesize lutein (Kim and DellaPenna, 2006) has been proposed. By using tomato fruit transient

silencing assays coupled to carotenoid profiling, Fantini et al (2013) provided evidence that suggests the existence of two different metabolons in tomato chromoplasts, PDS/ZISO and ZDS/CRTISO (i.e. desaturase and the downstream isomerase).

Different plastid types display a different carotenoid profile, a different enzymatic repertoire and, in particular cases like chromoplasts, unique subplastidial structures such as plastoglobules (PG). Based on these differences it would be expected that the nature and localization of the hypothetical multi-protein complexes would differ in different plastid types. In agreement, the enzymes ZDS, LCY-β, BCH1 and BCH2 were found to be part of the PG proteome in pepper fruit chromoplasts but not in Arabidopsis chloroplasts (Vidi et al., 2006; Ytterberg et al., 2006).

Section IV

Economic and nutritional value of tomato fruit and carotenoids

Tomato is one of the most important crops in the world, being positioned in the 11th position in the ranking of most produced crops. Nowadays, the production of tomato is highest in China and United States of America (USA), followed by Italy and Spain (http://www.fao.org/home/es/). As described above, carotenoid pigments are largely responsible for the color and aroma of ripe tomatoes. They also furnish with attractive colors many other fruits and flowers, improving consumer acceptance of vegetables and hence providing an economic value. Beyond these organoleptic properties, dietary carotenoids play an essential role in human and animal nutrition, as detailed in the next section.

Nutritional Quality

The human diet has suffered profound variations during history. The most pronounced change occurred quite recently, some 10,000 years ago, with the advent of agriculture and animal husbandry. Before that time, humans were hunter-gatherers and had a diet that was rich in fruits, vegetables and protein, and low in fat and starch (Pritchard, 2010). Unlike this diet, referred to as the *Paleolithic diet*, our *Modern diet* is typically starchier, higher in fat, and with lower intake of fresh fruits and vegetables. The human genome has evolved in the context of the *Paleolithic diet*, but there has not been enough time for it to adapt to the new diet. This evolutionary discordance has been proposed to be the reason of many modern chronic diseases (Cordain et al., 2000). In addition, due to a reduced variety of plants ingested and to selective breeding, the levels of phytonutrients consumed nowadays are decreasing (Willett, 2010).

For these reasons, most modern dietary recommendations include consumption of fresh and whole fruits and vegetables, generally, fruits containing high levels of phytonutrients such as polyphenols (e.g. flavonoids and stilbenes) and carotenoids. Polyphenols have gained significant importance recently, as they were proven to reduce the risk of chronic diseases such as cardiovascular disease, metabolic syndrome, cancer and obesity. A particular sub-group of polyphenols, anthocyanins, has the highest antioxidant capacity, and hence strong health-promoting effects. These metabolites reduce tumor initiation, suppress angiogenesis and minimize cancer-induced DNA damage in animal models (Frassetto et al., 2009; Morgan et al., 1999; Liu, 2003; Klonoff, 2009). Another important group of biologically active polyphenols comprises the hydroxycinnamic acid esters, been chlorogenic acid the major antioxidant in the average developed-world diet. Chlorogenic acid is also the most abundant soluble phenolic in *Solanaceous* species, including tomato.

Tomato fruit contains, depending on the variety, 8–40 μg of lycopene per gram of fresh weight (Martin et al., 2013). Lycopene is a potent lipophilic antioxidant, with greater antioxidant activity than other carotenoids. The antioxidant activity of lycopene is associated with its ability to act as a free radical scavenger for reactive oxygen species (ROS) that generate by partial reduction of oxygen (Friedman, 2013). The accumulation of ROS in the human body generates oxidative stress, which is a common feature of different processes like aging and development of chronic and degenerative illness such as cancer (Seren et al, 2008). The beneficial effects of lycopene are not only associated with its ROS scavenger ability, but also derive from its ability to interfere with key cancer-related processes (Ansari and Gupta, 2004). For instance, it has been observed that there is an inverse correlation between the ingestion of lycopene and the levels of *cyclin D1*, a known oncogene overexpressed in many primary tumors (Frusciante et al., 2007).

The second most abundant carotenoid in ripe tomatoes is β-carotene. β-carotene has provitamin A activity, as it can be converted into retinoids once ingested. In humans, β-carotene must be converted to all-*trans*-retinal to be further reduced to all-*trans*-retinol, which is finally esterified and stored in specialized cells in the liver and other tissues (D'Ambrosio et al., 2011). In eye's cells, retinoids can be metabolized into 11-*cis*-retinal, our visual chromophore. On the other hand, retinoids can be oxidized to

all-*trans*-retinoic acid, a hormone-like molecule that is able to influence gene expression in many physiologic processes (Von Lintig, 2012). β-carotene is also a strong antioxidant. For instance, several studies demonstrated that β-carotene can prevent photooxidative damage and sunburn in humans (Stahl and Sies, 2003). Phytoene, another abundant carotenoid in tomato fruit, has also been proposed to provide health benefits (Meléndez-Martínez et al., 2015).

The protective action of tomato is commonly attributed to the antioxidant activity of carotenoids. However, tomatoes are also a good source of other phytonutrients, including some of isoprenoid origin. The most abundant vitamin in tomato is vitamin E, that is, a family of compounds that includes tocopherols (α-, β -, γ-, and δ) and tocotrienols (α-, β -, γ-, and δ). While tocopherols contain a phytyl chain, tocotrienols contain a geranylgeranyl chain, both of them derived from the MEP pathway. These molecules are important antioxidants known to have a high synergistic effect with lycopene and β-carotene. Importantly, vitamin E consumption is associated with a decreased incidence of diabetes and cardiovascular diseases (Raiola et al., 2014).

Genetic engineering of carotenoid production in tomato fruits

Tomato has been established as a model for climacteric fruit but it is also a relevant crop in human nutrition. The successful use of the tomato fruit as a biotechnological platform to overproduce bioactive molecules is mainly based on the existence of a large quantity of genetic and molecular tools for tomato, including the recent release of its complete genome sequence (The Tomato Genome Consortium, 2012).

Different biotechnological strategies have been implemented to generate carotenoid-enriched tomato fruits (Table I3). Many of these strategies were based in the overexpression of genes encoding enzymes involved in carotenoid production, such as PSY or its bacterial homologue, crtB. Although many of these attempts were successful (i.e. the levels of carotenoids in the fruit were increased), there are still major problems that need to be overcome for an efficient, rational modification of the carotenoid pathway. To address these problems, it is essential to better understand fundamental aspects of the regulation of the carotenoid pathway in general and

particularly in tomato fruit during ripening. For example, detailed characterization of *PSY1* overexpressing lines showed that post-transcriptional mechanisms could be operating in the carotenoid pathway due to a lack of correlation between transcript levels, protein levels and enzyme activity (Fraser et al., 2007). Another example is the overexpression of *DXS*, which led to elevated phytoene levels without altering carotenoid end products or PSY1 activity, thus suggesting that the desaturation step might be limiting the progression through the pathway (Enfissi et al., 2005).

Table I3. Examples of genetic engineering for enhanced carotenoid content in tomato

*OE : Overexpression; DR: Down-regulation

Gene function	Target gene	OE/ DR*	Source	Fruit phenotype	Ref
MEP pathway	*DXS*	OE	*E. coli*	Increased phytoene and other carotenoids (2-fold).	(Enfissi et al., 2005)
Carotenoid biosynthesis	*crtB*	OE	*E. uredovora*	Increased (4-fold) phytoene, lycopene and β-carotene.	(Fraser et al., 2002)
	PSY1	OE	Tomato	Increased (1,5-fold) β-carotene	(Fray et al., 1995; Fraser et al., 2007)
	crtI	OE	*E. uredovora*	Increased (1,5-fold) β-carotene. Reduced lycopene and phytoene.	(Römer et al., 2000)
	LCY-β	OE	Tomato	Increased (7-fold) β-carotene.	(D'Ambrosio et al., 2004)
	CYC-β	OE	Tomato	Increased (31.7-fold) β-carotene. Reduced lycopene.	(Ronen et al., 2000)
	crtY	OE	*E. herbicola*	Increased β-carotene.	(Wurbs et al., 2007)
	LCY-β	DR	-	Increased (1,3 fold) lycopene.	(Rosati et al., 2000)
	CYC-β	DR	-	Increased lycopene.	(Ronen et al., 2000)
Carotenoid storage	*Fibrillin*	OE	Tomato	Increased (2-fold) carotenoids and derived volatiles.	(Simkin et al., 2007)
Light signaling	*Cry2*	DR	-	Increased (2-fold) carotenoid levels	(Giliberto et al., 2005)
	DET1	DR	-	10-fold increased β-carotene. 4-fold increased lycopene and increased	(Davuluri et al., 2005)

				flavonoid content.	
	COP1	DR	-	Increased (2-fold) carotenoid levels.	(Liu et al., 2004)
	CUL4	DR	-	Increased (2-fold) carotenoid levels.	(Wang et al., 2008)
Anthocyanin biosynthesis	*Delila1 /Rosea*	OE	Snapdragon	Increased anthocyanin content.	(Butelli et al., 2008)

Besides the overexpression of carotenoid biosynthetic enzymes, other biotechnological alternatives have also been implemented. Biotechnological strategies based on the manipulation of regulatory mechanisms underlying carotenoid biosynthesis have also been attempted (Fraser et al., 2009). Tomato fruits with altered activity of different components involved light signal transduction pathway were shown to display altered carotenoid profiles (Table I3). Interestingly, these approaches not only can improve the accumulation of carotenoids, but also of other important antioxidants such as flavonoids (Giliberto et al., 2005; Liu et al., 2004; Davuluri et al., 2005).

As mentioned before, carotenoids accumulate in specialized chromoplast substructures. One of the main proteins involved in the generation of these structures is fibrillin. In agreement with its role, transgenic tomato lines overexpressing a pepper fibrillin displayed a 2-fold increase in the levels of carotenoids and carotenoid-derived volatiles (Simkin et al., 2007). An improved storage capacity for carotenoids can also be achieved by increasing the size or/and number of plastids in a given cell. For example, tomato *high-pigment* (*hp*) mutants were found to have higher storage capacity due to increased chromoplast size and number. Both *hp1* and *hp2* mutants encode for regulators involved in light signaling (Levin et al. 2003; Mustilli et al. 1999 and Schroeder et al. 2002). Unlike *hp1* and *hp2*, the *hp3* mutant displays a reduction in ABA levels due to defective levels of ZEP, an enzyme that produces a carotenoid precursor of the hormone (Benvenuto et al., 2002; Davuluri et al., 2005; Galpaz et al., 2008; Kolotilin et al., 2007; Azari et al., 2010; Enfissi et al., 2010). Recently, a tomato transgenic plant overexpressing the ABA-related transcription factor ARABIDOPSIS PSEUDO RESPONSE

REGULATOR2-like (APRR2-like) was also found to display enhanced levels of carotenoids due to an increase in plastid number (Pan et al., 2013).

The implementation of new biotechnological strategies to generate plants enhanced in health-promoting metabolites, including carotenoids, will strongly benefit from applying to crops the knowledge generated in model systems. In the case of tomato fruits, the abundance of genetic and molecular resources available today facilitates this task. In this thesis, we will explore whether regulatory mechanisms known to regulate carotenoid biosynthesis in Arabidopsis can be successfully applied to improve the carotenoid content of tomato fruits.

Objectives

In order to test new biotechnological strategies to enhance the nutritional content of crops, we aimed to transfer the knowledge generated in the lab in the model plant *Arabidopsis thaliana* to improve the production of healthy carotenoids in tomato fruits as a proof of concept. In particular, we chose to manipulate two mechanisms known to regulate carotenoid biosynthesis in photosynthetic tissues (i.e. in chloroplasts) whose impact on carotenoid production and accumulation in chromoplast-containing tissues was virtually unexplored. Thus, the two specific goals of the thesis were:

1. Characterize the role of PIFs on the regulation of carotenoid biosynthesis during tomato fruit ripening and test their potential to improve the nutritional quality of the fruit.

2. Characterize the role of the Clp protease complex during tomato fruit ripening and evaluate the impact of its manipulation on carotenoid accumulation in ripe fruit.

Results

Chapter I

A role for shade signaling on the regulation of carotenoid biosynthesis during tomato fruit ripening.

Background and rationale: light, PSY and carotenoids

Light signals have a profound influence on tomato fruit ripening (Azari *et al*. 2010). In particular, fruit-localized phytochromes (PHYs) have been found to control different aspects of tomato ripening, including carotenoid accumulation (Alba *et al.* 2000, Gupta *et al.* 2014, Schofield and Paliyath 2005). Previous work in Arabidopsis has shown that when the active Pfr form of PHYs translocates to the nucleus, it interacts with a family of bHLH (basic helix-loop-helix) transcription factors named Phytochrome-Interacting Factor (PIFs), causing their inactivation mainly by proteasome-mediated degradation (Bae and Choi 2008, Leivar and Monte 2014). It has been previously demonstrated in our lab that Arabidopsis PIF1 and other members of the so called PIF quartet (PIF3, 4 and 5) can regulate carotenoid biosynthesis both in the dark and in response to a reduction in the R/FR ratio through the direct repression of *PSY* expression (Toledo-Ortiz et al., 2010, 2014; Bou-Torrent et al., 2015). The reduction in the R/FR ratio is known to be a plant proximity signal referred to as "shade", which is generated upon the preferential absorption of red light by chlorophyll-containing tissues like leaves of neighboring or canopy plants (Casal 2013; Martínez-García et al., 2010). In addition, it has been observed that the PIF1-dependent repression of *PSY* is antagonized by the bZIP transcription factor LONG HYPOCOTYL 5 (HY5). Oppositely to PIFq proteins, HY5 is degraded in the dark, but it accumulates in the light and induces *PSY* expression upon binding to the same promoter motif recognized by PIF1 (Toledo-Ortiz et al., 2014). In this way, the PIF1/HY5 module provides robutness to *PSY* regulation and hence carotenoid accumulation in Arabidopsis plants.

Arabidopsis and tomato diverged some 100 million years ago (Ku et al., 2000), and their different histories of polyploidization and subsequent gene loss have resulted in different numbers of paralogs for carotenoid biosynthesis enzymes, including PSY (Ruiz-Sola and Rodriguez-Concepcion 2012; Tomato Genome Consortium 2012). Three genes encode PSY in tomato (Table I2), but only one (*PSY1*) contributes to carotenoid biosynthesis during fruit ripening (Figure I3) (Fantini et al., 2013; Fray and Grierson 1993; Giorio et al., 2008; Tomato Genome Consortium 2012). The transcriptional induction of the *PSY1* gene actually fuels the burst in carotenoid biosynthesis that takes place at the onset of ripening (Fantini et al. 2013; Fray and Grierson 1993; Giorio et al.,

2008; Tomato Genome Consortium 2012). Many factors regulate *PSY1* transcriptional rate in tomato during ripening. They include ripening-associated transcription factors such as RIN and FUL1, which stimulate carotenoid biosynthesis by directly binding to the promoter of *PSY1* to induce gene expression (Fujisawa *et al.* 2013, Fujisawa *et al.* 2014, Martel *et al.* 2011, Shima *et al.* 2013). Similarly to Arabidopsis, light signaling component like HY5 are also known to positively regulate carotenoid accumulation in tomato fruit (Liu *et al.* 2004), whereas other light signaling components have been described as negative regulators of ripening and carotenoid biosynthesis (Azari *et al.* 2010). However, the molecular pathways connecting the perception of light signals with the regulation of carotenoid gene expression remain unknown.

In this chapter, I evaluate the putative role of a tomato PIF1 homologue as a regulator of *PSY1* expression and carotenoid biosynthesis during fruit ripening.

The ripening-induced tomato PIF1a is a true PIF1 homologue

Several studies have proposed that, PHYs control *PSY1* transcript levels and hence carotenoid biosynthesis during the ripening process in tomato (Alba *et al.* 2000, Gupta *et al.* 2015, Schofield and Paliyath 2005). When tomato fruits are irradiated with red light, PHYs are expected to accumulate mainly in the active Pfr form, re-locating from the cytosol to the nucleus and promoting changes in PIF stability and hence the transcription rate of several genes (Figure R1). Based on the knowledge generated in Arabidopsis, we speculated that the tomato *PSY1* gene might also be repressed by a tomato PIF1 homolog. Then, upon activation of PHYs the tomato PIF1 homologue would be degraded and *PSY1* de-repressed (Figure R1).

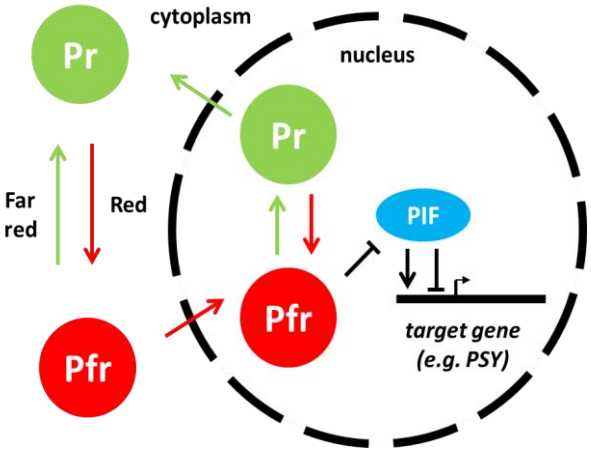

Figure R1. Schematic model of PHY-mediated regulation of gene expression. PHYs have two photoconvertible isoforms, the active (Pfr) form and the inactive (Pr) form. When Pr absorbs red light, it converts into the active Pfr form that translocates to the nucleus, causing the inactivation of PIFs, which directly regulate target genes (including those encoding PSY). Inversely, Pfr can be inactivated and excluded from the nucleus by far red light.

To test our hypothesis, we initially decided to confirm the role of PHYs in the regulation of *PSY1* gene expression in tomato fruits. MG tomato fruits (Moneymaker variety) were cut in two halves and one of the halves was incubated in the dark whereas the other half was irradiated with R light to activate PHYs. Similar experiments were done with O fruit to compare the effects of irradiation with white (W) light vs. FR-supplemented W light (i.e. simulated shade) on *PSY1* mRNA abundance by quantitative RT-PCR (RT-qPCR). As expected, while R light treatment induced *PSY1* transcription, tomato halves irradiated with W+FR accumulated lower levels of *PSY1* transcripts compared with W controls (Figure R2).

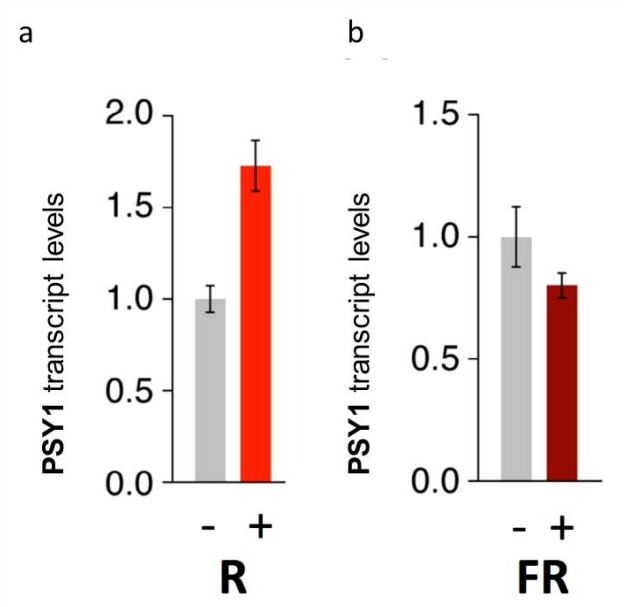

Figure R2. *PSY1* is regulated by PHYs. Quantitative PCR analysis of *PSY1* transcript levels in fruits halves irradiated with R or FR-enriched light. (a) Tomato fruits at the MG stage were cut in two halves. One of the halves was incubated in the dark (-) for 2h, whereas the other half was irradiated (+) with R light (30 µmol m^{-2} s^{-1} PAR) for the same time period. (b) Tomato fruits at the OR stage were cut in two halves and each of them was illuminated either with (-) white (W) light (25 µmol m^{-2} s^{-1} PAR, R/FR ratio of 3) or with (+) W light supplemented with FR (25 µmol m^{-2} s^{-1} PAR, R/FR ratio of 0.05) for 4h. Data correspond to mean ± SEM from n=3 (a) or n=4 (b) fruits.

While these data suggest a relevant role of PHYs in the regulation of tomato *PSY1*, the precise molecular mechanism acting during fruit ripening was unknown. PHYs are known to regulate the single Arabidopsis *PSY* gene by promoting the degradation of the PIF1 transcription factor, which functions as a direct *PSY* repressor (Toledo-Ortiz et al., 2010, 2014; Bou-Torrent et al., 2015). To check whether the same molecular components were involved in the regulation of the tomato fruit *PSY1* isoform, we first evaluated if tomato PIF1 homologues were present in the fruit. Survey of the tomato genome (Tomato Genome Consortium 2012) for PIF sequences found six genes (Table R1), including two with high similarity to Arabidopsis PIF1 (Figure R3).

Table R1. Tomato homologues Phytochrome Interacting factor (PIF)

*percentage of aminoacids which match exactly between both sequences

**Prediction with SUBA database

	Arabidopsis	Tomato			
Protein name	**Accession**	**Protein name**	**Identity (%)***	**Accesion**	**Loc Prediction****
PIF1	At2g20180	PIF1a	40	Solyc09g063010	nucleus
		PIF1b	40	Solyc06g008030	nucleus
PIF3	At1g09530	PIF3	35	Solyc01g102300	nucleus
PIF4	At2g43010	PIF4/5	36	Solyc07g043580	nucleus
PIF5	At3g59060		35		nucleus
PIF7	At5g61270	PIF7	30	Solyc06g069600	nucleus
PIF8	At4g00050	PIF8	49	Solyc01g090790	nucleus

The tomato gene encoding the protein most closely related to Arabidopsis PIF1 (Figure R3a) was named *PIF1a* (Solyc09g063010). Analysis of the Tomato Functional Genomics Database (http://ted.bti.cornell.edu/) and qPCR analysis of transcript levels (Figure R3b) showed that unlike the close homologue *PIF1b* (Solyc06g008030), *PIF1a* is expressed in the fruit and induced during ripening. As shown in Figure R3b, the level of transcripts encoding PIF1a remained virtually constant during the maturation process, i.e. when IG fruit grew to achieve its final size in the MG stage. Upon induction of ripening, however, *PIF1a* transcript levels increased ca. 2-fold in the O stage and ca. 5-fold in R fruit compared to MG samples (Figure R3b). We therefore selected PIF1a for further studies.

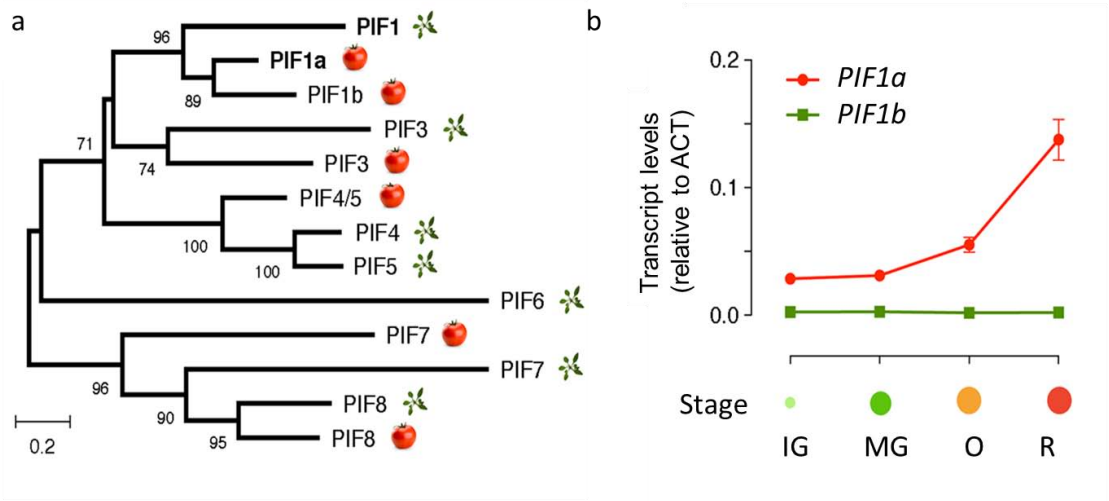

Figure R3. Identification of tomato PIF1 homologues. (a) Maximum-likelihood tree constructed using Arabidopsis and tomato PIF sequences. The percentage of trees in which the associated sequences clustered together with >70% reliability is shown next to the branches. The scale bar represents the mean number of substitutions per site. Images indicate the species. (b) Quantitative PCR analysis of transcript levels for the indicated tomato PIF1 homologs during fruit ripening. Values are means ± SEM of n ≥ 5 independent samples

To explore whether PIF1a could function as a true PIF transcription factor, we evaluated its light-dependent stability (Figure R4). Previous work in the lab had shown that a GFP-tagged PIF1a protein (PIF1a-GFP) localized in the nucleus of *Nicotiana benthamiana* leaf cells transiently expressing the protein as speckles or nuclear bodies (Botterweg 2015) (Figure R4a), as expected for a true PIF transcription factor (Al-Sady et al. 2006; Shen et al. 2008; Trupkin et al. 2015). Also as expected, the PIF1a-GFP protein was degraded when nuclei were irradiated with R light (i.e. upon activation of phytochromes), but not when irradiated with FR or when kept under dim light (Figure R4b).

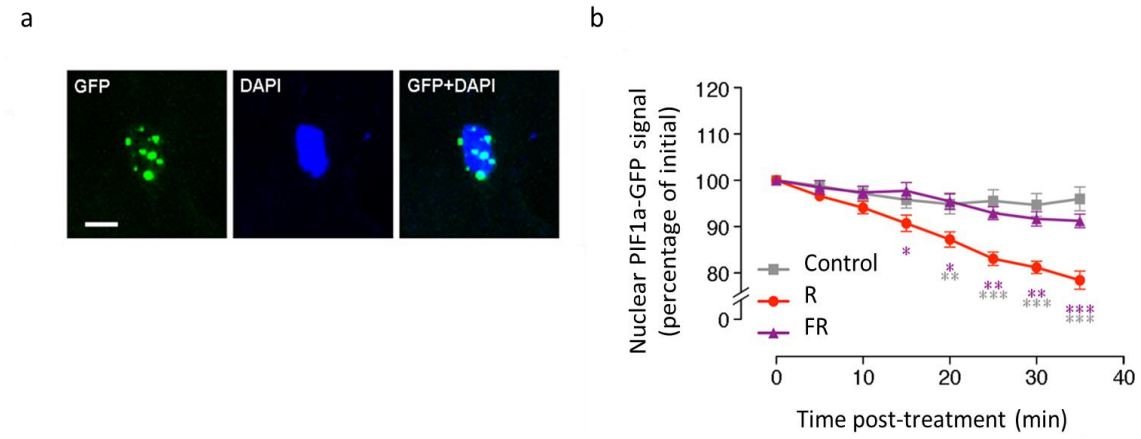

Figure R4. Tomato PIF1a is a photolabile nuclear protein. (a) Confocal microscopy images of GFP and DAPI fluorescence in the nucleus of a *N. benthamiana* leaf cell transiently expressing a GFP-tagged tomato PIF1a protein. Scale bar = 5 µm. (b) Quantification of PIF1a–GFP fluorescence in nuclei such as those shown in (a) for samples kept in the dim light of the microscope room (control) or illuminated with supplemental R or FR light for the indicated times (n ≥ 11). Values are means ± SEM, and significant differences (according to ANOVA followed by Newman–Keuls) compared with the symbols of corresponding color are indicated by asterisks (*P < 0.05, **P < 0.01, ***P < 0.001).

In Arabidopsis, PIFs participate in many physiological processes. For instance, the members of the so-called PIF quartet or PIFq (PIF1, PIF3, PIF4 and PIF5) are known to participate in the inhibition of hypocotyl elongation in the dark (Leivar and Quail 2011; Leivar et al., 2009; Shin et al. 2009). To evaluate whether the tomato PIF1a protein could function as the Arabidopsis PIF1 protein *in vivo*, we expressed the tomato *PIF1a* gene under the control of the constitutive *35S* promoter in an Arabidopsis *pifq* mutant (Figure R5). Then, we germinated the generated *PIF1a(pifq)* line together with the parental *pifq* line and the triple *pif3,4,5* mutant in the dark and measured the hypocotyl length of the seedlings grown after 4 days. As shown in the Figure R4, we found that the line expressing the tomato *PIF1a* gene showed longer hypocotyls that the *pifq* parental, reaching a length that was very similar to that of the triple mutant (i.e. to that of plants with a functional PIF1 protein). Thus, we concluded that the tomato PIF1a protein complements the loss of Arabidopsis PIF1 activity and hence that it functions as a true PIF1 protein *in vivo*.

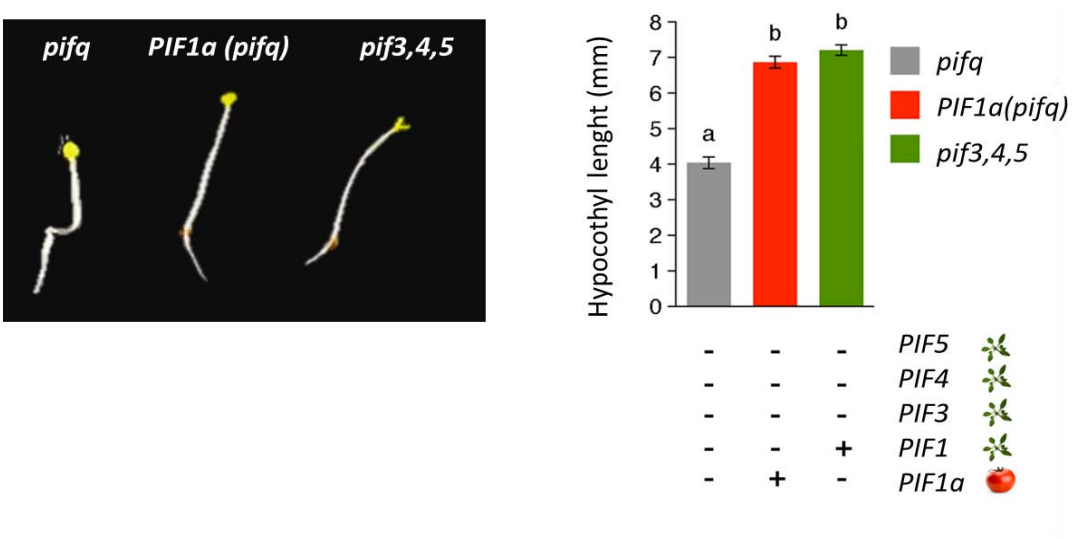

Figure R5. Tomato PIF1a is a true PIF1 homologue. The picture in the left shows representative seedlings of the indicated genotypes germinated and grown in the dark for 4 days. The graph in the right shows quantitative results. Values are means ± SEM (n=25), and significant differences (according to ANOVA followed by Newman–Keuls) are indicated by different letters ($P < 0.0001$)

PIF1a represses *PSY1* expression by binding to a PBE box in its promoter

We next explored the putative role of PIF1a in the control of tomato *PSY1* expression and fruit carotenoid biosynthesis during ripening. Transient overexpression of the PIF1a-GFP protein in tomato pericarp tissue by agroinjection of MG fruit resulted in the eventual development of carotenoid-devoid sections where the recombinant protein accumulated (Figure R6). This phenotype is consistent with a loss of PSY1 activity in these sections, which phenocopied the PSY1-defective *yellow flesh (r)* mutant (Fray and Grierson 1993).

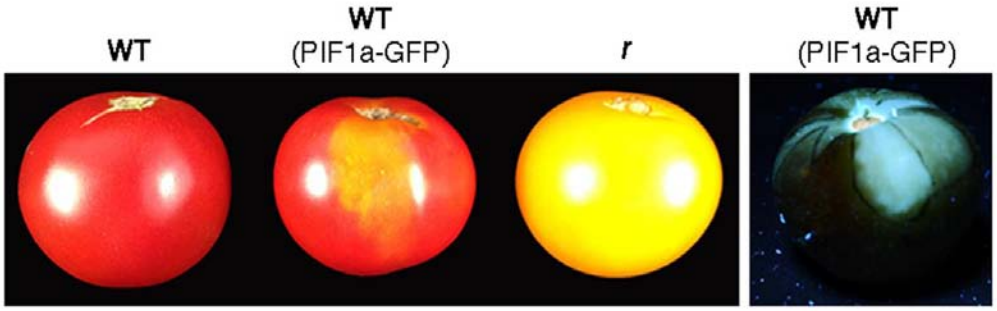

Figure R6. Transient overproduction of PIF1a-GFP in tomato fruits. Wild-type (WT) fruits at the MG stage were agroinjected with a construct to constitutively overexpress the PIF1a–GFP protein, and left attached to the plant until they reached the R stage. The fruit sections where the PIF1a–GFP protein was present (as deduced from GFP fluorescence detected by illumination with UV light, right panel) showed a reduced accumulation of carotenoids, resulting in a yellow color similar to that observed in ripe fruits of the PSY1-defective mutant *yellow ripe* (*r*).

To test whether PIF1a functions as a repressor of carotenoid biosynthesis in tomato fruit by downregulating *PSY1* gene expression (similar to that reported for PIF1 and *PSY* in Arabidopsis), we next reduced *PIF1a* transcript levels and analyzed the concomitant changes in *PSY1* expression. Using a similar approach to that described in next chapter for the *ClpR1* gene, we designed and generated an amiRNA construct specifically targeting the *PIF1a* gene and cloned it under the control of the *35S* promoter (Figure R7a). MicroTom (MT) plants harboring the generated *35S:amiPIF1a* construct were next generated and different lines were used to evaluate the impact of reducing PIF1a activity of *PSY1* expression and carotenoid content in the fruit (Figure R7b and R8). Transgenic T2 fruits at the R stage presented increased levels of *PSY1* transcripts that inversely correlated with the extent of *PIF1a* silencing in different lines (Pearson correlation coefficient: *r=-0. 9725*; *P=0.0055*) (Figure R7b).

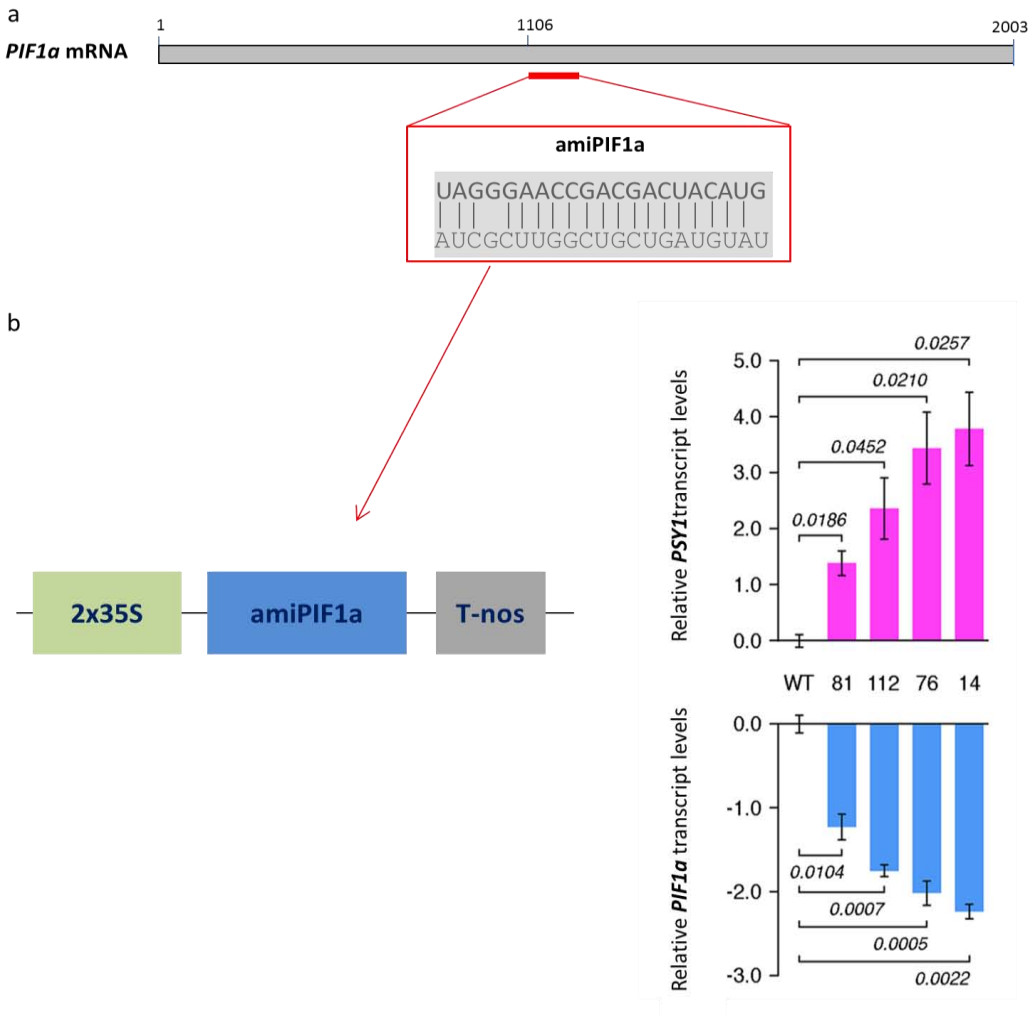

Figure R7. *PIF1a* silencing triggers *PSY1* up-regulation (a) The region in the tomato *PIF1a* mRNA targeted by an active amiRNAs (amiPIF1a). (b) amiPIF1a was cloned under the control of the 2x35S promoter. Constitutive silencing of PIF1a in fruits from various transgenic tomato lines expressing a specific artificial microRNA (amiPIF1a) leads to a concomitant induction in *PSY1* transcript levels compared to untransformed (WT) controls. Data is represented as relative log2. Values are means ± SEM (n ≥ 3). Italic numbers above the bars indicate P values (Student's t test). Values are reported relative to WT.

In agreement with the conclusion that higher *PSY1* transcript levels in amiPIF1a fruits resulted in increased PSY activity, metabolite profiling of transgenic O and R fruit showed higher amounts of phytoene, the direct product of PSY activity, than untransformed controls (Figure R8). Also consistent with the rate-limiting role demonstrated for PSY activity by metabolic flux control analysis (Fraser *et al.* 2002), levels of total carotenoids in transgenic fruits were significantly higher than those in untransformed controls (Figure R8).

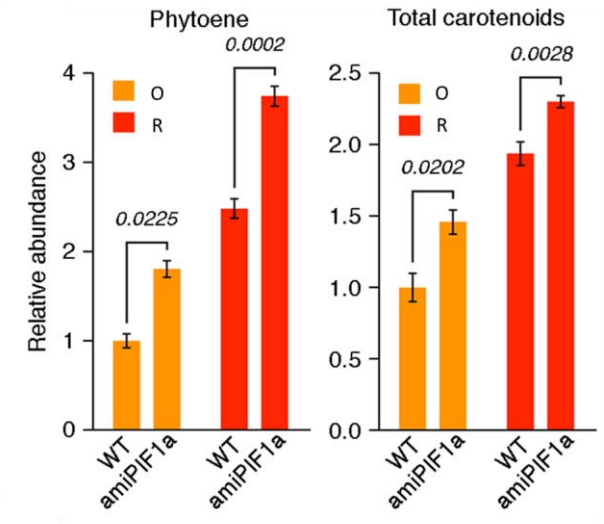

Figure R8. Reduced PIF1a levels result in higher carotenoid accumulation in tomato fruits. HPLC analysis of carotenoid levels in transgenic 35S:amiPIF1a fruits (line 112) shows an increased accumulation of phytoene (the direct product of PSY activity) and total carotenoids relative to untransformed (WT) controls at both O and R stages. Values are means ± SEM (n ≥ 3). Italic numbers above the bars indicate P values (Student's t test).

To this point, the data suggested that PIF1a negatively regulates the expression of the *PSY1* gene, similar to the observed for Arabidopsis PIF1 and *PSY*. To evaluate whether the proposed regulation occurred in a direct or in an indirect manner, we decided to evaluate if PIF1a was able to bind to the promoter of *PSY1* by Chromatin immunoprecipitation assays (ChIP) followed by qPCR (Figure R9). Examination of the genomic sequence 2000 nt upstream of the translation start codon (ATG) of *PSY1* revealed the existence of two conserved PIF-binding motifs (Toledo-Ortiz et al. 2003; Zhang et al. 2013), a G-box (CACGTG) and a PBE-box (CACATG) (Figure R9). We therefore selected these regions as possible motifs for PIF1a binding. Next, we transiently expressed the PIF1a-GFP protein in tomato fruit as shown above (Figure R6) and used pericarp sections showing GFP fluorescence for ChIP-qPCR assays. Chromatin associated with PIF1a-GFP was immunoprecipitated using antibodies against GFP. Then DNA was isolated and used for qPCR experiments with primers amplifying putatite PIF1a binding domains. The results indicated that PIF1a specifically binds to the PBE-box of the *PSY1* promoter *in vivo* (Figure R9).

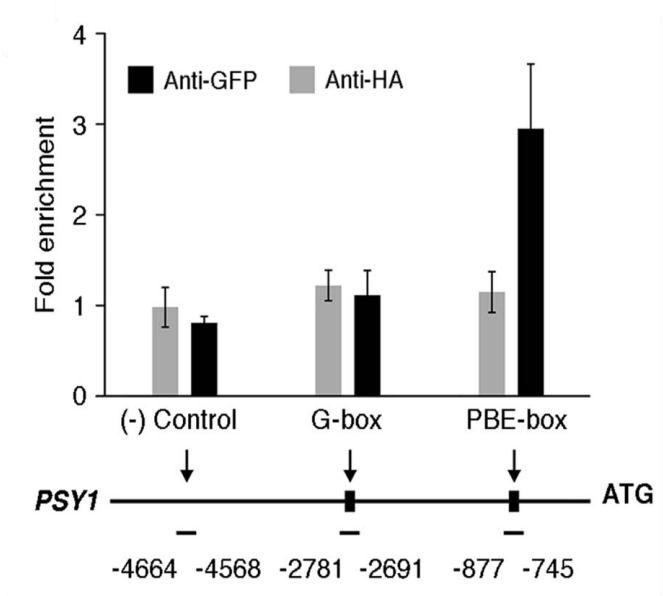

Figure R9. PIF1a binds directly to the promoter of *PSY1*. ChIP-qPCR analysis was performed using tomato fruit sections transiently expressing the PIF1a–GFP protein using anti-GFP antibodies. Control reactions were processed in parallel using anti-HA serum. The location of *PSY1* promoter amplicons used in qPCR quantification of ChIP-enriched DNA regions corresponding to control (-) and PIF-binding domains (G box and PBE box) are indicated in the map. Values are means ± SEM from two independent experiments. Values are reported relative to blank samples.

Based on these data, we conclude that PIF1a binds the promoter of *PSY1* to repress its expression and hence reduce PSY activity to eventually inhibit carotenoid biosynthesis.

Tomato fruit chlorophyll reduces the R/FR ratio of sunlight as it penetrates the fruit flesh

The ripening-dependent accumulation of *PIF1a* transcripts (Figure R3b) might function as a mechanism to repress *PSY1* expression and hence antagonistically balance the effect of other ripening-induced transcription factors such as RIN and FUL1, which are direct activators of *PSY1* expression during ripening (Fujisawa *et al.* 2013, Fujisawa *et al.* 2015, Martel *et al.* 2011, Shima *et al.* 2013). However, we decided to explore new regulatory roles for PIF1a based on its PHY-mediated degradation response. Most precisely, we focused in determining how changes in the R/FR ratio associated with the loss of chlorophyll might influence PIF1a stability during tomato fruit ripening (Figure R4). It has been shown that the amount of R that passes through the pericarp of tomato fruit exposed to sunlight is much lower in IG/MG stages compared to O/R stages, whereas the amount of FR changes very little (Alba *et al.* 2000). However, the dynamics of light quality changes within the tissues of tomato fruits and their potential biological relevance remain unknown. To address the first point, the quantity

(transmittance) and the quality (R/FR) of artificial W light when reaching increasing depths in the tomato pericarp were determined in collaboration with Dr. Jordi Andilla and Prof. Pablo Loza-Alvarez at the ICFO (Figure R10). Whereas the transmittance showed a similar decrease in MG and O fruit as W penetrated their flesh, the R/FR ratio only declined in MG fruits. Then, it was tentatively concluded that the preferential absorbance of R (but not FR) by the chlorophyll present in the chloroplasts of the pericarp cells could be responsible for the observed decrease in the R/FR ratio within the cells of MG fruit, whereas this ratio was virtually unaffected by the presence of increasing amounts of carotenoids in O fruits.

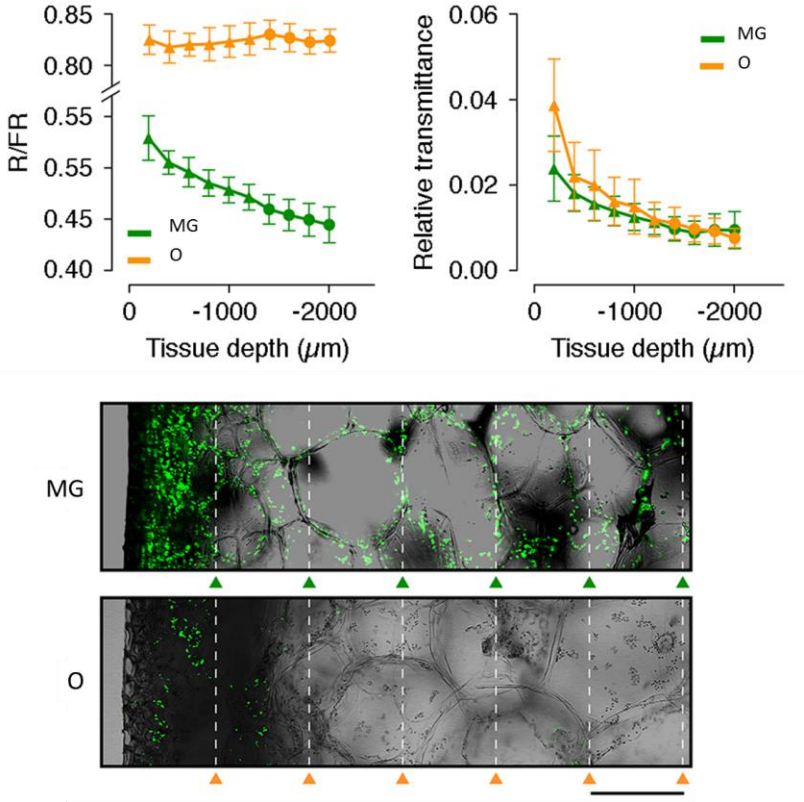

Figure R10. The R/FR ratio inside the fruit pericarp changes during ripening. Serial sections of the outer pericarp of MG and OR fruit were obtained using a vibratome. Starting with 2000 µm thick samples, 200 µm layers were sequentially removed from the internal side of the pericarp to obtain samples of decreasing thickness until only a thin section of the fruit surface was left. After removing each 200 µm layer, the remaining section was illuminated with artificial W light, and both the R/FR ratio and the intensity (transmittance) of the light that passed through it were determined. Bright-field images of MG and OR fruit pericarp tissue merged with chlorophyll autofluorescence (corresponding to chloroplasts, in green) are also shown. Dashed lines indicate the depths at which the last six light measurements were performed (represented by the triangles in the graphs). Values are means ± SEM (n = 3) relative to blank controls.

To next confirm whether the pigment composition of the fruit was responsible for the observed changes, an experimental system to mimic the natural filter formed by

these pigments was set up. Total chlorophyll and carotenoid pigments were extracted from MG, O and R fruit and used to characterize their composition and absorbance spectra. Pigment extracts from MG fruits showed an absorbance profile nearly identical to that observed in leaves, with a characteristic peak at 660 nm due to the presence of chlorophylls. By contrast, extracts from O and R fruits are almost completely devoid of this peak. As a consequence, sunlight or artificial W light passing through extracts made from O or R fruit maintained a high R/FR ratio whereas the light crossing those made from MG fruit showed low R/FR (Figure R11).

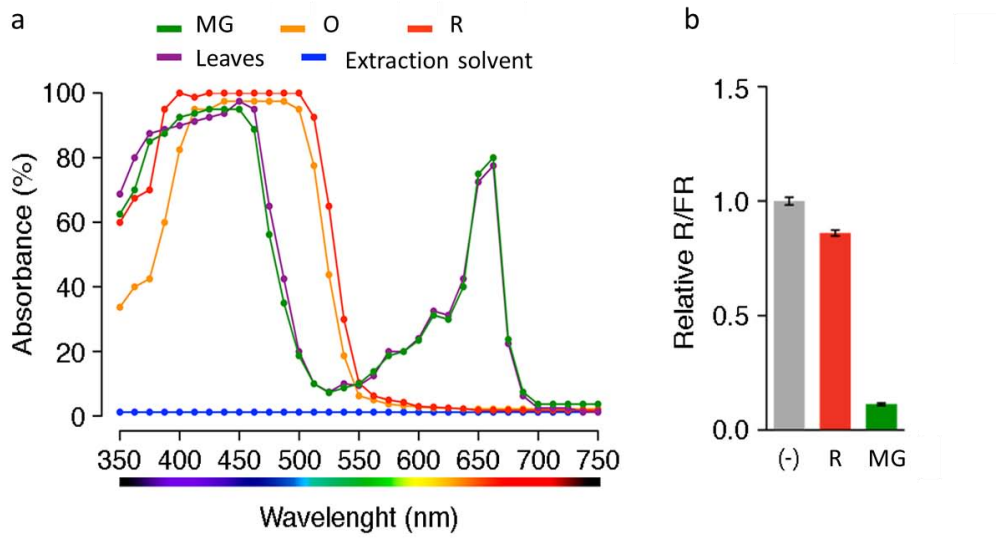

Figure R11. Light filtered through tomato fruit photosynthetic pigments changes its R/FR ratio. (a) Absorption spectra of organic extracts of photosynthetic pigments (chlorophylls and carotenoids) isolated from tomato leaves and fruits at various developmental stages.(b) R/FR ratio of artificial W light filtered through pigment extracts prepared from R or MG fruits relative to that of unfiltered light (-). Values are means ± SEM (n ≥ 6).

Fruit pigmentation-dependent changes in the R/FR ratio specifically influence *PSY1* expression

Once established that the pigment composition of the MG fruit resulted in a reduction in the R/FR ratio of the light reaching the inner layers of pericarp cells, whereas the pigment composition of O or R fruit (rich in carotenoids but virtually lacking chlorophylls) had little or no effect, we went on to confirm that this could have a biological relevance. A filter system based on placing a glass plate containing MG and RR fruit pigment extracts between the source of light (W) and the experimental samples was designed (Figure R12).

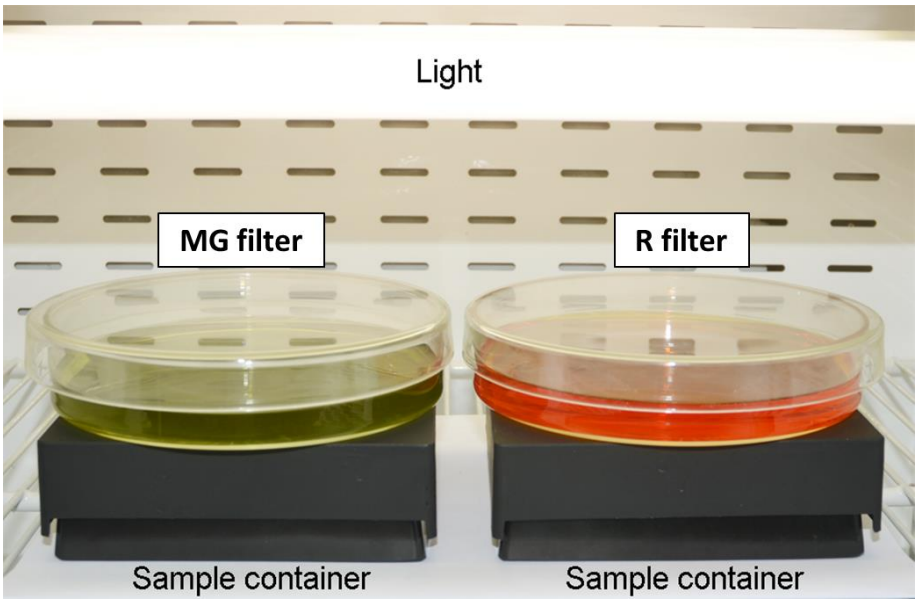

Figure R12. Setup for experiments with tomato fruit pigment extracts. Glass plates containing extracts of photosynthetic pigments (chlorophylls and carotenoids) isolated from tomato fruit pericarp tissue were placed on top of light-proof boxes with an opening in the lid so that all the light coming into the box passed through the corresponding pigment filter. Light sensors and biological samples were placed inside the corresponding box. When comparing different fruit extracts, the same control climate chamber and source of artificial white light (fluorescence tubes providing 90 µmol m^{-2} s^{-1} PAR) was used and the pigment concentration in the extracts was adjust so that the filtered light showed similar PAR values (40-50 µmol m^{-2} s^{-1} PAR).

To test whether the change in the R/FR ratio obtained after filtering of light through MG or R filters could impact gene expression, Arabidopsis, which is a well-established model to study molecular responses to shade (i.e. low R/FR) was used. Thus, Arabidopsis W-grown seedlings were exposed to W light filtered through MG or R filters and then we analyzed the expression of known shade-regulated genes: *PIL1*, *YUCCA8*, *XTR7* and *IAA29* (Leivar and Monte, 2014). As shown in Figure R13, transcripts from these shade-induced genes were accumulated at higher levels in samples exposed to W+MG when compared with W+RR. Altogether, these results demonstrate that the fruit pigments effectively alter the quality of the light that penetrates the tomato pericarp, generating signals that are able to eventually modulate the expression of shade-responsive genes.

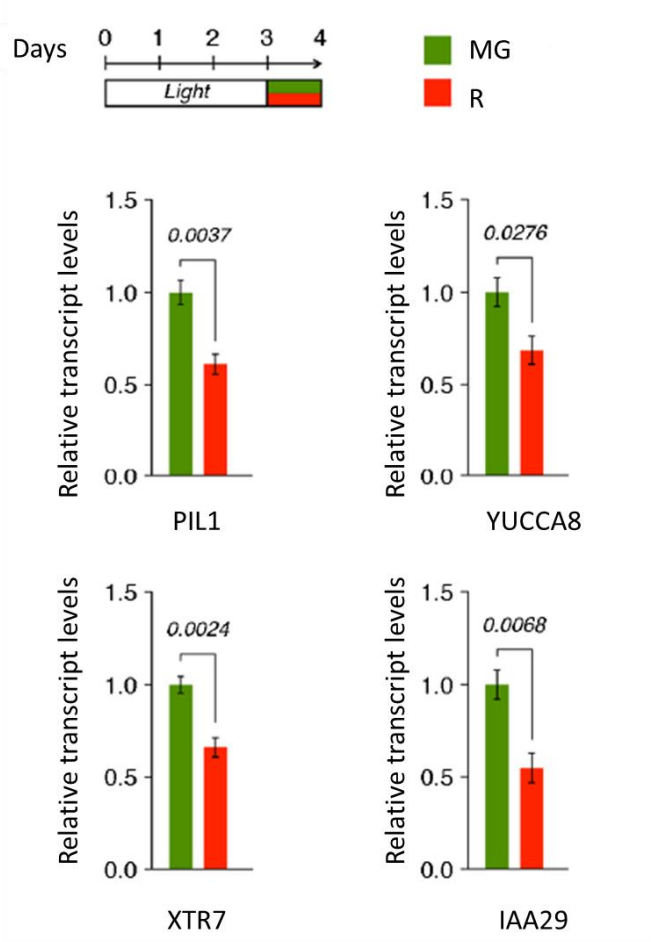

Figure R13. Effect of light filtered through tomato fruit pigment extracts on Arabidopsis shade-responsive gene expression. Arabidopsis wild-type seedlings germinated and grown under W light for 3 days were exposed for 24 h to W light filtered through MG or R filters. Transcript abundance of the indicated genes was assessed by quantitative PCR. The values and bars represent the mean ± SEM from n=4 biological replicates. Numbers above the bars show statistical P values according to the t-test. Values are reported relative to the MG filter condition.

To validate whether fruit pigment composition could also have an impact on the regulation of tomato carotenoid biosynthetic genes, we used pigment-devoid (white) tomato fruits obtained by preventing exposure to light from the very early stages of fruit set and development (Cheung et al., 1993). To do so, individual white fruits were longitudinally cut into two halves in the dark, and each of the halves was then treated with the corresponding light (W+MG or W+R) for 2h (Figure R14). Expression analysis of genes encoding enzymes of the carotenoid biosynthesis pathway, including *DXS1*, *PSY1*, *PSY2*, *PSY3*, *PDS*, *LCY-E*, *LCY-B* and *CYC-B* (Figures I4 and I5), revealed that only *PSY1* exhibited significant changes, showing levels approximately 2-fold higher in the halves placed under the R filter compared to those illuminated with W+MG (Figure R14). Higher levels of *PSY1* transcripts in samples exposed to light with higher R/FR ratio were expected as a consequence of the instability of the PIF1a repressor under such conditions (Figure R14).

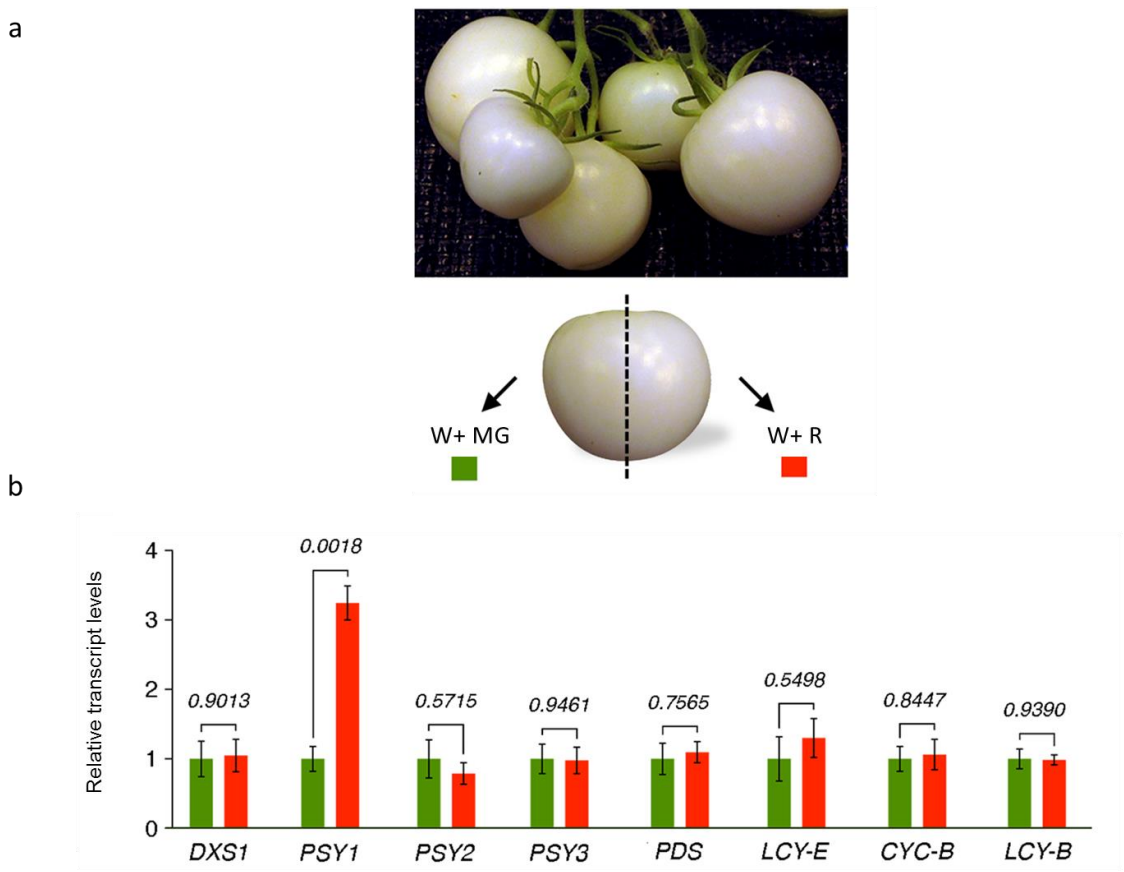

Figure R14. Light filtered through tomato fruit photosynthetic pigments specifically affects the expression of *PSY1*. (a) Tomato fruits lacking any kind of endogenous pigments were obtained approximately 40 days after covering whole inflorescences with light-proof bags. The resulting white fruits were collected in the bags and then cut in two halves in the dark. Each of the halves was immediately exposed for 2 h to W light filtered through MG or R filters. (b) Quantitative PCR analysis of samples treated as described in Figure R12 to estimate the abundance of transcripts for tomato genes encoding carotenoid biosynthetic enzymes. Values are means ± SEM from n=3 biological replicates relative to the W+MG condition. The numbers above the bars indicate P values (Student's t test).

Changes in the R/FR ratio of the light sensed in pericarp cells likely adjust carotenoid biosynthesis to the actual progress of ripening

We next tested whether the differential light-filtering properties of fruit pigments could also impact carotenoid metabolism during fruit ripening. Because this experiment required irradiating fruits in a pre-ripening stage and visually identifying the developmental stage was not possible in the case of white fruit, we used MG fruits. Individual fruits were split in two halves immediately before exposing each half to either W+MG or W+R. Exposure was maintained for a few days until both halves had

entered into the breaker stage (i.e. started losing chlorophylls and accumulating carotenoids). Reaching this stage typically took longer for fruit halves illuminated with W+MG (Figure R15a). Similar to that observed with white fruits, halves illuminated with W+R also showed a significantly increased accumulation of *PSY1* transcripts, while no changes were observed in other carotenoid-related genes (Figure R15b).

PSY1 gene is regulated both directly and indirectly by several ripening-associated transcription factors like RIN and FUL1 (Fujisawa *et al.* 2013, Fujisawa *et al.* 2015, Martel *et al.* 2011, Shima *et al.* 2013). To confirm whether the effect triggered by the changes in the R/FR ratio were due to a direct regulation on *PSY1*, and not a general effect in the ripening process, we analyzed the expression of several well-characterized ripening-related genes in the same samples. We selected genes that encode for proteins involved in different ripening-associated molecular processes, such as the master ripening-regulators RIN, TAGL1, AP2a and FUL1, and others involved in ethylene metabolism like ACS2, E8 and NR. Notably, no statistical differences were found between halves exposed to W+MG or W+R filters (Figure R15c), suggesting that the light treatments did not have a significant influence on ripening but specifically affected fruit carotenoid biosynthesis by modulating *PSY1* expression.

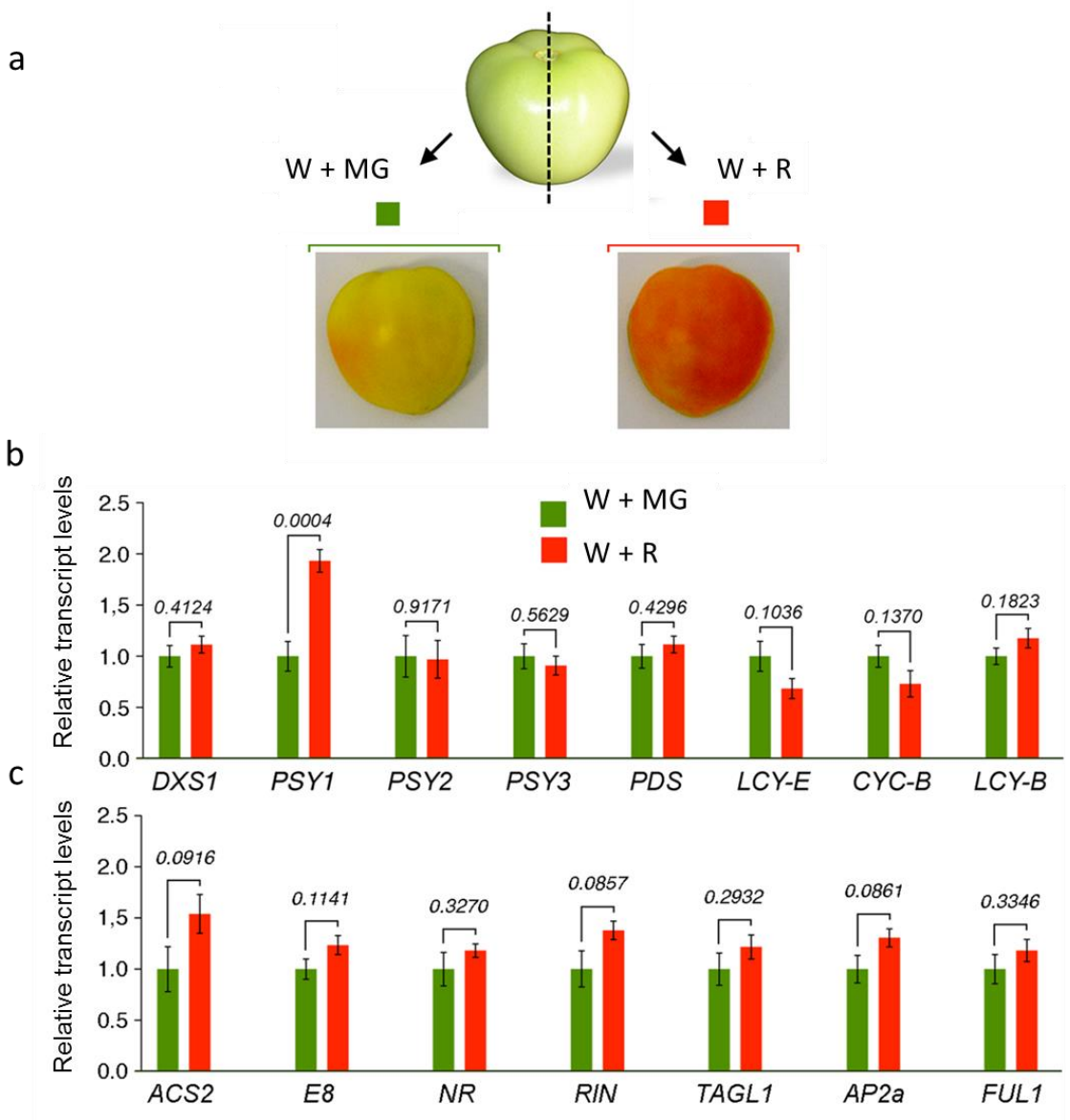

Figure R15. The light-absorbing properties of fruit photosynthetic pigments influence carotenoid biosynthesis but not ripening. (a) Fruits at the MG stage were cut in two and exposed to W light filtered through MG or R filters until pigmentation changes were visually observed in both halves. (b-c) Quantitative PCR analysis of transcript abundance of the indicated tomato genes in fruit halves treated as described in (a). (b) Genes for carotenoid biosynthetic enzymes. (c) Ripening-related genes. Values are means ± SEM from n=6 biological replicates relative to the W+MG condition. The numbers above the bars indicate P values (Student's t test).

In agreement with the conclusion that the R/FR ratio of the light reaching the pericarp cells affects carotenoid biosynthesis by specifically modulating *PSY1* gene expression, breaker fruits showed higher levels of *PSY1* transcripts and derived carotenoids such as phytoene (the immediate PSY product) and lycopene in the outer

side of the pericarp tissue (Figure R16), which shows a R/FR ratio higher than internal sections (Figure R10). Furthermore, PIF1a appears to be the main factor regulating *PSY1* expression in response to this signal, since the difference in *PSY1* transcript levels observed in fruit halves exposed to W+MG or W+R is strongly attenuated in transgenic 35S:amiPIF1a fruits (Figure R16b).

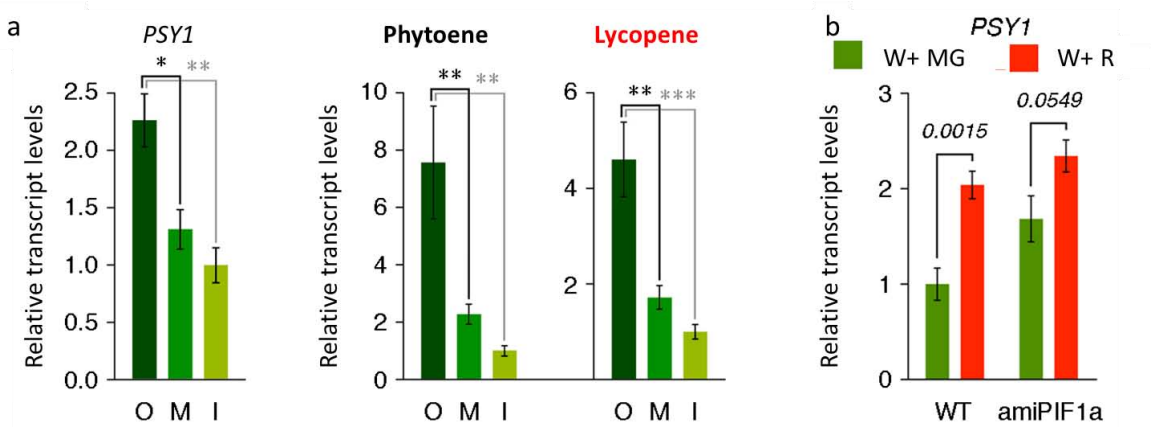

Figure R16. PIF1a regulates PSY1 expression in response to changes in R/FR ratio. (a) PSY1 expression and carotenoid levels in various regions of the pericarp. The graphs represent quantitative PCR analysis of PSY1 transcript levels and HPLC analysis of phytoene and lycopene accumulation in the outer section, i.e. that most exposed to sunlight (O), the middle section (M) and the inner section (I) (approximately 1 mm) of the pericarp of fruits at the breaker stage (n ≥ 5). Values are means ± SEM relative to inner pericarp samples. Significant differences (ac- cording to ANOVA followed by Newman–Keuls) are indicated by asterisks (*P < 0.05, **P < 0.01, ***P < 0.001). (b) Quantitative PCR analysis of PSY1 transcript abundance in untransformed (WT) and transgenic amiPIF1a fruit halves treated as described in Figure 12. Values are means ± SEM from n = 5 biological replicates relative to the W+MG condition. The numbers above the bars indicate P values (Student's t test).

Chapter II

A role for the Clp protease complex during tomato fruit ripening

Background and rationale: the Clp protease complex in plants

The ATP-dependent Clp complex is the most abundant serine-protease in plant chloroplasts. The Clp protease complex is formed by different subunits that are organized in two well-characterized multiprotein domains: the **chaperone** domain and the **protease core (**Figure R17).

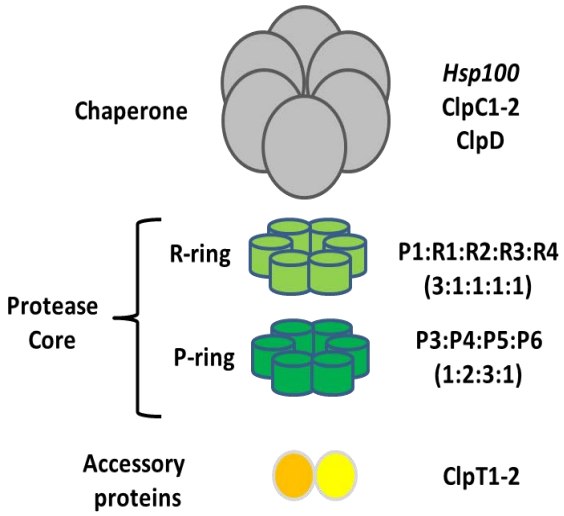

Figure R17. The stromal Clp protease complex. The complex consists of (I) a chaperone domain formed by three Hsp100 chaperones (C1, C2, and D), and (II) a proteolytic core formed by five catalytic ClpP subunits (P1 and P3-6) and four non-catalytic ClpR subunits (R1-4). ClpP and ClpR subunits are arranged in two blocks (R-Ring and P-Ring) with a specific stoichiometry. The R-ring is made up of plastome-encoded ClpP1 and nuclear genome-encoded ClpR1-4 subunits, while the P-ring only contains nuclear genome-encoded ClpP3-6 subunits. Two additional members (T1 and T2) are essential to properly assemble the complex.

The **chaperone domain** is made up of chaperones of the Hsp100 family (ClpC1, ClpC2 and ClpD) involved in recognizing, unfolding, and delivering substrates into the protease core to be degraded (Tryggvesson et al., 2012). The **protease core** consists of two types of very similar blocks called ClpP (Proteolytic) and ClpR (Regulatory) subunits. While ClpP subunits are known to have a catalytic triad Ser:His:Asp in their sequence, inactive R subunits lack these conserved amino acids (Porankiewlcz et al., 1999). ClpP1 is the only plastome-encoded subunit of the complex. At the protease core, ClpP and ClpR subunits are arranged in two heptameric rings (Figure R17) (Olinares et al., 2011a; Sjögren et al., 2006). As the ClpPR protease core is a complex machinery, plants have evolved components that ensure its correct assembly, namely the ClpT chaperones (ClpT1 and ClpT2) (Sjögren and Clarke, 2011). The actual model suggests that, first ClpT1 and then ClpT2 attach to the P-ring generating a stable complex. Subsequently, this transient complex associates with the R-ring to form the tetradecameric protease core (Kim et al., 2015).

Reverse genetics in combination with systems biology approaches have been

used to assess the role and substrates of the Clp protease in plants (Sjögren et al., 2006; Kim et al., 2009; Zybailov et al., 2009; Stanne et al., 2009; Olinares et al., 2011b; Kim et al., 2013; Rudella et al., 2006; Koussevitzky et al., 2007). Plant mutants defective in ClpP1, ClpP4 or ClpP5 (each with more than 1 copy per ring) are not viable, whereas loss-of-function mutants for ClpR2, ClpR4 and ClpP3 subunits (each 1 copy per ring) develop white embryos and smaller seeds than WT plants but they can grow and develop true leaves in sucrose-supplemented media (Rudella et al., 2006; Kim et al., 2009, 2013). In contrast, ClpP3 null mutants and ClpP6-defective transgenic lines have a pale phenotype but they can develop and produce viable seeds (Kim et al., 2013; Sjögren et al., 2006). ClpR1 knock out mutants display a very mild virescent phenotype with normal fertility (Koussevitzky et al., 2007; Flores-Perez et al., 2008), possibly due to a partial redundancy with ClpR3. These results suggest that most of the plastidial Clp protease subunits make non-redundant, specific structural and/or functional contributions. They also show that deficiency in at least one subunit of the protease core leads to a reduction in total Clp proteolytic activity.

Quantitative proteomic approaches have shown that reduced Clp activity in Arabidopsis mutants triggers a set of similar changes in the plastidial proteome and subsequent alterations in chloroplast functions (summarized in Figure R18 (Nishimura and van Wijk, 2015)). These include the following:

A) reduced photosynthetic capacity due to photosystems disassembly. This is in accordance with Transmission Electron Microscopy (TEM) analyses that show small chloroplasts with disorganized thylakoid ultrastructure (Flores-Perez et al., 2008). Moreover, plastoglobule-associated proteins are highly up-regulated. The general energetic loss explains the up-regulation of ATP/ADP envelope transporters (NTTs) that import ATP from the cytosol to the plastid.

B) altered levels of components of the plastidial PQC such as chaperones (stromal chaperone systems and ClpB3 unfoldase) and proteases (EGY2, SPPA, PREP1, LAP2, SPP), as well as proteins involved in plastid protein import (Sec machinery).

C) a strong up-regulation of plastidial protein translation factors and tRNA synthases, but not plastid ribosomes.

D) overaccumulation of enzymes involved in plastidial metabolic pathways (biosynthesis of thiamin, amino acids, carbohydrates, fatty acids and isoprenoid

precursors). Specifically, enzymatically active forms of MEP pathway enzymes such as DXS and DXR accumulate at higher levels in Clp-defective mutants such as *clpr1* and *clpc1* (Flores-Perez et al., 2008; Pulido et al., 2016).

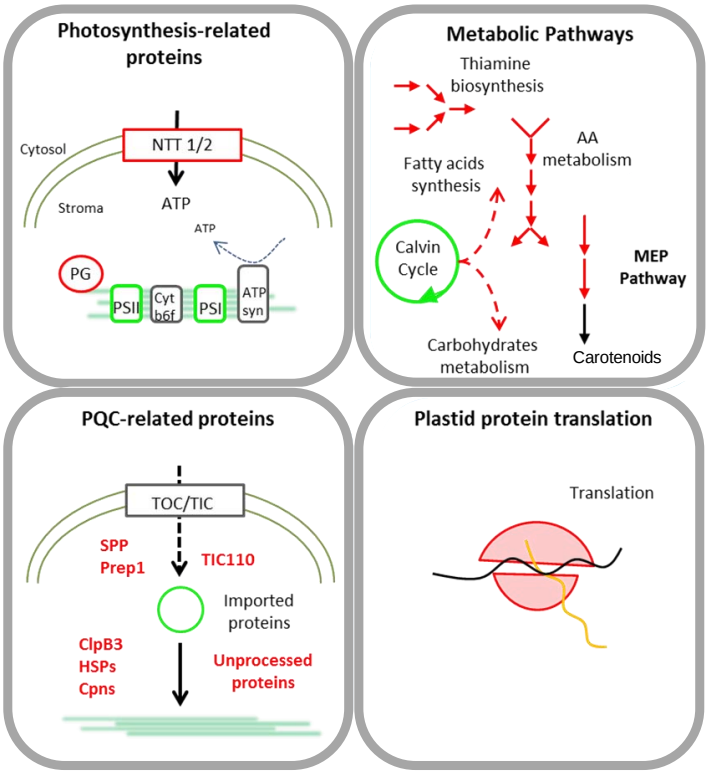

Figure R18. Potential Clp targets in Arabidopsis deduced from the analysis of the proteome of Clp-defective mutants. Processes that are less active in Clp protease defective mutants are colored in green, while those that are more active are colored in red.

While some of the proteins that over-accumulate when the Clp protease activity is decreased are expected to be potential Clp direct targets, further evidence is necessary to ascertain whether their accumulation is indirect (i.e. due to secondary effects). So far, two different approaches are being used to identify real substrates of the Clp protease: (1) interaction with the protein adaptors that help deliver the substrates to the complex, and (2) analysis of protein stability in Clp protease-defective mutant backgrounds (Tapken et al., 2015; Flores-Perez et al., 2008; Pulido et al., 2016).

The Arabidopsis ClpS1 protein is a well-characterized adaptor protein that targets to proteolysis proteins involved in aromatic amino acid metabolism such as 3-deoxy-D-arabino-heptulosonate 7-phosphate (DAHP) synthase and chorismate synthase (CS), and tetrapyrrole biosynthesis such as glutamyl-tRNA reductase (GluTR) (Czarnecki and Grimm, 2012). A recent publication proposed a new adaptor protein

named ClpF, which form a binary module together with ClpS1 (Nishimura et al., 2015). Alternative to the ClpS1/ClpF pathway, it has been proposed that ClpC1 could also function as an adaptor. Proteins delivered to degradation by the ClpC1 pathway include the thylakoid-located copper transporter PAA2/HMA8 (P-type ATPase of Arabidopsis2/Heavy-metal-associated8), which mediates copper delivery to plastocyanin for photosynthetic electron transport (Abdel-Ghany et al., 2005; Tapken et al., 2012) and DXS (Pulido et al., 2013, 2016).

Besides Arabidopsis, the role of the Clp protease has been analyzed in two monocot crops (rice and maize). Clp-defective rice and maize mutants display a yellow leaf phenotype similar to that reported in Arabidopsis, likely due to altered size and ultrastructure of chloroplasts (Dong et al., 2013; Xing et al., 2014). The Clp proteolytic complex is found in all plastid types, including tomato chromoplasts (Barsan et al. 2012; Peltier et al. 2004), but no information is available on whether altering Clp proteolytic activity in tomato fruit could impact the accumulation of carotenoid biosynthetic enzymes or/and the differentiation of chromoplasts. Here, I evaluated this possibility.

Genes encoding Clp protease subunits are induced during tomato fruit ripening

We reasoned that reducing the levels of the Clp protease in tomato fruit chromoplasts we could increase the levels of MEP pathway enzymes and hence induce the production of carotenoids without interfering with fundamental processes that take place in chloroplasts, such as photosynthesis. To test this hypothesis, we decided to silence genes encoding plastidial Clp protease subunits in tomato. We first searched for tomato homologues of Arabidopsis subunits of the Clp complex using BLAST (Basic Local Alignment Search Tool) and two different coding sequence (CDS) databases: *Solanaceae* Genomics Network (http://solgenomics.net) and the National Center for Biotechnology Information (NCBI). As the tomato genome suffered a wide gene triplication event (Tomato Genome Consortium, 2012), we expected to find a larger *ClpPR* gene family in tomato compare with Arabidopsis. Surprisingly, only *ClpP1* was found to have two different homologues in tomato (Figure R19). An identical sequence was retrieved from the tomato plastid genome and the nuclear genome (Solyc01g007490). As the latter is actually flanked by other sequences belonging to the plastome, we speculate that this might be an assembly artifact. We therefore conclude

that the two sequences likely correspond to the same plastome gene, encoding the isoform we named ClpP1a. A second ClpP1 homologue, referred to as ClpP1b, was found in chromosome 9 (Solyc09g065790) but algorithms such as TargetP and ChloroP failed to detect a plastid-targeting signal in the corresponding protein (Table R2), suggesting that it might not be part of the stromal Clp protease complex. In agreement with this conclusion, ClpP1b lacks two of the three conserved residues of the catalytic triad present in the Arabidopsis subunits and in tomato ClpP1a and ClpP3-6 (Figure R20). It is therefore possible that ClpP1b lacks proteolytic activity.

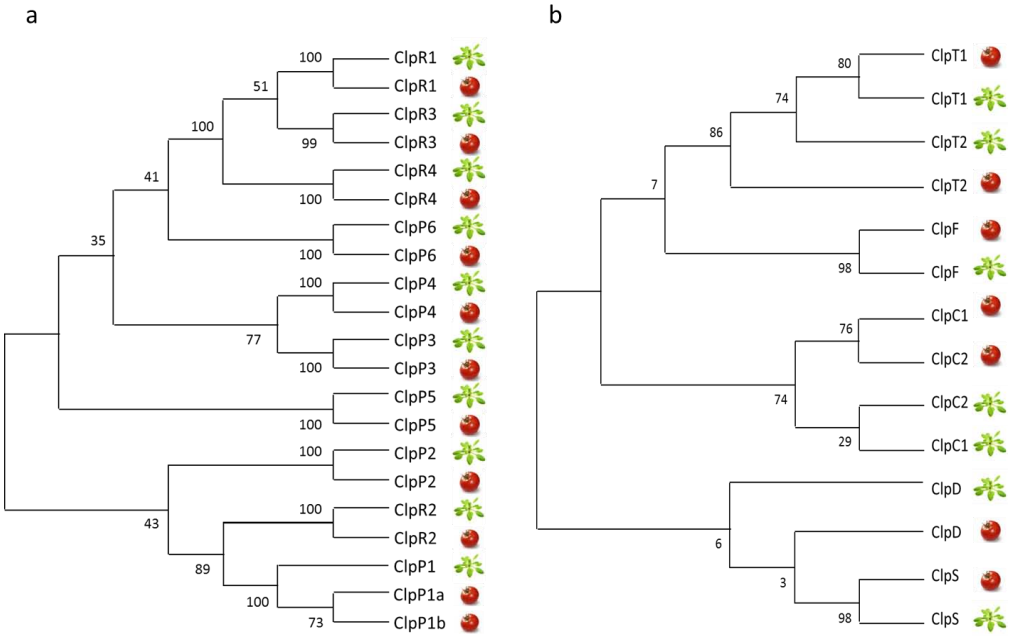

Figure R19. Tomato has a similar *ClpPR* gene dosage to Arabidopsis with the exception of *ClpP1*. (a) Maximum Likelihood tree constructed with Arabidopsis and putative tomato ClpP and ClpR protein sequences. ClpP1 has two homologues in tomato, annotated as Clp1a and Clp1b. (b) Maximum Likelihood tree constructed with Arabidopsis and putative tomato ClpC, ClpD, ClpT, ClpS and ClpF protein sequences.

Table R2. Tomato homologues Clp protease subunits
*percentage of aminoacids which match exactly between both sequences
**Prediction with TargetP
***Prediction is not possible.

	Arabidopsis	Tomato			
Protein Name	**Accession**	**Protein name**	**Identity (%)***	**Accession**	**Loc Predict****
ClpP1	AtCg00670	ClpP1a	75	Solyc01g007490	-***
ClpP1		ClpP1b	71	Solyc09g065790	-
ClpP2	At5g23140	ClpP2	85	Solyc04g009310	Mithocondria
ClpP3	At1g66670	ClpP3	75	Solyc02g091280	Chloroplast
ClpP4	At5g45390	ClpP4	64	Solyc08g075750	Chloroplast
ClpP5	At1g02560	ClpP5	78	Solyc01g100520	Chloroplast
ClpP6	At1g11750	ClpP6	70	Solyc10g051310	Chloroplast
ClpR1	At1g49970	ClpR1	66	Solyc10g049710	Chloroplast
ClpR2	At1g12410	ClpR2	68	Solyc08g079620	Chloroplast
ClpR3	At1g09130	ClpR3	77	Solyc01g099690	Chloroplast
ClpR4	At4g17040	ClpR4	76	Solyc08g077890	Chloroplast
ClpC1	At5g50920	ClpC1	90	Solyc12g042060	Chloroplast
ClpC2	At3g48870	ClpC2	86	Solyc03g118340	Chloroplast
ClpD	At5g51070	ClpD	67	Solyc03g117950	Chloroplast
ClpT1	At4g25370	ClpT1	56	Solyc03g007110	Chloroplast
ClpT2	At4g12060	ClpT2	47	Solyc08g079660	Chloroplast
ClpS	At1g68660	ClpS	74	Solyc03g119700	-
ClpF	At2g03390	ClpF	64	Solyc05g012620	Mithocondria

We next analyzed the expression of the nuclear-localized genes encoding the protease core subunits using different transcript expression databases (ESTs and microarrays) linked in the *Solanaceae* Genomics Network and Tomato eFP Browser (http://bar.utoronto.ca/efp_tomato/cgi-bin/efpWeb.cgi). Most subunits were found to be expressed in fruits, while ClpP1a and ClpP1b transcripts were hardly detected (Figure R21).

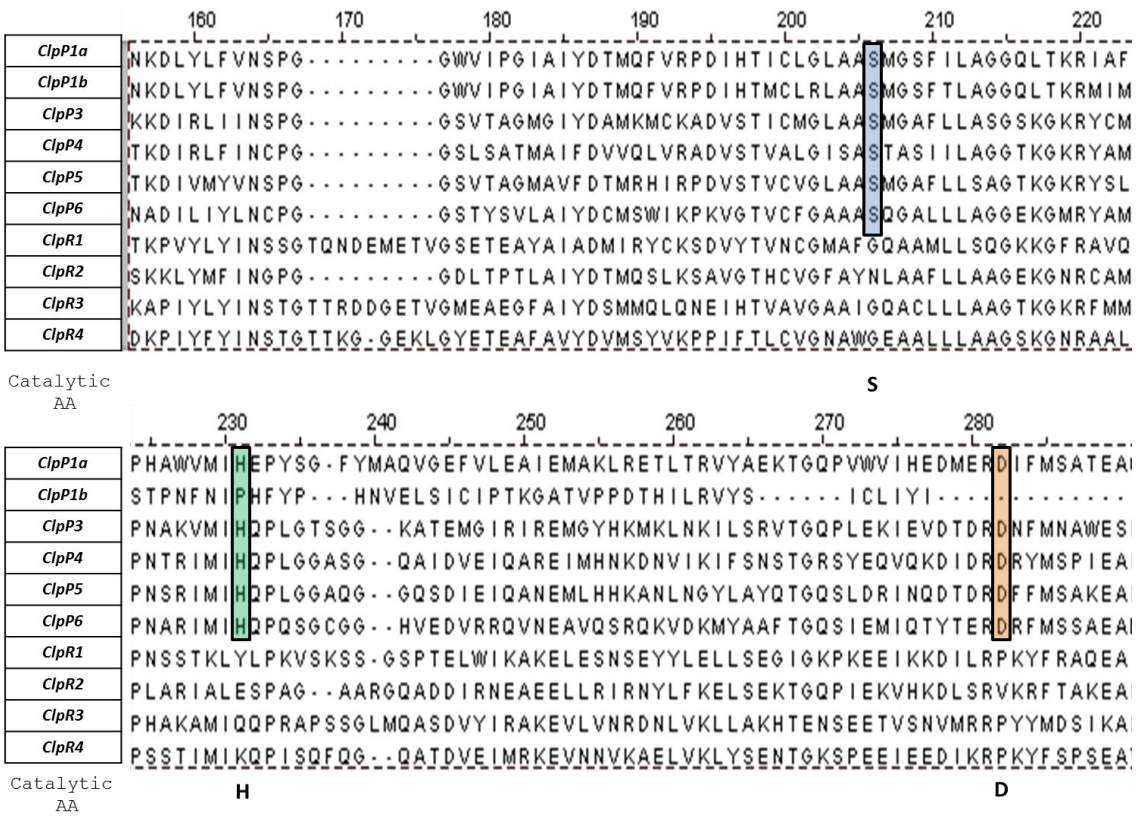

Figure R20. Alignment of the region harboring the catalytic triad of Clp serine proteases. While ClpP1a and ClpP3-6 conserve the three residues of the catalytic triad [serine (S); histidine (H) and aspartic acid (D)], ClpP1b has a mutation in the H position and it lacks the D residue.

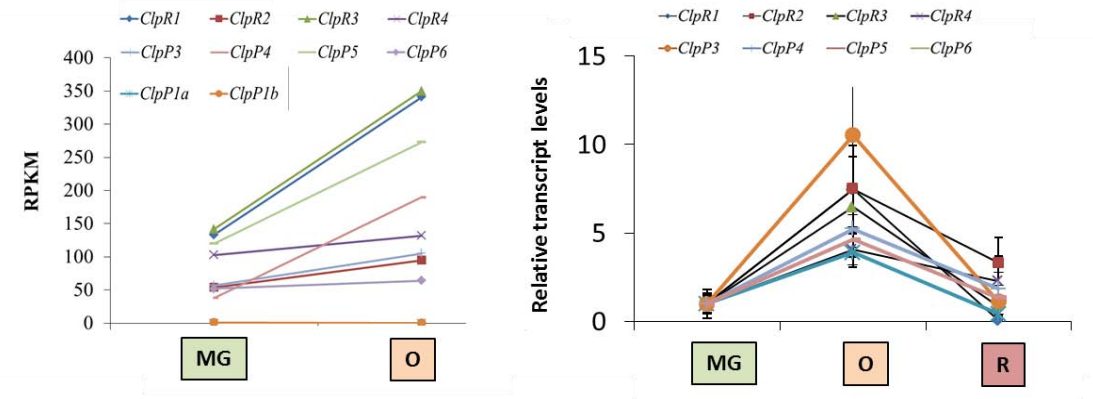

Figure R21. Transcript levels for nuclear-encoded subunits of the Clp protease core during fruit ripening. The graph in the left shows microarray data from the eFP-tomato browser in Mature Green (MG) and Orange (O) stages. Reads per Million Kilobase (RPKM) are plotted. The graph on the right shows the results of qPCR analysis of transcript levels in MicroTom fruit of the indicated stages, including ripe (R) fruit. Data correspond to mean and standard error of the media (SEM) of n≥3 independent fruits.

In agreement with tomato transcriptomic databases, RT-qPCR assays showed that the genes encoding ClpP3-6 and ClpR1-4 subunits are up-regulated during fruit ripening, reaching their peak levels at the O stage and then declining at the R stage (Figure R21). We were unable to detect *ClpP1a* or *Clp1b* transcripts. The same profile of upregulation from MG to O and downregulation from O to R is shared by core carotenoid biosynthetic genes such as *PSY1* and *DXS1* (Lois et al. 2000). However, the levels of DXS1 (a protein whose Arabidopsis homologue is degraded by the Clp protease; Pulido et al. 2016) do not increase but decrease when chloroplasts are differentiated into chromoplasts in the transition from MG to O (Figure R22). These observations suggest that tomato DXS enzymes might also be targets of the Clp protease complex during fruit ripening.

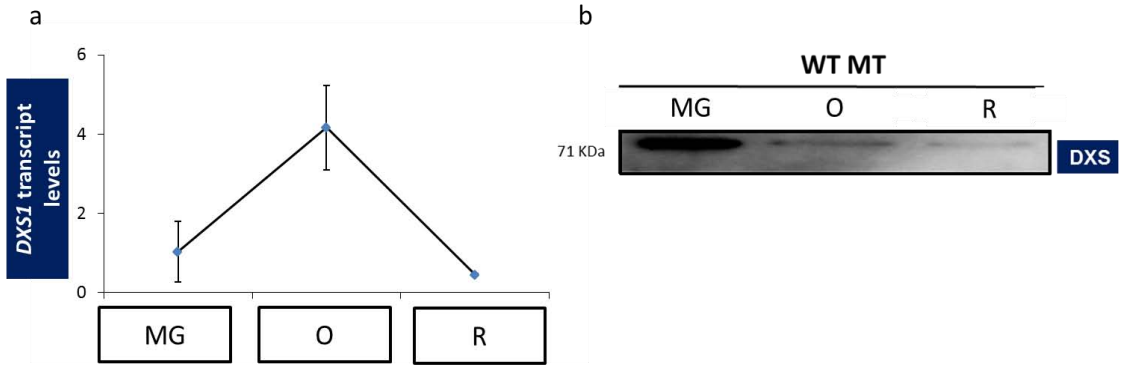

Figure R22. Changes in DXS transcript and protein levels during fruit ripening. (a) *DXS1* transcripts in MicroTom fruits of the indicated stages (n=3) (b) Western blot analysis of DXS protein levels at the same stages analyzed in (a). Data correspond to mean ± SEM of n≥3 independent fruits.

Silencing of the tomato *ClpR1* gene during fruit ripening affects carotenoid accumulation profile

To explore the role of the Clp protease during tomato fruit ripening, we decided to decrease its activity by silencing the expression of individual subunits. We first used a recently developed Virus Induced Gene Silencing (VIGS) approach based on a visual reporter (Orzaez et al., 2009). Briefly, this system takes advantage of transgenic tomatoes that overexpress in a fruit ripening-specific manner two transcription factors, *Delila* (*Del)* and *Rosea1* (*Ros1*), both involved in anthocyanin biosynthesis. These *Delila*-

Rosea1 (DR1) tomatoes turn purple when ripe due to a dramatic accumulation of anthocyanins that mask the red color provided by lycopene. Additionally, special VIGS vectors based on Tobacco Rattle Virus (TRV) were developed. These vectors contain (1) a sequence that triggers the silencing of *Del* and *Ros1* (DR module) and (2) a site that allows the cloning of around a ca. 200-bp sequence triggering the silencing of a Gene Of Interest (GOI). In this way, silencing can be visually followed by the disappearance of the purple color in ripe fruit. Because the co-silencing of the DR module and the tandem GOI is very high, fruit zones that are anthocyanin-free are also presumably silenced for the GOI.

We initially aimed to generate a VIGS vector able to trigger the simultaneous silencing of all the transcriptionally active ClpR subunits. To choose the target sequence, we aligned all these ClpR subunits and selected a region that is highly conserved in all of them, but less in ClpP subunits (Annex I and II). A representative sequence was cloned using the tomato *ClpR1* cDNA as template (Figure R23a). Once we obtained the corresponding construct, TRV2_DR/*ClpR1* (VIGS_*ClpR1*), we performed agro-injections in MG tomato fruits of DR1 plants of the Moneymaker variety as described (Orzaez et al., 2009). As a positive control, we used a construct that is able to trigger the silencing of the *PDS* gene (VIGS_*PDS*), which encodes the second enzyme of the carotenoid pathway (Figure I5). *PDS* silencing results in yellow fruits devoid of carotenoids similar to those treated with the PDS inhibitor norflurazon (Figure I6). As shown in Figure R23b, VIGS_*PDS* fruits developed yellow areas due to *PDS* silencing and purple zones where silencing has not occurred. In sharp contrast, we observed that VIGS_*ClpR1* fruits showed areas of a greenish-brown color in silenced sectors of the fruit.

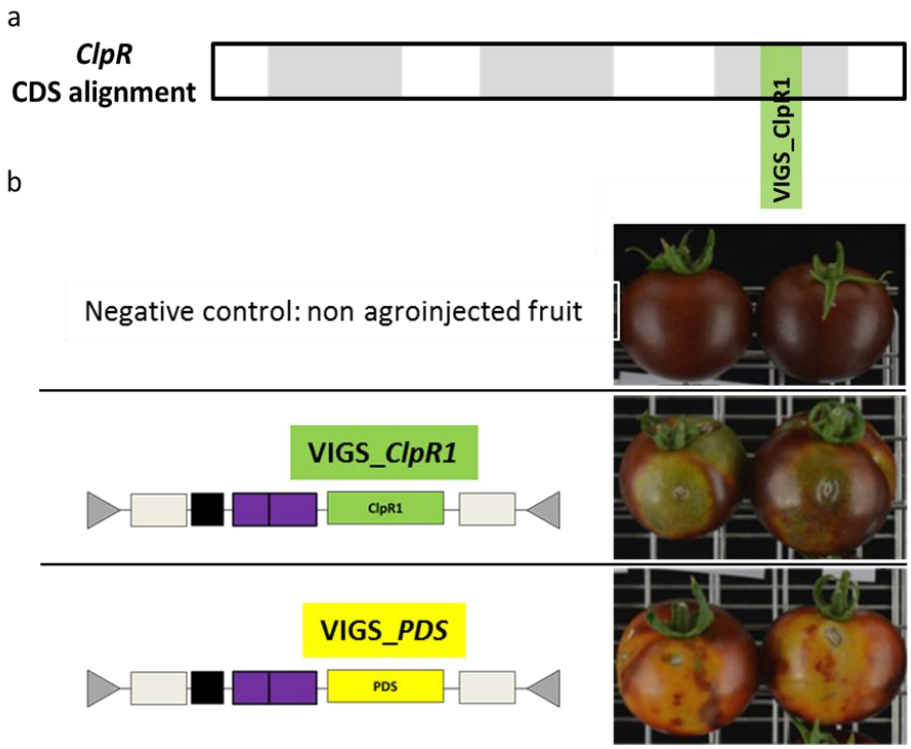

Figure R23. VIGS-mediated silencing of *ClpR1* in tomato fruit (a) Scheme representing conserved sequences (grey boxes) in the tomato ClpR subtunits. The sequence used to generate the VIGS_*ClpR1* vector is marked in green (See Alignment in Annex I and II). (b) Phenotype of ripe DR1 tomatoes that were agroinjected (or not) with the indicated constructs at the MG stage. While tomatoes agroinjected with VIGS_*PDS* show yellow silenced zones due to the absence of carotenoids, tomatoes that were injected with VIGS_*ClpR1* display greenish-brown silenced zones.

To evaluate if the VIGS-targeted ClpPR subunits were actually silenced, we analyzed transcript levels by RT-qPCR in three independent VIGS_*ClpR1* tomato fruits. Tissue corresponding to the silenced (S) and non-silenced (NS) zones of each fruit were collected separately. Because the coloration of S sections was suggestive of a developmental delay, we first compared the levels of *DXS1* transcripts in S and NS areas as a ripening stage marker (Figure R22) that is not affected by changes in Clp protease activity, as deduced from the analysis of *DXS* expression in Arabidopsis mutants (Flores-Perez et al. 2008; Pulido et al. 2016) (Figure R24).

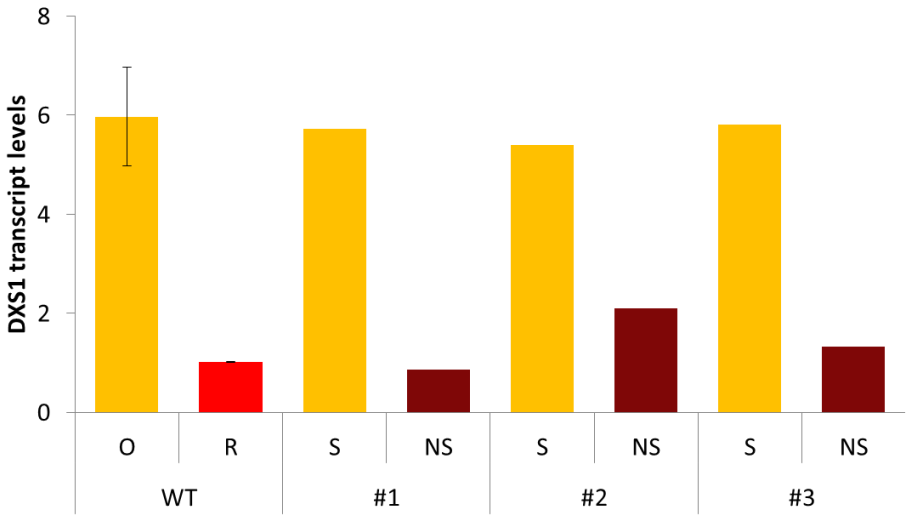

Figure R24. VIGS_*ClpR1* silenced zones have a *DXS1* expression pattern similar to WT orange fruits. *DXS1* mRNA levels were measured by RT-qPCR in silenced (S) and non-silenced (NS) zones of 3 independent tomato fruits (#1, #2 and #3) agroinjected with the VIGS_*ClpR1* construct. Results are compared with WT fruits (n=3) at the orange and red developmental stages. Data correspond to mean ± SD.

While *DXS1* transcript levels in NS areas of VIGS_*ClpR1* fruits were similar to those in non-injected ripe fruits, as expected, S zones showed transcript levels that were more similar to those in orange fruits (Figure R24). This result confirmed that S areas showed a developmental delay and did not ripe as fast as NS areas of the same fruit. Taking this into consideration, we investigated the possible silencing of ClpPR-encoding genes by comparing transcript levels in S sectors of VIGS_*ClpR1* fruits to those found in non-injected O fruits and those in NS sectors to R fruits (Figure R25). Analysis of S sectors showed dramatically decreased levels of *ClpR1* transcripts (10-fold lower than in control O fruit), as expected, but also of other ClpPR-encoding subunits (Figure R25a). By contrast, no significant differences relative to R fruit were observed in NS zones of VIGS_*ClpR1* samples with the only exception of *ClpP6* in NS3 (Figure R25b).

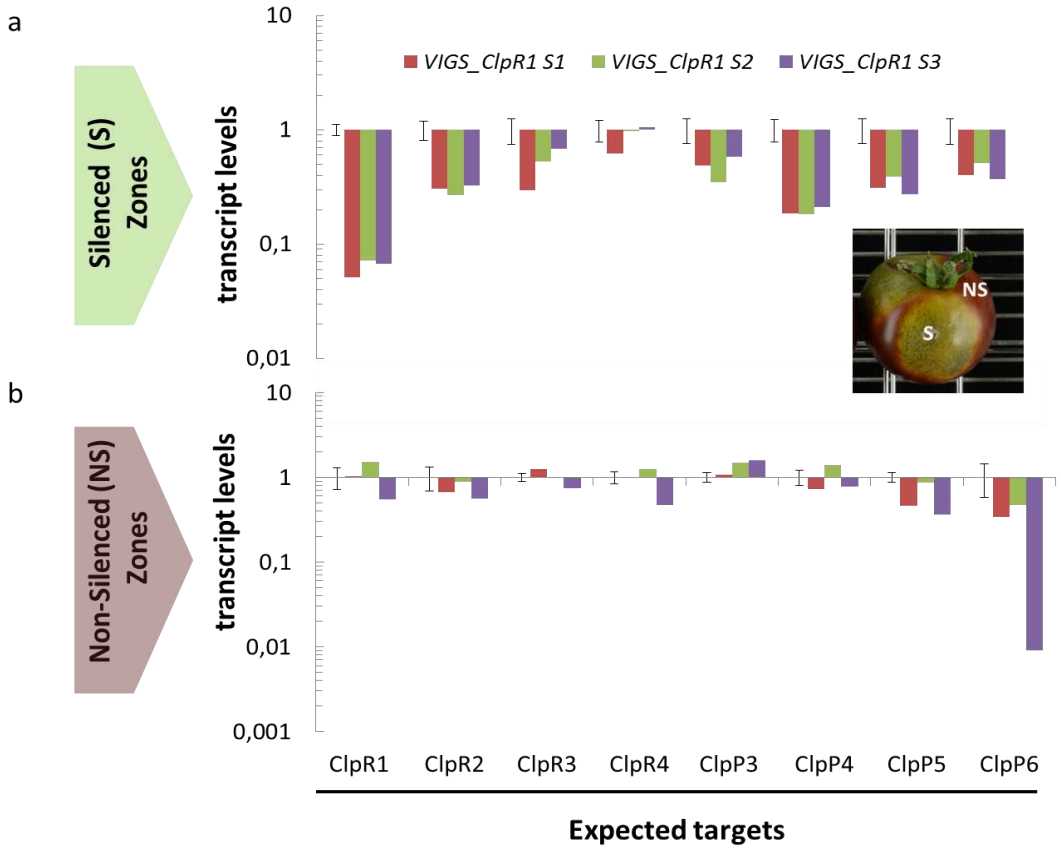

Figure R25. VIGS-mediated silencing of *ClpR1* and other ClpPR-encoding genes. (a) Transcript levels of *ClpR1-4* and *ClpP3-6* in S zones of three VIGS_*ClpR1* fruits (S1, S2 and S3). Levels are relative to non-injected O fruit of the same genotype (DR1). (b) Transcript levels of *ClpR1-4* and *ClpP3-6* in NS zones of the same fruits used in (a). Levels are relative to non-injected R fruit. Data correspond to mean ± SD and are represented in a logarithmic scale.

Next, we analyzed the impact of presumably reducing Clp protease activity on carotenoid biosynthesis. We used HPLC analysis to separate and quantify major tomato carotenoids such as phytoene, lycopene, β-carotene and lutein (Figure R26). S zones showed a carotenoid profile closely resembling that observed in non-injected O fruit, with detectable levels of lutein and chlorophylls (Figure R26a) and a relatively high proportion of β-carotene (Figure R26b). By contrast, NS sectors had the expected carotenoid composition, with high levels of phytoene and lycopene characteristic of R fruit (Figure R26). As a result, the β-carotene/lycopene ratio (a parameter that directly impacts tomato fruit color) in S sectors of VIGS_ClpR1 fruit were similar to that in O fruit whereas in NS sectors was undistinguishable from that in R fruits (Figure R26b).

Considering the molecular and metabolic data obtained from VIGS_*ClpR1* fruits,

we hypothesized that the S zones where the levels of transcripts encoding ClpR1 and other ClpPR subunits and reduced had a reduced activity of the Clp protease complex and this somehow resulted in a developmental arrest in the a ripening stage similar to the O stage in untreated, control fruits.

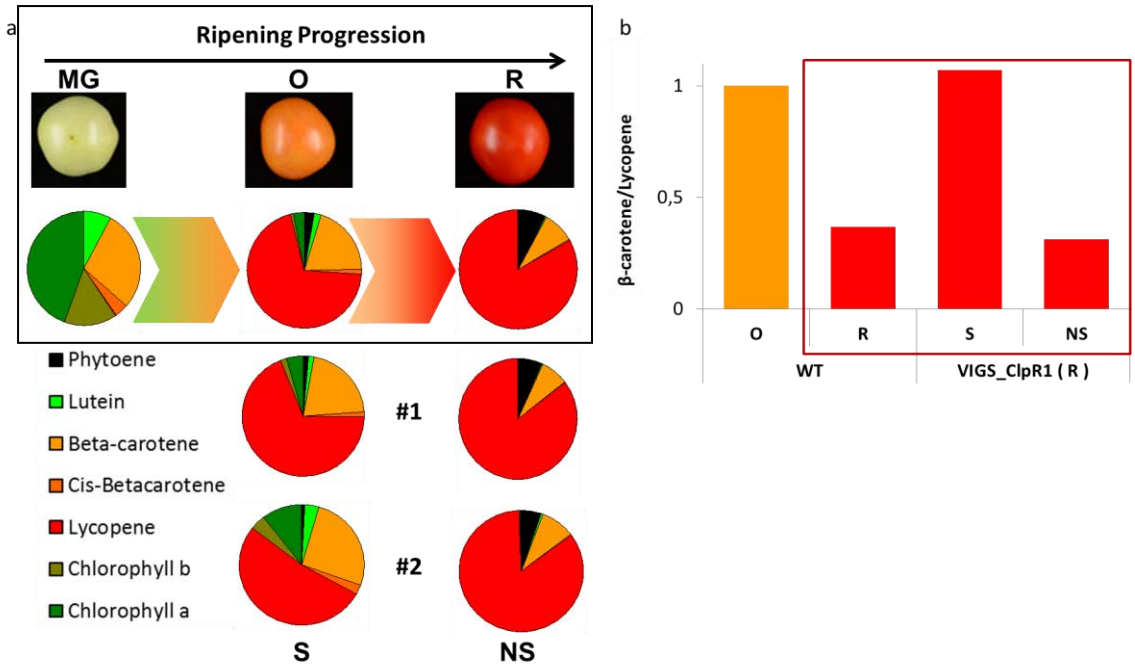

Figure R26. Carotenoid profile of VIGS_*ClpR1* fruit sectors. (a) Profile of carotenoids and chlorophylls in whole DR1 fruits at different ripening stages (boxed) and S and NS sectors of two individual VIGS_*ClpR1* fruit at the ripe stage. (b) β-carotene/lycopene ratio in DR1 (WT) O and R fruit and S and NS zones of VIGS_*ClpR1* ripe fruits.

Transgenic *E8:amiR1* fruits show an orange color when ripe due to an enrichment in β-carotene, the main pro-vitamin A carotenoid

VIGS experiments suggested that the Clp protease complex might be involved in ripening progression. Then, taking into account the Clp protease complex sub-cellular localization, we reasoned that its loss of function could be specifically impairing the chloroplast-to-chromoplast transition, hence affecting carotenoid accumulation. However, a deeper analysis was needed to confirm this idea. To facilitate this analysis, we decided to generate transgenic plants transformed with an artificial microRNA (amiRNA) designed to specifically reduce the levels of *ClpR1* transcripts in order to downregulate the activity of the whole Clp protease complex. The amiRNA silencing

method uses a very short sequence (21bp) to specifically downregulate an mRNA target (Ossowski et al., 2008). *ClpR1* mRNA was selected as the amiRNA target because: (1) ClpR1-defective Arabidopsis mutants have reduced Clp protease activity levels but are viable; (2) VIGS experiments were also based on *ClpR1* mRNA. Specific amiRNA sequences were designed and amplified following the recommendations of the Web MicroRNA Designer (WMD3) (http://wmd3.weigelworld.org/cgi-bin/webapp.cgi). Two amiRNA sequences (amiR1.1 and amiR1.2) were selected that match the *ClpR1* mRNA in different regions (Figure R27a). As a control, an inactive amiRNA was generated by inverting nucleotides at positions 10 and 11 of the amiR1.1 construct (amiC) (Figure R27a). Subsequently, the active and inactive sequences were cloned into specific pENTRY vectors (see Materials and Methods).

To check the affectivity of amiR1.1 and amiR1.2 sequences, we first subcloned them into expression vectors between two copies of the *35S* promoter (2x35S) and the T-nos terminator (see Materials and Methods). Agroinfiltration assays in tomato leaves allowed evaluating the effect of the generated constructs on *ClpR1* mRNA levels. While the inactive amiC sequence had no effect on *ClpR1* transcript levels, both functional amiR1.1 and amiR1.2 sequences successfully downregulated *ClpR1* mRNA levels, being amiR1.1 slightly more effective (Figure R27b). Based on these results, amiR1.1 and amiC sequences were selected to generate stably transformed tomato plants.

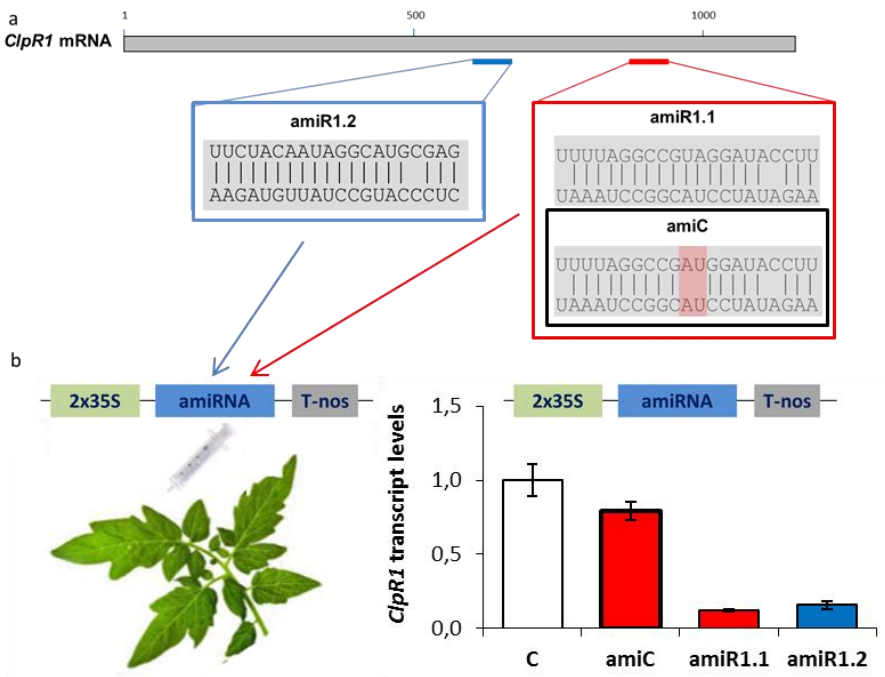

Figure R27. Design and validation of amiRNA sequences. (a) The regions in the tomato *ClpR1* mRNA targeted by two different active amiRNAs (amiR1.1 and amiR1.2) and one inactive amiC are indicated. Nucleotides mutated in amiC are highlighted in red. (b) Testing of the generated amiRNAs in tomato leaves. All amiRNAs were cloned under the control of the 2x35S promoter and the generated constructs were agroinfiltrated in tomato leaves. *ClpR1* transcript levels were measured by RT-qPCR. Data are presented relative to *ClpR1* transcript levels in leaves agroinfiltrated with a similar vector harboring an unrelated-amiRNA (C) and correspond to mean ± SEM of n=3 leaves.

To generate transgenic plants with a decreased Clp protease activity during fruit ripening without affecting its levels in chloroplast-containing tissues, we searched the pENFRUIT vector collection for fruit-specific promoters (Estornell et al, 2009). We selected the E8 promoter, because the *E8* gene is poorly expressed in early stages of fruit development (up to the MG stage) but highly up-regulated at the onset of ripening (Figure R28a). The profile of *E8* expression, with peak levels at the O stage, is actually very similar to that observed for *ClpR1* and other ClpPR-encoding genes (Figure R21). We therefore constructed vectors for the expression of selected amiRNAs under the control of the *E8* promoter, generating constructs E8:amiR1 (harboring the amiR1.1 sequence) and E8:C (Figure R28b).

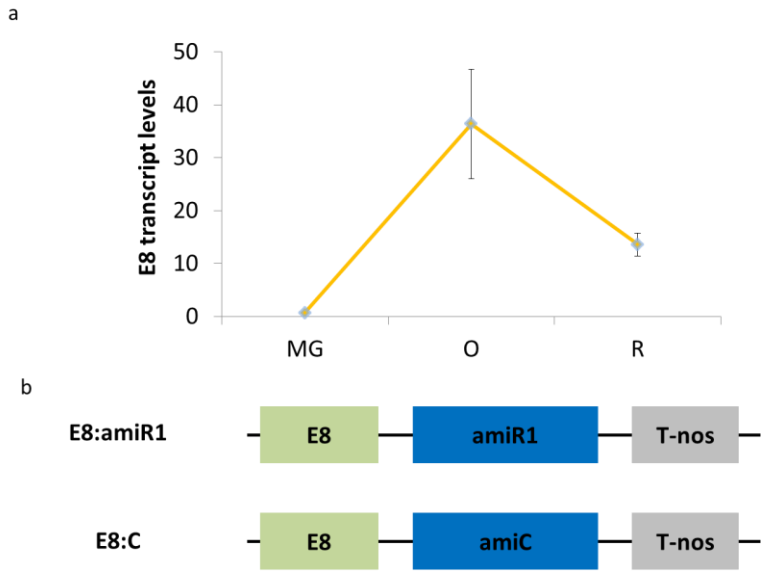

Figure R28. *E8* expression pattern and use as a promoter to drive the expression of amiRNAs. (a) *E8* transcript levels during MIcroTom fruit ripening are shown relative to the MG stage and correspond to mean ± SEM (n>3). (b) Scheme of the vectors used for stable transformation of tomato plants.

Tomato plants of the MicroTom variety were transformed following an *in vitro* technique optimized at CRAG (Material and Methods section). Although the method was adapted to maximize transformation efficiency, a high percentage of cotyledons developed explants (68.5 %) but only 3 % of them generated mature plants (Figure R29a).

a

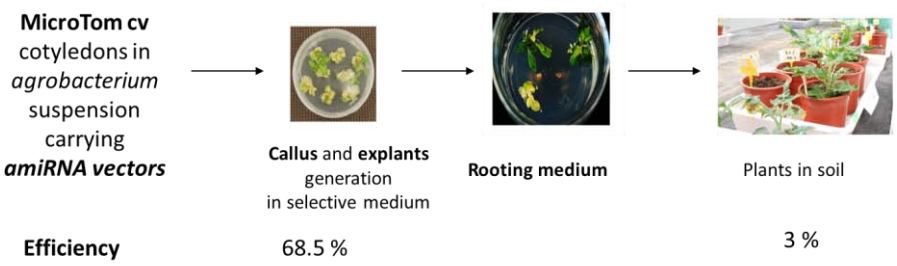

b

	# T1 independent Lines	# T2 independent Lines	Colour Ripe Fruit T2
E8:amiR1	10	3:2	O:R
E8:C	7	3	R

Figure R29. Stable transformation of tomato (MicroTom) with E8:amiR1 and E8:C constructs. (a) Summary of transformation phases. The percentage of explants regenerated from cotyledons and plants that survived greenhouse acclimation is shown. Efficiencies were calculated based on the initial number of transformed cotyledons. (b) Independent lines obtained in T1 and T2 generations. The number of T2 plants with reduced levels of *ClpR1* and the color of their ripe fruits (either orange or red) are shown.

We obtained 10 independent T1 plants transformed with E8:amiR1 and 7 plants harboring the inactive E8:C construct (Figure R29b). However, only half of them developed ripe fruits with fertile seeds. All T2 fruits from the remaining E8:C lines (#C7, #C25 and #C23) developed visually normal red ripe fruits. By contrast, only two of the E8:amiR1 lines (#R16 and #R52) showed red ripe fruits, whereas the remaining three lines (#R22, #R94 and #R66) generated fruits that were distinctively orange when ripe (Figure R30a). Quantification of *ClpR1* transcript accumulation showed similar levels in ripe fruits from E8:C lines and untransformed MicroTom wild-type (WT) plants (Figure R30b). E8:amiR1 lines developing red ripe fruits (#R52 and #R16) also showed *ClpR1* transcript levels that were similar or slightly higher than in the WT fruit. However, E8:amiR1 lines #R22, #R94 and #R66, whose fruits remained orange when ripe, presented downregulated *ClpR1* transcript levels (Figure R30b).

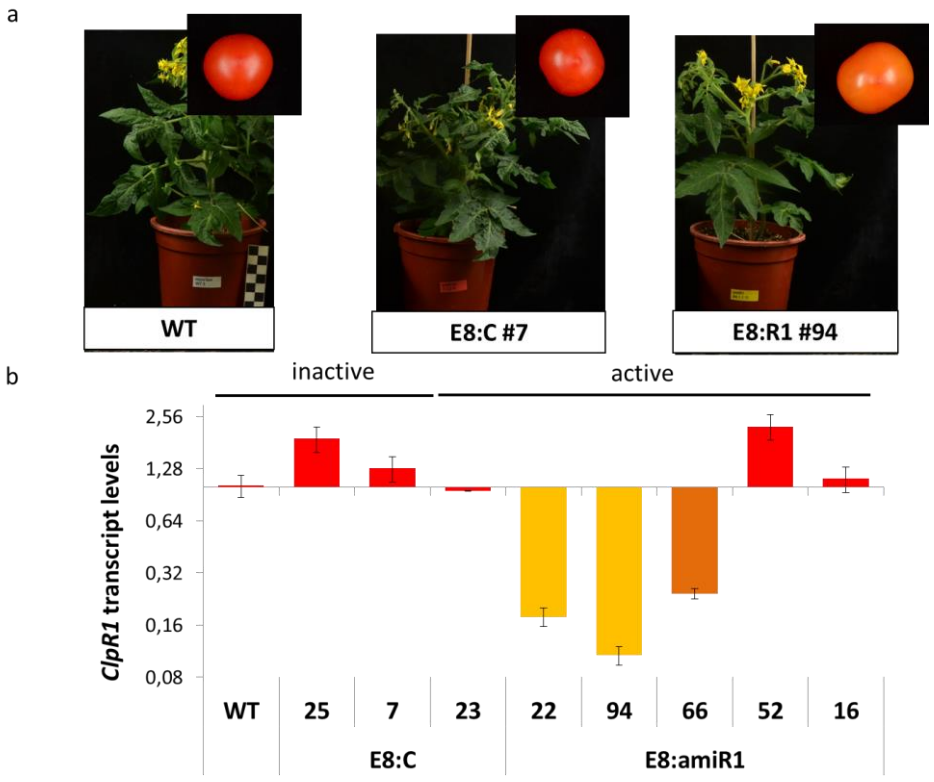

Figure R30. Phenotype of tomato lines with reduced *ClpR1* transcript levels. (a) Phenotype of MicroTom plants either untransformed (WT) or transformed with E8:C or E8:amiR1 (T2 generation). A representative ripe fruit produced by each genotype is also shown. (b) RT-qPCR analysis of *ClpR1* mRNA levels in ripe fruit from WT and independent T2 lines harboring the indicated constructs. Data is represented as relative log2. Values are relative to WT fruit and correspond to mean ± SEM (n>2). Column colors represent fruit colors when ripe.

T3 generation fruits from the amiR1 lines with silenced *ClpR1* expression were also orange when ripe, indicating a stable phenotype. An important point to note is that these transgenic lines had no evident differential phenotype at the vegetative level (Figure R30a), suggesting that the E8 promoter worked as expected. To investigate the metabolic basis of the coloration of transgenic ripe fruit, the carotenoid profile of fruit at the R stage (i.e., 52 days after anthesis) from E8:amiR1 lines #R66 and #R94 was compared to that of WT and E8:C (#C7) controls collected at the same stage. WT fruit at the O stage were also used for HPLC analysis of carotenoid contents as they display an orange color similar to that of R fruit from the selected E8:amiR1 lines (Figure R31c). In terms of total carotenoids, all genotypes tested accumulated similar levels in R fruit. However, the qualitative carotenoid profile of R E8:amiR1 fruit, was characterized by a substantial enrichment in orange-colored β-carotene (Figure R31a). The levels of this pro-vitamin A carotenoid increased between 40% (#R66) and 70% (#R94) in transgenic fruit. Because the accumulation of lycopene was similar in all the genotypes analyzed, the resulting β-carotene:lycopene ratio in R fruit was up to 2-fold higher in #R94 fruit compared to WT and #C7 controls (Figure R31c). This β-carotene:lycopene ratio, which influences whether the fruit pericarp color is closer to orange (high ratio) or to red (low ratio), was actually similar in ripe #R94 and O WT fruit (Figure R31c). Interestingly, a negative correlation was found between β-carotene:lycopene ratio (i.e. fruit color) and *ClpR1* silencing (Figure R30), suggesting a direct relationship. Altogether, we conclude that silencing of the *ClpR1* gene during tomato fruit ripening impairs normal carotenoid accumulation, eventually resulting in a specific enrichment in β-carotene that provides a characteristic orange color to the ripe fruit.

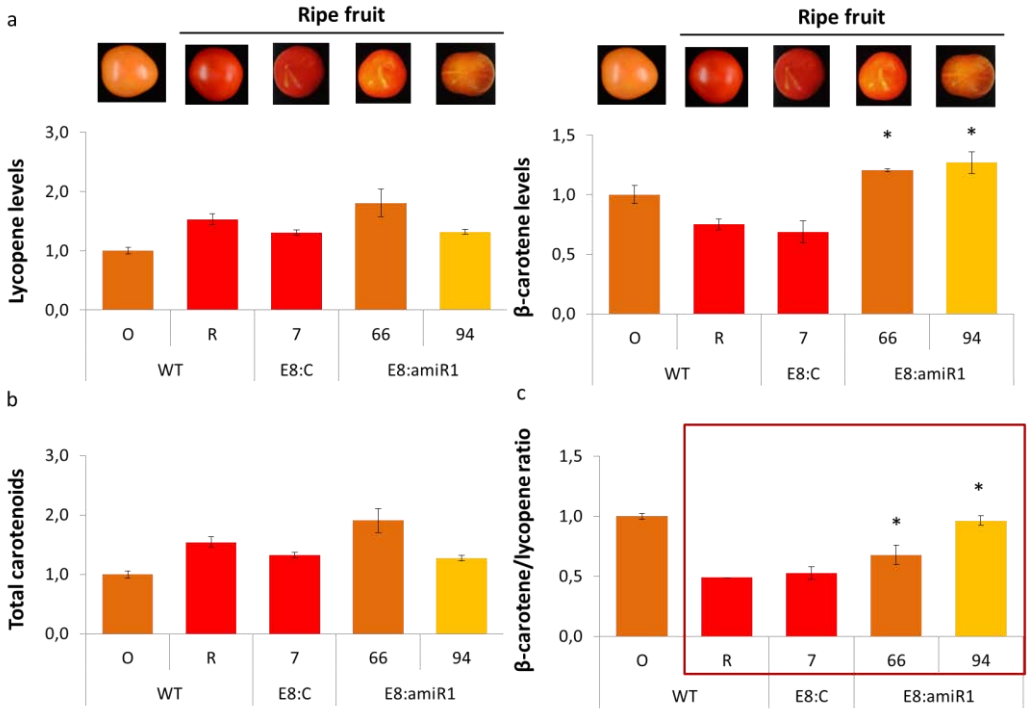

Figure R31. Carotenoid profile of transgenic fruit. (a) Levels of individual (lycopene and β-carotene) and (b) total carotenoids in WT fruits at the O and R stage and transgenic fruits of the indicated lines at the R stage. (c) β-carotene/lycopene ratio of the fruits analyzed in (a). Data are represented relative to WT fruit at the O stage. Data correspond to mean ± SEM of n=2 fruits per genotype. Statistical significance differences with WT Ripe fruit were calculated using t test. * indicates when p-value<0.05.

E8:amiR1 fruits do not fully differentiate typical chromoplasts

The Clp protease complex controls many plastidial processes in Arabidopsis, including plastid development (Figure R18). To test whether the observed phenotypes of transgenic amiR1 fruits were due to an altered differentiation of chromoplasts, we analyzed plastid ultrastructure by Transmision Electronic Microscopy (TEM). For consistency, we only observed the cells of the collenquima (i.e. the internal layer of the exocarp; Figure I1). As shown in Figure R32, control E8:C fruits at the O and R stages displayed the typical globular/crystalline chromoplasts, with many of them showing large plastoglobules and the remnants of lycopene crystals (the crystalloids are lost during the dehydration procedure and their expanded membrane envelopes shrunken into an undulating shape). While E8:amiR1 plastids at the O stage do not display clear differences when compared with the E8:C control, the ripe fruits of this silenced line did harbor chromoplasts with a completely altered architecture. In particular, chromoplasts with abundant plastoglobules but very low levels of lycopene-associated

membranes (Figure R32d) coexisted with other chromoplasts that did contain such membranes but lacked plastoglobules (Figure R32e) and chromoplasts with both types of carotenoid-accumulating structures (Figure R32f).

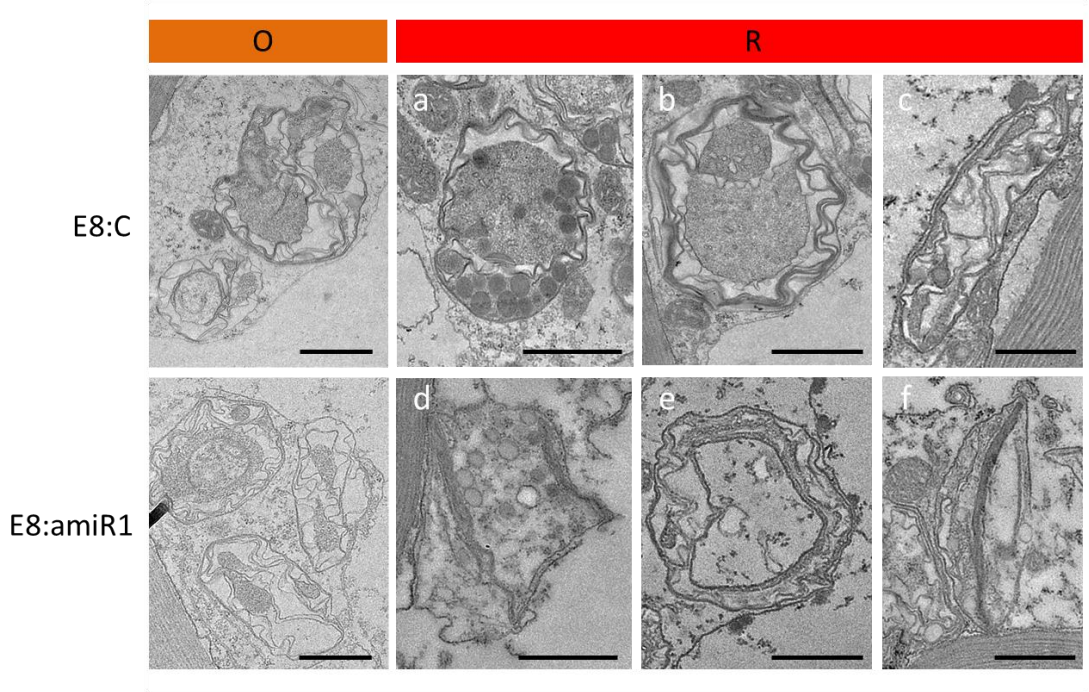

Figure R32. Transmission electron microscopy of amiR1 chromoplasts. Pictures show representative images of chromoplasts from E8:C (line #C7) and E8:amiR1 (line #R94) fruits at the indicated stages. Several chromoplasts are shown in the case of the R stage to illustrate the differences in their ultrastructure. Bars correspond to 1 µm.

To test whether the different chromoplast ultrastructures observed by TEM in amiR1 fruit samples had an impact on their carotenoid composition, we used Raman spectral imaging in collaboration with Dr. Monica Marro and Prof. Pablo Loza-Alvarez at the Institute of Photonic Sciences (ICFO) in Castelldefels, Barcelona, Spain (https://www.icfo.eu/). Analysis of the distribution of β-carotene and lycopene in chromoplasts of fresh tomato pericarp samples from control E8:C fruit showed that both carotenoids were present in the chromoplasts of ripe fruit, as expected (Figure R33). In ripe E8:amiR1 fruit, however, we found chromoplasts that almost exclusively contained β-carotene, others that primarily accumulated lycopene, and others that produced both (Figure R33). We speculate that the first type might correspond to those harboring abundant plastoglobules (Figure R32d), while the lycopene-accumulating

type likely corresponds to chromoplasts that lacked plastoglobules but were enriched in lycopene-associated membranes (Figure R32e). Together, our findings strongly indicate that tomato fruits with reduced levels of *ClpR1* transcripts and hence lower plastidial Clp protease activity show an altered chromoplastogenesis that might explain their metabolic (carotenoid) and visual phenotype.

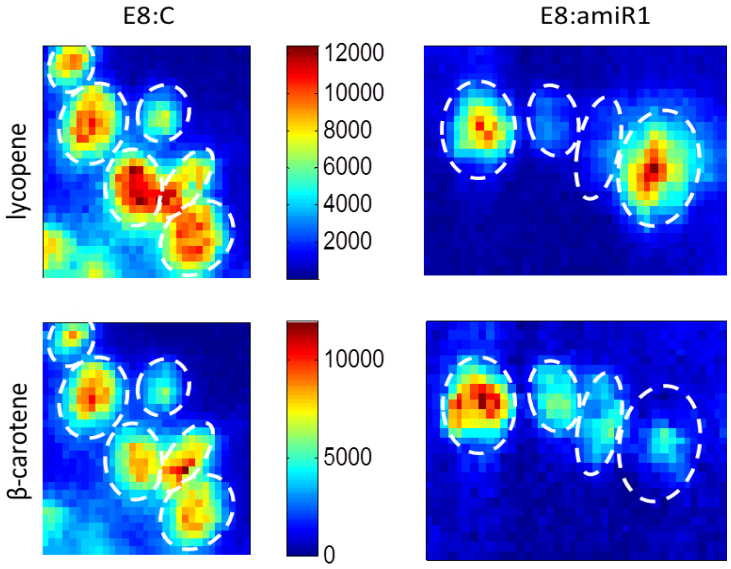

Figure R33. Raman mapping of lycopene and β-carotene in tomato chromoplasts. Representative maps of chromoplasts from E8:C (line #C7) and E8:amiR1 (line #R94) fruits at the R stage are shown. Map colors correspond to the band intensity in the corresponding range (heatmap). Chromoplast perimeter is indicated with a dashed while line for reference.

Higher levels of DXS protein (but not transcripts) in transgenic amiR1 fruits are consistent with a reduction in Clp protease activity.

If DXS is a target of the Clp protease in tomato chromoplasts as it is in Arabidopsis plants (Pulido et al., 2016), it was expected that amiR1 fruits with reduced *ClpR1* transcript levels showed increased levels of this enzyme in chromoplasts. To evaluate this prediction, we analyzed DXS protein levels in ripe fruits from silenced lines E8:amiR1 #R22 and #R94 and compared them with those in control WT and E8:C (#C7) lines. Western blot analysis using an antibody against the Arabidopsis DXS enzyme showed that both E8:amiR1 lines accumulated statistically higher levels of DXS protein (ca. 3-fold higher relative to the controls) (Figure R34a). Then, we compared the levels of DXS-encoding transcripts between ripe fruits of the DXS-accumulating E8:amiR1 #R94 line and the non-silenced #C7 control (Figure R34b). Because fruit DXS activity is predominantly supplied by the product of the *DXS1* gene, we carried out RT-qPCR experiments to quantify *DXS1* transcripts and observed that they accumulate

similarly in all the analyzed lines (Figure R34b). Altogether, these results show that DXS overaccumulation in E8:amiR1 ripe fruits results from an altered mechanism acting at the post-transcriptional level, most likely a reduced Clp protease activity.

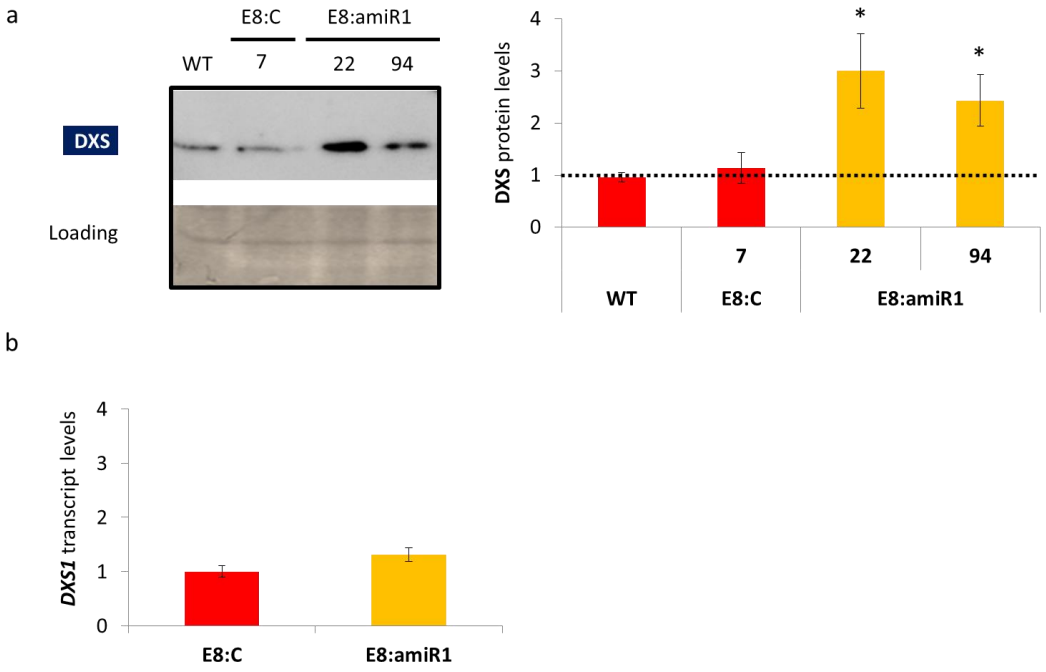

Figure R34. DXS protein post-transcriptionally accumulates in E8:amiR1 fruits. (a) Western blot against DXS protein. DXS (left panel) and quantification of signals (right panel) from several blots. Mean and SD (n≥3) are shown. (b) RT-qPCR experiments showing the mRNA levels of *DXS1* in ripe fruits from the incicated lines. Mean and SD (n≥3) are shown. Statistical significance differences with WT were calculated using t test. * indicates when p-value<0.05.

Clp-defective amiR1 fruits have a similar chromoplast proteome to control fruits at the R stage

We next aimed to explore whether other proteins besides DXS were misaccumulated in chromoplasts as a result of decreased Clp protease activity during ripening, perhaps explaining the phenotypes of the transgenic fruits. To assess that point, we decided to characterize the proteome of transgenic fruits by a quantitative proteomic approach named Tandem Mass Tag (TMT) (Thompson et al., 2003). The experimental design is presented in Figure R35. I made this experiment as part of a short-term stay at Prf. Li Li's lab, Cornell University (Ithaca, New York, USA). We compared non-transformed (WT) fruits at two stages of ripening, O (47 DPA) and R (52 DPA), with E8:amiR1 (line #R94) fruits at the R stage (52 DPA). To obtain statistically

significant results, three biological replicates were performed per each proteome. As the total number of samples was nine (3 WT-O replicates, 3 WT-R replicates and 3 #R94-R replicates), a 10-plex TMT was used in this experiment. Given that we were interested in characterizing changes in the plastidial proteome, we analyzed proteins solubilized from previously isolated chromoplasts. Once protein extracts were obtained, all replicates were processed following the instructions from Dr Theodore Thannhauser (USDA-Proteomic Service, Cornell University). Proteins from different replicates were labeled using specific tags (Figure R35). Then, all replicates were mixed and proteins were separated according to their size by liquid chromatography (HPLC) into six different fractions. Proteins in different fractions were identified by tandem mass spectrometry (MS/MS) (Material and Method section).

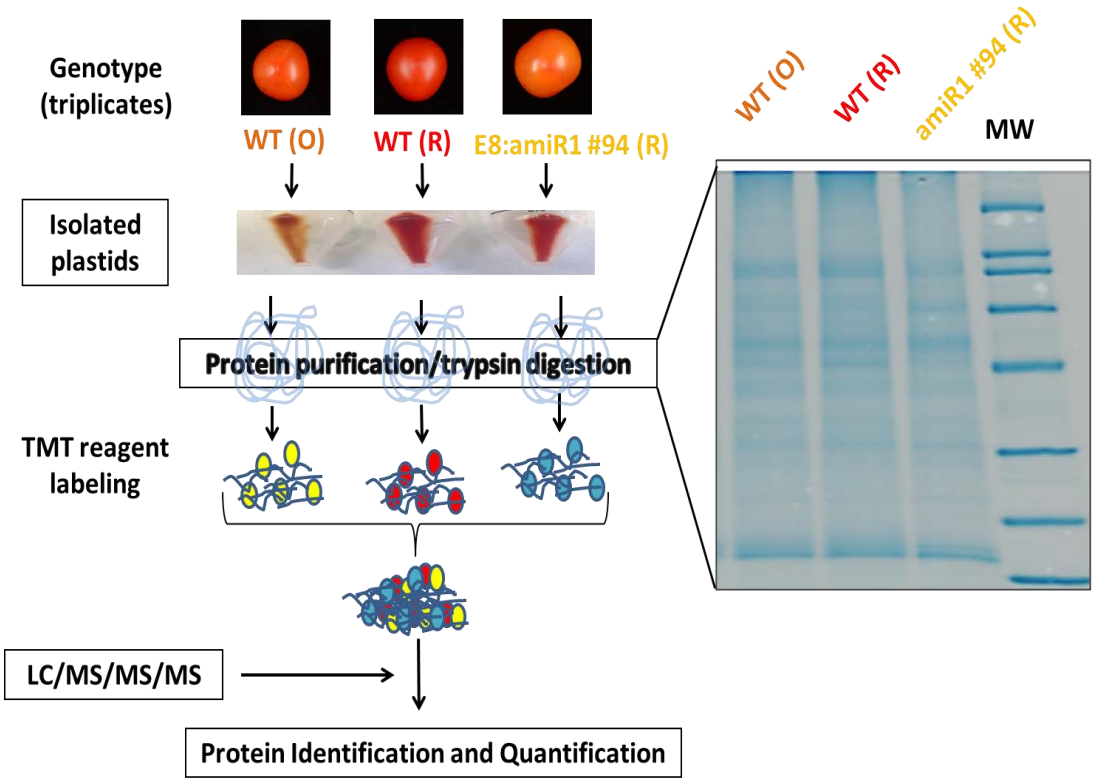

Figure R35. Schematic workflow for the proteomic study. Each biological replicate was generated by isolating chromoplasts from WT fruits in orange (O) and red (R) stages and #R94 fruits in the R stage. Plastid proteins were purified and checked by SDS-PAGE followed by Coomassie blue staining. Subsequently, proteins from different replicates were digested and labeled with different TMT® reagents (symbolized by yellow, red and blue balls). Finally, samples were mixed and analyzed by liquid-chromatography (LC) coupled to three tandem mass spectrometers (MS/MS/MS).

A total of 2223 proteins were confidently identified with more than two unique peptides and were subsequently used for further analyses. The percentage of proteins predicted to localize in plastids was estimated using 4 different programs (ChloroP, BaCelLo, EpiLoc and iPSORT) integrated in the SUBA database (http://suba.plantenergy.uwa.edu.au/), which houses large scale proteomics data and contains precompiled bioinformatic predictions for protein subcellular localizations from Arabidopsis. Among the 2223 initially identified proteins, 1998 homologues were identified and analyzed by SUBA database. About 60% of these proteins were predicted to be plastid-localized by at least one algorithm, 10 of which were plastome-encoded. These *in-silico* studies confirm the enrichment in plastidial proteins expected from the use of isolated chromoplasts as the source of protein extracts. However, it becomes evident that many (ca. 40%) of the proteins detected in this experiment are not plastid-localized. One possibility is that these non-plastidial proteins are contaminations coming from other cell compartments, like mitochondria. Alternatively, some predicted non-plastidial proteins might be attached to the plastid outer envelope membrane. Another possibility is that those proteins that are not predicted to harbor a transit peptide can be directed to the plastid by a different mechanism. Therefore, we decided to follow the analysis with all the identified proteins independent of their predicted localization.

To estimate the global impact of silencing Clp in the chromoplast proteome, all the obtained proteomes were compared by Principal Component Analysis (PCA) (Figure R36). While WT-R and WT-O proteomes clustered separately, as expected, #R94-R grouped together with WT-R proteomes. This analysis indicates that, although E8:amiR1 ripe fruits are phenotypically orange, their chromoplastidial proteome is similar to ripe WT fruit of the same age, independently of their different color.

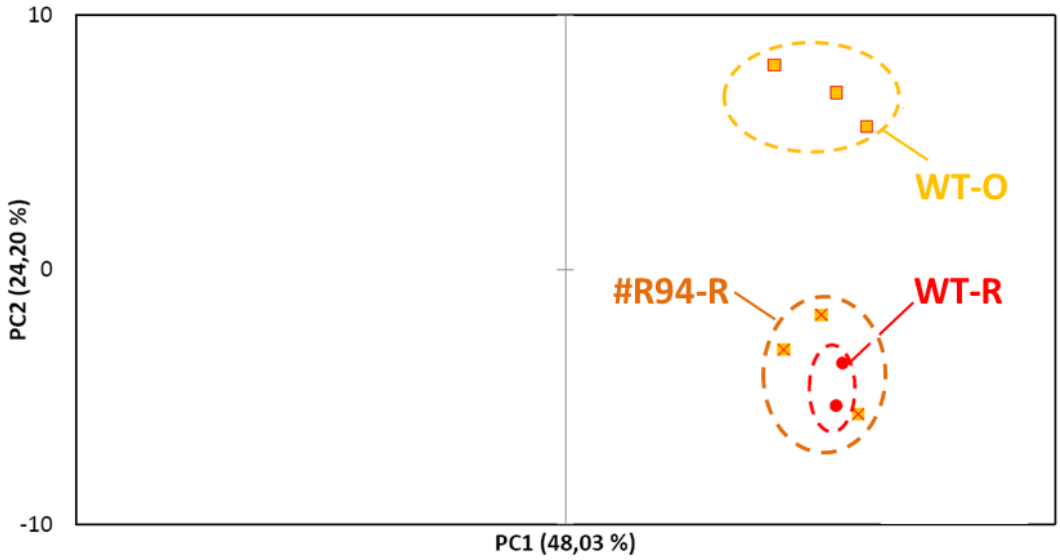

Figure R36. Principal Component Analysis (PCA) of chromoplast proteomes. The PCA analysis was performed with XLSTAT. Each symbol represents a replicate. PCA 1 and PCA2 explain 72.23% of the variance within the overall dataset.

Clp protease-dependent protein turnover plays an important role during tomato fruit ripening.

Because the amiR1 construct is under the regulation of the E8 promoter, it is expected that the silencing would progress together with the ripening process. We reasoned that if the decrease in Clp activity starts to be most effective at the O stage, the consequences of its reduction in the proteome should be observed later during ripening and hence be most obvious in the R stage. This is in agreement to what we observe in terms of chromoplast differentiation. With that in mind, we looked for proteins whose levels changed at the R stage in WT and #R94 fruits compared to WT-O samples.

First, we compared the levels of all the proteins present in WT-O and WT-R proteomes and selected those that exhibited statistically significant changes (i.e. those changing during normal ripening). Then, we compared the levels of all of the proteins present in WT-O and #R94-R proteomes and again selected those that exhibited significant changes (i.e. those changing during ripening with a reduced Clp protease activity). Subsequently, both groups of proteins (labeled as “WT ripening” and

"E8:amiR1 ripening") were compared to create three different groups (Figure R37):

Group A.- Proteins de-regulated specifically in WT fruits. Among these, the proteins that are down-regulated in this group are potential Clp targets as their levels decrease during ripening (Table R3).

Group B.- Proteins de-regulated specifically in amiR1 fruits. Among these, the proteins that are up-regulated in this group are potential Clp targets (Table R4).

Group C.- Proteins de-regulated during both normal and Clp-defective ripening.

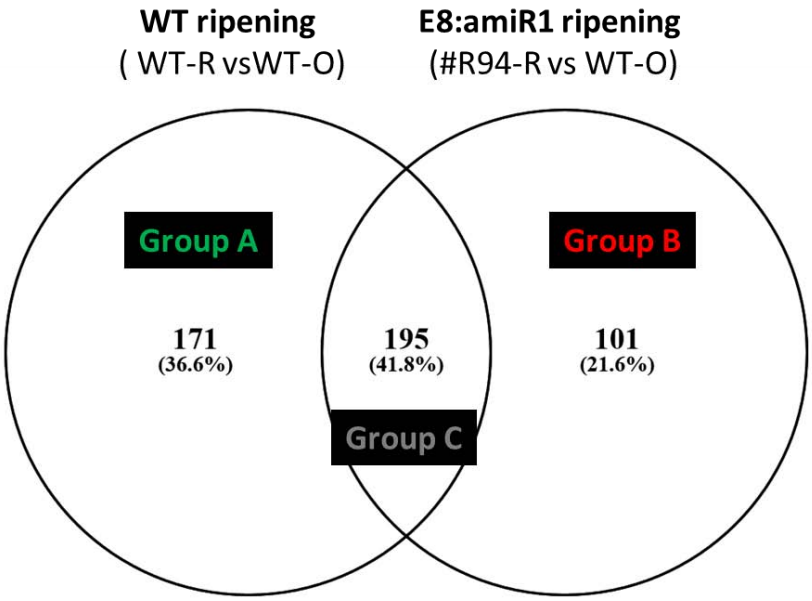

Figure R37. Identification of putative Clp targets during tomato fruit ripening. Venn diagram comparing the proteome of the indicated samples. Proteins were separated into three groups. Group A represents proteins that change in a statistically significant ($p<0.05$) manner during WT ripening and not in E8:amiR1, whereas Group B represents those that only change in E8:amiR1 fruits and Group C represents proteins that significantly change in both genotypes.

In total, we found 101 proteins from group A (Table I) and 59 from group B- (Table II), a total of 160 proteins that could be putative Clp protease targets.

Table R3. Group A down-regulated proteins
*numbers in bold are statistically significant (p<0.05)

Tomato accession	Description	Ratio R/O*
Solyc02g071040.2.1	starch synthase 4	**0.96**
Solyc03g112910.2.1	pantothenate kinase 2	**0.95**
Solyc11g005330.1.1	actin 7	**0.95**
Solyc07g053260.2.1	general regulatory factor 9	**0.93**
Solyc01g102510.2.1	Transducin/WD40 repeat-like superfamily protein	**0.93**
Solyc01g094410.2.1	C2 calcium/lipid-binding plant phosphoribosyltransferase family protein	**0.92**
Solyc02g062970.2.1	aminopeptidase P1	**0.92**
Solyc11g066560.1.1	vacuolar protein sorting 41	**0.91**
Solyc11g039840.1.1	Ubiquinol-cytochrome C reductase iron-sulfur subunit	**0.91**
Solyc05g005750.2.1	trehalose phosphate synthase	**0.91**
Solyc01g058730.2.1	Unknown	**0.91**
Solyc07g008320.2.1	autoinhibited Ca(2+)-ATPase 10	**0.90**
Solyc01g087250.2.1	carotenoid cleavage dioxygenase 1	**0.90**
Solyc02g062110.2.1	Protein of unknown function (DUF1712)	**0.90**
Solyc02g020980.2.1	disproportionating enzyme 2	**0.89**
Solyc06g019170.2.1	delta1-pyrroline-5-carboxylate synthase 1	**0.89**
Solyc03g098790.1.1	Kunitz family trypsin and protease inhibitor protein	**0.89**
Solyc06g008520.2.1	BET1P/SFT1P-like protein 14A	**0.89**
Solyc03g113730.2.1	B12D protein	**0.89**
Solyc09g065540.2.1	methylcrotonyl-CoA carboxylase alpha chain(MCCA)	**0.88**
Solyc08g080240.2.1	Cox19-like CHCH family protein	**0.88**
Solyc11g065920.1.1	xanthine dehydrogenase 1	**0.88**
Solyc05g052200.2.1	Protein kinase family protein with ARM repeat domain	**0.88**
Solyc04g048900.2.1	calreticulin 3	**0.88**
Solyc04g082700.2.1	tonoplast monosaccharide transporter2	**0.87**
Solyc11g072880.1.1	endomembrane-type CA-ATPase 4	**0.87**
Solyc07g032100.2.1	Coatomer. alpha subunit	**0.87**
Solyc07g056010.2.1	Unknown	**0.87**
Solyc05g054350.2.1	alpha/beta-Hydrolases superfamily protein	**0.87**
Solyc07g064910.2.1	EPS15 homology domain 1	**0.87**
Solyc06g009530.2.1	Carbohydrate-binding-like fold	**0.86**
Solyc02g084690.2.1	FG-GAP repeat-containing protein	**0.86**
Solyc04g076430.2.1	RAB geranylgeranyl transferase alpha subunit 1	**0.86**
Solyc06g066790.2.1	tetratricopeptide repeat (TPR)-containing protein	**0.86**
Solyc00g059500.1.1	aminoalcoholphosphotransferase 1	**0.85**
Solyc03g093830.2.1	Encodes a close homolog of the Cauliflower OR (Orange) protein.	**0.85**
Solyc12g014250.1.1	phosphoenolpyruvate carboxylase 1	**0.85**
Solyc06g007320.2.1	ubiquitin-activating enzyme 1	**0.84**
Solyc09g031600.2.1	sorting nexin 2B	**0.84**
Solyc01g106770.2.1	target of rapamycin	**0.84**
Solyc03g111720.2.1	peptidemethionine sulfoxide reductase 1	**0.83**
Solyc01g006360.2.1	glucan synthase-like 10	**0.83**

Solyc04g080340.2.1	flavodoxin family protein / radical SAM domain-containing protein	**0.83**
Solyc01g112240.2.1	alpha-1.3-mannosyl-glycoprotein beta-1.2-N-acetylglucosaminyltransferase	**0.82**
Solyc02g082350.2.1	plant intracellular ras group-related LRR 4	**0.82**
Solyc03g097440.2.1	hydroxysteroid dehydrogenase 1	**0.81**
Solyc03g083970.2.1	BCL-2-associated athanogene 7	**0.81**
Solyc02g067470.2.1	SPFH/Band 7/PHB domain-containing membrane-associated protein family	**0.81**
Solyc09g015670.2.1	vacuolar sorting receptor homolog 1	**0.81**
Solyc02g085350.2.1	succinate dehydrogenase 1-1	**0.80**
Solyc05g008600.2.1	Aldolase superfamily protein	**0.80**
Solyc04g055170.2.1	annexin 2	**0.80**
Solyc02g088270.2.1	Unknown	**0.79**
Solyc09g090140.2.1	Lactate/malate dehydrogenase family protein	**0.78**
Solyc03g097250.2.1	Unknown	**0.78**
Solyc07g005210.2.1	temperature-induced lipocalin	**0.78**
Solyc03g120700.2.1	Vps51/Vps67 family (components of vesicular transport) protein	**0.78**
Solyc10g012370.2.1	cysteine synthase C1	**0.77**
Solyc01g005520.2.1	protein containing PDZ domain. a K-box domain. and a TPR region	**0.77**
Solyc07g066610.2.1	Phosphoglycerate kinase family protein	**0.76**
Solyc12g009990.1.1	signal recognition particle receptor alpha subunit family protein	**0.76**
Solyc01g006280.2.1	10-formyltetrahydrofolate synthetase	**0.75**
Solyc02g087290.2.1	golgi alpha-mannosidase II	**0.73**
Solyc07g061790.2.1	SOUL heme-binding family protein	**0.73**
Solyc01g087730.2.1	Ribosomal protein L1p/L10e family	**0.73**
Solyc03g111570.2.1	glucan synthase-like 8	**0.72**
Solyc04g058070.2.1	UDP-sugar pyrophosphorylase	**0.72**
Solyc07g062530.2.1	phosphoenolpyruvate carboxylase 3	**0.71**
Solyc08g043170.2.1	delta1-pyrroline-5-carboxylate synthase 1	**0.71**
Solyc04g009960.2.1	threonine aldolase 1	**0.71**
Solyc01g097880.2.1	Cytidine/deoxycytidylate deaminase family protein	**0.71**
Solyc04g025990.2.1	Potassium transporter family protein	**0.70**
Solyc03g111560.2.1	glucan synthase-like 8	**0.70**
Solyc05g051570.2.1	RAB GTPase homolog H1E	**0.70**
Solyc11g010480.1.1	Unknown	**0.70**
Solyc03g113400.2.1	H(+)-ATPase 11	**0.70**
Solyc01g110290.2.1	squalene synthase 1	**0.70**
Solyc08g005800.2.1	Pectinacetylesterase family protein	**0.69**
Solyc07g064610.2.1	calmodulin-domain protein kinase 9	**0.69**
Solyc08g023440.2.1	Early-responsive to dehydration stress protein (ERD4)	**0.69**
Solyc02g080630.2.1	glyoxalase I homolog	**0.69**
Solyc09g082460.2.1	homocysteine S-methyltransferase 3	**0.69**
Solyc01g090550.2.1	DNAJ homologue 2	**0.68**
Solyc07g019440.2.1	ADPGLC-PPase large subunit	**0.67**
Solyc07g055320.2.1	FtsH extracellular protease family	**0.66**
Solyc10g045220.1.1	photosynthetic electron transfer A	**0.66**
Solyc12g088450.1.1	Unknown	**0.66**

Solyc08g066690.2.1	Exostosin family protein	**0.66**
Solyc10g047320.1.1	Disease resistance protein (CC-NBS-LRR class) family	**0.65**
Solyc04g082250.2.1	FtsH extracellular protease family	**0.64**
Solyc08g008210.2.1	vacuolar ATP synthase subunit E1	**0.64**
Solyc05g010340.2.1	Phosphoribulokinase / Uridine kinase family	**0.61**
Solyc02g067580.2.1	B12D protein	**0.61**
Solyc01g080280.2.1	glutamine synthetase 2	**0.58**
Solyc06g065990.1.1	ATPase. F0 complex. subunit B/B'. bacterial/chloroplast	**0.56**
Solyc10g085230.1.1	UDP-glucosyl transferase 76E1	**0.56**
Solyc07g006380.2.1	low-molecular-weight cysteine-rich 75	**0.52**
Solyc03g115980.1.1	Pyridine nucleotide-disulphide oxidoreductase family protein	**0.39**
Solyc06g063370.2.1	light harvesting complex of photosystem II 5	**0.32**
Solyc10g007690.2.1	photosystem I light harvesting complex gene 3	**0.24**
Solyc02g079950.2.1	photosystem II subunit Q-2	**0.23**
Solyc07g066150.1.1	photosystem I subunit G	**0.11**

Table R4. Group B up-regulated proteins
*numbers in bold are statistically significant ($p<0.05$)

Tomato accession	Description	Ratio E8:amiR1/O*
Solyc05g015060.2.1	P-loop containing nucleoside triphosphate hydrolases superfamily protein	**2.34**
Solyc01g109920.2.1	Dehydrin family protein	**1.99**
Solyc04g064870.2.1	pathogenesis-related family protein	**1.75**
Solyc05g055870.2.1	F-box family protein	**1.66**
Solyc09g010280.2.1	LETM1-like protein	**1.63**
Solyc02g082760.2.1	catalase 2	**1.50**
Solyc03g097670.2.1	DNA binding;ATP binding	**1.49**
Solyc03g123630.2.1	pectin methylesterase 3	**1.47**
Solyc11g013810.1.1	nitrate reductase 2	**1.45**
Solyc02g069640.2.1	gamma-soluble NSF attachment protein	**1.43**
Solyc10g085040.1.1	SOUL heme-binding family protein	**1.42**
Solyc01g100650.2.1	haloacid dehalogenase-like hydrolase family protein	**1.39**
Solyc05g052480.2.1	histidine acid phosphatase family protein	**1.39**
Solyc03g114640.2.1	signal peptide peptidase	**1.38**
Solyc09g065550.2.1	kinase interacting (KIP1-like) family protein	**1.36**
Solyc02g072160.2.1	NAD(P)-binding Rossmann-fold superfamily protein	**1.35**
Solyc03g082720.2.1	Yippee family putative zinc-binding protein	**1.34**
Solyc02g078950.2.1	beta-galactosidase 8	**1.34**
Solyc11g006300.1.1	3-oxo-5-alpha-steroid 4-dehydrogenase family protein	**1.34**
Solyc04g009630.2.1	Glycosyl hydrolases family 31 protein	**1.31**
Solyc03g034140.2.1	Quinone reductase family protein	**1.30**
Solyc03g114580.2.1	Phosphoribulokinase / Uridine kinase family	**1.29**
Solyc03g097110.2.1	RNA-binding (RRM/RBD/RNP motifs) family protein	**1.25**
Solyc02g062700.2.1	AAA-type ATPase family protein	**1.25**
Solyc02g086600.2.1	polyribonucleotide nucleotidyltransferase. putative	**1.24**

Solyc03g117430.2.1	plastid transcriptionally active 17	**1.24**
Solyc07g043320.2.1	Unknown	**1.24**
Solyc07g022910.2.1	Unknown	**1.23**
Solyc11g006550.1.1	uricase / urate oxidase / nodulin 35. putative	**1.23**
Solyc09g064200.2.1	myosin 2	**1.23**
Solyc12g099360.1.1	acyl-activating enzyme 7	**1.23**
Solyc09g059040.2.1	Oxidoreductase. zinc-binding dehydrogenase family protein	**1.22**
Solyc10g081650.1.1	carotenoid isomerase	**1.22**
Solyc07g053830.2.1	ADP/ATP carrier 3	**1.22**
Solyc03g095620.2.1	Protein kinase superfamily protein	**1.22**
Solyc04g072400.2.1	Unknown	**1.21**
Solyc07g042550.2.1	sucrose synthase 4	**1.21**
Solyc07g056420.2.1	glutathione S-transferase TAU 25	**1.20**
Solyc05g055000.2.1	chloroplastic NIFS-like cysteine desulfurase	**1.20**
Solyc02g077240.2.1	pyruvate decarboxylase-2	**1.19**
Solyc11g027810.1.1	RING/U-box protein with domain of unknown function (DUF 1232)	**1.18**
Solyc10g008640.2.1	diacylglycerol kinase 5	**1.17**
Solyc03g026320.2.1	non-intrinsic ABC protein 8	**1.17**
Solyc05g005490.2.1	beta carbonic anhydrase 4	**1.16**
Solyc01g007920.2.1	nicotinamidase 2	**1.16**
Solyc11g066130.1.1	Pathogenesis-related thaumatin superfamily protein	**1.15**
Solyc02g070810.2.1	embryo defective 3012	**1.15**
Solyc01g099100.2.1	long-chain acyl-CoA synthetase 7	**1.14**
Solyc07g009320.2.1	metaxin-related	**1.13**
Solyc04g054310.2.1	alanine:glyoxylate aminotransferase 2	**1.12**
Solyc11g019920.1.1	PDI-like 5-2	**1.12**
Solyc01g106050.2.1	dynamin-related protein 3A	**1.11**
Solyc11g040390.1.1	aspartate kinase-homoserine dehydrogenase i	**1.11**
Solyc05g053590.2.1	pleiotropic drug resistance 12	**1.11**
Solyc08g075720.1.1	Ribosomal L18p/L5e family protein	**1.10**
Solyc05g018130.2.1	2-oxoglutarate (2OG) and Fe(II)-dependent oxygenase superfamily protein	**1.09**
Solyc05g052510.2.1	Clathrin. heavy chain	**1.09**
Solyc06g051730.2.1	ABC2 homolog 9	**1.09**
Solyc08g080110.2.1	Protein of unknown function (DUF544)	**1.09**
Solyc12g044740.1.1	ubiquitin-specific protease 6	**1.06**

We next used MapMan software (http://mapman.gabipd.org) to cluster the potential Clp targets in Tables R2 and R3 in different groups depending on the biological process they are involved in. Then, we used that data to calculate the percentage of proteins in each biological process. In parallel, we made the same calculation with a WT-R proteome. Finally, we compared both data sets to find out those biological processes that were differentially represented (Figure R38). We

observed that proteins involved in plastidial processes like photosynthesis (PS), nitrogen (N) metabolism, and secondary metabolism were over-represented in the list of putative Clp targets. Other over-represented processes were cell wall, nucleotide, and carbohydrate (CHO) metabolism. In contrast, other functional groups are under–represented, likely as a secondary effect of the loss of Clp protease activity (Figure R38).

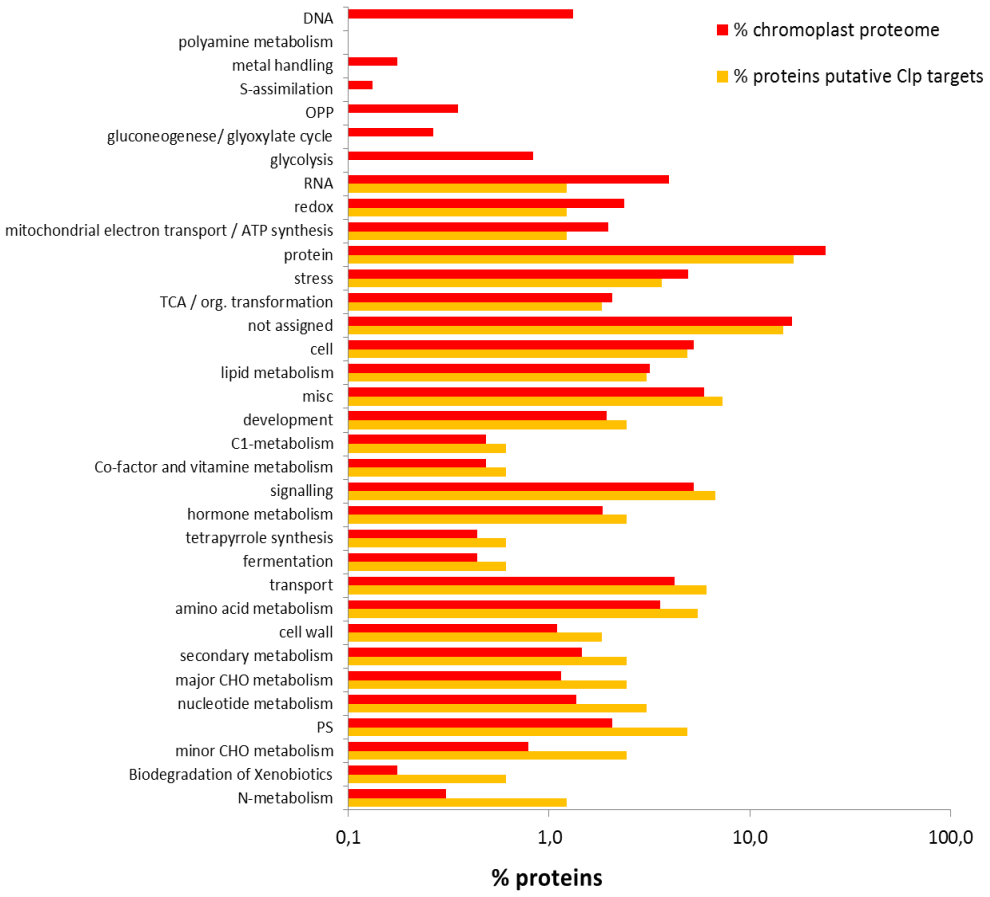

Figure R38. Decreased Clp activity in tomato fruit affects the levels of proteins involved in specific biological processes. The data represents % of proteins in the MapMan functional classes in WT-R samples (red bars) and in Tables I and II (orange bars).

As mentioned before, the effect of a reduction in Clp protease activity in the chloroplast proteome has been extensively studied in Arabidopsis plants. So, we decided to compare the impact of silencing Clp in Arabidopsis chloroplasts and in tomato fruit chromoplasts. To do so, we created a list with proteins found to be mis-regulated in, at least, one of the following Arabidopsis mutants: *clpr1*, *clpr2*, *clpr4* and *clpp3* (Stanne et al., 2009; Zybailov et al., 2009; Kim et al., 2009). Then, we classified

these proteins by biological processes using a similar strategy to that explained before, with the only difference that as a control we used the whole Arabidopsis proteome. To facilitate interpretation, we calculated a variable named Enrichment factor (EF). The EF was determined as the proportion of proteins of a given MapMan class in the proteome of Clp-defective mutants relative to the proportion of proteins of the same class in the proteome of Arabidopsis WT plants. EF was also calculated for tomato Clp-defective fruits by dividing the % of proteins of a given MapMan class in Tables R3 and R4 by the total number of protein identified the WT-R proteome. Figure R39 shows the comparison between EF values in Arabidopsis in tomato.

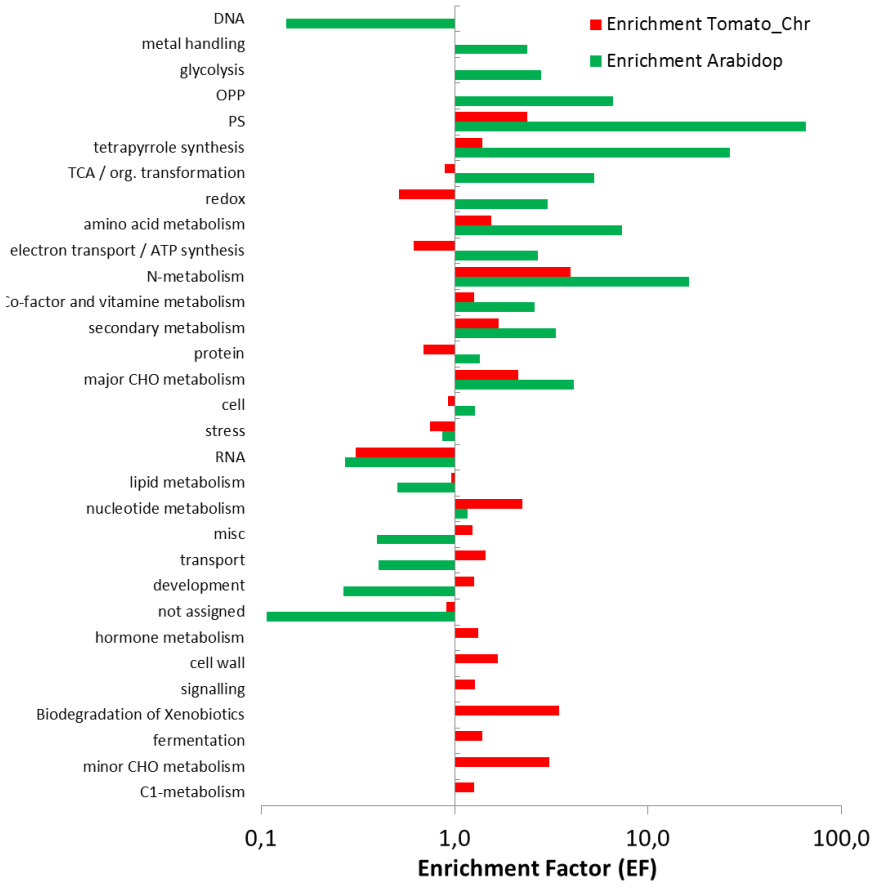

Figure R39. The Clp protease complex has both conserved and plastid-specific targets. Comparison of the enrichment factor (EF) of MapMan functional classes when Clp protease activity decreases in tomato fruits (red bars) and Arabidopsis seedlings (green bars).

We observed that tomato fruit (chromoplasts) and Arabidopsis seedlings (chloroplasts) share putative Clp targets involved in similar biological processes but also include proteins implicated in completely different processes. For instance, as expected

for a photosynthetic plastid, proteins involved in PS and chlorophyll metabolism (tetrapyrrole biosynthesis) are mainly enriched in chloroplasts of Clp-defective seedlings and not so much in fruit chromoplasts. Oppositely, proteins involved in nucleotide, hormone and cell wall metabolism, transport and signaling are enriched in the Clp-defective fruits. In the “development” group, storage proteins were found to be over-represented in tomato fruits. From these data, we conclude that the Clp protease likely controls both common and distinct pathways in chloroplasts and chromoplasts, consistent with the differential protein composition and function of these two plastid types.

The rate-limiting enzymes of the MEP and carotenoid pathways might be targets of the Clp protease in tomato fruit chromoplasts

Following our initial hypothesis based on the accumulation of active DXS enzymes in Arabidopsis mutants with reduced Clp protease activity (Flores-Perez et al. 2008; Pulido et al. 2016) and western blot data showing a decline in DXS protein levels during tomato fruit ripening (Figure R34) and an accumulation in amiR1 fruits (Figure R34), we expected to observe higher DXS protein levels in #R94-R samples compared to WT-R or WT-O samples. While we did not obtain any significant differences in the levels of DXS when comparing these samples, we did observe the expected tendency of higher DXS accumulation in Clp-defective chromoplasts (Figure R40). Similarly, other proteins involved in carotenoid biosynthesis, including PSY1, displayed a similar partner. By contrast, ClpR1 and other ClpPR subunits detected in our proteomics experiment were down-regulated (albeit not significantly) in ripe amiR1 fruits compared to WT controls, as expected (Figure R40).

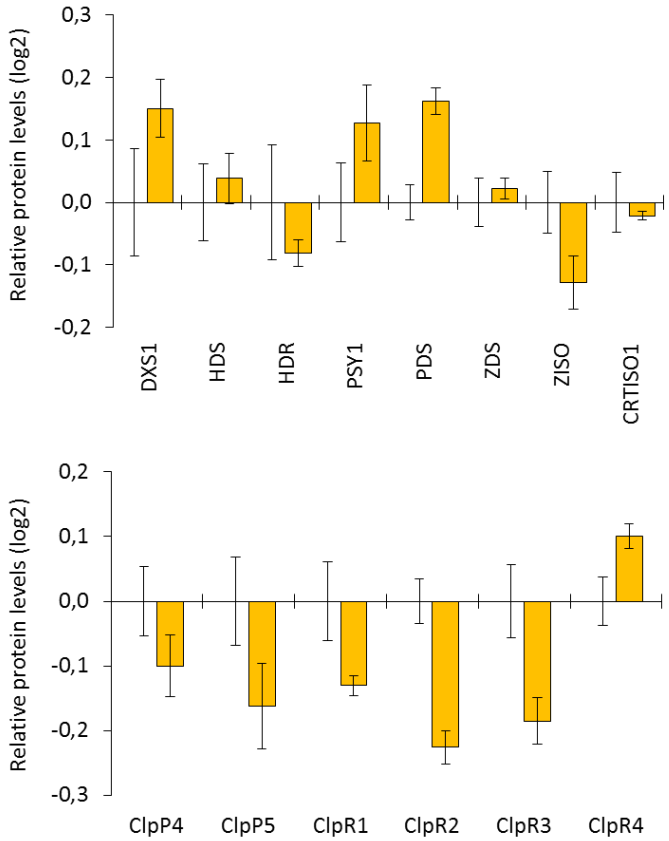

Figure R40. Changes in the level of proteins of the MEP and carotenoid pathways and the Clp protease core in Clp-defective E8:amiR1 fruits. Data correspond to mean and SEM values of TMT quantitative results for the indicated proteins in #R94-R (orange columns) and WT-R samples relative to the levels in WT-R. No statistically significant differences were found.

To evaluate whether the differences in the levels of PSY enzyme deduced from the proteomic data were real, we carried out Western blot analysis of protein samples from ripe WT and amiR1 (#R94) fruits. As shown in Figure R30a, we found that PSY proteins were over-accumulated in E8:amiR1 fruits. Quantification of the data from several blots showed a similar degree of accumulation of DXS and PSY enzymes in fruits with decreased Clp protease activity (Figure R41a). These data not only confirm the tendency observed in the proteomic (TMT) experiments and our previous results with DXS (Figure R34), but also suggest for the first time that the main rate-limiting enzyme of the carotenoid pathway, PSY, might be a Clp protease target. In agreement with this conclusion, incubation of ripe fruit pericarp fragments in the presence of the protein synthesis inhibitor cycloheximide resulted in a lower degradation rate for PSY in amiR1 (#R94) fruits compared to WT controls (Figure R41b).

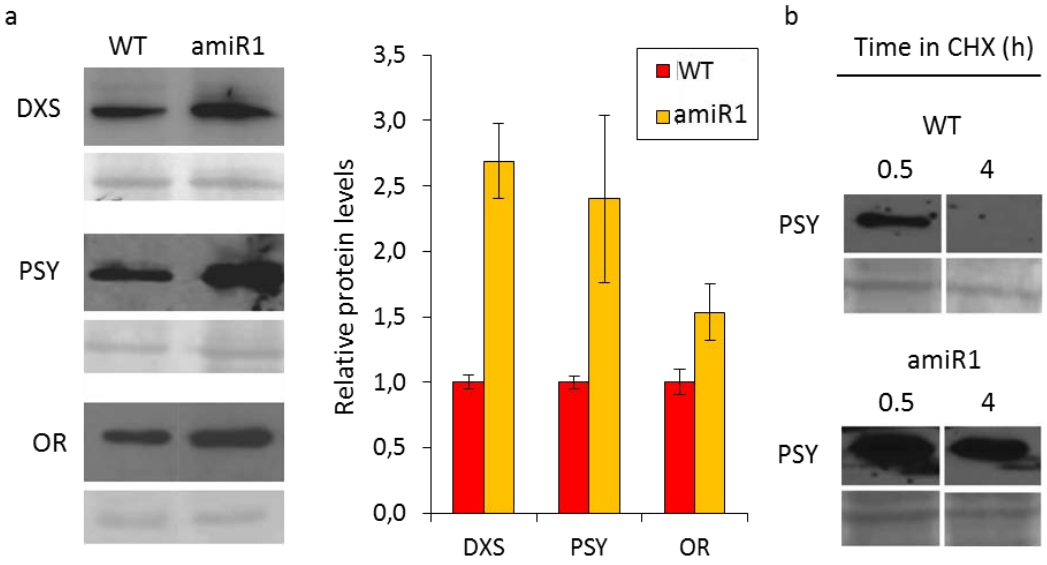

Figure R41. Western blot analysis of proteins involved in carotenoid biosynthesis in tomato fruit with decreased Clp protease activity. (a) Western blot analysis of the levels of the indicated proteins in ripe fruit of WT and amiR1 (#R94) lines. The left panel shows representative blots whereas the graph shows quantitative data (mean and SEM) from several blots corresponding to n>3 fruits. PSY protein levels were determined by densitometry, normalized to loading controls, and represented relative to the WT samples. (b) Western blot analysis of PSY protein levels in WT and amiR1 (#R94) pericarp samples cut from the fruit and incubated in the presence of cycloheximide (CHX) for the indicated times. Lower panels in all the Western blots correspond to loading controls.

Strikingly, a tomato protein with homology to the DnaJ-like co-chaperone Orange (OR) protein involved in regulating PSY protein stability was found among the putative Clp protease candidates in the fruit (Solyc03g093830.2.1, Table R3). OR has been proposed to trigger chromoplastogenesis, promoting the accumulation of β-carotene (Yuan et al., 2015; Li and Yuan, 2013). In addition, it has been demonstrated that it can physically interact with PSY enzymes to increase its stability and enzyme activity, possibly by promoting correct folding or preventing proteolytic degradation (Zhou et al., 2015). As expected from the TMT data (Table R3), Western blot analysis showed that the levels of the tomato OR protein decreased during ripening in WT fruit (Figure R42). Most interestingly, this decrease was prevented when Clp protease activity was reduced in amiR1 fruits (Figure R42), eventually resulting in the accumulation of higher OR levels in the ripe fruit of the transgenic plants compared to WT controls (Figure R41 and Figure R42).

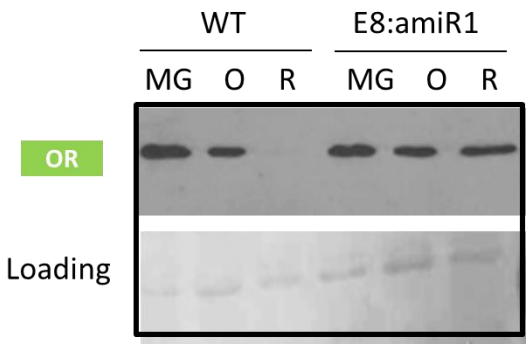

Figure R42. Western blot analysis of tomato OR levels during fruit ripening. A representative blot is shown (note that the lane corresponding to WT fruits at the MG and R stages contains less protein than the rest).

Discussion

Section I

A role for shade signaling on the regulation of carotenoid biosynthesis during tomato fruit ripening

The self-shading model: recycling of a PIF-based mechanism to monitor tomato fruit ripening.

As carotenoids are essential for photoprotection and contribute to the communication of plants with their environment via colored carotenoid pigments and apocarotenoid hormones and volatiles, it is not surprising that their production is tightly regulated by different environmental factors, including light (Ruiz-Sola and Rodriguez-Concepción, 2012; Azari et al., 2010; Fraser and Bramley, 2004). In many fleshy fruits, including tomatoes, carotenoids accumulate during ripening and provide bright colors as a signal of ripeness for animals to disperse the enclosed seeds only when their development has been completed and hence are fertile. For example, carotenoids give yellow color to bananas, orange color to peaches and oranges, and red color to tomatoes. Carotenoid-derived products (including apocarotenoids aromas) also contribute to the function of attracting animals that disperse mature seeds.

In the second chapter of this Thesis, I showed that carotenoid biosynthesis in ripening tomatoes is regulated by a PIF-based molecular mechanism virtually identical to that regulating carotenogenesis in response to light in Arabidopsis as both are based on specifically repressing PSY-encoding genes to inhibit carotenoid biosynthesis when PHYs are inactivated (e.g. in the dark or under shade). A striking difference, however, is that this mechanism appears to fulfill a completely new function in tomato fruit, as it uses signals usually involved in an inter-plant communication process (the shade avoidance syndrome or SAS) to sense the progression of an endogenous developmental process (i.e. ripening). The SAS is an important biological process triggered by a decrease in the R/FR ratio that allows plants to respond to the presence of nearby vegetation (i.e. potential light-competing neighbors) by allowing them to adapt their growth (e.g. elongate in search of light) and hence improve fitness. Because

changes in the R/FR ratio also occur within the pericarp of tomato fruit during ripening, SAS components could be readapted in this system to gather information on the progression of ripening based on the levels of chlorophyll.

Fruits can be viewed as modified leaves that, besides enclosing the seeds, have suffered a change in organ geometry, namely, a shift from a nearly planar conformation to an expanded three-dimensional anatomy. This anatomy imposes spatial constrains coercing light to pass through successive cell layers, so that the quality of the light that reaches inner sections of the fruit is influenced by the pigment composition of cells located in the outer pericarp sections. A self-shading effect due to the presence of high R-absorbing chlorophyll levels in green fruit alters the spectral composition of the light that penetrates the pericarp, resulting in a low R/FR ratio that maintains a relatively high proportion of PHYs in their inactive Pr form. In this context, PIF1a accumulates and represses *PSY1* gene expression by directly binding to its promoter (Figure R7 and R9). When the ripening developmental program starts, chlorophylls begin to degrade, progressively reducing the self-shading effect and consequently displacing the photoequilibrium of PHYs to their active Pfr form. This promotes PIF1a degradation, resulting in *PSY1* derepression and a subsequent boost in carotenoid biosynthesis (Figure R8). A model summarizing the proposed mechanism is presented in Figure D1.

Similar to the general mechanism involved in the PIF-mediated control of carotenoid biosynthesis in Arabidopsis shoot tissues, tomato PIF1a might be part of an antagonistic module to regulate the expression of the *PSY1* gene in tomato fruit. Thus, the levels of transcripts encoding direct negative regulators such as PIF1a (Figure R3), but also direct positive regulators such as RIN and FUL1 (Fujisawa et al., 2013, 2014; Martel et al., 2011) increase during ripening, finely tuning the expression of *PSY1*. This might function as a gas-and-brake mechanism to provide a more robust control of *PSY1* expression during ripening, similar to that proposed to regulate Arabidopsis *PSY* expression and carotenoid biosynthesis in response to light and temperature cues (Bou-Torrent et al., 2015; Toledo-Ortiz et al., 2014). However, we speculate that the main function of PIF1a during ripening is to modulate the developmental control of *PSY1* expression and hence carotenoid biosynthesis by finely adjusting the transcription rate of the gene to the actual progression of ripening (Figure D1). Based on the described data, we propose that the developmental induction of *PSY1* expression

directly mediated by general ripening activators like RIN would be additionally promoted by a reduced PIF1a activity when chlorophylls degrade at the onset of ripening (due to the pigmentation-derived increase in the R/FR ratio). As ripening progresses, however, increasing levels of *PIF1a* transcripts might produce more protein as a buffering mechanism to counterbalance the positive effects of transcriptional activators on *PSY1* expression.

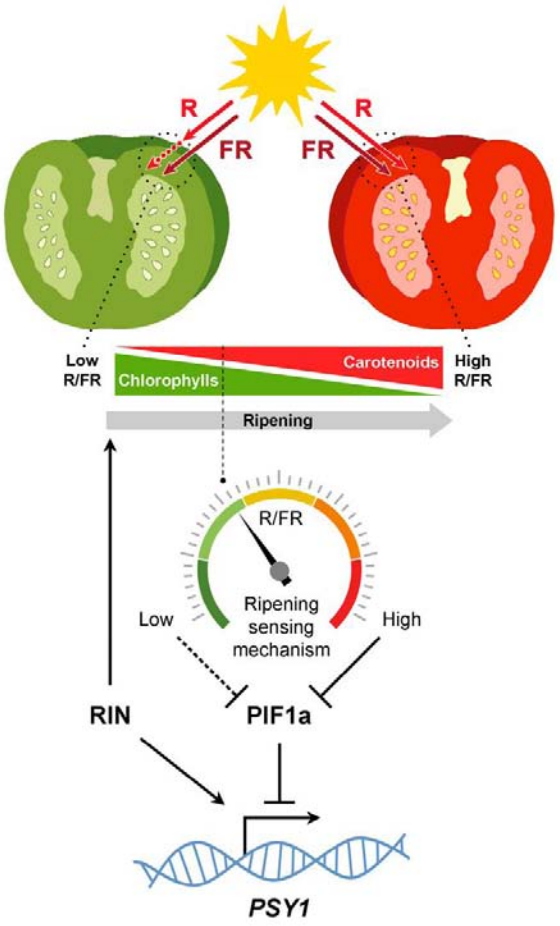

Figure D1. Self-shading model for the light mediated modulation of carotenoid biosynthesis in tomato fruits. Chlorophylls in green fruits preferentially absorb R light, generating a self-shading effect characterized by low R/FR ratios that maintain PHYs predominantly in the inactive form and relatively high levels of PIF1a repressing *PSY1*. Once seeds mature, the developmental program induces the expression of genes encoding master activators of the ripening process. Some of them, like RIN and FUL1/TDR4, induce *PSY1* gene expression directly. Chlorophyll breakdown reduces the self-shading effect so that the R/FR ratio within the cells gradually increases, consequently displacing PHYs to their active form, reducing PIF1a levels and derepressing *PSY1* expression. By sensing the spectral composition of the light filtered through the fruit pericarp, this mechanism diagnoses actual ripening progression to finely adjust fruit carotenoid biosynthesis.

It is striking that the described self-shading pathway specifically targets *PSY1*, the main gene controlling the metabolic flux into the carotenoid pathway during tomato ripening (Figures R14 and R15). Indeed, the specificity observed in the regulation of *PSY,* is in parallel with that previously described in Arabidopsis, where PIF1 specifically targets the *PSY* gene to regulate the whole carotenoid pathway (Toledo-Ortiz et al., 2010). Although *cis*-elements for PIF1a binding were found in the

promoter of important ripening master regulator genes such as *RIN,* RT-qPCR experiments showed that, at least in our experimental conditions, they are not regulated by this transcription factor (Figure R15). However, we cannot exclude the possibility that other ripening-dependent genes are being regulated by this transcription factor. ChIP-seq and RNA-seq approaches will be carried out in the lab to further characterize PIF1a-regulated genes (both direct and indirect) to further explore the role of this transcription factor beyond carotenoid biosynthesis during tomato fruit ripening.

It remains unknown whether the same mechanism is also active in tomato leaves or deetiolating tomato seedlings. If so, other PIF homologues and PSY-encoding genes might be involved, as PIF1a and PSY1 appear to be mostly restricted to fruit ripening. While it is possible that the direct transcriptional control of genes encoding PSY by PIF transcription factors may be a conserved mechanism in nature for the light-mediated regulation of the carotenoid pathway, PIFs are not required to regulate *PSY* expression in Arabidopsis roots in response to ABA or salt signals that promote a root-specific up-regulation of *PSY* (Ruiz-Sola et al., 2014). These results suggest that PIFs might only be relevant for the control of *PSY* gene expression and carotenoid biosynthesis in organs that are normally exposed to light.

Carotenoids and seed-dispersion: an evolutionary perspective

Based on the widespread occurrence of ripening-associated fruit pigmentation changes as an adaptive characteristic for attracting animals that disperse viable seeds, we propose that similar PIF-mediated mechanisms might operate in other plant species bearing fleshy fruits that lose their green color and accumulate pigments when ripe. Translation of molecular insights from tomato to other fleshy-fruited plants has indicated that many regulatory networks are conserved across a wide range of species (Seymour et al., 2013). Thus, given the ubiquitous nature of PHYs in land plants and the widespread occurrence of ripening-associated fruit pigmentation changes that typically involve the substitution of an initially chlorophyll-based green color with distinctive non-green (i.e. non-R-absorbing) eye-catching colors, it is possible that similar self-shading regulatory mechanisms might operate in other fruits with an exocarp thick enough that allows the differential absorption of light and hence to inform on the

actual stage of ripening (based on the pigment profile of the fruit at every moment) and thus finely coordinate fruit color change (Llorente et al., 2016).

From an evolutionary perspective, light signaling pathways already established in land plants may have had the chance to explore novel phenotypic space in fleshy fruits. Subsequent adaptations under selection in the fruit may have then integrated these pathways as modulatory components of the pigmentation process during ripening. For instance, the self-shading regulation of the tomato fruit carotenoid pathway likely evolved by co-option of components from the preexisting shade-avoidance responses (Mathews, 2006; Casal et al., 2013). Having been color cues a relevant factor determining visually driven selection in Cretaceous animals, as it is now becoming clear (Eriksson 2014), the establishing of fruit colors as ripening signals may actually be a legacy from the time when dinosaurs walked the earth.

Section II

A role for the Clp protease complex during tomato fruit ripening

A role for the Clp protease in carotenoid biosynthesis

During the last decades, tomato has become a model plant to study molecular and metabolic events associated with fleshy fruit development, specifically the ripening process. In the case of tomato fruit, the progression of ripening involves an enhancement in the levels of carotenoids such as lycopene (a red pigment that prevents some types of cancer) and β-carotene (an orange pigment used as the main precursor of vitamin A). Ripening also triggers the development of appropriate structures for carotenoid storage after the differentiation of chloroplasts into specialized plastids named chromoplasts. This system has also gained relevance as a biotechnological platform to generate fruits with enhanced levels of these health-promoting metabolites.

In tomato fruit, an increase in the levels of the MEP pathway rate-limiting enzyme DXS results in higher levels of total carotenoids (Lois et al., 2000; Enfissi et al., 2005). In addition to transcriptional regulation of DXS-encoding genes, the accumulation of active DXS enzymes in Arabidopsis is regulated by the chloroplastidial Clp protease complex (Pulido et al., 2013, 2016). In this thesis we aimed to explore a novel way to generate tomato fruits with enhanced levels of carotenoids based on the manipulation of the Clp protease complex (and hence of DXS protein levels) in tomato fruit chromoplasts.

Most of the studies regarding the structure, stoichiometry and protein targets of the Clp protease were centered in Arabidopsis (i.e. in chloroplasts). However, much less was known about the composition, nature and role of the Clp protease complex in other plants and plastidial contexts (Barsan et al., 2012; Nishimura and van Wijk, 2015). Initially, we found that Arabidopsis and tomato might have a similar Clp protease complex composition (Figures R19, R20 and R21). Phylogenetic studies revealed that

the tomato genome has one homologue for each Arabidopsis Clp subunit, with only one exception: ClpP1 (Figure R19). In this particular case, we detected two very close ClpP1 homologues, that we named ClpP1a and ClpP1b. In Arabidopsis and tobacco, ClpP1 is the only Clp protease subunit encoded in the plastome (plastid genome). In the case of tomato, an identical sequence encoding ClpP1a was retrieved from the tomato plastid genome and the nuclear genome (Solyc01g007490). As the latter is actually flanked by other sequences belonging to the plastome, we speculate that this might be an assembly artifact. We therefore conclude that the two sequences likely correspond to the same plastome gene. On the other hand, the gene encoding ClpP1b (Solyc09g065790) was found exclusively in the nuclear genome. More interestingly, analysis of the two tomato ClpP1 subunits showed that only the plastome-encoded ClpP1a has the catalytic amino acid triad (Figure R20). Finally, if *ClpP1b* was expressed (i.e. if transcripts were found in any experimental condition different to those tested in this work), it might not produce a plastidial protein since ClpP1b seems to lack a plastid transit peptide. Based on these data, I hypothesize that *ClpP1b* is probably a pseudo-gene. Supporting a scenario of non-active ClpP1-encoding genes, it has been shown that *Acacia ligulata* encodes for an inactive *ClpP1* in its plastome. However, the existence of an active nuclear-encoded ClpP1 isoform was not reported (Williams et al., 2015). In any case, it is highly probable that tomato has a Clp protease complex with a similar gene dose (*ClpP1*; *ClpP3-6* and *ClpR1-4*) to Arabidopsis, with ClpP1 activity provided by the plastome.

Based on previous results, transgenic tomato fruits with a reduced Clp protease activity were generated by silencing the *ClpR1* subunit during ripening (E8:amiR1 lines). These transgenic fruits were shown to accumulate higher amounts of β-carotene than control fruits when fully ripe, which we propose to be responsible for their characteristic orange color (Figure R31). Our proteomic analysis did not allow concluding whether the described phenotype results from an altered accumulation of the enzymes that produce β-carotene from lycopene or that transform β-carotene into downstream xanthophylls or apocarotenoids (Figure R40). This is similar to other proteomic studies of fruit ripening, which also failed in identifying biosynthetic enzymes downstream of lycopene (Wang et al. 2013). However, we did detect the presence of higher levels of rate-determining enzymes of the MEP pathway (DXS) and

the carotenoid pathway (PSY) in Clp-defective fruits (Figure R40 and Figure R41). Thus, it is expected that the isoprenoid precursors IPP and DMAPP are overproduced and more efficiently channeled to the carotenoid biosynthesis pathway in transgenic fruits. The fact that a decrease in the Clp protease activity triggers an increment in the levels of the DXS protein suggests that DXS could be a Clp protease target in tomato fruit chromoplasts, in agreement with our initial hypothesis. Hence, we conclude that DXS is a conserved Clp protease target in chloroplasts and chromoplasts (Figure R34). This conclusion provides an explanation to the sharp decrease in the levels of the DXS protein observed during tomato fruit ripening, as this inversely correlates with the up-regulation of the subunits of the Clp protease transcripts (Figure R34b). Nevertheless, these observations are quite surprising. Previous studies have shown that an increase in *DXS1* transcripts could support the production of higher DXS enzyme levels to supply the isoprenoid precursors needed to boost carotenoid biosynthesis during tomato fruit ripening (Lois et al., 2000). Tomato genome encodes three different paralogues with DXS activity named DXS1, DXS2 and DXS3, which contribute to the biosynthesis of isoprenoid precursors in a non-redundant manner. For instance, *DXS1* and *DXS2* transcripts are expressed in MG fruits, but as the ripening proceeds, only *DXS1* is up-regulated, becoming the major isogene expressed in ripe fruits. Although no experimental data regarding their enzymatic properties (vmax and Km) are available to date, we speculate that if DXS1 is more active than DXS2 less protein might be necessary to generate the IPP and DMAPP needed to boost carotenoid production during ripening. Additionally, DXS1 stability might decrease as fruit ripening progresses. In this scenario, the Clp protease might be important to adjust the DXS protein levels during ripening, possibly preventing carotenoid overproduction.

The levels of PSY protein were also found to be higher in fruits with a decreased Clp protease activity (Figure R41). It is worth to mention that the antibody used to detect this enzyme presumably recognize all PSY isoforms (PSY1, PSY2 and PSY3). However, and in agreement with previous reports, in our proteomic experiments we only detected the PSY1 isoform. Even though more experimental evidence is necessary, these results strongly suggest that tomato PSY1 isoform is a target of the Clp protease in tomato fruit chromoplasts. Our findings are in agreement with a recent discovery made in Prof. Li Li's lab (Cornell University) suggesting that the Arabidopsis PSY enzyme

might also be a Clp protease target (personal communication). We therefore speculate that the delivery of both DXS and PSY enzymes to the Clp protease for degradation might be a novel mechanism, ensuring a tight coordination between the MEP pathway and the carotenoid pathway in plants. How this delivery might be regulated (i.e. coordinated) will need to be explored in future work. At the transcriptional level, Fujisawa et al. (2013) showed that the genes encoding DXS1 and PSY1 are both regulated by the master ripening regulator RIN. A tight, coordinated regulation of both transcription rate and the stability/activity of DXS1 and PSY1 during tomato fruit ripening, likely ensures the correct supply of isoprenoid precursors when needed to boost carotenoid production.

An increased flux to the production of carotenoid by upregulated DXS and PSY activities in E8:amiR1 fruits do not fully explain the observed phenotype of β-carotene accumulation in the mutant ripe fruit. So it is likely that other proteins somehow involved in carotenoid production, accumulation (i.e. storage) and/or degradation could also be targets of the Clp protease. Thus, quantitative proteomic analysis was performed to determine potential Clp targets in tomato fruit chromoplasts. Quantitative proteomic approaches allow the identification and quantification of most of the proteins from a particular proteome. Recently, using a free-labeling quantitative proteomic technique, the changes that occur during tomato chloroplast-to-chromoplast transition were identified (Barsan et al., 2012). In addition, the chromoplastidial proteomes of six different carotenoid-enriched crops were also characterized (Wang et al., 2013). In this Thesis, I used a labeling technique named Tandem Mass Tags (TMT) technology to characterize changes associated with a decrease in the Clp protease activity in tomato fruit chromoplasts. Although labeling techniques require additional steps when compared with free-labeling techniques, they have a significant reduction in technical variability, as it is possible to work in multiplexing. In addition, the data processing and comparison is less time-consuming, as the reporter ions (labels) quantify the same peptide from different samples in the same spectrum (Figure R35).

Once data was obtained and processed to check for statistically significant changes, only one carotenoid biosynthetic enzyme was found to be significantly up-regulated ($p<0.05$) in ripe E8:amiR1 fruits (Table R4). The identified enzyme, carotenoid

isomerase 1 (CRTISO1, Solyc10g081650.1.1), is involved in the isomerization of tetra-*cis*-lycopene (i.e. prolycopene, an orange pigment), to the red-colored all-*trans*-lycopene (Figure I5). In agreement, tomato *tangerine* mutants with a deletion in the *CRTISO1* gene (Figure I5) produce orange fruits due to the accumulation of prolycopene (Isaacson et al., 2002). From the fact that both, E8:amiR1 and *tangerine* tomato plants produce orange fruits when ripe, we reasoned that maybe the color of transgenic ripe fruits could be due to the presence of higher amounts of prolycopene because CRTISO1 accumulates in an enzymatically inactive form. Our HPLC method does not to reliably identify and quantify prolycopene and therefore we could not verify whether this carotenoid accumulates at higher levels in transgenic fruits. On the other hand, the statistical analysis of proteomic data also revealed that one of the two carotenoid cleavage dioxygenases of the CCD1 type present in tomato, CCD1A (Solyc01g087250.2), was another putative substrate of the Clp protease in tomato fruit (Table R3). CCD1 enzymes use oxygen to cleave a variety of carotenoid substrates downstream of phytoene, generating volatile (di)aldehydes and ketones. Consistent with its proposed role in contributing to the characteristic flavors and fragances of ripe fruits, CCD1 proteins have been found in most chromoplast proteomes (Vogel et al., 2008; Wang et al., 2013). Additionally, Arabidopsis *ccd1* mutants have increased seed carotenoid content, suggesting a role in carotenoid turnover (Auldridge et al., 2006). Similar to the CCD1B isoform, the tomato CCD1A enzyme cleaves β-carotene to produce the volatile β-ionone during fruit ripening (Simkin et al., 2004). Although it is tempting to speculate that an impaired Clp-mediated degradation of CCD1A might result in the accumulation of inactive enzymes and hence a reduced CCD1A activity and increased β-carotene content in E8:amiR1 fruits, reduced *CCD1A* expression in transgenic tomato plants resulted in lower β-ionone levels but no significant alterations in phytoene, lycopene, β-carotene, or lutein content in the fruit (Simkin et al., 2004). Additionally, and oppositely to E8:amiR1 transgenic fruits, *tangerine* fruits exhibit a significant reduction in all carotenoids downstream prolycopene, including lycopene and β-carotene (Isaacson et al., 2004). Furthermore, it is unclear why decreasing Clp protease activity could lead to higher levels of inactive (instead of active) CRTISO1 or CCD1A enzymes but presumably active DXS1 and PSY1. In Arabidopsis and other systems such as *Chlamydomonas*, loss of Clp protease activity results in the induction of an unfolded

protein response in the chloroplast (Ramundo et al. 2014; Pulido et al. 2016). In the case of DXS, the ClpB3 unfoldase accumulates to disaggregate inactive enzymes, eventually resulting in higher levels of active DXS protein (Pulido et al. 2016). However, it is unknown whether ClpB3 could also reactivate PSY1 or why CRTISO1 and CCD1A would not be regulated by this refolding pathway. In this context, it is difficult to conclude whether the orange color of ripe E8:amiR1 fruits results from a putative accumulation of prolycopene, from a reduced cleavage of β-carotene, from both, or from additional mechanisms.

Our data also indicated that the tomato OR (Orange) protein (Solyc03g093830.2) was another putative Clp protease target (Table R3) that accumulated at higher levels in E8:amiR1 fruits (Figure R42). OR has been shown to be a major post-translational regulator of PSY in Arabidopsis plants, by either stabilizing the enzyme and/or protecting it from degradation (Zhou et al., 2015). Similar to that described above for ClpB3 and DXS in Arabidopsis, it is possible that OR, a protein with similarity to cochaperones, could interact with inactive forms of PSY to promote their refolding. Therefore, an increment in the levels of OR protein might be translated into higher levels of active PSY1 in ripe E8:amiR1 fruits (Figure R41). Additionally, OR has been proposed to be a major factor promoting chromoplast development in several plant systems (Li and Yuan, 2013). The next section will discuss other potential Clp candidates that could also influence the differentiation of chromoplasts and hence the carotenoid storage capacity of plastids.

A role for the Clp protease in chromoplast ultrastructure

Chromoplasts are non-photosynthetic plastids specialized to storage high levels of lipophilic molecules, such as carotenoids. In the case of the tomato fruit, chromoplasts arise from pre-existing chloroplasts during the ripening process (Egea et al., 2011). Although plastid biogenesis is crucial for plant survival, there is not much information regarding the molecular mechanisms directly regulating this process. The only known protein regulating the chromoplastogenesis is the OR protein. Besides its role in PSY stabilization, the mutant version of the *OR (orange)* gene was shown to act as a *bona fide* molecular switch capable of converting non-colored plastids into chromoplasts (Li and Yuan, 2013). Hence, it could be assumed that the OR protein plays an important

role in the interconnection between carotenoid biosynthesis and chromoplastogenesis. In this regard, increased levels of this cochaperone in Clp-deficient fruits (Figure R42) might at least partially explain the atypical chromoplast population, both in structure (Figure R32) and carotenoid content (Figure R33), found in the orange-colored ripe fruits of transgenic E8:amiR1 lines (Figure R38).

In addition, and correlating with the atypical chromoplast ultrastructure (Figure R32), proteins involved in plastid division and plastid structure maintenance were found to be strongly de-regulated in transgenic ripe fruit chromoplasts. For instance while in control fruits the levels of Dynamin-related protein 3A (DRP) (Solyc01g106050) do not change during the transition from O to R stages, they are up-regulated in E8:amiR1 ripe fruits (Table R4). In addition, the ripening-associated decrease in the levels of proteins such as Curvature thylakoid protein 1 (CURT1) (Solyc11g010480) and FtsH homologues (Solyc07g055320 and Solyc04g082250) is attenuated in the E8:amiR1 mutant (Table R3). Dynamin-related proteins (DRPs) belong to a large family of GTPases involved in inter-organellar trafficking and plastid division (Fujimoto and Tsutsumi, 2014). For instance, in the primitive red alga *Cyanidioschyzon*, DRPs were found to localize in the chloroplast division ring (Miyagishima et al., 2003). Similarly, the dynamin-related protein ARC5 is also recruited to the division ring at the outer surface of the chloroplast in plants, and Arabidopsis *arc5* mutants harbor constricted dumbbell-shaped chloroplasts (Miyagishima et al., 2006). On the other hand, CURT1 belongs to a family of plastid-localized proteins involved in chloroplast vesicle transport and grana architecture maintenance (Armbruster et al., 2013). Disruption of the thylakoid membrane-bound metalloprotease FtsH impairs the proper thylakoid membrane formation (Janska et al., 2013). Thus, I conclude that the de-regulation of these proteins might explain some of the features of the atypical chromoplast architecture found in E8:amiR1 fruits.

The Clp protease complex has been studied at different levels, including gene expression. In Arabidopsis and pea, the expression profile of Clp subunit genes during plant development revealed that they are highly expressed in organs where plastids are differentiating (Nishimura and van Wijk, 2015). In the case of tomato, something similar seems to happen. Both public microarrays and RT-qPCR data show that all the Clp protease nuclear-encoded subunits are up-regulated during fruit ripening, that is,

when chloroplast-to-chromoplast transition occurs (Figure R21). Even though previous studies have supported the idea that plastidial PQC systems (including the Clp protease complex) are central players in the differentiation of carotenoid-accumulating chromoplasts during fruit ripening (Barsan et al., 2012; Zeng et al., 2015), to the best of our knowledge, no direct evidence of the role of the Clp protease for plastid differentiation was available until this thesis work. Our data strongly indicate that the tomato Clp protease plays an important role in chromoplast differentiation during tomato fruit ripening, ensuring a proper turnover of proteins involved in carotenoid biosynthesis (DXS, PSY, CRTISO) and degradation (CCD1) but also storage (OR, DRP, CURT1) during chromoplastogenesis. Interference with this process eventually results in altered plastid ultrastructure and carotenoid accumulation.

Section III

All roads lead to Rome: PSY as a central regulator of carotenogenesis in tomato fruit.

Here, I present data that unveil two different molecular mechanisms regulating the production of carotenoids in tomato fruit during ripening. These mechanisms rely on two interconnected layers of regulation. While the PIF-dependent self-shading mechanism adjusts carotenoid biosynthesis to actual ripening by regulating gene expression (i.e. transcription), the Clp protease regulates protein turnover (i.e. post-translational). Interestingly, both mechanisms converged at the level of PSY activity. On one hand, the self-shading effect appeared to only regulate *PSY1* gene expression among all the genes tested, including other carotenoid biosynthetic enzymes and ripening regulators (Figure R14 and R15). On the other hand, the Clp protease regulates PSY protein accumulation and, possibly (via OR), its enzymatic (i.e. folding) status. A model summarizing the main mechanisms regulating tomato fruit carotenogenesis in this thesis are presented in Figure D2.

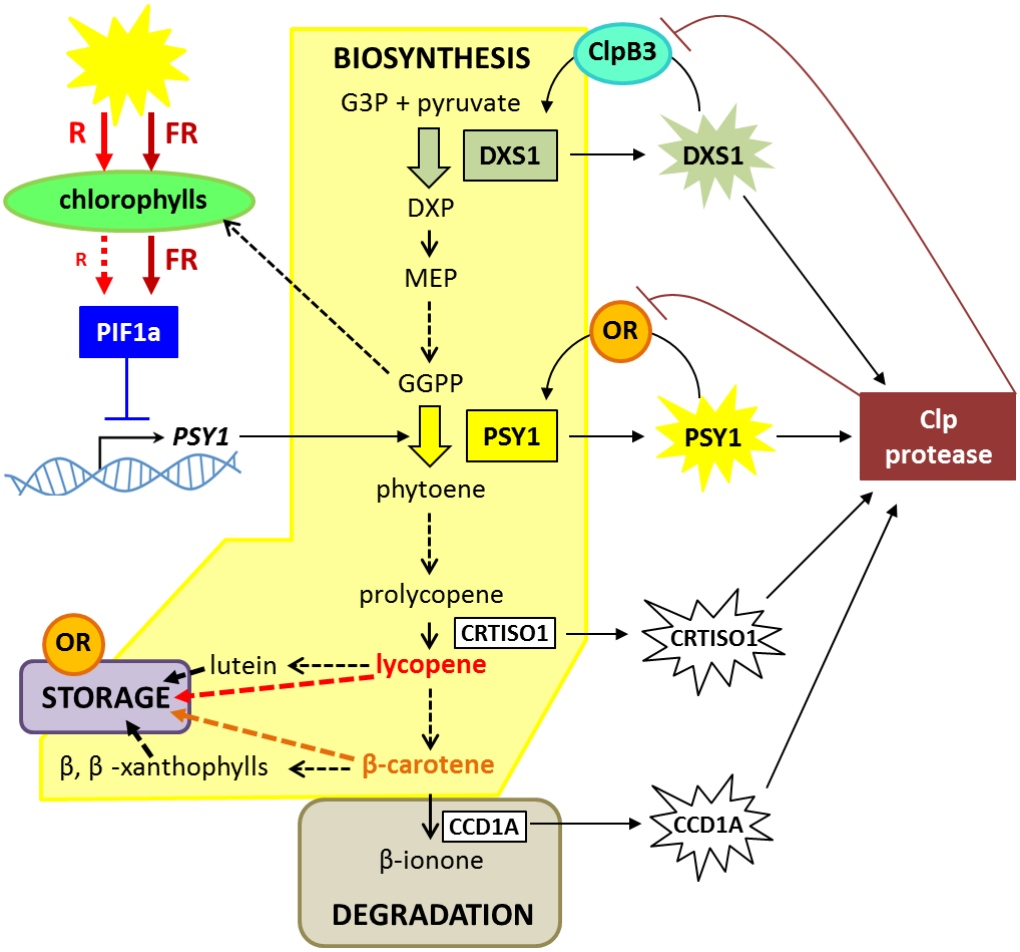

Figure D2. Integrative model for the mechanisms regulating tomato fruit carotenogenesis unveiled in this thesis. Carotenoid levels depend on the rate of biosynthesis and degradation and the storage capacity of the plastid. Among the biosynthetic enzymes, DXS1, PSY1, CRTISO1 and CCD1 might be targets of the Clp protease that degrades inactive (star-shaped) forms of the enzymes. A decreased Clp protease activity, however, triggers the accumulation of chaperones such as ClpB3 and OR that promote the refolding and hence activation of DXS and PSY enzymes, respectively. Therefore, tomato E8:amiR1 fruit would have higher levels of active DXS1 and PSY1 enzymes (i.e. an increased flux to the carotenoid pathway) but inactive CRTISO1 (perhaps causing an accumulation of prolycopene) and CCD1 (which might contribute to a decreased degradation of β-carotene), resulting in orange-colored fruits. The Clp protease also influences chromoplast differentiation (and hence storage capacity) via OR and likely other protein targets. An interconnected layer of regulation involves the transcriptional PIF1a-dependent self-shading mechanism that adjusts carotenoid biosynthesis to actual ripening by regulating *PSY1* gene expression.

Metabolic control analysis has shown that PSY displays the highest control coefficient among the carotenoid pathway enzymes, i.e. it is the main rate-limiting enzyme in the pathway (Fraser et al., 2002). While many biotechnological efforts trying to improve the carotenoid content in tomato fruit were based on increasing PSY activity through the overexpression of bacterial or plant enzymes, these approaches did not always generated the expected enhancement in carotenoid accumulation,

presumably due to the existence of important unknown mechanisms operating at the post-translational level (Fraser et al., 2009). While the role of the Clp protease unveiled in this thesis will need to be taken into account in the future, further work will be necessary to fully understand how to manipulate it for optimal carotenoid accumulation. As shown in this work, reducing Clp protease activity at the onset of ripening results in tomato fruits enriched in provitamin A (β-carotene), an interesting biotechnological feature. Manipulation of the self-shading mechanism discovered in the thesis by silencing the *PIF1a* gene was also shown here to effectively increase the accumulation of total carotenoids in the fruit. Work is currently in progress in the lab to investigate whether the levels of other phytonutrients (including MEP-derived plastidial isoprenoids such as vitamins E and K) are also improved in fruits with reduced Clp protease or PIF1a levels.

Altogether, our results highlight the essential role of PSY in the modulation of the carotenoid biosynthesis during fruit ripening. Besides adding new components to the intricate regulatory network controlling the activity of this essential enzyme, our work opens completely new biotechnological avenues to generate tomato fruits with enhanced levels of health-promoting metabolites like carotenoids. Surely, advancing in our knowledge of the unveiled mechanisms will give us the opportunity to dive into new strategies on our way to produce highly valuable food.

Conclusions

1) The tomato genome has six homologues to Phytochrome-Interacting Factors (PIFs), including two with similarity to Arabidopsis PIF1: PIF1a and PIF1b.

2) PIF1a is a true PIF that preferentially accumulates in fruits. It is located in the nucleus, degraded by phytochromes, and it complements the loss of function of PIF1 in Arabidopsis.

3) Silencing of *PIF1a* results in fruits with enhanced levels of *PSY1* transcripts, increased production of phytoene (the product of PSY activity), and a higher accumulation of total carotenoids.

4) PIF1a represses carotenoid biosynthesis in green tomato fruits by directly binding to a PBE-box motif in the promoter of the *PSY1* gene to inhibit its expression.

5) Chlorophyll degradation at the onset of ripening results in a higher R/FR ratio of the light that penetrates the pericarp, causing the degradation of PIF1a to specifically derepress *PSY1* expression and activate carotenoid biosynthesis.

6) The PIF1a-dependent self-shading mechanism unveiled here likely adjusts carotenoid biosynthesis to the actual progression of tomato fruit ripening.

7) The tomato genome has homologues for all the Clp protease subunits identified so far. In the case of ClpP1, a plastome-encoded subunit and a likely non-functional nuclear-encoded copy exist.

8) All the nuclear-encoded subunits of the Clp protease catalytic core are up-regulated during tomato fruit ripening, peaking at the O stage.

9) The fruit-specific silencing of *ClpR1* results in fruits of an orange color when ripe, presumably due to an enrichment in β-carotene, the main pro-vitamin A carotenoid.

10) Ripe fruits with decreased Clp protease activity show a heterogeneous population of chromoplasts with different ultrastructure and carotenoid composition. Proteome changes are in agreement with a role of this protease in chromoplast development during fruit ripening.

11) The tomato fruit Clp protease complex might target several enzymes involved in carotenoid biosynthesis, including the rate-limiting enzymes DXS1 (similar to Arabidopsis) and PSY1.

12) Other Clp protease targets in tomato chromoplasts might also include proteins involved in carotenoid degradation and storage, including OR (a protein kwon to promote chromoplastogenesis).

13) Our data unveil two different interconnected mechanisms that converge at the PSY step to regulate the production of carotenoids during tomato fruit ripening. These mechanisms rely on two layers of regulation: transcriptional (via PIF1a and self-shading) and post-translational (via Clp protease).

14) Biotechnological manipulation of the uncovered mechanisms produces fruits with increased nutritional quality.

MATERIALS AND METHODS

Plant material and growth conditions

During this Thesis, two varieties of *Solanum lycopersicum* (tomato) plants were used, named MoneyMaker (MM) and MicroTom (MT). Particular experiments were done using *Arabidopsis thaliana* (Col 0 ecotype) and *Nicotiana benthamiana*.

- Plant material

Tomato and Arabidopsis transgenic lines are listed in Tables MM1 and MM2, respectively.

Table MM1. Tomato transgenic lines

Transgenic line	Description	Reference
E8:amiR1	Plants with an artificial microRNA (amiRNA) against the mRNA of *ClpR1*. The amiRNA expression is controlled by the tomato fruit ripening-dependent *E8* promoter.	This thesis
E8:C	Plants with a mutated version of the amiRNA against *ClpR1*. The amiRNA expression is controlled by the *E8* promoter.	This thesis
2x35S:amiPIF1a	Plants with an amiRNA against the *PIF1a* mRNA. The amiRNA expression is controlled by the constitutive 2x35S promoter.	This thesis
Del/Ros1	Plants over-expression the transcription factors Delila(Del) and Rosea1(Ros1) under the control of the *E8* promoter.	(Orzaez et al., 2009)

Table MM2. Arabidopsis mutants and transgenic lines

Mutant line	Background	Reference
pifq	Arabidopsis plants (Col 0 ecotype) with reduce levels of PIF1, PIF3, PIF4 and PIF5 proteins.	(Leivar et al., 2009)
pif3,4,5	Arabidopsis plants (Col 0 ecotype) with reduce levels of PIF3, PIF4 and PIF5 proteins	(Shin et al., 2009)
Transgenic line		
pifq(PIF1a)	Pifq mutant plants overexpressing tomato *PIF1a* under the control of the 2x35S promoter.	This thesis.

- Plant growth conditions

Tomato and *Nicotiana benthamiana* plants were grown under standard greenhouse conditions (14 h light at 27 ± 1°C and 10 h dark at 24 ± 1°C). On the other hand, Arabidopsis plants were grown under standard greenhouse conditions (14 h light at 25 ± 1°C and 10 h dark at 22 ± 1°C).

Albino tomatoes used in Chapter II, were obtained from Moneymaker plants as described previously (Cheung et al., 1993). Briefly, tomato flower at anthesis stage were covered with several layers of dark paper and cotton fabric in such a way to allow oxygen interchange. Tomato fruit developed in the absence of light, with a complete deprivation of pigments and hence completely white. Tomatoes with a similar size to non-covered fruits were used to further experiments.

Light-filtering experiments with fruit pigment filters were performed in climate-controlled growth chambers equipped with fluorescent tubes providing continuous white light (22°C; 90 µmol m^{-2} sec^{-1} PAR). Fluence rates were measured using a SpectroSense2 meter associated with a four-channel sensor (Skye Instruments, http://www.skyeinstruments. com/), which measures PAR (400–700 nm) and 10 nm windows in the R (664–674 nm) and FR (725–735 nm) regions. Fruit pigment filters were freshly prepared for each experiment. Pericarp samples were homogenized at a 1:2 w/v ratio of tissue (fresh weight) to cold extraction solvent (hexane/acetone/methanol, 2:1:1) using a stainless steel blender. The homogenate was incubated in the dark at 4°C with agitation (320 rpm) for 2 h, and then centrifuged at 5000 g for 30 min at 4°C. The organic phase enriched in chlorophylls and carotenoids was recovered and directly transferred to glass plates to create the filters (Figure R12). When required, pigment concentration was adjusted by adding extraction solvent to the extracts in the plate until the PAR value of the light passing through the filters was approximately 40–50 µmol m^{-2} sec^{-1}.

Etiolation experiments were done as follows. Arabidopsis seeds were surface-sterilized and sown on sterile Murashige and Skoog (MS) medium containing 1% agar and no sucrose. Seeds were stratified for 3 days at 4°C before use. After stratification, seeds were exposed to light during 1 hour and then kept in darkness during 4 days at 24°C. Hypocotyl length was quantified using ImageJ (http://rsb.info.nih.gov/) as described previously (Sorin et al., 2009).

Nucleic acids techniques

- PCR. Cloning and colony screening

Two different DNA polymerase enzymes were used depending on the experiment.

Table MM3. *Taq DNA polymerase enzymes*

Enzyme	Description	T° extension	Fidelity
Taq	*GoTaq* Green Master Mix (Promega)	72°C	Low
Taq DNA hf	AccuPrime *Taq* DNA Polymerase, High Fidelity (Invitrogen)	68°C	Low

The standard PCR mix composition was as follow:

Reagent	[initial]	[final]	Volume
Buffer	10x	1x	3 µL
$MgCl_2$	50 mM	1.5 mM	1 µL
dNTPs	2.5 mM (each)	200 µM	2.4 µL
Primer F	10 µL	0.3 µM	0.6 µL
Primer R	10 µL	0.3 µM	0.6 µL
Taq (1 U/ µL)	1 U/ µL	1 U	1 µL
DNA	25 ng/ µL	10 ng	2.2 µL
Water	-	-	19.2 µL
			30 µL

The PCR program was determined in every case depending on the primer melting temperature (Tm), the Taq optimal temperature and the length of the expected fragment.

- Gateway cloning
  - Virus induced gene silencing (VIGS) cloning

For **VIGS**, a 180-200 bp fragment of the *PIF1a* and *ClpR1* cDNA was PCR-amplified (Table MM6) and cloned into the pDONR207 vector by a BP reaction prior to sub-cloning into pTRV2/DR/Gateway vector by an LR reaction (Orzaez et al., 2009). Both reactions were performed following the recommendation given by Invitrogen for Gateway cloning .

Table MM4. BP reaction

Reagent	Volume
attB-PCR product (15-150 ng)	1-7 µL

pDONR vector (150 ng)	1 µL
TE buffer pH=8	Up to 8 µL
BP clonase	2 µL
	10 µL

BP reaction was incubated at room temperature for 1 h and then used for *Escherichia coli* competent cells.

Table MM5. LR reaction

GOI: Gene Of Interest

pDEST: vector: Destination Vector

Reagent	Volume
pDONR-GOI (50-150 ng)	1-7 µL
pDEST vector (150 ng)	1 µL
TE buffer pH=8	Up to 8 µL
LR clonase	2 µL
	10 µL

To enhance cloning efficiency, LR reactions were incubated overnight at room temperature. The fragments used in VIGS experiments were designed to minimize off-target silencing by BLAST.

- Artificial microRNA (amiRNA) cloning

The **amiRNAs** were designed as described previously (Ossowski et al., 2008) to specifically silence *PIF1a (amiPIF1a)* or *ClpR1 (amiR1.1 and amiR1.2)* in stably transformed tomato lines. An inactive amiRNA was generated by site-directed mutagenesis, which introduced two point mutations in the 10^{th} and 11^{th} microARN positions (amiC). Briefly, plasmid pRS300 was used as template to introduce the amiRNA sequence into the miR319a precursor by site-directed mutagenesis (Schwab et al., 2006). The overlapping PCR amplification steps were performed as described previously (Fernandez et al., 2009), with the exception that primers A and B were re-designed (Table MM6). The resulting PCR product was cloned into the multisite Gateway vector pDONR221P4r-P3r to generate the plasmid pEF4r-GOI-3r (i.e. Gene of Interest). In the case of amiPIF1a, plasmids pEF1-2x35S-4, pEF4r-amiPIF1a-3r and pEF3-Tnos-2 were recombined (Estornell et al., 2009), and the resulted triple recombination was sub-cloned into the binary vector pKGW (Karimi et al., 2005) to obtain the plasmid

pKGW-amiPIF1a. In the case of amiR1.1, amiR1.2 and amiC, plasmids were recombined in such a way to obtain the microRNA under the control of the 2X35S promoter (pKGW-2x35S:amiR1.1; pKGW-2x35S:amiR1.2 and pKGW-2x35S:amiC) or under the ripening-specific E8 promoter (pKGW-E8:amiR1.1; and pKGW-E8:amiC).

Table MM6. Primers used for cloning experiments

Assay	Primer	Sequence
VIGS	SlPIF1a VIGS F	GGGGACAAGTTTGTACAAAAAAGCAGGCTGCTCCTCGACCGCCTATAC
	SlPIF1a VIGS R	GGGGACCACTTTGTACAAGAAAGCTGGGTCCCTGTAATTGGAGTTACGTTTG
	SlClpR1 VIGS F	GGGGACAAGTTTGTACAAAAAAGCAGGCTAGGTCAGCAAATCCAGTGGATC
	SlClpR1 VIGS R	GGGGACCACTTTGTACAAGAAAGCTGGGTTTATCTGCAAGGCCATAGTC
amiRNA	A	GGGGACAACTTTTCTATACAAAGTTGCTCCCCAAACACACGCTCGGA
	B	GGGGACAACTTTATTATACAAAGTTGTCCCCATGGCGATGCCTTAA
	amiR1.1I miR-s	GATTTTAGGCCGATGGATACCTTCTCTCTTTTGTATTCCA
	amiR1.1II miR-a	AGAAGGTATCCATCGGCCTAAAATCAAAGAGAATCAATGA
	amiR1.1III miR*s	AGAAAGTATCCATCGCCCTAAATTCACAGGTCGTGATATG
	amiR1.1IV miR*a	GAATTTAGGGCGATGGATACTTTCTACATATATATTCCTA
	amiR1.2I miR-s	GATTCTACAATAGGCATGCGCAGCTCTCTTTTGTATTCCA
	amiR1.2II miR-a	AGCTGCGCATGCCTATTGTAGAATCAAAGAGAATCAATGA
	amiR1.2III miR*s	AGCTACGCATGCCTAATGTAGATTCACAGGTCGTGATATG
	amiR1.2IV miR*a	GAATCTACATTAGGCATGCGTAGCTACATATATATTCCTA
	amiCI miR-s	GATTTTAGGCCGTAGGATACCTTCTCTCTTTTGTATTCCA
	amiCII miR-a	AGAAGGTATCCTACGGCCTAAAATCAAAGAGAATCAATGA
	amiCIII miR*s	AGAAAGTATCCTACGCCCTAAATTCACAGGTCGTGATATG
	amiCIV miR*a	GAATTTAGGGCGTAGGATACTTTCTACATATATATTCCTA
	amiPIF1aI miR-s	GATATGTAGTCGTCGGTTCGCTACTCTCTTTTGTATTCCA
	amiPIF1aII miR-a	AGTAGCGAACCGACGACTACATATCAAAGAGAATCAATGA
	amiPIF1aIII miR*s	AGTAACGAACCGACGTCTACATTTCACAGGTCGTGATATG
	amiPIF1aIV miR*a	GAAATGTAGACGTCGGTTCGTTACTACATATATATTCCTA

BP reactions were done as described for VIGS cloning. LR multisite reactions were done as follows:

Table MM8. Multisite LR reaction

Reagent	Volume
Entry clone (10 fmol each)	1-7 µL
pDEST vector (20 fmol)	1 µL
TE buffer pH=8	Up to 8 µL
LR clonase	2 µL
	10 µL

fmol/µL was calculated using the following equation:

$$\mathbf{ng/\mu L = (x\ fmol/\mu L)(N)(660fg/fmol)(1ng/10^6\ fg)}$$

Where **x** is the number of fmol per µL and **N** is the size of the DNA in bp.

- Bacteria transformation by heat shock

Different bacteria strains were used during this thesis. For cloning and most plasmid amplifications, competent *E. coli* DH5α cells were used. In the case of empty gateway vectors, which expressed a toxin that kills DH5α, an strain with the antitoxin system named DB3.1 was used. For plant transformation experiments, *Agrobacterium tumefaciens* GV3101-pMP90 was used.

Competent cells were incubated with plasmidic DNA for 20 min on ice.

In the case of *E. coli* a heat shock was applied by incubating the cells at 42C during 1 min. After 5 min on ice, 900 µL of sterile LB was added and cells were allowed to recovered during at least 1 h at 37C. Finally, bacteria were plated on selective medium(LB with the corresponding antibiotic) to select those cells that efficiently incorporate the plasmid.

In the case of *A. tumefaciens:* a heat shock was by incubating the cell in liquid nitrogen during 1 min. After 5 min on ice, 900 µL of sterile YEB was added and cells were allowed to recovered during at least 1 h at 28C. Finally, bacteria were plated on selective medium(LB with the corresponding antibiotic) to select those cells that efficiently incorporate the plasmid. The strain GV3101 harbors the pMP90 plasmid that gives the extra-resistance to rifampicin and gentamicin.

- Plasmidic DNA extraction

Colonies were first checked by colony-PCR. Positive colonies were used to inoculate LB medium (5 ml) with the corresponding antibiotic and incubated at 37C and 180 rpm.

Grown cultures were centrifuge at 13000 rpm during 5 min and the pellets were collected and used for plasmid DNA extraction using the High pure plasmid isolation kit (Roche).

Plasmids were confirmed by restriction mapping and DNA sequencing (Sanger and Coulson, 1975).

- Gel purification

After all PCR and enzyme restriction reactions, the fragment size was checked by 1%-2% agarose gele, comparing with a DNA molecular marker.

In the case of molecular cloning, DNA fragments were purified from the PCR reaction, to avoid the cloning of undesirable DNA fragments. To do that, PCR reactions were load in a low % agarose gel (0.7-0.8 %). Then, once the expected band size was checked, the desire amplicon was slide from the gel using a sterile razor blade and placed in a labeled tube. The DNA was purified from the agarose using the commercial kit “High pure PCR purification kit”, Roche ®. Finally, to check the purification procedure, the purified DNA fragment was run in an agarose gel.

- RNA extraction

In this thesis two different RNA methods were used. In all those experiments performed in Chapter II, RNA was isolated using from previous grinded frozen tissue using the PureLinkTM RNA Mini (Life Technologies, https://www.thermofisher.com/) and TRIzol (Invitrogen, https://www.thermofisher.com/) according to the manufacturer’s instructions. In the case of those RNA extractions performed in Chapter I, this molecule was isolated from lyophilized tissue by automated system supply by Promega ® Maxwell® 16 LEV Plant RNA Kit according to the manufacturer’s instructions.

In all the cases, RNA was quantified using a NanoDrop 1000 spectrophotometer

(Thermo Scientific, http://www.nanodrop. com/), and checked for integrity by 1% agarose gel electrophoresis.

- cDNA synthesis

The cDNA synthesis was performed following the recommendations of the Transcriptor First Strand cDNA synthesis kit (Roche).

Table MM8. cDNA synthesis

Reagent	[initial]	[final]	Volume
Template RNA	1 ug total RNA		Up to 11 µL
Oligo dT	10 µ	0.5 µ	1 µL
Water			Up to 13 µL
			5 min to 55 °C
Buffer	5x	1x	4 µL
dNTPs	2.5 mM (each)	1 m	2 µL
RNase inhibitor	40 U/ µL	20U	0.5 µL
RTase	20 U/ µL	10U	0.5 µL
			20 µL
			30 min to 45 °C
			5 min to 65 °C

cDNA was used as template in amplification reactions with two different objectives: gene expression analysis by quantitative PCR (RT-qPCR) or cloning.

- Gene expression analysis

Relative mRNA abundance was evaluated via quantitative PCR using LightCycler 480 SYBR Green I Master Mix (Roche) on a LightCycler 480 real-time PCR system (Roche). At least two technical replicates of each biological replicate were performed, and the mean values were used for further calculations. Normalized transcript abundances were calculated as described previously (Simon, 2003) using tomato ACT (Solyc04g011500) and Arabidopsis UBC (At5g25760) as endogenous reference genes.

For all the transcripts measured in this thesis, primers efficiencies were calculated using serial genomic DNA dilutions. Primers are listed in Table MM11.

The PCR mix reaction was made as follows:

Table MM9. qPCR mix reaction

Reagent	Volume
SYBR Green I master MIX	10 µL

Primer F (300 nM)	0.6 mL
Primer R (300 nM)	0.6 mL
Template cDNA (50 ng template)	1 mL
Water	7.8 mL

Table MM10. qPCR program

Step	Tº	Time
Taq activation	95 °C	10 min
Denaturalization	95 °C	10 seg
Annealing and extension	60 °C	30 seg
		45 cycles

Table MM11. Primers used for qPCR in this Thesis

Biological process	Primer	Sequence
Reference gene	SlACT qPCR F	CCTTCCACATGCCATTCTCC
	SlACT qPCR R	CCACGCTCGGTCAGGATCT
	AtUBC qPCR F	TCAAATGGACCGCTCTTATC
	AtUBC qPCR F	CACAGACTGAAGCGTCCAAG
Carotenoid biosynthetic genes	SlDXS1 qPCR F	TGACCATGGATCTCCTGTTG
	SlDXS1 qPCR R	GCCTCTCTGGTTTGTCCAAG
	SlPSY1 qPCR F	GCCATTGTTGAAAGAGAGGGTG
	SlPSY1 qPCR R	AGGCAAACCAACTTTTCCTCAC
	SlPSY2 qPCR F	CTCTAGTGCCCCCTAAGTCAAC
	SlPSY2 qPCR R	TTTAGAAACTTCATTCATGTCTTTGC
	SlPSY3 qPCR F	TTGGATGCAATAGAGGAGAATG
	SlPSY3 qPCR R	ATTGAATGGCTAAACTAGGCAAAG
	SlPDS qPCR F	AGCAACGCTTTTTCCTGATG
	SlPDS qPCR R	TCGGAGTTTTGACAACATGG
	SlLCY-E qPCR F	GCCACAAGAACGAAAACGAC
	SlLCY-E qPCR R	CGCGGAAAAATGACCTTATC
	SlLCY-B qPCR F	TTGTGGCCCATAGAAAGGAG
	SlLCY-B qPCR R	GGCATCGAAAAACCTTCTTG
	SlCYC-B qPCR F	TGGCAAGGGTTCCTTTCTTC
	SlCYC-B qPCR R	AGTCATGTTTGAGCCATGTCC
Ripening-associated genes	SlACS2 qPCR F	CGTTTGAATGTCAAGAGCCAGG
	SlACS2 qPCR R	TCGCGAGCGCAATATCAAC
	SlE8 qPCR F	AGCTGCAAGTTGGAGAGACACG
	SlE8 qPCR R	CCGCATGGAGTTGGAAATTC
	SlNR qPCR F	CTCCCAGAGGCAGATTGAAC
	SlNR qPCR R	TTCACAGACATCCCACCATC
	SlRIN qPCR F	GCTAGGTGAGGATTTGGGACAA
	SlRIN qPCR R	AATTTGCCTCAATGATGAATCCA
	SlTAGL1 qPCR F	GCCATTGGTAGAGTCCGTTC
	SlTAGL1 qPCR R	GATACATGTTGGCGTTCTGC
	SlAP2a qPCR F	AACGGACCACAATCTTGAC

	SlAP2a qPCR R	CTGCTCGGAGTCTGAACC
	SlFUL1 qPCR F	CAACAACTGGACTCTCCTCACCTT
	SlFUL1 qPCR R	TCCTTCCACTTCCCCATTATCTATT
PIF1 homologs	SlPIF1a qPCR F	TCGAACCAGCCAAGACTTCC
	SlPIF1a qPCR R	CGGTAATGCAACTTGCGC
	SlPIF1b qPCR F	TCAGGAAGTGGAACAGCTGAG
	SlPIF1b qPCR R	TTGATGATTCCCTCTACTTCCTTC
	SlPIF1c qPCR F	GAAATCCACAATATGAAGAAATCATG
	SlPIF1c qPCR R	TTGCTCGGGAAAAAGGTTAG
Clp protease subunit homologs	SlClpR1 qPCR F	CCACTTTCTTGCCCTACTC
	SlClpR1 qPCR R	GAAGAGAATCTGAAAAGAAG
	SlClpR2 qPCR F	CACTGCTAAAGAAGCTCTTG
	SlClpR2 qPCR R	CAGTGATATCCCTCGGCG
	SlClpR3 qPCR F	TTCTTTTCAAGCTTCCGTTGA
	SlClpR3 qPCR R	CAACCGCAAGCACGTGGC
	SlClpR4 qPCR F	ATGGAAGCTGTCACTATTGC
	SlClpR4 qPCR R	TGAGGCACGGCAACTCGC
	SlClpP1a qPCR F	GCATTCCCTCACGCTTGGG
	SlClpP1a qPCR R	TATACCGTGTTCATCCGCTTAAAC
	SlClpP1b qPCR F	CATACCTCATTTTTACCCCCACA
	SlClpP1b qPCR R	TATGGGTATCTGGTGGAACC
	SlClpP3 qPCR F	TTGGTTGATGCTGTTATAGATGAC
	SlClpP3 qPCR R	TTTTGGTGGAGGTGCATCCT
	SlClpP4 qPCR F	ATTGACGGTGTAATTGACAGAGA
	SlClpP4 qPCR R	ATTTCATAGGGTCTTGGATCAAA
	SlClpP5 qPCR F	TCATGAGCGCAAAGGAAGCT
	SlClpP5 qPCR R	CAAGTGGTTGAAGGGCTTTCA
	SlClpP6 qPCR F	GTTCAATGAGTACGAATCCGG
	SlClpP6 qPCR R	GGCATGATGGGCGGATTAG

- Chromatin immunoprecipitation (ChIP) coupled to qPCR

The ChIP-qPCR assay is used to study the binding of transcription factors to a DNA region. In our particular case, we tested if PIF1a was able to bind to previously defined conserved cis-elements. To prove PIF1a binding to those regions, a tagged version of PIF1a (PIF1a-GFP) was transiently expressed in tomato fruit pericarp as described previously (Orzaez et al., 2009). GFP fluorescence in pericarp sections was monitored using a Blak-Ray B–100AP high-intensity UV lamp (Ultra-Violet Products). Pericarp sections showing fluorescence were then excised using a scalpel, fixed with 1% formaldehyde for 15 min under vacuum, and then grounded to fine powder under liquid nitrogen. The DNA/PIF1a-GFP complex was immunoprecipitated with an antibody against GFP (Life Technologies). ChIP assays were performed as described

previously (Osnato et al., 2012). An anti-HA antibody (Santa Cruz Biotechnology) was used in parallel control reactions. Primers used in this assay are listed in Table MM12.

Table MM12. ChIP-qPCR primers used in this Thesis

Primer	Sequence
SlPSY1(Up-Ctrl) ChIPqPCR F	CGGACAGAGACGAATCCAAG
SlPSY1(Up-Ctrl) ChIPqPCR R	TTTTGTGCGGAATTGAAACC
SlPSY1(G-box) ChIPqPCR F	AGTACCCAATTTTCCCAAAAC
SlPSY1(G-box) ChIPqPCR R	ATTTGAAGTGCCGTCATTGG
SlPSY1(PBE-box) ChIPqPCR F	TGATTCCACTGTCATAGGAGG
SlPSY1(PBE-box) ChIPqPCR R	CCCAAAACTACAACAAAATCAGC

Protein techniques

- Protein extraction

Fruits at different developmental stages and leaves were collected and immediately frozen in liquid nitrogen. Then, samples were lyophilized and kept at 4C in the dark.

Protein extraction was done using the TKMES method. Briefly, plant tissue was pulverized using a Tissue Lyzer equipment (Quiagen) and then 150 µl TKMES buffer (100 mM tricine-KOH pH7.5; 10 mM KCl; 1 mM MgCl2; 1 Mm EDTA; 10% (p/v) sucrose) was added. The mix was centrifuged at maximum speed for 10 min at 4C and the supernatant was collected.

Protein concentration was determined by the Bradford method using the Coomasie Plus Protein Assay Reagent (Thermo).

- SDS-PAGE

Based on the protein concentration obtained using the Bradford method, the volume necessary to achieve a certain quantity (µg) of protein was calculated. Depending on the protein, different µg of protein were used. In the case of DXS, 20 µg were used, while in the case of PSY and Or, 50 ug were loaded in the gels. Samples were prepared adding to the tissue an extraction buffer (0.2% (v/v) Triton X-100, 1mM DTT, 100 µg/mL PMSF, 3 µg/mL E64, 20 µg/mL Protease inhibitor cocktail (Sigma)).

Then, protein samples were denatured during 5 min at 95C.

The gels used in SDS-PAGE PAGE experiments were building using Mini-Protean II Bio-Rad equipment.

- Western blot

In this assay, denatured proteins were separated according to their molecular weight by SDS-PAGE gels, and then transferred to a PVDF membrane (Hybond-p, Amersham Biosciences) using a Trans-Blot Semi-dry Transfer Cell (BioRad).

The membrane was then recovered and incubated during 1 h with a solution of milk dissolved in PBS + TWEEN20 at 0,05% (v/v). Then, the primary antibody was added to the desire dilution (DXS 1:500; PSY 1:200 and Or 1:2000) and the membrane was incubated overnight under agitation. After the incubation with the primary antibody, the membrane was washed 3 times in PBS-TWEEN. Then, the corresponding secondary antibody coupled to horseradish peroxidase (1:10000 dilution) was added and incubated during 1 h at room temperature. Finally, the membrane was washed 3 times in PBS-TWEEN and used for protein quimioluminiscence detection. DXS and DXR western blots were obtained using the LAS4000 equipment (Multi Gauge software). PSY and Or western blots were obtained using photographic film exposure (Kodak).

Total proteins in membranes were finally stained by incubating with Coomassie blue (Coomassie 0,6% (w/v), ethanol 40% (v/v), acetic acid 10% (v/v) and 50% water (v/v)). To eliminate the background signal, membranes were incubated with a distaining solution (ethanol 40% (v/v), acetic acid 10% (v/v) and 50% water (v/v)).

- Densitometry

The intensities of the bands obtained by western blot analysis were quantified using ImageJ (http://rsb.info.nih.gov/), following the software instructions. Band intensities were normalized to the Coomassie blue stained membranes (loading control). Fold changes were calculated in each individual membrane by relativizing against a control WT signal.

Metabolite techniques

- Plastidial isoprenoids analysis by HPLC

HPLC is a type of chromatography that allows the separation and quantification of metabolites. To separate plastidial isoprenoids an hydrophobic chromatography (C-18 column) approach was used. Hence, the separation is achieved based on the metabolite differential hydrophobicity.

Isoprenoids were purified from 15 mg lyophilized tissue using 1 ml cold extraction solvent as described previously (Saladie et al., 2014). HPLC profiling was performed using an Agilent 1200 series HPLC system (Agilent Technologies) as described previously (Fraser et al., 2000).

Cantanxanthin, a carotenoid not present in plants, was used as an internal standard in HPLC experiments. Individual peaks in chromatograms were quantified by integrating the area under the curve using the software provided by the supplier and normalized to the cantaxanthin value.

Plant molecular biology techniques

- Seed sterilization and sowing

Tomato seeds were surface-sterilized by incubating them under a laminar flow chamber with sterilized water during 30 min. After discarding water, a Sterilization Solution (40% bleach; two drops of tween-20) was added and incubated during 20-30 min. Finally, seeds were wash with water at least three times and sowed in a jar with corresponding medium. The jar was wrapped with aluminum paper and incubates during 2 days at 24-36 C.

In the case of Arabidopsis, seeds were surface-sterilized with 70% of ethanol method in sterilized conditions. Then, seed were sow in petri plates with the corresponding medium, wrapped with aluminum paper and incubated during 2 days at 4C. Finally, they were transfered to growing conditions

- Plant transformation

The Arabidopsis transgenic plants pifq(PIF1a) were generated by Águila Ruiz-

Sóla, PhD by floral dip (Bechtold and Pelletier, 1998).

- MicroTom (MT) stable transformation

Tomato MT plants were transformed with the previously described plasmids pKGW-PIF1a and pKGW-E8:amiR1.1; and pKGW-E8:amiC as previously described (Fernandez et al., 2009). Briefly:

1) Surface-sterile MT seeds are sown in 50% MSO medium (50% MS salts; 30g/l sucrose; Vitamin B5; agar 8 g/l; pH=5.8) and grown during 10 days at 25C in long day conditions (16 h light; 8 h dark).
2) Cut cotyledons in two halves and incubate in KCMS medium (50% MS salts; 20g/l sucrose; KH_2PO_4 200 mg/l; Tiamin 0.9 mg/l; 2,4 D 2 mg/l, Kinetin 1 mg/l; acetosyringone 200 µM; agar 8 g/l; pH=5.8) 24 hs at 25C in long day conditions.
3) Incubate cotyledons during 30 min with an agrobacterium suspension in liquid KCMS harboring the desired plasmid. Cotyledons are then transfer to a fresh solid KCMS medium and incubated in dark 48 hs at 25C;
4) Transfer the cotyledons to 2Z medium (50% MS salts; 30g/l sucrose; Nistch vitamins; Zeatin 2 mg/l; Timentin 250 mg/l; antibiotic (pKGW plasmids is Kanamycin 100 mg/l); agar 8 g/l; pH=5.8) during 15 days at 25C in long day conditions.
5) Every 15 days refresh the cotyledons transferring to new 2Z medium until regenerated plants appear (approximately 30 days);
6) Transfer the re-generated explants to the rooting medium (50% MS salts; 10g/l sucrose; Nitsch vitamins; Zeatin 2 mg/l; Timentin 75 mg/l; antibiotic (pKGW plasmids is Kanamycin 100 mg/l); agar 8 g/l; pH=5.8);
7) Once roots appear, plants are transferred to soil and acclimated at the greenhouse.

- Transient transformation

Transient expression assays were performed using the same protocol in *Nicotiana benthamiana* and tomato leaves.

In the case of *Nicotiana benthamiana* 2X35S:PIF1a–GFP was infiltrated to determine the subcellular localization and protein stability of PIF1a under red light.

Tomato leaves were agroinfiltrated with pKGW-2x35S:amiR1.1; pKGW-2x35S:amiR1.2 and pKGW-2X35S:amiC constructs to access their silencing efficiency. A detailed protocol is presented:

1) Pre-inoculum: Inoculate a *Agrobacterium* colony (transformed with the corresponding plasmid) in 5 ml YEB (with the corresponding antibiotics) and incubate during one night at 28 C under agitation (180 rpm).
2) Inoculate 20 ml YEB (with the corresponding antibiotics) with 0.5% of the pre-inoculum. Incubate at 28 C during 16-20 h until an OD_{600}=0.5-1 is achieved.
3) Centrifuge during 20 min at 3500 rpm and discard the supernatant.
4) Dilute the pellet with suspension buffer ($MgCl_2$ 10 mM; MES 10 mM pH=6; acetosyringone 150 µM) to get a culture with a final OD_{600}=1.
5) Incubate 2 h at room temperature.
6) Agroinfiltrate the solution in young and fully expanded leaves.

Tomato fruit agroinjection for VIGS experimetns was performed as described previously (Orzaez et al., 2009; Fantini et al., 2013). Constructs harboring VIGS sequences to trigger the silencing of a gene of interest (GOI) (*PIF1a* or *ClpR1)* and the anthocyanin-related genes (*Rosea 1(R)* and *Delila(D)*) at the same time were used to agroinject R/D fruits (Butelli et al., 2008). Thus, this system works as a silencing visual reporter, because those zones where silencing occurs do not accumulate anthocyanins (due to R/D silencing) and the red pigment lycopene is observed. A plasmid with a silencing sequence against *phytoene desaturase* (*PDS*) was used as a positive control. *PDS* silencing generates yellow zones due to the absence of carotenoids.

For transient over-expression, the 2X35S:PIF1a–GFP construct was used (Orzaez et al., 2006) following a similar protocol to that used to agroinfiltrate leaves. The only difference was that the *Agrobacterium* cultures were use with an OD_{600}=0.5.

- Selection of transgenic plants

Transgenic T1 tomato plants that grew in selective medium (Kanamycin) were analyzed by PCR to confirm the presence of the transgene.

- Genomic DNA extraction

Tomato genomic DNA extraction was performed using the CTAB protocol. Briefly, a piece of tomato leaf was grinded in liquid nitrogen and extraction buffer was added (50 mM Tris.HCl pH 8 and 20 mM EDTA pH 8). After adding 20 µl of SDS 10%, samples were vortex and incubated at room temperature during 10 min. Then, 45 µl of NaAc pH 5.2 3M was added to the mix and incubated on ice during 30 min. Smples were centrifuged at 10000 rpm during 10 min and resuspended the pellet in 500 µl Tris-HCl pH 8.0 10mM. After that, the sample was mixed with 500 µl CTAB (2% CTAB, 2M NaCl, 0,2 M Tris.HCl pH 8, 0.05 M EDTA) and incubated at 65 C during 15 min. Finally, one volume of chloroform was added, mixed and centrifuged during 5 min at maximum speed. The pellet was resuspend with 50 µl of water.

- Genotyping PCR

Genomic DNA was used as template to detect transgenes by PCR. The oligonucleotides used for genotyping are presented in Table MM13.

Table MM13. Primers used for transgenic tomato plant genotyping.

Primer	Sequence
Att4_seq F	CAACTTTTCTATACAAAGTTG
amiRNA_universal_R	CATGTGTAATATGCGTCCGAGCGTG
E8_promoter F	TACAACCTCCATGCCACTTG
Att2_T-nos R	GGGGACCACTTTGTACAAGAAAGCTGGGTACCCGATCTAGTAACATAG

- <u>Cycloheximide (CHX) experiment</u>

E8:amiR1 and WT ripe fruits were cut into small pieces (approximately 1 cm^2) and incubated with a solution of 300 µM CHX. Samples were collected at two different time points: 30 min and 4 h. Finally, samples were frozen in liquid nitrogen to further studies.

Microscopy and imaging

- Laser confocal microscopy

After agroinfiltration of *N. benthamiana* leaves with pGWB405-PIF1a as described previously (Sparkes et al., 2006), PIF1a–GFP fluorescence was detected using a Leica TCS SP5 confocal laser-scanning microscope. Nuclei were identified by directly incubating the leaf samples with 4',6–diamidino-2–phenylindole (DAPI) (1 mg ml^{-1}). Excitation filters of 450–490 nm and 410–420 nm were used for detection of GFP fluorescence and DAPI signal, respectively. PIF1a–GFP levels in individual nuclei were estimated by quantifying the GFP fluorescence signal in z–stacks of optical sections separated by 0.5 lm using the integrated microscope software. To estimate PIF1a–GFP stability in response to light, GFP fluorescence in the nuclei found in a given field was quantified in the dim light of the microscope room and then the microscope stage was moved down to expose the sample to either R (30 µmol m^{-2} sec^{-1}) or FR (30 µ.mol m^{-2} sec^{-1}) using a portable QBEAM 2200 LED lamp (Quantum Devices). After illumination for 5 min, the microscope stage was moved up to quantify the GFP signals in the same field. GFP excitation was limited to image acquisition steps to minimize photo-bleaching. Control samples were treated similarly except that they were not irradiated. Tomato pericarp sections were obtained using a Vibratome series 1000 sectioning system (Vibratome). Chloroplasts were identified using excitation at 488 nm and a 610–700 nm filter to detect chlorophyll autofluorescence.

- Transmission electronic microscopy (TEM)

TEM samples were prepared by "Unitat de crio-microscopia electronica" that belongs to the "Centres Cientifics i Tecnologics de la Universitat de Barcelona" following the general procedure for chemical fixation.

TEM observations were done using a crio-microscopy TEM Tecnai G2 F20 (FEI) 200KV with a CCD Eagle 4k x 4k. In all the cases the sub-epideral cell layers (third layer) were observed.

- Raman imaging

Tomato fruit pericarp sections were embedded in low-melting agarose and cut into

300 µm thick sections using a vibratome. Samples were kept in water to avoid dehydration.

Observations were done using an inVia confocal Raman microscope equipped with a 60× WI lens (NA = 1, Nikon) and a 532 nm laser using a 2.69 s integration time, 20 mW power and 0.6um pixel size. In all the cases the sub-epideral cell layers (third layer) were observed.

Data analysis and visualization were done by Dr. Monica Marro and Prof. Pablo Loza-Alvarez at the Institute of Photonic Sciences (ICFO) in Castelldefels, Barcelona, Spain, following previous recommendations (Baranska et al., 2006; Gierlinger and Schwanninger, 2007).

- Photography

Photographs were done using a Nikon D7000 camera coupled to the objective AF-S NIKOR 18-70 MM 1:3.5-4.5G and AF-S MICRO NIKKOR 105 mm 1:2.8G.

Biophotonics

The quantity (transmittance) and quality (R/FR ratio) of white light (400–800 nm) filtered through pericarp sections of tomato fruit was determined using a Lambda 950 UV/VIS/NIR spectrophotometer (Perkin-Elmer). Data were sequentially acquired after removing successive layers (200 lµm thick) of inner pericarp tissue using a VT12000 S vibrating-blade microtome (Leica).

System biology techniques

The chromoplast proteomes were obtained in a short-term stay at the Cornell University in the laboratory of Dr Li Li and in collaboration with Dr Theodore Tannhauser that belongs to USDA Robert Holley Institute - Proteomic Services.

- Plastid isolation

Firstly plastids were isolated following a previously established procedure based on sucrose gradient (Wang et al., 2013).

- Protein solubilization from isolated plastids

Isolated chromoplasts were solubilized with 50 ul Tris-HCl pH=7.2-8. Afterwards, plastids were broken by 5 freeze-and-thaw cycles using liquid nitrogen. Then, 100 µl of resuspension buffer (Urea 8M + 2% SDS) were added and incubated overnight at 4C. The morning after, the samples were centrifuge at 13000 rpm during 10 min and the supernatant, where plastid proteins are located, was taken (after the centrifuge step it is observed a white pellet and a color supernatant).

Protein extraction procedure was checked by loading 10 µg of protein in a 10%-20% gradient SDS-PAGE gel and observed by Coomassie Blue staining.

- Proteomic analysis.
  - Sample preparation

Protein pellets were dissolved in a solution of 8M urea/2% SDS (sodium dodecyl sulfate). Protein concentrations were determined by Bradford protein assay. Prior to trypsin digestion, protein samples were subjected to reduction and cysteine blocking steps. 100 ug of each protein sample was added to an eppendorf tube and brought up to a starting volume of 65 µl, with 8M Urea/2% SDS. Proteins were reduced by adding TCEP (tris (2-carboxethyl) phosphine hydrochloride) to a final concentration of 5 mM TCEP in the sample volume and incubation at 35°C for 1h. The cysteines were then blocked using a modification of the general method of Thannhauser et al. (1997) for blocking thiols with alkyl alkanethiosulfonates. Briefly, MMTS (methyl methanethiosulfonate) was added to the sample to a final concentration of 10 mM MMTS, and the reaction was allowed to proceed at room temperature for 1h. Prior to adding the trypsin for protein digestion, the urea concentration was brought below 1M by diluting the samples with 50 mM TEAB (triethylammonium bicarbonate) buffer. Sequence grade modified Trypsin (Promega) was resuspended in 50 mM TEAB and 3 µg of the trypsin enzyme was added to each of the 9 samples. Digestion was carried out at 30°C overnight (18h). The tryptic digests were then dried under reduced pressure in a CentriVap concentrator (Labconco).

  - TMT Labeling

The TMT labeling was carried out according to the manufacturer's instructions

(Thermo) with minor modifications. The vacuum dried tryptic digests were reconstituted with 40 ul of 500 mM TEAB. The TMT reagents (0.8 mg) were dissolved in 50 µl of acetonitrile. For the nine-plex experiment, each of the labeling reaction mixtures contained 45 µl of the TMT reagent and 40 µl (100 µg) of the tryptic digest in TEAB. The "E8:amiR1 ripe stage" samples A, B and C were labeled with TMT reagent numbers, 126, 127C, and 130N, respectively. The "WT O stage" samples A, B, and C were labeled with TMT reagent numbers, 128N, 130C, and 129N, respectively. The "WT RR stage" samples A, B, and C were labeled with TMT reagent numbers 127N, 131, and 129C, respectively. For the labeling, reaction mixtures were incubated at room temperature, protected from light, for 1h. After completion of the labeling reaction, 8 µl of 5% hydroxylamine/200 mM TEAB solution was added to each reaction mixture to quench the labeling reaction. Equal amounts of each of the 9 individually TMT-labeled digests were pooled into a single tube and mixed. The pooled 9–plex sample was then dried at reduced pressure. To remove detergent, excess-labeling reagents, and to desalt the samples, prior to analysis, the 9-plex pooled samples were cleaned by Solid Phase Extraction (SPE) procedures first by Strong Cation Exchange (SCX) and then by reverse phase (RP). Briefly, for the SCX procedure, the 9-plex vacuum-dried sample was reconstituted in SCX Load Buffer (10 mM potassium phosphate, 25% acetonitrile, pH 3.0). A PolySulfoethyl A cartridge (PolyLC Inc) was conditioned with Load Buffer, and the 9-plex sample was loaded onto the cartridge. The sample was washed with Load buffer, and then eluted from the cartridge with SCX Elution Buffer (10 mM potassium phosphate, 25% acetonitrile, 350 mM potassium chloride, pH 3.0) The elution was dried at reduced pressure and brought up in 0.1% trifluoroacetic acid (TFA) for RP-SPE desalting. For the SPE procedure, a SepPak, 1 cc, C18 cartridge (Waters) was conditioned with acetonitrile, and then equilibrated with 0.1% TFA. The sample was loaded onto the cartridge, and then washed with 2% acetonitrile/0.1% TFA. The sample was then eluted with 50% acetonitrile/0.1% TFA. The SPE elution volume was vacuum dried and submitted for analysis.

- High pH reverse phase (hpRP) fractionation

The hpRP chromatography was carried out by Ultra Performance Liquid Chromatography (UPLC*)*. The peptide separation was using an Acquity UPLC System

and UV detection (Waters, Milford, MA) coupled with a robotic fraction collector (Probot; Dionex, Sunnyvale, CA, USA) as reported previously (Okekeogbu et al, 2014). Specifically, the TMT 10-plex tagged tryptic peptides were reconstituted in buffer A (20 mM ammonium formate pH 9.5 in water), and loaded onto an Acquity UPLC BEH C18 column (1.7 µm, 2.1x100 mm, Waters, Milford, MA) with 20 mM ammonium formate (NH_4FA), pH 9.5 as buffer A and 90% ACN/10% 20 mM NH_4FA as buffer B. The LC was performed using a gradient from 10-45% of buffer B in 12 minutes at a flow rate 200 µL/min. Forty-eight fractions were collected at 15 second intervals and pooled into a total of 6 fractions based on the UV absorbance at 214 nm and with multiple fraction concatenation strategy (Zhou et al, 2013). All of the fractions were dried and reconstituted in 30 µL of 2% ACN/0.5% FA for nanoLC-MS/MS analysis**.**

- Nano-scale reverse phase chromatography and tandem mass spectrometry (nanoLC-MS/MS)

The nanoLC-MS/MS analysis was carried out using both Orbitrap Elite and Orbitrap Fusion (Thermo-Fisher Scientific, San Jose, CA) mass spectrometer equipped with nano ion source using high energy collision dissociation (HCD) similar to previous report (Zhou et al, 2013). Both instruments were coupled with the UltiMate3000 RSLCnano (Dionex, Sunnyvale, CA). Each reconstituted fraction (5 µL) was injected onto a PepMap C-18 RP nano trap column (3 µm, 75 µm × 20 mm, Dionex) with nanoViper Fittings at 20 µL/min flow rate for on-line desalting and then separated on a PepMap C-18 RP nano column (3 µm, 75µm x 15cm), and eluted in a 120 min gradient of 5% to 38% acetonitrile (ACN) in 0.1% formic acid at 300 nL/min., followed by a 5-min ramping to 95% ACN-0.1% FA and a 7-min hold at 95% ACN-0.1% FA. The column was re-equilibrated with 2% ACN-0.1% FA for 20 min prior to the next run. The Orbitrap Elite was operated in positive ion mode with nano spray voltage set at 1.6 kV and source temperature at 275 °C. The instrument was externally calibrated using Ultramark 1621 for the FT mass analyzer. An internal calibration was performed using the background polysiloxane ion signal at *m/z* 445.120025 as the celebrant. The instrument was operated in data-dependent acquisition (DDA) mode. In all experiments, full MS scans were acquired over a mass range of *m/z* 400-1,400, with detection in the Orbitrap mass analyzer at a resolution setting of 60,000. Fragment ion spectra produced via high

energy collision dissociation (HCD) were acquired in the Orbitrap mass analyzer with a resolution setting of 15,000 for the mass range of *m/z* 100-2000. In each cycle of DDA analysis, following each survey scan, the 20 most intense multiply charged ions above a threshold ion count of 5,000 were selected for fragmentation at a normalized collision energy of 45%. Dynamic exclusion parameters were set at repeat count 1 with a 40 s repeat duration with ±10 ppm exclusion mass width. The activation time was 0.1 ms for HCD analysis. All data were acquired with Xcalibur 2.2 software (Thermo-Fisher Scientific).

The Orbitrap Fusion was operated in positive ion mode with nano spray voltage set at 1.6 kV and source temperature at 275 °C. External calibration for FT, IT and quadrupole mass analyzers was performed. The instrument was operated in data-dependent acquisition (DDA) mode using FT mass analyzer for one survey MS scan for selecting precursor ions followed by Top 3 second data-dependent HCD-MS/MS scans for precursor peptides with 2-7 charged ions above a threshold ion count of 10,000 with normalized collision energy of 37.5%. MS survey scans at a resolving power of 120,000 (fwhm at m/z 200), for the mass range of m/z 400-1600 and MS/MS scans at 30,000 resolution for the mass range m/z 105-2000. Dynamic exclusion parameters were set at 1 within 40s exclusion duration with ±10 ppm exclusion mass width. All data are acquired under Xcalibur 3.0 operation software and Orbitrap Fusion Tune 2.0 (Thermo-Fisher Scientific).

- Data processing, protein identification and data analysis

All MS and MS/MS raw spectra from TMT experiments were processed and searched using Sequest HT and Mascot Daemon software within the Proteome Discoverer 1.4 (PD1.4, Thermo). The ITAG2.4_proteins.fasta sequence database containing 34725 sequence entries were used for database searches. The search settings used for 10-plex TMT quantitative processing and protein identification in the PD1.4 searching software were: trypsin with up to two missed cleavage, fixed Methylthion modification of cysteine, fixed 10-plex TMT modifications on lysine and N-terminal amines. Variable modifications were allowed for methionine oxidation and deamidation on asparagines/glutamine residues. The peptide mass tolerance and fragment mass tolerance values were 10 ppm and 50 mDa, respectively. Identified peptides were

filtered for maximum 1% FDR using the Percolator algorithm in PD 1.4 along with additional peptide confidence set to high. The TMT 10-plex quantification method within Proteome Discoverer 1.4 software was used to calculate the reporter ratios with mass tolerance ±10 ppm. Only peptide spectra containing all reporter ions were designated as "quantifiable spectra" and used for peptide/protein quantitation. A protein ratio was expressed as a median value of the ratios for all quantifiable spectra of the unique peptides pertaining to that protein. For each relative ratio group, normalization on protein median was applied. The comparison between groups was undertaken with Micosoft Excel software.

Statistical analysis

Student's t test and Pearson correlation coefficients (r values) were calculated using Excel. PCA analysis was done using the Excel complement XLSTAT (https://www.xlstat.com/es/).

Bioinformatic Analysis

- Gene expression analysis from microarray and RNA-seq data

Gene expression data was downloaded from the EFP-tomato browser (http://bar.utoronto.ca/efp_tomato/cgi-bin/efpWeb.cgi).

- MapMan

The quantitative proteomic data was analyzed using tomato accessions or Arabidopsis homolog accession numbers, depending on the bioinformatics analysis and the available information. Protein descriptions were performed using annotations associated with each protein entry (https://solgenomics.net/) and through homology-based comparisons with the TAIR9 protein database (http://www.arabidopsis.org/) using BasicLocal Alignment Search Tool BLASTX (Altschul et al., 1990) with an e-value cutoff of 1e-5 to avoid false positives.

MapMan Bins were used for class functional assignments (http://gabi.rzpd.de/projects/MapMan/) (Thimm et al., 2004). Arabidopsis total proteome was downloading from Arabidopsis official page

(http://www.arabidopsis.org/).

The proteins listed were used to predict their subcellular localization using four predictors (ChloroP: (Emanuelsson et al., 1999) http://www.cbs.dtu.dk/services/ChloroP/; iPSORT: (Bannai et al., 2002); http://ipsort.hgc.jp/; BaCelLo: (Pierleoni et al., 2006) http://gpcr.biocomp.unibo.it/bacello/; EpiLoc: (Brady and Shatkay, 2008) http://epiloc.cs.queensu.ca/). Predictions were made on the basis of tomato and Arabidopsis homolog proteins when harboring an N-terminal sequence.

- Sequence alignment and phylogenetic trees

Arabidopsis ClpPR sequences (Nishimura and van Wijk, 2015) were used as queries to search for putative tomato homologs using BLAST on the SolGenomics Network website (http://solgenomics.net/). Alignments were performed using MUSCLE (Edgar, 2004) and an unrooted tree was constructed using MEGA6 (Hall, 2013) as described previously (Hall, 2013).

References

Abdel-Ghany, S.E., Burkhead, J.L., Gogolin, K.A., Andrés-Colás, N., Bodecker, J.R., Puig, S., Peñarrubia, L., and Pilon, M. (2005). AtCCS is a functional homolog of the yeast copper chaperone Ccs1/Lys7. FEBS Lett. 579: 2307–2312.

Adato, A. et al. (2009). Fruit-surface flavonoid accumulation in tomato is controlled by aSLMYB12-regulated transcriptional network. PLoS Genet. 5: 1–23.

Alba, R., Cordonnier-Pratt, M.-M., and Pratt, L.H. (2000). Fruit-Localized Phytochromes Regulate Lycopene Accumulation Independently of Ethylene Production in Tomato. Plant Physiol. 123: 363–370.

Alder, A., Jamil, M., Marzorati, M., Bruno, M., Vermathen, M., Bigler, P., Ghisla, S., Bouwmeester, H., Beyer, P., and Al-babili, S. (2012). The Path from b-Carotene to Carlatone, a Strigolactone-like Plant Hormone. Science. 335: 1348–1351.

Al-Sady, B., Ni, W., Kircher, S., Schòfer, E., and Quail, P.H. (2006). Photoactivated Phytochrome Induces Rapid PIF3 Phosphorylation Prior to Proteasome-Mediated Degradation. Mol. Cell 23: 439–446.

Altschul SF, Gish W, Miller W, Myers EW, Lipman DJ (1990) Basic local alignment search tool. J Mol Biol 215:403–410

Ament, K., Van Schie, C.C., Bouwmeester, H., Haring, M.A., and Schuurink, R.C. (2006). Induction of a leaf specific geranylgeranyl pyrophosphate synthase and emission of (E,E)-4,8,12-trimethyltrideca-1,3,7,11-tetraene in tomato are dependent on both jasmonic acid and salicylic acid signaling pathways. Planta 224: 1197–1208.

Ansari, M.S. and Gupta, N.P. (2004). Lycopene: a novel drug therapy in hormone refractory metastatic prostate cancer. Urol. Oncol. 22: 415–420.

Armbruster, U. et al. (2013). Arabidopsis CURVATURE THYLAKOID1 proteins modify thylakoid architecture by inducing membrane curvature. Plant Cell 25: 2661–78.

Auldridge, M., Block, A., Vogel, J.T., Dabney-Smith, C., Mila, I., Bouzayen, M., Magallanes-Lundback, M., DellaPenna, D., McCarty, D.R., and Klee, H.J. (2006). Characterization of three members of the Arabidopsis carotenoid cleavage dioxygenase family demonstrates the divergent roles of this multifunctional enzyme family. Plant J. 45: 982–993.

Austin, J.R., Frost, E., Vidi, P.-A., Kessler, F., and Staehelin, L.A. (2006). Plastoglobules are lipoprotein subcompartments of the chloroplast that are permanently coupled to thylakoid membranes and contain biosynthetic enzymes. Plant Cell 18: 1693–1703.

Avendaño-Vázquez, A.-O., Cordoba, E., Llamas, E., San Román, C., Nisar, N., De la Torre, S., Ramos-Vega, M., Gutiérrez-Nava, M.D.L.L., Cazzonelli, C.I., Pogson, B.J., and León, P. (2014). An Uncharacterized Apocarotenoid-Derived Signal Generated in ζ-Carotene Desaturase Mutants Regulates Leaf Development and the Expression of Chloroplast and Nuclear Genes in Arabidopsis. Plant Cell 26: 2524–2537.

Azari, R., Tadmor, Y., Meir, A., Reuveni, M., Evenor, D., Nahon, S., Shlomo, H., Chen, L., and Levin, I. (2010). Light signaling genes and their manipulation towards modulation of phytonutrient content in tomato fruits. Biotechnol. Adv. 28: 108–118.

Bae, G. and Choi, G. (2008). Decoding of light signals by plant phytochromes and their interacting proteins. Annu. Rev. Plant Biol. 59: 281–311.

Bai, L., Kim, E.H., Dellapenna, D., and Brutnell, T. (2009). Novel lycopene epsilon cyclase activities in maize revealed through perturbation of carotenoid biosynthesis. Plant J. 59: 588–599.

Ballester, A.R.; Molthoff, J.; de Vos, R.; Hekkert, B.; Orzaez, D.; Fernández-Moreno, J.P.; Tripodi, P.; Grandillo, S.; Martin, C.; Heldens, J.; Ykema, M.; Granell, A.; Bovy, A. (2010). Biochemical and molecular analysis of pink tomatoes: deregulated expression of the gene encoding transcription factor SlMYB12 leads to pink tomato fruit color. Plant Physiol. 152: 71–84.

Balmer, Y., Koller, A., del Val, G., Manieri, W., Schürmann, P., and Buchanan, B.B. (2003). Proteomics gives insight into the regulatory function of chloroplast thioredoxins. Proc. Natl. Acad. Sci. U. S. A. 100: 370–375.

Bannai, H., Tamada, Y., Maruyama, O., Nakai, K., and Miyano, S. (2002). Extensive feature detection of N-terminal protein sorting signals. Bioinformatics 18: 298–305.

Bannai, H., Tamada, Y., Maruyama, O., Nakai, K., and Miyano, S. (2002). Extensive feature detection of N-terminal protein sorting signals. Bioinformatics 18: 298–305.

Baranska, M., Schütze, W., and Schulz, H. (2006). Determination of lycopene and β-carotene content in tomato fruits and related products: Comparison of FT-raman, ATR-IR, and NIR spectroscopy. Anal. Chem. 78: 8456–8461.

Barry, C., Blume, B., Bouzayen, M., Hamilton, A., and Grierson, D. (1996). Differential expression of the 1-aminocyclopropane-1-carboxylate oxidase gene family of tomato. Plant J. 9: 525–535.

Barry, C., McQuinn, R.P., Chung, M.Y., Besuden, A., and Giovannoni, J.J. (2008). Amino acid substitutions in homologs of the STAY-GREEN protein are responsible for the green-flesh and chlorophyll retainer mutations of tomato and pepper. Plant Physiol. 147: 179–187.

Barsan, C., Zouine, M., Maza, E., Bian, W., Egea, I., Rossignol, M., Bouyssie, D., Pichereaux, C., Purgatto, E., Bouzayen, M., Latche, A., and Pech, J.C. (2012). Proteomic Analysis of Chloroplast-to-Chromoplast Transition in Tomato Reveals Metabolic Shifts Coupled with Disrupted Thylakoid Biogenesis Machinery and Elevated Energy-Production Components. Plant Physiol. 160: 708–725.

Bartley, G. and Scolnik, P. (1993). cDNA Cloning, Expression during Development, and Genome Mapping of a second phytoenen synthase. Biochemistry 268: 25718–25721.

Bechtold, N. and Pelletier, G. (1998) In planta Agrobacterium-mediated transformation of adult Arabidopsis thaliana plants by vacuum infiltra- tion. Methods Mol. Biol. 82, 259–266

Bemer, M., Karlova, R., Ballester, A.-R., Tikunov, Y.M., Bovy, A., Wolters-Arts, M., Rossetto, P.D.B., Angenent, G.C., and de Maagd, R. a (2012). The tomato FRUITFULL homologs TDR4/FUL1 and MBP7/FUL2 regulate ethylene-independent aspects of fruit ripening. Plant Cell 24: 4437–4451.

Benvenuto, G., Formiggini, F., Laflamme, P., Malakhov, M., and Bowler, C. (2002). The photomorphogenesis regulator DET1 binds the amino-terminal tail of histone H2B in a nucleosome context. Curr. Biol. 12: 1529–1534.

Bick, J.A. and Lange, B.M. (2003). Metabolic cross talk between cytosolic and plastidial pathways of isoprenoid biosynthesis: Unidirectional transport of intermediates across the chloroplast envelope membrane. Arch. Biochem. Biophys. 415: 146–154.

Bleecker, A.B. (1999). Ethylene perception and signaling: An evolutionary perspective. Trends Plant Sci. 4: 269–274.

Botella-Pavía, P., Besumbes, Ó., Phillips, M. a., Carretero-Paulet, L., Boronat, A., and Rodríguez-Concepción, M. (2004). Regulation of carotenoid biosynthesis in plants: Evidence for a key role of hydroxymethylbutenyl diphosphate reductase in controlling the supply of plastidial isoprenoid precursors. Plant J. 40: 188–199.

Botterweg, E. (2014) PIFILa: a novel regulator of carotenoid biosynthesis in tomato fruit. Tesis de Máster. Máster en Biotecnología molecular. Universitat de Barcelona.

Bou-Torrent, J., Toledo-Ortiz, G., Ortiz-Alcaide, M., Cifuentes-Esquivel, N., Halliday, K.J., Martinez-García, J.F., and Rodríguez-Concepción, M. (2015). Regulation of carotenoid biosynthesis by shade relies on specific subsets of antagonistic transcription factors and co-factors. Plant Physiol. 168: 1584–1594..

Bouvier, F., Rahier, A., and Camara, B. (2005). Biogenesis, molecular regulation and function of plant isoprenoids. Prog. Lipid Res. 44: 357–429.

Brady, S. and Shatkay, H. (2008). EpiLoc: a (working) text-based system for predicting protein subcellular location. Pacific Symp. Biocomput. 615: 604–615.

Brady, S. and Shatkay, H. (2008). EpiLoc: a (working) text-based system for predicting protein subcellular location. Pacific Symp. Biocomput. 615: 604–615.

Büch, K., Stransky, H., and Hager, A. (1995). FAD is a further essential cofactor of the NAD (P) H and O 2-dependent zeaxanthin-epoxidase. FEBS Lett. 376: 45–48.

Burg, S.P. and Burg, E. a (1965). Ethylene Action and the Ripening of Fruits. Science 148: 1190–1196.

Butelli, E., Titta, L., Giorgio, M., Mock, H.-P., Matros, A., Peterek, S., Schijlen, E.G.W.M., Hall, R.D., Bovy, A., Luo, J., and Martin, C. (2008). Enrichment of tomato fruit with

health-promoting anthocyanins by expression of select transcription factors. Nat. Biotechnol. 26: 1301–1308.

Carol, P. and Kuntz, M. (2001). A plastid terminal oxidase comes to light: Implications for carotenoid biosynthesis and chlororespiration. Trends Plant Sci. 6: 31–36.

Casal, J.J., Candia, A.N., and Sellaro, R. (2013). Light perception and signalling by phytochrome A. J. Exp. Bot. 65: 2835–2845.

Cazzonelli, C.I. and Pogson, B.J. (2010). Source to sink: regulation of carotenoid biosynthesis in plants. Trends Plant Sci. 15: 266–274.

Chen, G.; Hackett, R.; Walker, D.; Taylor, A.; Lin, Z.; and Grierson, D. (2004). Identification of a Specific Isoform of Tomato Lipoxygenase (TomloxC) Involved in the Generation of Fatty Acid-Derived Flavor Compounds. Plant Physiol. 136: 2641–2651.

Cherian, S., Figueroa, C.R., and Nair, H. (2014). "Movers and shakers" in the regulation of fruit ripening: A cross-dissection of climacteric versus non-climacteric fruit. J. Exp. Bot. 65: 4705–4722.

Cheung, Y., McNellis, T., and Piekos, B. (1993). Maintenance of Chloroplast Components during Chromoplast Differentiation in the Tomato Mutant Green Flesh. Plant Physiol. 101: 1223–1229.

Chung, M.Y., Vrebalov, J., Alba, R., Lee, J., McQuinn, R., Chung, J.D., Klein, P., and Giovannoni, J. (2010). A tomato (Solanum lycopersicum) APETALA2/ERF gene, SlAP2a, is a negative regulator of fruit ripening. Plant J. 64: 936–947.

Cookson, P.J., Kiano, J.W., Shipton, C.A., Fraser, P.D., Romer, S., Schuch, W., Bramley, P., and Pyke, K.A. (2003). Increases in cell elongation, plastid compartment size and phytoene synthase activity underlie the phenotype of the high pigment-1 mutant of tomato. Planta 217: 896–903.

Cordain, L., Miller, J.B., Eaton, S.B., Mann, N., Holt, S.H.A., and Speth, J.D. (2000). Plant-animal subsistence ratios and macronutrient energy estimations in worldwide hunter-gatherer diets. Am. J. Clin. Nutr. 71: 682–692.

Cordoba, E., Porta, H., Arroyo, A., San Román, C., Medina, L., Rodríguez-Concepción, M., León, P. (2011). Functional characterization of the three genes encoding 1-deoxy-D-xylulose 5-phosphate synthase in maize. J. Exp. Bot. 62: 2023–2038.

Cunningham, F.X. and Gantt, E. (1998). Genes and Enzymes of Carotenoid Biosynthesis in Plants. Annu. Rev. Plant Physiol. Plant Mol. Biol. 49: 557–583.

Cunningham, F.X., Pogson, B., Sun, Z., McDonald, K. a, DellaPenna, D., and Gantt, E. (1996). Functional Analysis of the B and e Lycopene Cyclases for Control of Cyclic Carotenoid Formation. Society 8: 1613–1626.

Czarnecki, O. and Grimm, B. (2012). Post-translational control of tetrapyrrole biosynthesis in plants, algae, and cyanobacteria. J. Exp. Bot. 63: 1675–1687.

D'Ambrosio, C., Giorio, G., Marino, I., Merendino, A., Petrozza, A., Salfi, L., Stigliani, A.L., and Cellini, F. (2004). Virtually complete conversion of lycopene into beta-carotene in fruits of tomato plants transformed with the tomato lycopene beta-cyclase (tlcy-b) cDNA. Plant Sci. 166: 207–214.

D'Ambrosio, D.N., Clugston, R.D., and Blaner, W.S. (2011). Vitamin A metabolism: An update. Nutrients 3: 63–103.

Davuluri, G.R. et al. (2005). Fruit-specific RNAi-mediated suppression of DET1 enhances carotenoid and flavonoid content in tomatoes. Nat. Biotechnol. 23: 890–895.

Demmig-Adams, B., Gilmore, A.M., and Adams, W.W. (1996). In vivo functions of carotenoids in higher plants. Faseb 10: 403–412.

Dogbo, O., Laferriere, A., d'Harlingue, A., and Camara, B. (1988). Carotenoid Biosynthesis: Isolation and Characterization of a Bifunctional Enzyme Catalyzing the Synthesis of Phytoene. Proc Natl Acad Sci USA 85: 7054–7058.

Dong, H., Fei, G., Wu, C., Wu, F., Sun, Y., Chen, M. Ren, Y., Zhou, K., Cheng, Z., Wang, J., Jiang, L., Zhang, X., Guo, X., Lei, C., Su, N., Wang, H., Wan, J. (2013). A Rice Virescent-Yellow Leaf Mutant Reveals New Insights into the Role and Assembly of Plastid Caseinolytic Protease in Higher Plants. Plant Physiol. 162: 1867–1880.

Dong, T., Hu, Z., Deng, L., Wang, Y., Zhu, M., Zhang, J., and Chen, G. (2013). A tomato MADS-box transcription factor, SlMADS1, acts as a negative regulator of fruit ripening. Plant Physiol. 163: 1026–36.

Edgar, R.C. (2004). MUSCLE: Multiple sequence alignment with high accuracy and high throughput. Nucleic Acids Res. 32: 1792–1797.

Egea, I., Bian, W., Barsan, C., Jauneau, A., Pech, J.C., Latchè, A., Li, Z., and Chervin, C. (2011). Chloroplast to chromoplast transition in tomato fruit: Spectral confocal microscopy analyses of carotenoids and chlorophylls in isolated plastids and time-lapse recording on intact live tissue. Ann. Bot. 108: 291–297.

Emanuelsson, O., Nielsen, H., and von Heijne, G. (1999). ChloroP, a neural network-based method for predicting chloroplast transit peptides and their cleavage sites. Protein Sci. 8: 978–984.

Enfissi, E., Fraser, P., Lois, L.M., Boronat, A., Schuch, W., and Bramley, P. (2005). Metabolic engineering of the mevalonate and non-mevalonate isopentenyl diphosphate-forming pathways for the production of health-promoting isoprenoids in tomato. Plant Biotechnol. J. 3: 17–27.

Enfissi, E.M. a, Barneche, F., Ahmed, I., Lichtlé, C., Gerrish, C., McQuinn, R.P., Giovannoni, J.J., Lopez-Juez, E., Bowler, C., Bramley, P.M., and Fraser, P.D. (2010). Integrative transcript and metabolite analysis of nutritionally enhanced DE-ETIOLATED1 downregulated tomato fruit. Plant Cell 22: 1190–1215.

Eriksson, E.M., Bovy, A., Manning, K., Harrison, L., Andrews, J., De Silva, J., Tucker, G. a, and Seymour, G.B. (2004). Effect of the Colorless non-ripening mutation on cell wall

biochemistry and gene expression during tomato fruit development and ripening. Plant Physiol. 136: 4184–4197.

Eriksson, O. (2014). Evolution of angiosperm seed disperser mutualisms: the timing of origins and their consequences for coevolutionary interactions between angiosperms and frugivores. Biol. Rev. Camb. Philos. Soc. 91, 168–186.

Estévez, J.M., Cantero, A., Reindl, A., Reichler, S., and León, P. (2001). 1-Deoxy-D-xylulose-5-phosphate Synthase, a Limiting Enzyme for Plastidic Isoprenoid Biosynthesis in Plants. J. Biol. Chem. 276: 22901–22909.

Esther Botterberg (2014) PIFILa: a novel regulator of carotenoid biosynthesis in tomato frui. Máster en Biotecnologia Molecular.. Universitat de Barcelona.

Estornell, L.H., Orzáez, D., López-Peña, L., Pineda, B., Antón, M.T., Moreno, V., and Granell, A. (2009). A multisite gateway-based toolkit for targeted gene expression and hairpin RNA silencing in tomato fruits. Plant Biotechnol. J. 7: 298–309.

Fanciullino, A.L., Cercós, M., Dhuique-Mayer, C., Froelicher, Y., Talón, M., Ollitrault, P., and Morillon, R. (2008). Changes in carotenoid content and biosynthetic gene expression in juice sacs of four orange varieties (Citrus sinensis) differing in flesh fruit color. J. Agric. Food Chem. 56: 3628–3638.

Fantini, E., Falcone, G., Frusciante, S., Giliberto, L., and Giuliano, G. (2013). Dissection of Tomato Lycopene Biosynthesis through Virus-Induced Gene Silencing. Plant Physiol. 163: 986–998.

Fernandez, A.I. et al. (2009). Flexible Tools for Gene Expression and Silencing in Tomato. Plant Physiol. 151: 1729–1740.

Flores-Perez, U., Sauret-Gueto, S., Gas, E., Jarvis, P., and Rodriguez-Concepcion, M. (2008). A Mutant Impaired in the Production of Plastome-Encoded Proteins Uncovers a Mechanism for the Homeostasis of Isoprenoid Biosynthetic Enzymes in Arabidopsis Plastids. Plant Cell 20: 1303–1315.

Fraser, P. and Bramley, P. (2004). The biosynthesis and nutritional uses of carotenoids. Prog. Lipid Res. 43: 228–265..

Fraser, P.D., Enfissi, E., and Bramley, P. (2009). Genetic engineering of carotenoid formation in tomato fruit and the potential application of systems and synthetic biology approaches. Arch. Biochem. Biophys. 483: 196–204.

Fraser, P.D., Enfissi, E.M. a, Halket, J.M., Truesdale, M.R., Yu, D., Gerrish, C., and Bramley, P. (2007). Manipulation of phytoene levels in tomato fruit: effects on isoprenoids, plastids, and intermediary metabolism. Plant Cell 19: 3194–3211.

Fraser, P.D., Kiano, J.W., Truesdale, M.R., Schuch, W., and Bramley, P. (1999). Phytoene synthase-2 enzyme activity in tomato does not contribute to carotenoid synthesis in ripening fruit. Plant Mol. Biol. 40: 687–698.

Fraser, P.D., Pinto, M.E., Holloway, D.E., and Bramley, P. (2000). Technical advance: application of high-performance liquid chromatography with photodiode array detection to the metabolic profiling of plant isoprenoids. Plant J. 24: 551–558.

Fraser, P.D., Romer, S., Shipton, C. a, Pb, M., Jw, K., N, M., R, D., Schuch, W., and Bramley, P. (2002). Evaluation of transgenic tomato plants expressing an additional phytoene synthase in a fruit-specific manner. Proc. Natl. Acad. Sci. 99: 1092–1097.

Fraser, P.D., Truesdale, M.R., Bird, C.R., Schuch, W., and Bramley, P. (1994). Carotenoid biosynthesis during tomato fruit development (evidence for tissue-specific gene expression). Plant Physiol. 105: 405–413.

Frassetto, L. a, Schloetter, M., Mietus-Synder, M., Morris, R.C., and Sebastian, a (2009). Metabolic and physiologic improvements from consuming a paleolithic, hunter-gatherer type diet. Eur. J. Clin. Nutr. 63: 947–955.

Fray, R., Grierson, D.(1993). Molecular-genetics of tomato fruit ripening. Trends in Genetics. 9,438–443.

Fray, R.G., Wallace, A., Fraser, P.D., Valero, D., Hedden, P., Bramley, P., and Grierson, D. (1995). Constitutive expression of a fruit phytoene synthase gene in transgenic tomatoes from the gibberellin pathway. Plant J. 8: 693–701.

Friedman, M. (2013). Anticarcinogenic, cardioprotective, and other health benefits of tomato compounds lycopene, α-tomatine, and tomatidine in pure form and in fresh and processed tomatoes. J. Agric. Food Chem. 61: 9534–9550.

Frigaard, N., Maresca, J. a, Yunker, C.E., Jones, D., Bryant, D. a, and Jones, a D. (2004). Genetic Manipulation of Carotenoid Biosynthesis in the Green Sulfur Bacterium Chlorobium tepidum Genetic Manipulation of Carotenoid Biosynthesis in the Green Sulfur Bacterium Chlorobium tepidum. J. Bacteriol. 186: 5120–5220.

Frusciante, L., Carli, P., Ercolano, M.R., Pernice, R., Di Matteo, A., Fogliano, V., and Pellegrini, N. (2007). Antioxidant nutritional quality of tomato. Mol. Nutr. Food Res. 51: 609–617.

Fujimoto, M. and Tsutsumi, N. (2014). Dynamin-related proteins in plant post-Golgi traffic. Front. Plant Sci. 5: 1–8.

Fujisawa, M., Nakano, T., and Ito, Y. (2011). Identification of potential target genes for the tomato fruit-ripening regulator RIN by chromatin immunoprecipitation. BMC Plant Biol. 11: 26–40.

Fujisawa, M., Nakano, T., Shima, Y., and Ito, Y. (2013). A large-scale identification of direct targets of the tomato MADS box transcription factor RIPENING INHIBITOR reveals the regulation of fruit ripening. Plant Cell 25: 371–86.

Fujisawa, M., Shima, Y., Higuchi, N., Nakano, T., Koyama, Y., Kasumi, T., and Ito, Y. (2012). Direct targets of the tomato-ripening regulator RIN identified by transcriptome and chromatin immunoprecipitation analyses. Planta 235: 1107–1122.

Fujisawa, M., Shima, Y., Nakagawa, H., Kitagawa, M., Kimbara, J., Nakano, T., Kasumi, T., and Ito, Y. (2014). Transcriptional regulation of fruit ripening by tomato FRUITFULL homologs and associated MADS box proteins. Plant Cell 26: 89–101.

Galpaz, N., Ronen, G., Khalfa, Z., Zamir, D., and Hirschberg, J. (2006). A Chromoplast-Speci c Carotenoid Biosynthesis Pathway Is Revealed by Cloning of the Tomato white-ower Locus. Plant Cell 18: 1–14.

Galpaz, N., Wang, Q., Menda, N., Zamir, D., and Hirschberg, J. (2008). Abscisic acid deficiency in the tomato mutant high-pigment 3 leading to increased plastid number and higher fruit lycopene content. Plant J. 53: 717–730.

Galvao, V.C. and Fankhauser, C. (2015). Sensing the light environment in plants: Photoreceptors and early signaling steps. Curr. Opin. Neurobiol. 34: 46–53.

Gapper, N.E., McQuinn, R.P., and Giovannoni, J.J. (2013). Molecular and genetic regulation of fruit ripening. Plant Mol. Biol. 82: 575–591.

Ghassemian, M., Lutes, J., Tepperman, J.M., Chang, H.S., Zhu, T., Wang, X., Quail, P.H., and Markus Lange, B. (2006). Integrative analysis of transcript and metabolite profiling data sets to evaluate the regulation of biochemical pathways during photomorphogenesis. Arch. Biochem. Biophys. 448: 45–59.

Gierlinger, N., Keplinger, T., and Harrington, M. (2012). Imaging of plant cell walls by confocal Raman microscopy. Nat. Protoc. 7: 1694–1708.

Giliberto, L., Perrotta, G., Pallara, P., Weller, J.L., Fraser, P.D., Bramley, P., Fiore, A., Tavazza, M., and Giuliano, G. (2005). Manipulation of the blue light photoreceptor cryptochrome 2 in tomato affects vegetative development, flowering time, and fruit antioxidant content. Plant Physiol. 137: 199–208.

Giménez, E., Pineda, B., Capel, J., Antón, M.T., Atarés, A., Pérez-Martín, F., García-Sogo, B., Angosto, T., Moreno, V., and Lozano, R. (2010). Functional analysis of the Arlequin mutant corroborates the essential role of the ARLEQUIN/TAGL1 gene during reproductive development of tomato. PLoS One 5: 1–16.

Giorio, G., Stigliani, A.L., and D'Ambrosio, C. (2008). Phytoene synthase genes in tomato (*Solanum lycopersicum L.*) - New data on the structures, the deduced amino acid sequences and the expression patterns. FEBS J. 275: 527–535.

Giovannoni, J.J. (2007). Fruit ripening mutants yield insights into ripening control. Curr. Opin. Plant Biol. 10: 283–289.

Giuliano, G., Tavazza, R., Diretto, G., Beyer, P., and Taylor, M. a. (2008). Metabolic engineering of carotenoid biosynthesis in plants. Trends Biotechnol. 26: 139–145.

Gupta, S.K., Sharma, S., Santisree, P., Kilambi, H.V., Appenroth, K., Sreelakshmi, Y., and Sharma, R. (2014). Complex and shifting interactions of phytochromes regulate fruit development in tomato. Plant, Cell Environ. 37: 1688–1702.

Hall, B.G. (2013). Building phylogenetic trees from molecular data with MEGA. Mol. Biol. Evol. 30: 1229–1235.

Han, H., Gao, S., Li, B., Dong, X.C., Feng, H.L., and Meng, Q.W. (2010). Overexpression of violaxanthin de-epoxidase gene alleviates photoinhibition of PSII and PSI in tomato during high light and chilling stress. J. Plant Physiol. 167: 176–183.

Harjes, C.E., Rocheford, T.R., Bai, L., Brutnell, T., Kandianis, C.B., Sowinski, S.G., Stapleton, A.E., Vallabhaneni, R., Williams, M., and Wurtzel, E.T. (2007). Natural Genetic Variation in Lycopene Epsilon Cyclase Tapped for Maize Biofortification. Science (80-.). 171: 16–18.

Hirschberg, J. (2001). Carotenoid biosynthesis in flowering plants. Curr Opin Plant Biol 4: 210–218.

Hörtensteiner, S. (2009). Stay-green regulates chlorophyll and chlorophyll-binding protein degradation during senescence. Trends Plant Sci. 14: 155–162.

Huang, F.C., Molnar, P., and Schwab, W. (2009). Cloning and functional characterization of carotenoid cleavage dioxygenase 4 genes. J. Exp. Bot. 60: 3011–3022.

Ilg, A., Bruno, M., Beyer, P., and Al-Babili, S. (2014). Tomato carotenoid cleavage dioxygenases 1A and 1B: Relaxed double bond specificity leads to a plenitude of dialdehydes, mono-apocarotenoids and isoprenoid volatiles. FEBS 4: 584–593.

Isaacson, T., Ohad, I., Beyer, P., and Hirschberg, J. (2004). Analysis in vitro of the enzyme CRTISO establishes a poly-cis-carotenoid biosynthesis pathway in plants. Plant Physiol. 136: 4246–55.

Isaacson, T., Ronen, G., Zamir, D., and Hirschberg, J. (2002). Cloning of tangerine from tomato reveals a carotenoid isomerase essential for the production of beta-carotene and xanthophylls in plants. Plant Cell 14: 333–42.

Itkin, M., Seybold, H., Breitel, D., Rogachev, I., Meir, S., and Aharoni, A. (2009). TOMATO AGAMOUS-LIKE 1 is a component of the fruit ripening regulatory network. Plant J. 60: 1081–1095.

Ito, Y., Kitagawa, M., Ihashi, N., Yabe, K., Kimbara, J., Yasuda, J., Ito, H., Inakuma, T., Hiroi, S., and Kasumi, T. (2008). DNA-binding specificity, transcriptional activation potential, and the rin mutation effect for the tomato fruit-ripening regulator RIN. Plant J. 55: 212–223.

Janska, H., Kwasniak, M., and Szczepanowska, J. (2013). Protein quality control in organelles - AAA/FtsH story. Biochim. Biophys. Acta - Mol. Cell Res. 1833: 381–387.

Jeffery, J., Holzenburg, A., and King, S. (2012). Physical barriers to carotenoid bioaccessibility. Ultrastructure survey of chromoplast and cell wall morphology in nine carotenoid-containing fruits and vegetables. J. Sci. Food Agric. 92: 2594–2602.

Kachanovsky, D.E., Filler, S., Isaacson, T., and Hirschberg, J. (2012). Epistasis in tomato color mutations involves regulation of phytoene synthase 1 expression by cis-carotenoids. Proc. Natl. Acad. Sci. 109: 19021–19026.

Karimi, M., De Meyer, B., and Hilson, P. (2005). Modular cloning in plant cells. Trends Plant Sci. 10: 103–105.

Kevany, B.M., Tieman, D.M., Taylor, M.G., Cin, V.D., and Klee, H.J. (2007). Ethylene receptor degradation controls the timing of ripening in tomato fruit. Plant J. 51: 458–467.

Kim, J. and DellaPenna, D. (2006). Defining the primary route for lutein synthesis in plants: the role of Arabidopsis carotenoid beta-ring hydroxylase CYP97A3. Proc. Natl. Acad. Sci. U. S. A. 103: 3474–3479.

Kim, J., Kimber, M.S., Nishimura, K., Friso, G., Schultz, L., Ponnala, L., and van Wijk, K.J. (2015). Structures, Functions, and Interactions of ClpT1 and ClpT2 in the Clp Protease System of Arabidopsis Chloroplasts. Plant Cell 27: 1477–1496.

Kim, J., Olinares, P.D., Oh, S., Ghisaura, S., Poliakov, A., Ponnala, L., and van Wijk, K.J. (2013). Modified Clp protease complex in the ClpP3 null mutant and consequences for chloroplast development and function in Arabidopsis. Plant Physiol. 162: 157–79

Kim, J., Rudella, A., Ramirez Rodriguez, V., Zybailov, B., Olinares, P.D.B., and van Wijk, K.J. (2009). Subunits of the plastid ClpPR protease complex have differential contributions to embryogenesis, plastid biogenesis, and plant development in Arabidopsis. Plant Cell 21: 1669–1692.

Klassen, J.L. (2010). Phylogenetic and evolutionary patterns in microbial carotenoid biosynthesis are revealed by comparative genomics. PLoS One 5: 1–20.

Klee, H.J. and Giovannoni, J.J. (2011). Genetics and Control of Tomato Fruit Ripening and Quality Attributes. Annu. Rev. Genet. 45: 41–59.

Klonoff, D.C. (2009). The beneficial effects of a Paleolithic diet on type 2 diabetes and other risk factors for cardiovascular disease. J. Diabetes Sci. Technol. 3: 1229–32.

Kolotilin, I., Koltai, H., Tadmor, Y., Bar-Or, C., Reuveni, M., Meir, A., Nahon, S., Shlomo, H., Chen, L., and Levin, I. (2007). Transcriptional profiling of high pigment-2dg tomato mutant links early fruit plastid biogenesis with its overproduction of phytonutrients. Plant Physiol. 145: 389–401.

Koussevitzky, S., Stanne, T.M., Peto, C.A., Giap, T., Sjögren, L.L.E., Zhao, Y., Clarke, A.K., and Chory, J. (2007). An Arabidopsis thaliana virescent mutant reveals a role for ClpR1 in plastid development. Plant Mol. Biol. 63: 85–96.

Kovàcs, K., Fray, R.G., Tikunov, Y., Graham, N., Bradley, G., Seymour, G.B., Bovy, A., and Grierson, D. (2009). Effect of tomato pleiotropic ripening mutations on flavour volatile biosynthesis. Phytochemistry 70: 1003–1008.

Krushkal, J., Pistilli, M., Ferrell, K.M., Souret, F.F., and Weathers, P.J. (2003). Computational analysis of the evolution of the structure and function of 1-deoxy-D-xylulose-5-phosphate synthase, a key regulator of the mevalonate-independent pathway in plants. Gene 313: 127–138.

Laguna, L., Casado, C.G., and Heredia, A. (1999). Flavonoid biosynthesis in tomato fruit cuticles after in vivo incorporation of H-3-phenylalanine precursor. Physiol. Plant. 105: 491–498.

Lanahan, M.B., Yen, H.-C., Giovannoni, J.J., and Klee, H.J. (1994). The Never Ripe Mutation Blocks Ethylene Perception in Tomato. Plant Cell 6: 521–530.

Laule, O., Fürholz, A., Chang, H.-S., Zhu, T., Wang, X., Heifetz, P.B., Gruissem, W., and Lange, M. (2003). Crosstalk between cytosolic and plastidial pathways of isoprenoid biosynthesis in Arabidopsis thaliana. Proc. Natl. Acad. Sci. U. S. A. 100: 6866–6871.

Leivar, P. and Monte, E. (2014). PIFs: systems integrators in plant development. Plant Cell 26: 56–78.

Leivar, P. and Quail, P.H. (2011). PIFs: Pivotal components in a cellular signaling hub. Trends Plant Sci. 16: 19–28.

Leivar, P., Tepperman, J.M., Monte, E., Calderon, R.H., Liu, T.L., and Quail, P.H. (2009). Definition of early transcriptional circuitry involved in light-induced reversal of PIF-imposed repression of photomorphogenesis in young Arabidopsis seedlings. Plant Cell 21: 3535–3553.

Lemaire, S., Guillon, B., Le Marechal, P., Keryer, E., Miginiac-Maslow, M., and Decottignies, P. (2004). New thioredoxin targets in the unicellular photosynthetic eukaryote Chlamydomonas reinhardtii. Proc. Natl. Acad. Sci. 101: 7475–7480.

Leseberg, C.H., Eissler, C.L., Wang, X., Johns, M.A., Duvall, M.R., and Mao, L. (2008). Interaction study of MADS-domain proteins in tomato. J. Exp. Bot. 59: 2253–2265.

Levin I, Frankel P, Gilboa N, Tanny S, Lalazar A (2003) The tomato dark green mutation is a novel allele of the tomato homolog of the DEETIOLATED1 gene. Theor Appl Genet 106 454–460

Lewinsohn, E., Sitrit, Y., Bar, E., Azulay, Y., Ibdah, M., Meir, A., Yosef, E., Zamir, D., and Tadmor, Y. (2005). Not just colors - Carotenoid degradation as a link between pigmentation and aroma in tomato and watermelon fruit. Trends Food Sci. Technol. 16: 407–415.

Li, L. and Yuan, H. (2013). Chromoplast biogenesis and carotenoid accumulation. Arch. Biochem. Biophys. 539: 102–109.

Lincoln, J.E., Cordes, S., Read, E., and Fischer, R.L. (1987). Regulation of gene expression by ethylene during Lycopersicon esculentum (tomato) fruit development. Proc. Natl. Acad. Sci. U. S. A. 84: 2793–2797.

Liu, L., Shao, Z., Zhang, M., and Wang, Q. (2015). Regulation of Carotenoid Metabolism in Tomato. Mol. Plant 8: 28–39.

Liu, R.H. (2003). Health benefits of fruit and vegetables are from additive and synergistic combinaions of phytochemicals. Am. J. Clin. Nutr. 78: 3–6.

Liu, Y., Roof, S., Ye, Z., Barry, C., Van Tuinent, A., Vrebalov, J., Bowler, C., Giovannoni, J., van Tuinen, A., Vrebalov, J., Bowler, C., and Giovannoni, J. (2004). Manipulation of light signal transduction as a means of modifying fruit nutritional quality in tomato\r10.1073/pnas.0400935101. Proc. Natl. Acad. Sci. U. S. A. 101: 9897–9902.

Llorente, B., D'Andrea, L., and Rodríguez-Concepción, M. (2016). Evolutionary Recycling of Light Signaling Components in Fleshy Fruits: New Insights on the Role of Pigments to Monitor Ripening. Front. Plant Sci. 7: 1–7.

Lois, L.M., Rodríguez-Concepción, M., Gallego, F., Campos, N., and Boronat, A. (2000). Carotenoid biosynthesis during tomato fruit development: Regulatory role of 1-deoxy-D-xylulose 5-phosphate synthase. Plant J. 22: 503–513.

Luo, Z., Zhang, J., Li, J., Yang, C., Wang, T., Ouyang, B., Li, H., Giovannoni, J., and Ye, Z. (2013). A STAY-GREEN protein SlSGR1 regulates lycopene and β-carotene accumulation by interacting directly with SlPSY1 during ripening processes in tomato. New Phytol. 198: 442–452.

Manning, K., Tör, M., Poole, M., Hong, Y., Thompson, A.J., King, G.J., Giovannoni, J.J., and Seymour, G.B. (2006). A naturally occurring epigenetic mutation in a gene encoding an SBP-box transcription factor inhibits tomato fruit ripening. Nat. Genet. 38: 948–952.

Maresca, J. a, Graham, J.E., Wu, M., Eisen, J. a, and Bryant, D. a (2007). Identification of a fourth family of lycopene cyclases in photosynthetic bacteria. Proc. Natl. Acad. Sci. U. S. A. 104: 11784–9.

Marin, E., Nussaume, L., Quesada, a, Gonneau, M., Sotta, B., Hugueney, P., Frey, a, and Marion-Poll, a (1996). Molecular identification of zeaxanthin epoxidase of Nicotiana plumbaginifolia, a gene involved in abscisic acid biosynthesis and corresponding to the ABA locus of Arabidopsis thaliana. EMBO J. 15: 2331–2342.

Martel, C., Vrebalov, J., Tafelmeyer, P., and Giovannoni, J.J. (2011). The Tomato MADS-Box Transcription Factor RIPENING INHIBITOR Interacts with Promoters Involved in Numerous Ripening Processes in a COLORLESS NONRIPENING-Dependent Manner. Plant Physiol. 157: 1568–1579.

Martin, C., Zhang, Y., Tonelli, C., and Petroni, K. (2013). Plants, diet, and health. Annu. Rev. Plant Biol. 64: 19–46.

Martinez-Garcia JF, Galstyan A, Salla-Martret M, Cifuentes-Esquivel N, Gallemí M, et al. (2010) Regulatory components of shade avoidance syndrome. Adv Bot Res53: 65–116.

Mathews, S. (2006). Phytochrome-mediated development in land plants: Red light sensing evolves to meet the challenges of changing light environments. Mol. Ecol. 15: 3483–3503.

McQuinn, R.P., Giovannoni, J.J., and Pogson, B.J. (2015). More than meets the eye: from carotenoid biosynthesis, to new insights into apocarotenoid signaling. Curr. Opin. Plant Biol. 27: 172–179.

Meier, S., Tzfadia, O., Vallabhaneni, R., Gehring, C., and Wurtzel, E.T. (2011). A transcriptional analysis of carotenoid, chlorophyll and plastidial isoprenoid biosynthesis genes during development and osmotic stress responses in Arabidopsis thaliana. BMC Syst. Biol. 5: 1–19.

Meléndez-Martínez, A.J., Mapelli-Brahm, P., Benítez-González, A., and Stinco, C.M. (2015). A comprehensive review on the colorless carotenoids phytoene and phytofluene. Arch. Biochem. Biophys. 572: 188–200.

Meng, X., Wang, J.R., Wang, G.D., Liang, X.Q., Li, X.D., and Meng, Q.W. (2015). An R2R3-MYB gene, LeAN2, positively regulated the thermo-tolerance in transgenic tomato. J. Plant Physiol. 175: 191–197.

Mialoundama, A.S., Heintz, D., Jadid, N., Nkeng, P., Rahier, A., Deli, J., Camara, B., and Bouvier, F. (2010). Characterization of plant carotenoid cyclases as members of the flavoprotein family functioning with no net redox change. Plant Physiol. 153: 970–9.

Mintz-oron, S., Mandel, T., Rogachev, I., Feldberg, L., Lotan, O., Yativ, M., Wang, Z., Jetter, R., Venger, I., Adato, A., and Aharoni, A. (2008). Gene Expression and Metabolism in Tomato Fruit. 147: 823–851.

Miyagishima, S., Froehlich, J.E., and Osteryoung, K.W. (2006). PDV1 and PDV2 mediate recruitment of the dynamin-related protein ARC5 to the plastid division site. Plant Cell 18: 2517–2530.

Miyagishima, S.-Y., Nishida, K., Mori, T., Matsuzaki, M., Higashiyama, T., Kuroiwa, H., and Kuroiwa, T. (2003). A plant-specific dynamin-related protein forms a ring at the chloroplast division site. Plant Cell 15: 655–665.

Moise, A.R., Al-Babili, S., and Wurtzel, E.T. (2014). Mechanistic aspects of carotenoid biosynthesis. Chem. Rev. 114: 164–193.

Morgan, H.D., Sutherland, H.G., Martin, D.I., and Whitelaw, E. (1999). Epigenetic inheritance at the agouti locus in the mouse. Nat. Genet. 23: 314–318.

Mustilli, A.C., Fenzi, F., Ciliento, R., Alfano, F., and Bowler, C. (1999). Phenotype of the tomato high pigment-2 mutant is caused by a mutation in the tomato homolog of DEETIOLATED1. Plant Cell 11: 145–157.

Nambara, E. and Marion-Poll, A. (2010). Abscisic Acid Biosynthesis and Catabolism. Annu. Rev. Plant Biol. 56: 165–185.

Nashilevitz, S., Melamed-Bessudo, C., Izkovich, Y., Rogachev, I., Osorio, S., Itkin, M., Adato, A., Pankratov, I., Hirschberg, J., Fernie, A.R., Wolf, S., Usadel, B., Levy, A., Rumeau, D., Aharoni, A. (2010). An orange ripening mutant links plastid NAD(P)H dehydrogenase complex activity to central and specialized metabolism during tomato fruit maturation. Plant Cell 22: 1977–1997.

Neff, M.M., Fankhauser, C., and Chory, J. (2000). Light: an indicator of time and place. Genes Dev. 14: 257–271.

Nishimura, K. and van Wijk, K.J. (2015). Organization, function and substrates of the essential Clp protease system in plastids. Biochim. Biophys. Acta - Bioenerg. 1847: 915–930.

Nishimura, K., Apitz, J., Friso, G., Kim, J., Ponnala, L., Grimm, B., and van Wijk, K.J. (2015). Discovery of a Unique Clp Component, ClpF, in Chloroplasts: A Proposed Binary ClpF-ClpS1 Adaptor Complex Functions in Substrate Recognition and Delivery. Plant Cell 27: 2677–2691.

North, H.M., Almeida, A.D., Boutin, J.P., Frey, A., To, A., Botran, L., Sotta, B., and Marion-Poll, A. (2007). The Arabidopsis ABA-deficient mutant aba4 demonstrates that the major route for stress-induced ABA accumulation is via neoxanthin isomers. Plant J. 50: 810–824.

Okekeogbu, I.Y., Z.J.; Sangireddy, S. R.; Li, H.; Bhatti, S.; Hui, D.F.; Zhou, S. P.; Howe, K. J.; Fish, T. L.; Yang, Y and Thannhauser, T. W. (2014). Effect of Aluminum Treatment on Proteomes of Radicles of Seeds Derived from Al-Treated Tomato Plants. Proteomes, 2: p. 169-190.

Olinares, P.D.B., Kim, J., and Van Wijk, K.J. (2011b). The Clp protease system; A central component of the chloroplast protease network. Biochim. Biophys. Acta - Bioenerg. 1807: 999–1011.

Olinares, P.D.B., Kim, J., Davis, J.I., and van Wijk, K.J. (2011a). Subunit stoichiometry, evolution, and functional implications of an asymmetric plant plastid ClpP/R protease complex in arabidopsis. Plant Cell 23: 2348–2361.

Orzaez, D., Medina, A., Torre, S., Fernandez-Moreno, J.P., Rambla, J.L., Fernandez-del-Carmen, A., Butelli, E., Martin, C., and Granell, A. (2009). A Visual Reporter System for Virus-Induced Gene Silencing in Tomato Fruit Based on Anthocyanin Accumulation. Plant Physiol. 150: 1122–1134.

Orzaez, D., Mirabel, S., Wieland, W.H., and Granell, A. (2006). Agroinjection of Tomato Fruits. A Tool for Rapid Functional Analysis of Transgenes Directly in Fruit\r10.1104/pp.105.068221. Plant Physiol. 140: 3–11.

Osnato M, Castillejo C, Matías-Hernández L, Pelaz S (2012) TEMPRANILLO genes link photoperiod and gibberellin pathways to control flowering in Arabidopsis. Nat Commun 3: 808.

Osorio, S., Ruan, Y.-L., and Fernie, A.R. (2014). An update on source-to-sink carbon partitioning in tomato. Front. Plant Sci. 5: 1–11.

Ossowski, S., Schwab, R., and Weigel, D. (2008). Gene silencing in plants using artificial microRNAs and other small RNAs. Plant J. 53: 674–690.

Paetzold, H., Garms, S., Bartram, S., Wieczorek, J., Urós-Gracia, E.M., Rodríguez-Concepción, M., Boland, W., Strack, D., Hause, B., and Walter, M.H. (2010). The isogene 1-deoxy-D-xylulose 5-phosphate synthase 2 controls isoprenoid profiles, precursor pathway allocation, and density of tomato trichomes. Mol. Plant 3: 904–916.

Pan, I.L., McQuinn, R., Giovannoni, J.J., and Irish, V.F. (2010). Functional diversification of AGAMOUS lineage genes in regulating tomato flower and fruit development. J. Exp. Bot. 61: 1795–1806.

Pan, Y., Bradley, G., Pyke, K.; Ball, G., Lu, C., Fray, R., Marshall, A., Jayasuta, S., Baxter, C., Van Wijk, R., Boyden, L., Cade, R., Chapman, N.H., Fraser, P.D., Hodgman, C.; Seymour, G.B. (2013). Network inference analysis identifies an APRR2-like gene linked to pigment accumulation in tomato and pepper fruits. Plant Physiol. 161: 1476–85.

Peltier, J.B., Ripoll, D.R., Friso, G., Rudella, A., Cai, Y., Ytterberg, J., Giacomelli, L., Pillardy, J., and Van Wijk, K.J. (2004). Clp Protease Complexes from Photosynthetic and Non-photosynthetic Plastids and Mitochondria of Plants, Their Predicted Three-dimensional Structures, and Functional Implications. J. Biol. Chem. 279: 4768–4781.

Penarrubia, L., Aguilar, M., Margossian, L., and Fischer, R.L. (1992). An Antisense Gene Stimulates Ethylene Hormone Production during Tomato Fruit Ripening. Plant Cell 4: 681–687.

Perello, C., Llamas, E., Burlat, V., Ortiz-Alcaide, M., Phillips, M.A., Pulido, P., and Rodríguez-Concepción, M. (2016). Differential subplastidial localization and turnover of enzymes involved in isoprenoid biosynthesis in chloroplasts. PLoS One 11: 1–17.

Pierleoni, A., Martelli, P.L., Fariselli, P., and Casadio, R. (2006). BaCelLo: A balanced subcellular localization predictor. Bioinformatics 22: 408–416.

Pogson, B.J., McDonald, K. a, Truong, M., Britton, G., and DellaPenna, D. (1996). Arabidopsis carotenoid mutants demonstrate that lutein is not essential for photosynthesis in higher plants. Plant Cell 8: 1627–39.

Porankiewlcz, J., Wang, J., and Clarke, A.K. (1999). New insights into the ATP-dependent Clp protease: Escherichia coli and beyond. Mol. Microbiol. 32: 449–458.

Pritchard, J.K. (2010). How we are evolving. Sci. Am.: 41–47.

Pulido, P., Llamas, E., Llorente, B., Ventura, S., Wright, P., and Rodríguez-Concepción, M. (2016). Specific Hsp100 Chaperones Determine the Fate of the First Enzyme of the Plastidial Isoprenoid Pathway to Either Refolding or Degradation by the Stromal Clp Protease in Arabidopsis. PLoS Genet.: 1–19.

Pulido, P., Toledo-Ortiz, G., Phillips, M.A., Wright, L.P., and Rodríguez-Concepción, M. (2013). Arabidopsis J-protein J20 delivers the first enzyme of the plastidial isoprenoid pathway to protein quality control. Plant Cell 25: 4183–4194.

Pyke, K.A. and Howells, C.A. (2002). Plastid and stromule morphogenesis in tomato. Ann. Bot. 90: 559–566.

Qin, G., Wang, Y., Cao, B., Wang, W., and Tian, S. (2012). Unraveling the regulatory network of the MADS box transcription factor RIN in fruit ripening. Plant J. 70: 243–255.

Raiola, A., Rigano, M.M., Calafiore, R., Frusciante, L., and Barone, A. (2014). Enhancing the health-promoting effects of tomato fruit for biofortified food. Mediators Inflamm. 2014: 1–16.

Rambla, J.L.J.L., Tikunov, Y.M., Monforte, A.J., Bovy, A., and Granell, A. (2014). The expanded tomato fruit volatile landscape. J. Exp. Bot. 65: 4613–4623.

Ramundo S, Casero D, Muhlhaus T, Hemme D, Sommer F, Crèvecoeur M, et al. (2014) Conditional Depletion of the Chlamydomonas Chloroplast ClpP Protease Activates Nuclear Genes Involved in Autophagy and Plastid Protein Quality Control. Plant Cell 26: 2201–2222

Rock, C.D. and Zeevaart, J.A. (1991). The aba mutant of Arabidopsis thaliana is impaired in epoxy-carotenoid biosynthesis. Proc. Natl. Acad. Sci. U. S. A. 88: 7496–9.

Rodríguez-Concepción, M. (2010). Supply of precursors for carotenoid biosynthesis in plants. Arch. Biochem. Biophys.

Rodríguez-Concepción, M., Ahumada, I., Diez-Juez, E., Sauret-Güeto, S., María Lois, L., Gallego, F., Carretero-Paulet, L., Campos, N., and Boronat, A. (2001). 1-Deoxy-D-xylulose 5-phosphate reductoisomerase and plastid isoprenoid biosynthesis during tomato fruit ripening. Plant J. 27: 213–222.

Rodríguez-Villalón, A., Gas, E., and Rodríguez-Concepción, M. (2009a). Colors in the dark. Plant Signal. Behav. 4: 965–967.

Rodríguez-Villalón, A., Gas, E., and Rodríguez-Concepción, M. (2009b). Phytoene synthase activity controls the biosynthesis of carotenoids and the supply of their metabolic precursors in dark-grown Arabidopsis seedlings. Plant J. 60: 424–435.

Römer, S., Fraser, P.D., Kiano, J.W., Shipton, C. a, Misawa, N., Schuch, W., and Bramley, P. (2000). Elevation of the provitamin A content of transgenic tomato plants. Nat. Biotechnol. 18: 666–669.

Ronen, G., Carmel-Goren, L., Zamir, D., and Hirschberg, J. (2000). An alternative pathway to beta -carotene formation in plant chromoplasts discovered by map-based cloning of beta and old-gold color mutations in tomato. Proc. Natl. Acad. Sci. U. S. A. 97: 11102–11107.

Ronen, G., Cohen, M., Zamir, D., and Hirschberg, J. (1999). Regulation of carotenoid biosynthesis during tomato fruit development: expression of the gene for lycopene epsilon-cyclase is down-regulated during ripening and is elevated in the mutantDelta. Plant J. 17: 341–351.

Rosati, C., Aquilani, R., Dharmapuri, S., Pallara, P., Marusic, C., Tavazza, R., Bouvier, F., Camara, B., and Giuliano, G. (2000). Metabolic engineering of beta-carotene and lycopene content in tomato fruit. Plant J. 24: 413–419.

Rottmann, W., Peter, G., Oeller, P., Keller, J., Shen N., Nagy B., Taylor L., Campbell A., Theologis A.. (1991). 1-Aminocyclopropane-1-carboxylate synthase in tomato is encoded by a multigene family whose transcription is induced during fruit and floral senescence. Journal Mol Biol. 222,937–961.

Rudella, A., Friso, G., Alonso, J.M., Ecker, J.R., and van Wijk, K.J. (2006). Downregulation of ClpR2 Leads to Reduced Accumulation of the ClpPRS Protease Complex and Defects in Chloroplast Biogenesis in Arabidopsis. Plant Cell Online 18: 1704–1721.

Ruiz-Sola, A., M., Arbona, V., Gómez-Cadenas, A., Rodríguez-Concepción, M., and Rodríguez-Villalón, A. (2014). A root specific induction of carotenoid biosynthesis contributes to ABA production upon salt stress in arabidopsis. PLoS One 9: 1–7.

Ruiz-Sola, M.A. and Rodriguez-Concepción, M. (2012). Carotenoid Biosynthesis in Arabidopsis: A Colorful Pathway. Arab. B.: 1–28.

Ruiz-Sola, M.A., Rodríguez-Villalón, A., and Rodríguez-Concepción, M. (2014). Light-sensitive Phytochrome-Interacting Factors (PIFs) are not required to regulate phytoene synthase gene expression in the root. Plant Signal. Behav. 9: 1–4.

Ruyter-Spira, C., Al-Babili, S., van der Krol, S., and Bouwmeester, H. (2013). The biology of strigolactones. Trends Plant Sci. 18: 72–83.

Saladie, M., Wright, L.P., Garcia-Mas, J., Rodriguez-Concepcion, M., and Phillips, M.A. (2014). The 2-C-methylerythritol 4-phosphate pathway in melon is regulated by specialized isoforms for the first and last steps. J. Exp. Bot. 65: 5077–5092.

Sauret-Güeto, S., Botella-Pavía, P., Flores-Pérez, U., Martínez-García, J.F., San Román, C., León, P., Boronat, A., and Rodríguez-Concepción, M. (2006). Plastid cues posttranscriptionally regulate the accumulation of key enzymes of the methylerythritol phosphate pathway in Arabidopsis. Plant Physiol. 141: 75–84.

Schnurr, G., Misawa, N., and Sandmann, G. (1996). Expression, purification and properties of lycopene cyclase from Erwinia uredovora. Biochem. J. 315 (Pt 3: 869–874.

Schofield, A. and Paliyath, G. (2005). Modulation of carotenoid biosynthesis during tomato fruit ripening through phytochrome regulation of phytoene synthase activity. Plant Physiol. Biochem. 43: 1052–1060.

Schroeder, D.F., Gahrtz, M., Maxwell, B.B., Cook, R.K., Kan, J.M., Alonso, J.M., Ecker, J.R., and Chory, J. (2002). De-etiolated 1 and damaged DNA binding protein 1 interact to regulate Arabidopsis photomorphogenesis. Curr. Biol. 12: 1462–1472.

Schürmann, P. (2003). Redox Signaling in the Chloroplast: The Ferredoxin / Thioredoxin System. Antioxidants Redox Signal. 5: 69–78.

Schwab, R., Ossowski, S., Riester, M., Warthmann, N., and Weigel, D. (2006). Highly Specific Gene Silencing by Artificial MicroRNAs in Arabidopsis[W][OA]. Plant Cell 18: 1121–1133.

Schwechheimer, C. and Deng, X.W. (2000). The COP/DET/FUS proteins-regulators of eukaryotic growth and development. Semin. Cell Dev. Biol. 11: 495–503.

Seren S, Lieberman R, Bayraktar UD, Heath E, Sahin K, et al. (2008). Lycopene in cancer prevention and treatment. Am. J. Ther. 15:66–81

Seymour, G.B., Chapman, N.H., Chew, B.L., and Rose, J.K.C. (2013a). Regulation of ripening and opportunities for control in tomato and other fruits. Plant Biotechnol. J. 11: 269–278.

Seymour, G.B., Østergaard, L., Chapman, N.H., Knapp, S., and Martin, C. (2013b). Fruit Development and Ripening. Annu. Rev. Plant Biol 64: 219–241.

Shen, H., Zhu, L., Castillon, A., Majee, M., Downie, B., and Huq, E. (2008). Light-induced phosphorylation and degradation of the negative regulator PHYTOCHROME-INTERACTING FACTOR1 from Arabidopsis depend upon its direct physical interactions with photoactivated phytochromes. Plant Cell 20: 1586–1602.

Shima, Y., Fujisawa, M., Kitagawa, M., Nakano, T., Kimbara, J., Nakamura, N., Shiina, T., Sugiyama, J., Nakamura, T., Kasumi, T., and Ito, Y. (2014). Tomato FRUITFULL homologs regulate fruit ripening via ethylene biosynthesis. Biosci. Biotechnol. Biochem. 78: 231–7.

Shima, Y., Kitagawa, M., Fujisawa, M., Nakano, T., Kato, H., Kimbara, J., Kasumi, T., and Ito, Y. (2013). Tomato FRUITFULL homologues act in fruit ripening via forming MADS-box transcription factor complexes with RIN. Plant Mol. Biol. 82: 427–438.

Shin, J., Kim, K., Kang, H., Zulfugarov, I.S., Bae, G., Lee, C.-H., Lee, D., and Choi, G. (2009). Phytochromes promote seedling light responses by inhibiting four negatively-acting phytochrome-interacting factors. Proc. Natl. Acad. Sci. U. S. A. 106: 7660–5.

Simkin, A.J., Gaffé, J., Alcaraz, J.P., Carde, J.P., Bramley, P., Fraser, P.D., and Kuntz, M. (2007). Fibrillin influence on plastid ultrastructure and pigment content in tomato fruit. Phytochemistry 68: 1545–1556.

Simkin, A.J., Schwartz, S.H., Auldridge, M., Taylor, M.G., and Klee, H.J. (2004). The tomato carotenoid cleavage dioxygenase 1 genes contribute to the formation of the flavor volatiles β-ionone, pseudoionone, and geranylacetone. Plant J. 40: 882–892.

Simon, P. (2003). Q-Gene: Processing quantitative real-time RT-PCR data. Bioinformatics 19: 1439–1440.

Sjögren, L.L.E. and Clarke, A.K. (2011). Assembly of the chloroplast ATP-dependent Clp protease in Arabidopsis is regulated by the ClpT accessory proteins. Plant Cell 23: 322–332.

Sjögren, L.L.E., Stanne, T.M., Zheng, B., Sutinen, S., and Clarke, A.K. (2006). Structural and functional insights into the chloroplast ATP-dependent Clp protease in Arabidopsis. Plant Cell 18: 2635–49.

Sorin C, Salla-Martret M, Bou-Torrent J, Roig-Villanova I, Martinez-Garcia JF. (2009). ATHB4, a regulator of shade avoidance, modulates hormone response in Arabidopsis seedlings. Plant J. 59, 266–277

Stahl, W. and Sies, H. (2003). Antioxidant activity of carotenoids. Mol. Aspects Med. 24: 345–351.

Stanne, T.M., Sjögren, L.L.E., Koussevitzky, S., and Clarke, A.K. (2009). Identification of new protein substrates for the chloroplast ATP-dependent Clp protease supports its constitutive role in Arabidopsis. Biochem. J. 417: 257–268.

Stigliani, A.L., Giorio, G., and D'Ambrosio, C. (2011). Characterization of P450 Carotenoid β- And ε-hydroxylases of tomato and transcriptional regulation of xanthophyll biosynthesis in root, leaf, petal and fruit. Plant Cell Physiol. 52: 851–865.

Tapken, W., Kim, J., Nishimura, K., van Wijk, K.J., and Pilon, M. (2015). The Clp protease system is required for copper ion-dependent turnover of the PAA2/HMA8 copper transporter in chloroplasts. New Phytol. 205: 511–517.

Tapken, W., Ravet, K., and Pilon, M. (2012). Plastocyanin controls the stabilization of the thylakoid Cu-transporting P-type ATPase PAA2/HMA8 in response to low copper in Arabidopsis. J. Biol. Chem. 287: 18544–18550.

Thannhauser, T.W., Rothwarf, D.M. and Scheraga, H. A., Kinetic Studies of the Regeneration of Recombinant Hirudin Variant 1 with Oxidized and Reduced Dithiothreitol. Biochemistry, 1997, 36 (8), 2154–2165.

The tomato Genome Consortium (2012). The tomato genome sequence provides insights into fleshy fruit evolution. Nature 485: 635–641.

Thimm, O., Bläsing, O., Gibon, Y., Nagel, A., Meyer, S., Krüger, P., Selbig, J., Müller, L.A., Rhee, S.Y., and Stitt, M. (2004). MAPMAN: A user-driven tool to display genomics data sets onto diagrams of metabolic pathways and other biological processes. Plant J. 37: 914–939.

Thompson, A.J., Schofer, J., Kuhn, K., Kienle, S., Schwarz, J., Schmidt, G., Neumann, T., and Hamon, C. (2003). Tandem mass tags: A novel quantification strategy for comparative analysis of complex protein mixtures by MS/MS. Anal. Chem. 75: 1895–1904.

Thompson, A.J., Tör, M., Barry, C., Vrebalov, J., Orfila, C., Jarvis, M.C., Giovannoni, J.J., Grierson, D., and Seymour, G. (1999). Molecular and Genetic Characterization of a Novel Pleiotropic Tomato-Ripening Mutant. 120: 383–389.

Tieman, D.; Bliss, P.; McIntyre, L.M.; Blandon-Ubeda, A.; Bies, D.; Odabasi, A.Z.; Rodríguez, G.R.; Van Der Knaap, E.; Taylos, M. G.; Goulet, C.; Mageroy, M.H.; Snyder, D.J.; Colquhoun, T.; Moskowitz, H.; Clark, D.G.; Sims, C.; Bartoshuk,L.;Klee, H. J. (2012).

The chemical interactions underlying tomato flavor preferences. Curr. Biol. 22: 1035–1039.

Tieman, D.M., Taylor, M.G., Ciardi, J. a, and Klee, H.J. (2000). The tomato ethylene receptors NR and LeETR4 are negative regulators of ethylene response and exhibit functional compensation within a multigene family. Proc. Natl. Acad. Sci. U. S. A. 97: 5663–5668.

Toledo-Ortiz, G., Huq, E., and Quail, P.H. (2003). The Arabidopsis Basic / Helix-Loop-Helix Transcription Factor Family. Plant Cell 15: 1749–1770.

Toledo-Ortiz, G., Huq, E., and Rodríguez-Concepción, M. (2010). Direct regulation of phytoene synthase gene expression and carotenoid biosynthesis by phytochrome-interacting factors. Proc. Natl. Acad. Sci. U. S. A. 107: 11626–11631.

Toledo-Ortiz, G., Huq, E., and Rodríguez-Concepción, M. (2010). Direct regulation of phytoene synthase gene expression and carotenoid biosynthesis by phytochrome-interacting factors. Proc. Natl. Acad. Sci. U. S. A. 107: 11626–11631.

Toledo-Ortiz, G., Johansson, H., Lee, K.P., Bou-Torrent, J., Stewart, K., Steel, G., Rodríguez-Concepción, M., and Halliday, K.J. (2014). The HY5-PIF Regulatory Module Coordinates Light and Temperature Control of Photosynthetic Gene Transcription. PLoS Genet. 10: 1–14.

Trupkin, S.A., Legris, M., Buchovsky, A.S., Tolava Rivero, M.B., and Casal, J.J. (2014). Phytochrome B Nuclear Bodies Respond to the Low Red to Far-Red Ratio and to the Reduced Irradiance of Canopy Shade in Arabidopsis. Plant Physiol. 165: 1698–1708.

Tryggvesson, A., Ståhlberg, F.M., Mogk, A., Zeth, K., and Clarke, A.K. (2012). Interaction specificity between the chaperone and proteolytic components of the cyanobacterial Clp protease. Biochem. J. 446: 311–320.

Vallabhaneni, R. and Wurtzel, E.T. (2009). Timing and biosynthetic potential for carotenoid accumulation in genetically diverse germplasm of maize. Plant Physiol. 150: 562–572.

Van Norman, J.M., Zhang, J., Cazzonelli, C.I., Pogson, B.J., Harrison, P.J., Bugg, T.D.H., Chan, K.X., Thompson, A.J., and Benfey, P.N. (2014). Periodic root branching in Arabidopsis requires synthesis of an uncharacterized carotenoid derivative. Proc. Natl. Acad. Sci. U. S. A. 111: 1300–1309.

Vidi, P.A., Kanwischer, M., Baginsky, S., Austin, J.R., Csucs, G., Dormann, P., Kessler, F., and Bréhélin, C. (2006). Tocopherol cyclase (VTE1) localization and vitamin E accumulation in chloroplast plastoglobule lipoprotein particles. J. Biol. Chem. 281: 11225–11234.

Vogel, J.T., Tan, B.C., McCarty, D.R., and Klee, H.J. (2008). The carotenoid cleavage dioxygenase 1 enzyme has broad substrate specificity, cleaving multiple carotenoids at two different bond positions. J. Biol. Chem. 283: 11364–11373.

Von Lintig, J. (2012). Metabolism of carotenoids and retinoids related to vision. J. Biol. Chem. 287: 1627–1634.

Vrebalov, J., Pan, I.L., Arroyo, A.J.M., McQuinn, R., Chung, M., Poole, M., Rose, J., Seymour, G., Grandillo, S., Giovannoni, J., and Irish, V.F. (2009). Fleshy fruit expansion and ripening are regulated by the Tomato SHATTERPROOF gene TAGL1. Plant Cell 21: 3041–62.

Vrebalov, J., Ruezinsky, D., Padmanabhan, V., White, R., Medrano, D., Drake, R., Schuch, W., and Giovannoni, J.J. (2002). A MADS-Box Gene Necessary for Fruit Ripening at the Tomato Ripening-Inhibitor (Rin) Locus. Science. . 296: 343–346.

Walter, M.H., Fester, T., and Strack, D. (2000). Arbuscular mycorrhizal fungi induce the non-mevalonate methylerythritol phosphate pathway of isoprenoid biosynthesis correlated with accumulation of the “yellow pigment” and other apocarotenoids. Plant J. 21: 571–578.

Walter, M.H., Hans, J., and Strack, D. (2002). Two distantly related genes encoding 1-deoxy-D-xylulose 5-phosphate synthases: Differential regulation in shoots and apocarotenoid-accumulating mycorrhizal roots. Plant J. 31: 243–254.

Walter, M.H., Stauder, R., and Tissier, A. (2015). Evolution of root-specific carotenoid precursor pathways for apocarotenoid signal biogenesis. Plant Sci. 233: 1–10.

Wang, S., Liu, J., Feng, Y., Niu, X., Giovannoni, J., and Liu, Y. (2008). Altered plastid levels and potential for improved fruit nutrient content by downregulation of the tomato DDB1-interacting protein CUL4. Plant J. 55: 89–103.

Wang, Y.Q., Yang, Y., Fei, Z., Yuan, H., Fish, T., Thannhauser, T.W., Mazourek, M., Kochian, L. V., Wang, X., and Li, L. (2013). Proteomic analysis of chromoplasts from six crop species reveals insights into chromoplast function and development. J. Exp. Bot. 64: 949–961.

Weller, J.L., Schreuder, M.E.L., Smith, H., Koornneef, M., and Kendrick, R.E. (2000). Physiological interactions of phytochromes A, B1 and B2 in the control of development in tomato. Plant J. 24: 345–356.

Wilkinson, J.Q., Lanahan, M.B., Yen, H., Giovannoni, J.J., and Klee, H.J. (1995). An ethylene-inducible component of signal transduction encoded by Never-ripe. Science. 270: 1807–1809.

Willett, W.C. (2010). Fruits, vegetables, and cancer prevention: Turmoil in the produce section. J. Natl. Cancer Inst. 102: 510–511.

Williams, A. V., Boykin, L.M., Howell, K. a., Nevill, P.G., and Small, I. (2015). The complete sequence of the Acacia ligulata chloroplast genome reveals a highly divergent clpP1 gene. PLoS One 10: 1–19.

Wright, L.P., Rohwer, J.M., Ghirardo, A., Hammerbacher, A., Ortiz-Alcaide, M., Raguschke, B., Schnitzler, J.-P., Gershenzon, J., and Phillips, M. a (2014). Deoxyxylulose

5-Phosphate Synthase Controls Flux through the Methylerythritol 4-Phosphate Pathway in Arabidopsis. Plant Physiol. 165: 1488–1504.

Wurbs, D., Ruf, S., and Bock, R. (2007). Contained metabolic engineering in tomatoes by expression of carotenoid biosynthesis genes from the plastid genome. Plant J. 49: 276–288.

Xing, A., Williams, M.E., Bourett, T.M., Hu, W., Hou, Z., Meeley, R.B., Jaqueth, J., Dam, T., and Li, B. (2014). A pair of homoeolog ClpP5 genes underlies a virescent yellow-like mutant and its modifier in maize. Plant J. 79: 192–205.

Yang Y, Qiang X, Owsiany K, Zhang S, Thannhauser TW, Li L. 2011. Evaluation of different multidimensional LC-MS/MS pipelines for isobaric tags for relative and absolute quantitation (iTRAQ)-based proteomic analysis of potato tubers in response to cold storage. Journal of Proteome Research 10, 4647–4660.

Yanishlieva, N. V., Aitzetmüller, K., and Raneva, V. (1998). β-Carotene and lipid oxidation. Lipid - Fett 100: 444–462.

Ytterberg, A. J., Peltier, J.-B., Wijk, K.J. Van, and Van Wijk, K.J. (2006). Protein Profiling of Plastoglobules in Chloroplasts and Chromoplasts . A Surprising Site for Differential Accumulation of Metabolic Enzymes 1 [W]. Plant Physiol. 140: 984–997.

Yuan, H., Zhang, J., Nageswaran, D., and Li, L. (2015). Carotenoid metabolism and regulation in horticultural crops. Hortic. Res. 2: 1–11.

Zeng, Y., Du, J., Wang, L., Pan, Z., Xu, Q., Xiao, S., and Deng, X. (2015). A comprehensive analysis of chromoplast differentiation reveals complex protein changes associated with plastoglobule biogenesis and remodelling of protein systems in orange flesh. Plant Physiol. 168: 1648–1665.

Zhang, Y., Mayba, O., Pfeiffer, A., Shi, H., Tepperman, J.M., Speed, T.P., and Quail, P.H. (2013). A Quartet of PIF bHLH Factors Provides a Transcriptionally Centered Signaling Hub That Regulates Seedling Morphogenesis through Differential Expression-Patterning of Shared Target Genes in Arabidopsis. PLoS Genet. 9: 1–20.

Zhong, S., Fei, Z., Chen, Y.-R., Zheng, Y., Huang, M., Vrebalov, J., McQuinn, R., Gapper, N., Liu, B., Xiang, J., Shao, Y., and Giovannoni, J.J. (2013). Single-base resolution methylomes of tomato fruit development reveal epigenome modifications associated with ripening. Nat. Biotechnol. 31: 154–9.

Zhou, S., Palmer, M., Zhou, J. Bhatti, S., Howe, K. J., Fish, T. Thannhauser, T. W. (2013) Differential root proteome expression in tomato genotypes with contrasting drought tolerance exposed to dehydration. J. Amer. Soc. Hort. Sci., 138: 131-141.

Zhou, T.; Zhang, H.; Lai, T.; Qin, C.; Shi, N.; Wang, H.; Jin, M.; Zhong, S; Fan, Z; Liu, Y.; Wu, Z.; Jackson, S.; Giovannoni; J.J.; Rolin, D.; Gallusci, P.; Hong, Y.(2012). Virus-induced gene complementation reveals a transcription factor network in modulation of tomato fruit ripening. Sci. Rep.: 836–843.

Zhou, X., Welsch, R., Yang, Y., Álvarez, D., Riediger, M., Yuan, H., Fish, T., Liu, J., Thannhauser, T.W., and Li, L. (2015). Arabidopsis OR proteins are the major posttranscriptional regulators of phytoene synthase in controlling carotenoid biosynthesis. Proc. Natl. Acad. Sci.: 201420831.

Zybailov, B., Friso, G., Kim, J., Rudella, A., Rodríguez, V.R., Asakura, Y., Sun, Q., and van Wijk, K.J. (2009). Large scale comparative proteomics of a chloroplast Clp protease mutant reveals folding stress, altered protein homeostasis, and feedback regulation of metabolism. Mol. Cell. Proteomics 8: 1789–1810.

Annexes

Annex I. Alignment of the coding sequences (CDS) of tomato *ClpPR* subunits of tomato. CDS sequences for tomato ClpP3-6 and ClpR1-4 were aligned using ClustalW. The VIGS_*ClpR1* sequence is indicated (light green box). Dashes (-) indicate spaces introduced to promote optimal alignment, perfect matches are represented by an asterisk (*).

```
ClpR1           -ATGTCCATGGC---TTCTTCCTTG---C---------TTCTCT---CTC
ClpR2           -ATGG---CAG-TAGCTCT----TCCAAC---------ATCTTC------
ClpR3           CATTG--GTTA-TACTTCTAGACCTCAGTT--TCTTCT-TTTCAAGCTTC
ClpR4           -AATC-CTTCAC-T---CTT-----CACTCTCTTTGAG-TTTCAAAC-AC
ClpP3           TATAT--ATAA-TTGTTTT----TTCATC---CGAAATATATGA------
ClpP4           -GCAA-ATTCCC-T-TTCCT-----CATC-CCTT-GCG-GCTTACAC-AC
ClpP5           -ATTCTCGTAAATTGTTTA---CTCCAACA-CTCAACT-CTTTAAATTGC
ClpP6           -AT-G--GTAA---CGTCT-----GCAATT--GC------T-GGAACGTC


ClpR1           CAC--TTTCTTGCC-CTAC-T--CTT----GC--TAATAATCCCTCTCA-
ClpR2           -TT--CCTCGTATCTACAC-T--CTAAA---A--CT--------------
ClpR3           CGTTGAAAGAGACC-AGAA-G-AATC----GA--AATTCATCCGTGGAGA
ClpR4           -----AATGGAAGC-TGTC-ACTATT----GC--TTCCCATTTCT-----
ClpP3           GAG--AGTAATATC-TCTC-T-GTTAAAAGAA--GTGGA----------A
ClpP4           -----AAATTCTCC-TCTCTACCAAT----GGAGTCCCTAACTCT-----
ClpP5           CCC--AAAAAAACC-TATC-T-TTTT----CC--TCTTCATCT------A
ClpP6           -----AATTGTACC-AG-------T-----------CTCTTCCCGGC---
                             *

ClpR1           TATTGTACTCAAT-AA-ATCAACT------TT-CCTTCCCAC-CCCC-AA
ClpR2           ----AAAATTCCT-------AAGT--CTTCTT-TAAGCTGCTCCAGCAAA
ClpR3           AATCATGGCC-ACGTGCTTGCGGTTGCCCATGGCGT----CCT---C-AA
ClpR4           ------CGCCGGCT-A-CCGGAATACGGCTAT-CATCTACG----GCGAG
ClpP3           AAAAAAAATCAATC--TTTGGAGTCTCTTAGC-CAAAAACC----CCTAA
ClpP4           ------T-TCTACT-T-CTCTATCTCC-TCAC-TGTC-------------
ClpP5           CACCAAACTCAACC--CCCCCAATGGCTCATT-CTTGCATAGCCA-C-AA
ClpP6           -ACCA----A-ACGT-CT--------TTTT---CGT----CTCT--G-CT


ClpR1           TTTCT-TCT-TTTCAG-ATTCTCTTCATAGAC---CCAA-CGCCGG-CGT
ClpR2           GTTTA-TG----TCG-GATTAA----GAA---TC-CAAT-C-TC------
ClpR3           TTCCA-TGTTCTTCAT-CTTCA--TCGATGACACTGAAA-CACCGTAGCT
ClpR4           TTGC--CGTGCCTCAG-CTCC-----CAA---AC-GGACTC-TCA-----
ClpP3           TAGCAGAA----AAA-GAGTGG----AAG---AC-GAATGG-AGG-----
ClpP4           ------------CC------T-----CTT---T--CAATCT-CCG-----
ClpP5           CTTCA-TC----TCT-C--TCT----AAA---TA-CAAT-T-CCG-----
ClpP6           TTCC-----TCTAGAAGCT------TAAGG------AAA-A-ATG-----
                                                    *

ClpR1           T-------CG-AGGATA---T---TCTTACA-G--------CTC-TCCGG
ClpR2           -CAGGTTC-TTATGGGG---T---TGCGACA-T--------CTAATTCAA
ClpR3           TCAATTTTCG-GTGTGCAGCCTATAGCAATA-G--------CA-GTTCAA
ClpR4           -GAT-TTTC---TCCT-----T-CTACGAAA-T--------CTTCTCTAT
ClpP3           -GAAGTTG--TCTAACA---T--TTAGCACA-G--------CTTTGGCAC
ClpP4           -CCA-TGCC---T-CT-----C-TTCCTAAGCTTTCGCCCACTTTTTCAC
ClpP5           -CAATTTTCCCATCTGA---TTATTGCAATA-T--------TTCTCCCAT
ClpP6           -TAGT-TTCT-G--TTC----T-T--CGA-------------A-GTCCA-
                                      *

ClpR1           T-A-GCCCAG----TCTTTCAA-------------CCA------------
ClpR2           --ATGTTGAT----TTTTTCAA-------------CA-------GAGTTC
ClpR3           ACATTCCGATGCCTCCTTTTAA-------------CCCTAAGGACCCATT
ClpR4           ---CGACGA-----------------CCTTCATCTCC-------CCATTC
ClpP3           ---CAGCCAG----ACCTTCAA-----------CATG-------CC-TTC
ClpP4           C-ATACCCA-----TCTCGCAAAACACCCTTATCCCT-------CAAATC
```

```
ClpP5          --ATCTCTAC----AGTTTAAA-------------CG-------TCTTTC
ClpP6          -TATTCTGATTC------ATCA-------------G-ATAT---TGGATT
                       *

ClpR1          --T----------ATA-------CCCAAACAGT-TCAGA-----------
ClpR2          ATA-A---AAG-TATT--AAATC-CGGA----------ACTAAA-G--AT
ClpR3          TC-TAAGTAAGCTTGCCTCTGTTGCTG-------------CAAA-TAAT-
ClpR4          ATC-G--GCAG-CAGT--CTAT----------TCTCGGACTTATCGGGTC
ClpP3          ATT-A--CAAT-TCTA--CTTTTGTTAAACAGTTTCAGACAAATACAATC
ClpP4          TT----------CACT--CACT----------T--CTCACCAATCCACTT
ClpP5          TTTGAGGAAAG-TAAAGGCTGTTGGGAA----------AGTGAA-AAGTA
ClpP6          TT-CAAGCAAGAA-G------TT--------------------------

ClpR1          -----------CA-AGACTATCTC-AAAG-ATG-GACTACTGA-------
ClpR2          GGTAAAGC-AACA-CG---TGCAC-A------AGTTACCATGA-TG-CCC
ClpR3          CCAGATG----CAC-TCTT--CTC-TCGGCCTCAAAATTCTGA--T-AT-
ClpR4          AGAGAATTCGACC-CGATTCTCTT-TACC-CT--------T-CTTC-CTC
ClpP3          ACACCAAG-AAGA-GGATTATCAG-T------AAA-AGCGTCCACCCACA
ClpP4          CAAAACCCCTTTC-TGATTCTCATCTAGT-TG--------CGGATG-ATA
ClpP5          GGGGAAAT-AGCACCGTC-AAGGC-T------GTGTATTCTGG-AG-GTG
ClpP6          GGGGATC----C----C-----AT-TAAAG-------TTC--A----AT-

ClpR1          A--CAACTATAAGAATGCCCCTCAGT-ATCTTTACGGCCTTT-----CTC
ClpR2          A-TTG-------------------------------------------
ClpR3          -GCCGCCATTTTTG-GACA-TTTACGACTCCCCTAAGCTCATGGCTACTC
ClpR4          AACTGGCTTTATCCCCAAACGTGCCGT-TGTC-----------------
ClpP3          AGCCGACTTTATCGACGAACTG----------------------------
ClpP4          AATTGTCCTTG-----CTACTTGC-------C-----------------
ClpP5          A-CTGGGATTTAGCAAAGGCTTCACG-TTCTTCTGGAATTTGGTCTATCA
ClpP6          -GA------------------GTACGAATCCGGT--GCTCATACCAATTC

ClpR1          CGTCACAGA--------T-GG--ATATGTTCATGACAGAA-GAT--AACC
ClpR2          ----------------------GAACA------CC---AAAG-GTGCC-CT
ClpR3          CTGCT-------------------------------------------
ClpR4          ----------------------------------------A-CTAT--GG
ClpP3          ----------------------GGATG------TT---TCCAGTTACT-CA
ClpP4          -------------------------------------T-CTGCT-CC
ClpP5          GAGATGACG--------T-GCAAATACCATCATCACCTTATTTTCCTACA
ClpP6          AAGCTATGGTGTTATCGTAGCAAAAGAGGGGG----CTAAT-CCGCC-CA


ClpR1          CAGCCCGGCGACAGTCGGG---AAGCGTC-ACTG-AA--GAGAA----TA
ClpR2          ATAGAAATC-CAGTT----GACGCAT--C-A-T-GG-C-AATGGGTT---
ClpR3          -CA---GGTGGAG-AGATCAGT-ATCATA-CAATGAGCACAGAGCGAGTA
ClpR4          TT---ATTCCTTTCGGA-GGGGACCCATCGCAGGAT-C-ATCCTCCA---
ClpP3          A---AAGCCCCTGCT--TGGATGCCCA-G-A-T-TT-G-AAGAACTT---
ClpP4          TC---AGTCCCCGGGGA---TGG-CTAT-GCGTGGT-G-CTGAAGGA---
ClpP5          TATGCCGCCCAAGGTCAAGGACCACCGCC-AATGGTAC-AAGAACGATTT
ClpP6          TCA--TGCCCGCCGTGAT-GAC-ACC----AGTGGGC--GCGTTGGATCT

ClpR1          -----------T---------------------------------ATCT
ClpR2          ---------GA---TATATGGAATG-CTCTTTACCGCGAACGTGTTATTT
ClpR3          CACCTCCACCAGA-CTTGCC-CTCTATGTTGCTCCATGGTAGAATAGTTT
ClpR4          ---------GA---TTTAGCA-TCTTACTTGTTTAAGAATCGAATCGTCT
ClpP3          ---------GA---TACCACCAATA-TGCTTCTTCGTCAAAGGATTATCT
ClpP4          ---------GA---CGCAATG-GGGCTGTTGCTTAGGGAGAGGATAATTT
```

```
ClpP5          ---------CAGAGTGTGATCAGCC-AGCTCTTTCAATATAGGATCATAC
ClpP6          TT-----C----T----A-C-CG---TGTTATTCAGGAATCGAATTATCT
                                                              *

ClpR1          TCATCCCATA-ACTA-T--CTGAAAAA-----------------TGGTGG
ClpR2          TCATTGGAGA-AGAGATTACTGAAGAAT-TTAGCAACCAGATATTGGCAA
ClpR3          ATATTGGCAT-GCCGTTGGTGTCAGCAG-TCACAGAGCTTGTGATTGCAG
ClpR4          ACTTGGGAATG-TC-TCTAGTTCCATCAGTGACAGAATTGATTCTAGCTG
ClpP3          TCTTGGGTTC-TCAGGTAGATGATATTA-CTGCGGATTTTATTATAAGCC
ClpP4          TCTTGGGTAGTAGC-ATTGATGACTTCT-TCGCTGATGCTATTATTAGTC
ClpP5          GATGTGGTGG-AGCAGTTGATGATGATA-TGGCTAATGTCATAGTTGCTC
ClpP6          TCATTGGACA-ACCAGTCAACTCTGCAG-TTGCTCAGAAAGTAATATCAC
                                                          *

ClpR1          AATGTGGAGTATGT---CAGGCATGAATAA-ACAGGGCCCTTCAACATGC
ClpR2          CAATG-CTGTACCTTGACAG-TATTGATAATTCCAAG-----A-------
ClpR3          AGTTG-ATGTACCTACAATA-TATGGATCCTAAAGCGCCAATTT------
ClpR4          AATTT-CTTTACCTTCAGTA-TGAGGATGAGGATAAG-----C-------
ClpP3          AGCTA-TTAATTCTTGATGC-AGAAGATGATAAAAAG-----G-------
ClpP4          AGTTG-TTGTTGTTGGATGC-TCTGGATTCCACTAAA-----G-------
ClpP5          AGCTT-CTTTATCTTGATGC-TGTTGATCCCACAAAG-----G-------
ClpP6          AACTT-GTGACCCTTGCAAC-TATAGATGAAA-----ACGCAG-------
                           *           **

ClpR1          AGCATGAGCGTCAGCATGTA--------------------CGGAG---G-
ClpR2          -------AGCTCTACATGTTTATCAATGGGCCT------------G---G
ClpR3          -------ATCTATACATAAATTCTACTGGGACT------ACCCGTGATGA
ClpR4          -------CAATCTATTTTTATATAAATTCTACTGGGACTACCAAGGGT--
ClpP3          -------ACATCAGATTGATCATTAATTCACCT------------G---G
ClpP4          -------ATATTAGGCTCTTTATTAATTGCCCTGG---------------
ClpP5          -------ACATTGTTATGTATGTCAATTCTCCA------------G---G
ClpP6          -------ATATTTTGATCTATCTTAACTGTCCT------------G---G
                        *     *

ClpR1          ---AGGAGGAGCAAGAT-CTGATAGATCCCCAACTGCGCCTC--------
ClpR2          TGG------------TG-ATCTAACTCCAACCCTGGCCATTTATGACACA
ClpR3          TGGTGAAACGGTTG-GTATGGAAGCAGAAGGTTTTGCAATTTATGATTCC
ClpR4          -GGTGAAA-AGTTGGGTTATGAGACAGAGGCGTTTGCTGTATATGACGTT
ClpP3          TGG------------TT-CAGTAACTGCTGGAATGGGAATATATGATGCC
ClpP4          ------------TGGCT-CACTCAGCGCAACAATGGCTATCTTCGACGTT
ClpP5          AGG------------GT-CAGTAACAGCAGGAATGGCTGTTTTTGATACC
ClpP6          TGG------------AAGCACATACT-CTGTCTTGGCAATATATGACTGC
                                           *

ClpR1          CTGATTT------------GCCATCTTTGCTTTTAGATGCTAGAATTGTC
ClpR2          ATGCAAAGTCTG-AAAAGTGCTGTTGGTACC-CACTGTGTGGGCTTTGCC
ClpR3          ATGATGCAACTT-CAAAACGAGATACACACT-GTAGCAGTTGGTGCTGC-
ClpR4          ATGAGTTACGTC-AAGCCACCTATATTTACT-CTGTGTGTTGGGAATGC-
ClpP3          ATGAAAA-TGTGTAAGGCTGATGTTTCTACT-ATCTGCATGGGATTGG-C
ClpP4          GTGCAGTTGGTG-AGGGCTGATGTATCCACA-GTTGCACTTGGCATTTC-
ClpP5          ATGCGACATATT-CGACCCGATGTCTCAACT-GTCTGTGTTGGACTCGC-
ClpP6          ATGTCATGGATA-AAGCCTAAGGTTGGTACA-GTATGTTTTGGAGCTGC-
                **                    *     *           *

ClpR1          -TAT-CTG-GGCATGCCTATT-GTAGAAGCTGTTACAGA-GCTTATT-GT
ClpR2          TACAATC-TTGCCGCTTTTCTTCTTGCTGCTGGAGAAAAGGGCAATCGAT
ClpR3          CATAGGTCAGGCATGTCTATTGCTTGCAGCTGGTACTAAGGGCAAAAGGT
ClpR4          ATGGGGAGAAGCTGCCTTGCTTTTAGCAGCTGGTTCAAAAGGAAATCGTG
ClpP3          TGCATCCATGGGTGCGTTTCTCCTGGCTTCTGGCAGCAAGGGAAAGAGGT
ClpP4          AGCTTCCACAGCTTCAATAATCCTTGCCGGTGGCACCAAAGGAAAACGCT
```

```
ClpP5          TGCAAGTATGGGGGCTTTTCTTCTCAGTGCTGGCACTAAAGGGAAGAGAT
ClpP6          TGCAAGCCAAGGAGCACTTCTTCTTGCTGGTGGAGAAAAGGGCATGAGGT
                         *      *  *  *      **      * *

ClpR1          T-GCACAGTTTATGTGGTTGGATTTCGATAATCCAACAAAGCCCGTATAC
ClpR2          GTGCAATG-CCTCTTGCAAGGA---TTGCACTAGAATC-TCCAGCTGGAG
ClpR3          TTATGATG-CCACATGCCAAAG---CCATGATTCAACA-GCCCCGTGCAC
ClpR4          CTGCACTG-CCCTCATCTACAA---TTATGATTAAGCA-GCCAATTTCTC
ClpP3          ACTGCATG-CCAAACGCAAAAG---TGATGATCCATCA-ACCACTTGGAA
ClpP4          ACGCAATG-CCTAATACTCGAA---TTATGATACATCA-ACCACTTGGAG
ClpP5          ATAGCTTG-CCAAATTCAAGGA---TAATGATTCACCA-GCCTCTAGGTG
ClpP6          ATGCAATG-CCAAATGCACGTA---TAATGATTCATCA-ACCTCA---AA
                      *                       *  *      *

ClpR1          -CTATATATAAATTCATCTGGTACCCAG-AATGACGAAATGGAGACT--G
ClpR2          -CTGCACG-CGGA-----CA--GGCTGACGATATCCGTAATGAAGCAGAA
ClpR3          -CATCATCTGGATTAATGCA--GGCCAGCGATGTTTATATCCGGGCAAAG
ClpR4          AGTTTCAG--GGT-----CA--AGCAACAGATGTTGAGATCATGCGGAAA
ClpP3          -CTTCTGG-TGGT-----AA--AGCAACAGAGATGGGTATACGGATCAGA
ClpP4          -GTGCCAG-TGGT-----CA--AGCAATAGATGTAGAAATTCAAGCCCGA
ClpP5          -GTGCTCA-AGGT-----GG--TCAAAGTGATATAGAAATACAGGCTAAT
ClpP6          -GTGGATGT------GG-------------------A-------------


ClpR1          TCGGTTCTGA--AACAGAGGCATA--TGCCATTGCTGACATGATAAGATA
ClpR2          GAACTTCTCAGAATTAGAAATTACCTTTTCA-AGGAGTTGTCTGAGAAGA
ClpR3          GAGGTACTCGTTAACAGAGACAACCTTGTCA-AGCTTTTGGCTAAACATA
ClpR4          GAAGTAAATAATGTCAAAGCGGAATTGGTCA-AATTGTATTCAGAAAATA
ClpP3          GAAATGGGATACCACAAGATGAAGCTTAATA-AAATACTATCAAGAGTTA
ClpP4          GAAATAATGCATAACAAGGACAATGTTATCA-AAATCTTTTCCAATTCCA
ClpP5          GAGATGTTGCATCACAAAGCAAATTTGAATG-GTTACCTTGCCTACCAGA
ClpP6          --------------------------------------------------


ClpR1          CTGCAAATC----AGAT---GTAT------ATAC-GGTAAAC-----TGT
ClpR2          CAGGCCAGCCTATTGAAAAGGTTCACAAGGATTTGAGTCGAGTGAAGCGA
ClpR3          CTGAAAATTCGGAAGAGACTGTTTCCAATGTTATGAGAAGACCA---TAT
ClpR4          CTGGAAAATCACCTGAGGAGATTGAAGAAGACATAAAACGTCCA---AAA
ClpP3          CAGGCCAGCCTTTAGAAAAGATTGAAGTGGATACTGATCGTGAT---AAT
ClpP4          CTGGACGATCATATGAACAAGTTCAGAAAGATATTGATAGAGAT---CGT
ClpP5          CTGGTCAAAGCCTTGATAGGATTAATCAGGATACTGATCGTGAT---TTT
ClpP6          --------------------------------------------------


ClpR1          GGCATGGCTTTTGGTCAAGCAGCAATG-CTTCTGTCACAAGGAAAGAAAG
ClpR2          TTCA---CTGCTAAAGAAGCTCTTGAATACGGTCTTAT-TGACCGTATAG
ClpR3          TACATGGATTCTATCAAAGCTAGAGAATTTGGCGTTAT-TGATAAGATTC
ClpR4          TACTTTAGTCCTAGTGAAGCAGTAGAATATGGAATTAT-TGATAAGGTTG
ClpP3          TTTATGAATGCTTGGGAGTCTAAGGAATACGGGTTGGT-TGATGCTGTTA
ClpP4          TACATGTCCCCAATTGAAGCTTTAGAATTTGGGCTAAT-TGACGGTGTAA
ClpP5          TTCATGAGCGCAAAGGAAGCTAAGGAGTACGGGCTAAT-CGATGGTGTCA
ClpP6          --------------------------------------------------


ClpR1          GGT--TCCG--TGCTGTGCAGC-----CA-AATTCATCTA----CCAAAT
ClpR2          T---T-----------------------------------------------
ClpR3          TTT--GGCG--TGGCCAGGAGCAGGAGCAG--ATTA------TTGCAAGT
ClpR4          TATACAATG--A---GAGG---GGAAATAAAGATAGAGGA-GTTGTATCT
ClpP3          TAGATGACGGCAAACCAGGATTGGTAGCACCCATTACCGAGGATGCACCT
ClpP4          T------TG--A---CAGA---GATAGC---ATCATTCCA-CTTATGCCT
```

```
ClpP5           TCA-TGAATC-----CAAT---GAAAGC--CCTTCAACCA-CTTGCAGCA
ClpP6           --------------------------------------------------


ClpR1           -TGTATTTACCCA-AGG------TCAGCAAAT---CC-AGTGGAT--CA-
ClpR2           --------------------------------------AGG------
ClpR3           GTTGATGCACCAG-AGG------TGTGGGACA---AT-A--GGG---CAG
ClpR4           GAT-CTGAAGAAGGCCCAACTTATCTGAAAGGAGTCAAA--AGT-CCCAC
ClpP3           CCA-CCAAAAA-C-ACGAG----TTTGGTATAAGTGG-A--AGGCCGAAG
ClpP4           GTC----------------------CCTGAAAA-GGTTAAA----------
ClpP5           GCTGCTGAACAAT-CGTAG------TTGTATT---GC-A--AGG---AAG
ClpP6           --------------------------------------GGG---CAC


ClpR1           CCGA---------------CAGAGTTGTGGATAAAGGCCAAA---GAACT
ClpR2           ------------------------------------CCTAAC--CGTCT
ClpR3           GCAT---------------CAAAGTTGCTGATG-CTTTTT--AG----GT
ClpR4           CAGCCACGAAACCACAGGG-------ATTGAGG-CCC--GGGGGTGGCGT
ClpP3           GCACCAGGAAGAGAAAGAACAATTGG--------CCTTCTGAAGAAAAGT
ClpP4           --------------------------------------------------
ClpP5           GT-----------------TAATTTT--------CTACCTAT---CATTT
ClpP6           -------------------------GTGGAG-----------------


ClpR1           AGAATCAAACTCAGA----GTATTACCTT--GAGCTATTATCAGA-----
ClpR2           TGACGGAG----ATGCTC-----CGCCG--AGGGATA-TCACTGC-----
ClpR3           CCTTTCAATAT-ATAAT--------CCGATGGGAATATTGACGGAAGC--
ClpR4           --TTGGCATCT-ACCT---------------------TTCACC--GGC--
ClpP3           TATTCCAAAATGATGAGCAGAG-CAAT---GAACAGA-AAGATGAAGCTC
ClpP4           --------CGT-ACAT---------------------T-GAGA-------
ClpP5           TGTTTCTCATTAATACACT----CGTCTTTAGAGATTGTAATTGA-----
ClpP6           -----------------------------------GATGTGCGGC-----


ClpR1           -------AGG-A-----ATTGGA-AA-AC------------CAAAGGAA-
ClpR2           -------AGG-T-C----TTGGT-TAAGT------------C-TATAAGT
ClpR3           -ATTTCAACTATCAAGG----GGAC-TGAA------------A-CTCTTT
ClpR4           -AATTCA-TCAACAAGG----CTAT-TT-------------CCCATCATG
ClpP3           TAAGTCCTCTATAATGTATTGGGAT-ACATGTGGCCTTGAACAGATAGTC
ClpP4           -A--------ATCAAGA----TTTG-AT--------------C---CAAG
ClpP5           ---TTTTACTAAGTTG-----GG-TA-GA------------CACAACATT
ClpP6           ---GCCAAGTA------------AA-TGAA------------G-CGGTTC


ClpR1           --------------GAAATA--AAGAAAGATAT----CCTA-CGGCCT--
ClpR2           C-------------------------------------------------T
ClpR3           CATTTC-------ACTAGTA--AAGAGTGTTAC----CAAA-T-GAGAGA
ClpR4           AACGCTCCTTTTAAT--CTA--CAGATTGCCTCGAACTATA-T-TAGAGG
ClpP3           CCTACT-------G--AATATGA-----GATGT----CGTCTT-GAGGGT
ClpP4           A---CCCTATGAAAT--T-------TTT-----GAACC-----------
ClpP5           CCTGCT-------GCCAGGA--A-----GAAAA----TGTA-T-GCCA--
ClpP6           AATCTC-------GCCAG-----AAAGT-CGAC----AAAA-T-GTATGC


ClpR1           AAAT-ATTTCAGGGC-----GCAAG-AG-GCCA----------------
ClpR2           TGGCT--------------GCAAG-TGTTGT--TCTGCAAGAAAATTG-
ClpR3           AAAT-TCTGGTTTGT-----GCAAG-TCTTGAA--ATGTACGCACTCGC-
ClpR4           C----CACAGTT-GG-----GACAGCTATTATA--CTTGTTTTATACAGA
ClpP3           TCATTGTAAGATTATTAACAGGAAT-TTTTATATTATGGTCGACGTCAG-
ClpP4           -------CAG------------------ATATC--CCTGAT-GA------
```

```
ClpP5          AAATTTTTA-CTTGTT-G--GGAAA-GAGTGTA--ATGTACCTGCCCAG-
ClpP6          TGCT-TTTAC-----------------------------------TGGC-


ClpR1          ------------------TTGACTAT--GG----CCTTGCAG-ATAAGAT
ClpR2          T-TTAA---TCTGC-AT---ATTGAACG-------CTT-TTG-ATC---T
ClpR3          T-GTAGC--TCTC----CAAGATTATACAA----GTATCATG-ATGAGAT
ClpR4          TCCTAG---TCAC----TTAGATTCTGCATT---CTGTGTTGGCTCA-AC
ClpP3          T-TGAGCCTTCTGTTGTATCAATGTCTCCTCTTAGTAT-TTG-AACTGGT
ClpP4          ------------------TGAGAT-----------------------A---
ClpP5          ------A--TCT--TATATAGATGTTTCCTC-----AT-ATC-AGCA-AT
ClpP6          ------------------CA--ATCA-----------ATTGAG-ATGATAC


ClpR1          AAT-TAG-TTCA-AGTGACGAT--------GC---AT---------TTGA
ClpR2          ACT-TATT--CA------A-----AAATTTGC---AT-TGCTGTTG--AA
ClpR3          ACT-TAC-TACATAGTAACCAAG--AA-TAGG---AT-TTTCGCTTTGTA
ClpR4          GAAGTAG-CTTATAG--AACACG--T-GTG-----AA-GTTTGCACTAT-
ClpP3          CCTTTATCAACAAAGAGAACATTTGAAATGGT---AT-TTTTGTTGGGGA
ClpP4          -TATTAG-CTGGTGC--AACAGG--T-----------------------
ClpP5          TCTTTAC-CCCATGTTG-------------------T-TCATGTTGT--G
ClpP6          AA-------AC----ATACACTG--AA-AGGGATCGTTTTATGTCTTCCG


ClpR1          CAA--ACGGAAC------------------TAT--GAAGAGA--TGCTCA
ClpR2          GTA--AAAGAATTGAA-----GCTT---------------------A----
ClpR3          TTA--AAAGCATTGTA-----CA---------------------------
ClpR4          --TTT--AGAATGTTATG--GTCT-------------TAAGA--T-----
ClpP3          TTTATATAGCATATCACATCCTTTTAGGTCTATTAGTAGAGACTCACTCA
ClpP4          -------------------------------------AGGGA--T-----
ClpP5          TTTC--TTGAAGAGCACG--ATATT-------------------A----
ClpP6          CTG--AGGCCAT-GGA---------------------------------


ClpR1          T--CCAA----TC-----------TAG--A-ATGTCGAGACCAGGTGCTC
ClpR2          ------ATCTTTCAT----------------ATTATTT---TAT-TTTTC
ClpR3          ---CAAATTGTTG----TTGGTTTCTG--AATTTGTGA-GTGAGTCGAAC
ClpR4          --------GGTTC----CAATATTCAGTAAAATATTC---TAACTGCAAG
ClpP3          TGTCAAACCAATGATAATTGGTAGC-----AATTATGA---CAT-TGCTG
ClpP4          --------GGCTC----TTGG-CTCAG--AAATATCG---C-AT------
ClpP5          ------ATGTTTCG------AGTGC-----AATAATGT---CAGTTGAAG
ClpP6          ------GT---------TTGGTCTC-----ATTGACGG----GGTGCTAG
                                             *


ClpR1          -AAGCTGCT---CCCTC--CGGGT--T---CA-GGTGA
ClpR2          --ACAA---------AA--AAAAT---GT-----TCTG
ClpR3          -AATTATCAGCTCATGGGCAAATT--TTTTCTCTCTCT
ClpR4          -TCTTTACACCA-ATTTGTTAAGTGGAGATCTCAGAAA
ClpP3          TAACAACTA-T--AAACTAAAAAT--TGG---TTAGTA
ClpP4          -ACCTAACA-------TGCAGCGT--TGTCCTCATCGC
ClpP5          -AAGAAACA-C--ACACAC-ACAC--AGA-----GGAG
ClpP6          -AA---A-----------CAGAG-----T----ACTAG
```

Annex II. Alignment of the coding sequences (CDS) of tomato *ClpR* subunits of tomato. CDS sequences for tomato ClpR1-4 were aligned using ClustalW. The VIGS_*ClpR1* sequence is indicated (light green box). Dashes (-) indicate spaces introduced to promote optimal alignment, perfect matches are represented by an asterisk (*).

```
ClpR1           -ATGTCCATGGC---TTCTTCCTTG---C---------TTCTCT---CTC
ClpR2           -ATGG---CAG-TAGCTCT----TCCAAC---------ATCTTC------
ClpR3           CATTG--GTTA-TACTTCTAGACCTCAGTT--TCTTCT-TTTCAAGCTTC
ClpR4           -AATC-CTTCAC-T---CTT-----CACTCTCTTTGAG-TTTCAAAC-AC
ClpP3           TATAT--ATAA-TTGTTTT----TTCATC---CGAAATATATGA------
ClpP4           -GCAA-ATTCCC-T-TTCCT-----CATC-CCTT-GCG-GCTTACAC-AC
ClpP5           -ATTCTCGTAAATTGTTTA---CTCCAACA-CTCAACT-CTTTAAATTGC
ClpP6           -AT-G--GTAA---CGTCT-----GCAATT--GC------T-GGAACGTC


ClpR1           CAC--TTTCTTGCC-CTAC-T--CTT----GC--TAATAATCCCTCTCA-
ClpR2           -TT--CCTCGTATCTACAC-T--CTAAA---A--CT--------------
ClpR3           CGTTGAAAGAGACC-AGAA-G-AATC----GA--AATTCATCCGTGGAGA
ClpR4           -----AATGGAAGC-TGTC-ACTATT----GC--TTCCCATTTCT-----
ClpP3           GAG--AGTAATATC-TCTC-T-GTTAAAAGAA--GTGGA----------A
ClpP4           -----AAATTCTCC-TCTCTACCAAT----GGAGTCCCTAACTCT-----
ClpP5           CCC--AAAAAAACC-TATC-T-TTTT----CC--TCTTCATCT------A
ClpP6           -----AATTGTACC-AG-------T-----------CTCTTCCCGGC---
                             *

ClpR1           TATTGTACTCAAT-AA-ATCAACT------TT-CCTTCCCAC-CCCC-AA
ClpR2           ----AAAATTCCT-------AAGT--CTTCTT-TAAGCTGCTCCAGCAAA
ClpR3           AATCATGGCC-ACGTGCTTGCGGTTGCCCATGGCGT----CCT---C-AA
ClpR4           ------CGCCGGCT-A-CCGGAATACGGCTAT-CATCTACG----GCGAG
ClpP3           AAAAAAAATCAATC--TTTGGAGTCTCTTAGC-CAAAAACC----CCTAA
ClpP4           ------T-TCTACT-T-CTCTATCTCC-TCAC-TGTC--------------
ClpP5           CACCAAACTCAACC--CCCCCAATGGCTCATT-CTTGCATAGCCA-C-AA
ClpP6           -ACCA----A-ACGT-CT--------TTTT---CGT----CTCT--G-CT


ClpR1           TTTCT-TCT-TTTCAG-ATTCTCTTCATAGAC---CCAA-CGCCGG-CGT
ClpR2           GTTTA-TG----TCG-GATTAA----GAA---TC-CAAT-C-TC------
ClpR3           TTCCA-TGTTCTTCAT-CTTCA--TCGATGACACTGAAA-CACCGTAGCT
ClpR4           TTGC--CGTGCCTCAG-CTCC-----CAA---AC-GGACTC-TCA-----
ClpP3           TAGCAGAA----AAA-GAGTGG----AAG---AC-GAATGG-AGG-----
ClpP4           ------------CC------T-----CTT---T--CAATCT-CCG-----
ClpP5           CTTCA-TC----TCT-C--TCT----AAA---TA-CAAT-T-CCG-----
ClpP6           TTCC-----TCTAGAAGCT------TAAGG------AAA-A-ATG-----
                                                    *

ClpR1           T-------CG-AGGATA---T---TCTTACA-G--------CTC-TCCGG
ClpR2           -CAGGTTC-TTATGGGG---T---TGCGACA-T--------CTAATTCAA
ClpR3           TCAATTTTCG-GTGTGCAGCCTATAGCAATA-G--------CA-GTTCAA
ClpR4           -GAT-TTTC---TCCT-----T-CTACGAAA-T--------CTTCTCTAT
ClpP3           -GAAGTTG--TCTAACA---T--TTAGCACA-G--------CTTTGGCAC
ClpP4           -CCA-TGCC---T-CT-----C-TTCCTAAGCTTTCGCCCACTTTTTCAC
ClpP5           -CAATTTTCCCATCTGA---TTATTGCAATA-T--------TTCTCCCAT
ClpP6           -TAGT-TTCT-G--TTC----T-T--CGA------------A-GTCCA-
                                      *

ClpR1           T-A-GCCCAG----TCTTTCAA-------------CCA------------
ClpR2           --ATGTTGAT----TTTTTCAA-------------CA-------GAGTTC
ClpR3           ACATTCCGATGCCTCCTTTTAA-------------CCCTAAGGACCCATT
ClpR4           ---CGACGA-----------------CCTTCATCTCC-------CCATTC
ClpP3           ---CAGCCAG----ACCTTCAA-----------CATG-------CC-TTC
```

```
ClpP4           C-ATACCCA-----TCTCGCAAAACACCCTTATCCCT-------CAAATC
ClpP5           --ATCTCTAC----AGTTTAAA-------------CG-------TCTTTC
ClpP6           -TATTCTGATTC------ATCA-------------G-ATAT---TGGATT
                       *

ClpR1           --T----------ATA-------CCCAAACAGT-TCAGA-----------
ClpR2           ATA-A---AAG-TATT--AAATC-CGGA----------ACTAAA-G--AT
ClpR3           TC-TAAGTAAGCTTGCCTCTGTTGCTG-------------CAAA-TAAT-
ClpR4           ATC-G--GCAG-CAGT--CTAT----------TCTCGGACTTATCGGGTC
ClpP3           ATT-A--CAAT-TCTA--CTTTTGTTAAACAGTTTCAGACAAATACAATC
ClpP4           TT----------CACT--CACT----------T--CTCACCAATCCACTT
ClpP5           TTTGAGGAAAG-TAAAGGCTGTTGGGAA----------AGTGAA-AAGTA
ClpP6           TT-CAAGCAAGAA-G------TT----------------------------

ClpR1           -----------CA-AGACTATCTC-AAAG-ATG-GACTACTGA-------
ClpR2           GGTAAAGC-AACA-CG---TGCAC-A------AGTTACCATGA-TG-CCC
ClpR3           CCAGATG----CAC-TCTT--CTC-TCGGCCTCAAAATTCTGA--T-AT-
ClpR4           AGAGAATTCGACC-CGATTCTCTT-TACC-CT--------T-CTTC-CTC
ClpP3           ACACCAAG-AAGA-GGATTATCAG-T------AAA-AGCGTCCACCCACA
ClpP4           CAAAACCCCTTTC-TGATTCTCATCTAGT-TG--------CGGATG-ATA
ClpP5           GGGGAAAT-AGCACCGTC-AAGGC-T------GTGTATTCTGG-AG-GTG
ClpP6           GGGGATC----C----C-----AT-TAAAG-------TTC--A----AT-

ClpR1           A--CAACTATAAGAATGCCCCTCAGT-ATCTTTACGGCCTTT-----CTC
ClpR2           A-TTG-----------------------------------------------
ClpR3           -GCCGCCATTTTTG-GACA-TTTACGACTCCCCTAAGCTCATGGCTACTC
ClpR4           AACTGGCTTTATCCCCAAACGTGCCGT-TGTC-----------------
ClpP3           AGCCGACTTTATCGACGAACTG----------------------------
ClpP4           AATTGTCCTTG-----CTACTTGC-------C-----------------
ClpP5           A-CTGGGATTTAGCAAAGGCTTCACG-TTCTTCTGGAATTTGGTCTATCA
ClpP6           -GA------------------GTACGAATCCGGT--GCTCATACCAATTC

ClpR1           CGTCACAGA--------T-GG--ATATGTTCATGACAGAA-GAT--AACC
ClpR2           ----------------------GAACA------CC---AAAG-GTGCC-CT
ClpR3           CTGCT-----------------------------------------------
ClpR4           ----------------------------------------A-CTAT--GG
ClpP3           ----------------------GGATG------TT---TCCAGTTACT-CA
ClpP4           -------------------------------------T-CTGCT-CC
ClpP5           GAGATGACG--------T-GCAAATACCATCATCACCTTATTTTCCTACA
ClpP6           AAGCTATGGTGTTATCGTAGCAAAAGAGGGGG----CTAAT-CCGCC-CA


ClpR1           CAGCCCGGCGACAGTCGGG---AAGCGTC-ACTG-AA--GAGAA----TA
ClpR2           ATAGAAATC-CAGTT----GACGCAT--C-A-T-GG-C-AATGGGTT---
ClpR3           -CA---GGTGGAG-AGATCAGT-ATCATA-CAATGAGCACAGAGCGAGTA
ClpR4           TT---ATTCCTTTCGGA-GGGGACCCATCGCAGGAT-C-ATCCTCCA---
ClpP3           A---AAGCCCCTGCT--TGGATGCCCA-G-A-T-TT-G-AAGAACTT---
ClpP4           TC---AGTCCCCGGGGA---TGG-CTAT-GCGTGGT-G-CTGAAGGA---
ClpP5           TATGCCGCCCAAGGTCAAGGACCACCGCC-AATGGTAC-AAGAACGATTT
ClpP6           TCA--TGCCCGCCGTGAT-GAC-ACC----AGTGGGC--GCGTTGGATCT
```

```
ClpR1           ----------T-----------------------------------ATCT
ClpR2           ---------GA---TATATGGAATG-CTCTTTACCGCGAACGTGTTATTT
ClpR3           CACCTCCACCAGA-CTTGCC-CTCTATGTTGCTCCATGGTAGAATAGTTT
ClpR4           ---------GA---TTTAGCA-TCTTACTTGTTTAAGAATCGAATCGTCT
ClpP3           ---------GA---TACCACCAATA-TGCTTCTTCGTCAAAGGATTATCT
ClpP4           ---------GA---CGCAATG-GGGCTGTTGCTTAGGGAGAGGATAATTT
ClpP5           ---------CAGAGTGTGATCAGCC-AGCTCTTTCAATATAGGATCATAC
ClpP6           TT-----C----T----A-C-CG---TGTTATTCAGGAATCGAATTATCT
                                                             *

ClpR1           TCATCCCATA-ACTA-T--CTGAAAAA-----------------TGGTGG
ClpR2           TCATTGGAGA-AGAGATTACTGAAGAAT-TTAGCAACCAGATATTGGCAA
ClpR3           ATATTGGCAT-GCCGTTGGTGTCAGCAG-TCACAGAGCTTGTGATTGCAG
ClpR4           ACTTGGGAATG-TC-TCTAGTTCCATCAGTGACAGAATTGATTCTAGCTG
ClpP3           TCTTGGGTTC-TCAGGTAGATGATATTA-CTGCGGATTTTATTATAAGCC
ClpP4           TCTTGGGTAGTAGC-ATTGATGACTTCT-TCGCTGATGCTATTATTAGTC
ClpP5           GATGTGGTGG-AGCAGTTGATGATGATA-TGGCTAATGTCATAGTTGCTC
ClpP6           TCATTGGACA-ACCAGTCAACTCTGCAG-TTGCTCAGAAAGTAATATCAC
                                                           *

ClpR1           AATGTGGAGTATGT---CAGGCATGAATAA-ACAGGGCCCTTCAACATGC
ClpR2           CAATG-CTGTACCTTGACAG-TATTGATAATTCCAAG-----A-------
ClpR3           AGTTG-ATGTACCTACAATA-TATGGATCCTAAAGCGCCAATTT------
ClpR4           AATTT-CTTTACCTTCAGTA-TGAGGATGAGGATAAG-----C-------
ClpP3           AGCTA-TTAATTCTTGATGC-AGAAGATGATAAAAAG-----G-------
ClpP4           AGTTG-TTGTTGTTGGATGC-TCTGGATTCCACTAAA-----G-------
ClpP5           AGCTT-CTTTATCTTGATGC-TGTTGATCCCACAAAG-----G-------
ClpP6           AACTT-GTGACCCTTGCAAC-TATAGATGAAA-----ACGCAG-------
                             *           **

ClpR1           AGCATGAGCGTCAGCATGTA--------------------CGGAG---G-
ClpR2           -------AGCTCTACATGTTTATCAATGGGCCT------------G---G
ClpR3           -------ATCTATACATAAATTCTACTGGGACT------ACCCGTGATGA
ClpR4           -------CAATCTATTTTTATATAAATTCTACTGGGACTACCAAGGGT--
ClpP3           -------ACATCAGATTGATCATTAATTCACCT------------G---G
ClpP4           -------ATATTAGGCTCTTTATTAATTGCCCTGG---------------
ClpP5           -------ACATTGTTATGTATGTCAATTCTCCA------------G---G
ClpP6           -------ATATTTTGATCTATCTTAACTGTCCT------------G---G
                         *     *


ClpR1           ---AGGAGGAGCAAGAT-CTGATAGATCCCCAACTGCGCCTC--------
ClpR2           TGG------------TG-ATCTAACTCCAACCCTGGCCATTTATGACACA
ClpR3           TGGTGAAACGGTTG-GTATGGAAGCAGAAGGTTTTGCAATTTATGATTCC
ClpR4           -GGTGAAA-AGTTGGGTTATGAGACAGAGGCGTTTGCTGTATATGACGTT
ClpP3           TGG------------TT-CAGTAACTGCTGGAATGGGAATATATGATGCC
ClpP4           ------------TGGCT-CACTCAGCGCAACAATGGCTATCTTCGACGTT
ClpP5           AGG------------GT-CAGTAACAGCAGGAATGGCTGTTTTTGATACC
ClpP6           TGG------------AAGCACATACT-CTGTCTTGGCAATATATGACTGC
                                           *

ClpR1           CTGATTT------------GCCATCTTTGCTTTTAGATGCTAGAATTGTC
ClpR2           ATGCAAAGTCTG-AAAAGTGCTGTTGGTACC-CACTGTGTGGGCTTTGCC
ClpR3           ATGATGCAACTT-CAAAACGAGATACACACT-GTAGCAGTTGGTGCTGC-
ClpR4           ATGAGTTACGTC-AAGCCACCTATATTTACT-CTGTGTGTTGGGAATGC-
ClpP3           ATGAAAA-TGTGTAAGGCTGATGTTTCTACT-ATCTGCATGGGATTGG-C
ClpP4           GTGCAGTTGGTG-AGGGCTGATGTATCCACA-GTTGCACTTGGCATTTC-
ClpP5           ATGCGACATATT-CGACCCGATGTCTCAACT-GTCTGTGTTGGACTCGC-
ClpP6           ATGTCATGGATA-AAGCCTAAGGTTGGTACA-GTATGTTTTGGAGCTGC-
                 **                   *     *           *
```

```
ClpR1           -TAT-CTG-GGCATGCCTATT-GTAGAAGCTGTTACAGA-GCTTATT-GT
ClpR2           TACAATC-TTGCCGCTTTTCTTCTTGCTGCTGGAGAAAAGGGCAATCGAT
ClpR3           CATAGGTCAGGCATGTCTATTGCTTGCAGCTGGTACTAAGGGCAAAAGGT
ClpR4           ATGGGGAGAAGCTGCCTTGCTTTTAGCAGCTGGTTCAAAAGGAAATCGTG
ClpP3           TGCATCCATGGGTGCGTTTCTCCTGGCTTCTGGCAGCAAGGGAAAGAGGT
ClpP4           AGCTTCCACAGCTTCAATAATCCTTGCCGGTGGCACCAAAGGAAAACGCT
ClpP5           TGCAAGTATGGGGGCTTTTCTTCTCAGTGCTGGCACTAAAGGGAAGAGAT
ClpP6           TGCAAGCCAAGGAGCACTTCTTCTTGCTGGTGGAGAAAAGGGCATGAGGT
                          *      *  *  *      **      * *

ClpR1           T-GCACAGTTTATGTGGTTGGATTTCGATAATCCAACAAAGCCCGTATAC
ClpR2           GTGCAATG-CCTCTTGCAAGGA---TTGCACTAGAATC-TCCAGCTGGAG
ClpR3           TTATGATG-CCACATGCCAAAG---CCATGATTCAACA-GCCCCGTGCAC
ClpR4           CTGCACTG-CCCTCATCTACAA---TTATGATTAAGCA-GCCAATTTCTC
ClpP3           ACTGCATG-CCAAACGCAAAAG---TGATGATCCATCA-ACCACTTGGAA
ClpP4           ACGCAATG-CCTAATACTCGAA---TTATGATACATCA-ACCACTTGGAG
ClpP5           ATAGCTTG-CCAAATTCAAGGA---TAATGATTCACCA-GCCTCTAGGTG
ClpP6           ATGCAATG-CCAAATGCACGTA---TAATGATTCATCA-ACCTCA---AA
                       *                        *  *      *

ClpR1           -CTATATATAAATTCATCTGGTACCCAG-AATGACGAAATGGAGACT--G
ClpR2           -CTGCACG-CGGA-----CA--GGCTGACGATATCCGTAATGAAGCAGAA
ClpR3           -CATCATCTGGATTAATGCA--GGCCAGCGATGTTTATATCCGGGCAAAG
ClpR4           AGTTTCAG--GGT-----CA--AGCAACAGATGTTGAGATCATGCGGAAA
ClpP3           -CTTCTGG-TGGT-----AA--AGCAACAGAGATGGGTATACGGATCAGA
ClpP4           -GTGCCAG-TGGT-----CA--AGCAATAGATGTAGAAATTCAAGCCCGA
ClpP5           -GTGCTCA-AGGT-----GG--TCAAAGTGATATAGAAATACAGGCTAAT
ClpP6           -GTGGATGT------GG-------------------A-------------

ClpR1           TCGGTTCTGA--AACAGAGGCATA--TGCCATTGCTGACATGATAAGATA
ClpR2           GAACTTCTCAGAATTAGAAATTACCTTTTCA-AGGAGTTGTCTGAGAAGA
ClpR3           GAGGTACTCGTTAACAGAGACAACCTTGTCA-AGCTTTTGGCTAAACATA
ClpR4           GAAGTAAATAATGTCAAAGCGGAATTGGTCA-AATTGTATTCAGAAAATA
ClpP3           GAAATGGGATACCACAAGATGAAGCTTAATA-AAATACTATCAAGAGTTA
ClpP4           GAAATAATGCATAACAAGGACAATGTTATCA-AAATCTTTTCCAATTCCA
ClpP5           GAGATGTTGCATCACAAAGCAAATTTGAATG-GTTACCTTGCCTACCAGA
ClpP6           --------------------------------------------------

ClpR1           CTGCAAATC----AGAT---GTAT------ATAC-GGTAAAC-----TGT
ClpR2           CAGGCCAGCCTATTGAAAAGGTTCACAAGGATTTGAGTCGAGTGAAGCGA
ClpR3           CTGAAAATTCGGAAGAGACTGTTTCCAATGTTATGAGAAGACCA---TAT
ClpR4           CTGGAAAATCACCTGAGGAGATTGAAGAAGACATAAAACGTCCA---AAA
ClpP3           CAGGCCAGCCTTTAGAAAAGATTGAAGTGGATACTGATCGTGAT---AAT
ClpP4           CTGGACGATCATATGAACAAGTTCAGAAAGATATTGATAGAGAT---CGT
ClpP5           CTGGTCAAAGCCTTGATAGGATTAATCAGGATACTGATCGTGAT---TTT
ClpP6           --------------------------------------------------

ClpR1           GGCATGGCTTTTGGTCAAGCAGCAATG-CTTCTGTCACAAGGAAAGAAAG
ClpR2           TTCA---CTGCTAAAGAAGCTCTTGAATACGGTCTTAT-TGACCGTATAG
ClpR3           TACATGGATTCTATCAAAGCTAGAGAATTTGGCGTTAT-TGATAAGATTC
ClpR4           TACTTTAGTCCTAGTGAAGCAGTAGAATATGGAATTAT-TGATAAGGTTG
ClpP3           TTTATGAATGCTTGGGAGTCTAAGGAATACGGGTTGGT-TGATGCTGTTA
ClpP4           TACATGTCCCCAATTGAAGCTTTAGAATTTGGGCTAAT-TGACGGTGTAA
ClpP5           TTCATGAGCGCAAAGGAAGCTAAGGAGTACGGGCTAAT-CGATGGTGTCA
ClpP6           --------------------------------------------------
```

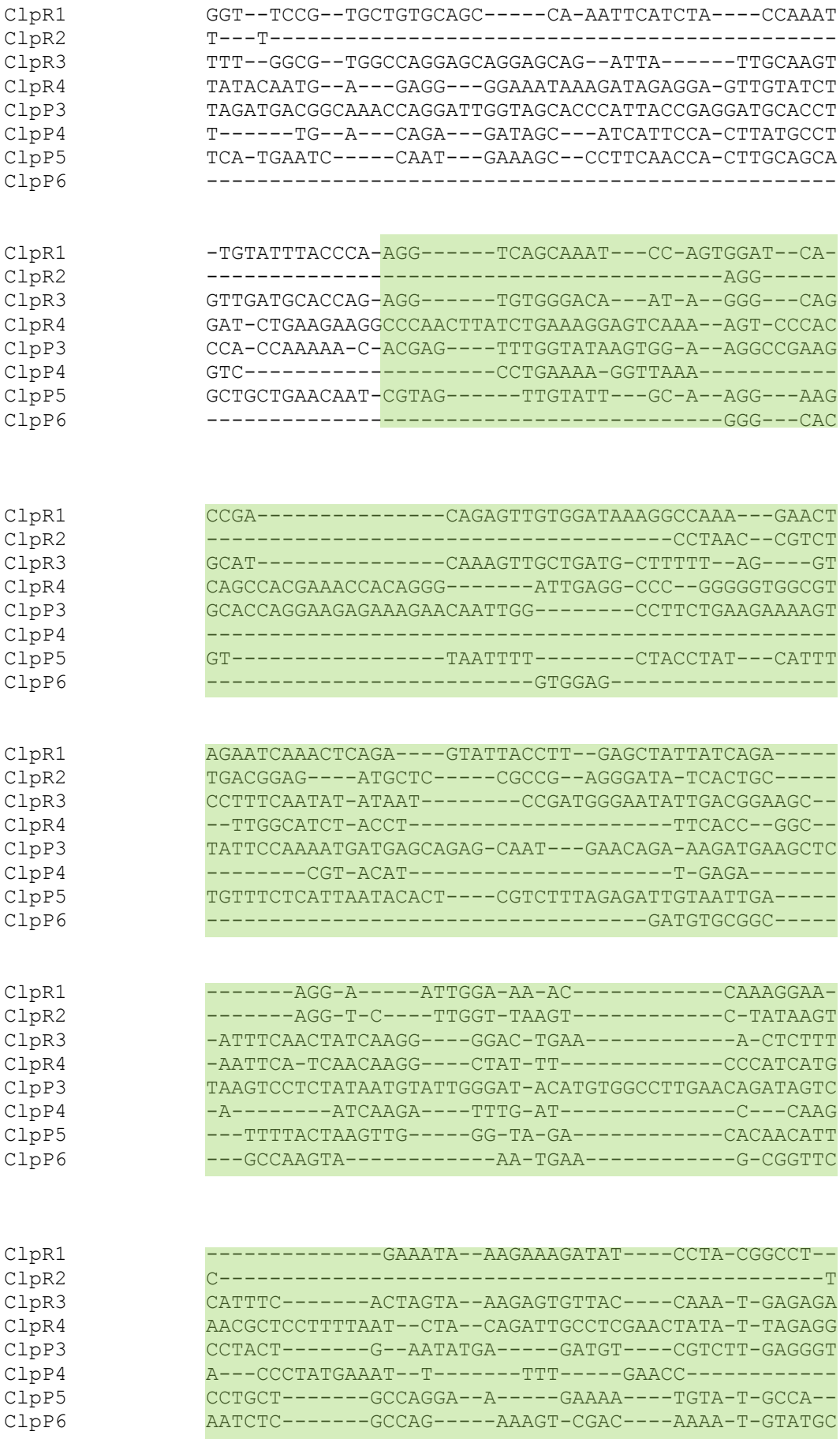
ClpR1 GGT--TCCG--TGCTGTGCAGC-----CA-AATTCATCTA----CCAAAT
ClpR2 T---T----------
ClpR3 TTT--GGCG--TGGCCAGGAGCAGGAGCAG--ATTA------TTGCAAGT
ClpR4 TATACAATG--A---GAGG---GGAAATAAAGATAGAGGA-GTTGTATCT
ClpP3 TAGATGACGGCAAACCAGGATTGGTAGCACCCATTACCGAGGATGCACCT
ClpP4 T------TG--A---CAGA---GATAGC---ATCATTCCA-CTTATGCCT
ClpP5 TCA-TGAATC-----CAAT---GAAAGC--CCTTCAACCA-CTTGCAGCA
ClpP6 ----------
ClpR1 -TGTATTTACCCA-AGG------TCAGCAAAT---CC-AGTGGAT--CA-
ClpR2 ----------AGG------
ClpR3 GTTGATGCACCAG-AGG------TGTGGGACA---AT-A--GGG---CAG
ClpR4 GAT-CTGAAGAAGGCCCAACTTATCTGAAAGGAGTCAAA--AGT-CCCAC
ClpP3 CCA-CCAAAAA-C-ACGAG----TTTGGTATAAGTGG-A--AGGCCGAAG
ClpP4 GTC----------CCTGAAAA-GGTTAAA----------
ClpP5 GCTGCTGAACAAT-CGTAG------TTGTATT---GC-A--AGG---AAG
ClpP6 ----------GGG---CAC
ClpR1 CCGA----------CAGAGTTGTGGATAAAGGCCAAA---GAACT
ClpR2 ----------CCTAAC--CGTCT
ClpR3 GCAT----------CAAAGTTGCTGATG-CTTTTT--AG----GT
ClpR4 CAGCCACGAAACCACAGGG-------ATTGAGG-CCC--GGGGGTGGCGT
ClpP3 GCACCAGGAAGAGAAAGAACAATTGG--------CCTTCTGAAGAAAAGT
ClpP4 ----------
ClpP5 GT----------TAATTTT--------CTACCTAT---CATTT
ClpP6 ----------GTGGAG----------
ClpR1 AGAATCAAACTCAGA----GTATTACCTT--GAGCTATTATCAGA-----
ClpR2 TGACGGAG----ATGCTC-----CGCCG--AGGGATA-TCACTGC-----
ClpR3 CCTTTCAATAT-ATAAT--------CCGATGGGAATATTGACGGAAGC--
ClpR4 --TTGGCATCT-ACCT----------TTCACC--GGC--
ClpP3 TATTCCAAAATGATGAGCAGAG-CAAT---GAACAGA-AAGATGAAGCTC
ClpP4 --------CGT-ACAT----------T-GAGA-------
ClpP5 TGTTTCTCATTAATACACT----CGTCTTTAGAGATTGTAATTGA-----
ClpP6 ----------GATGTGCGGC-----
ClpR1 -------AGG-A-----ATTGGA-AA-AC----------CAAAGGAA-
ClpR2 -------AGG-T-C----TTGGT-TAAGT----------C-TATAAGT
ClpR3 -ATTTCAACTATCAAGG----GGAC-TGAA----------A-CTCTTT
ClpR4 -AATTCA-TCAACAAGG----CTAT-TT----------CCCATCATG
ClpP3 TAAGTCCTCTATAATGTATTGGGAT-ACATGTGGCCTTGAACAGATAGTC
ClpP4 -A--------ATCAAGA----TTTG-AT----------C---CAAG
ClpP5 ---TTTTACTAAGTTG-----GG-TA-GA----------CACAACATT
ClpP6 ---GCCAAGTA----------AA-TGAA----------G-CGGTTC
ClpR1 ----------GAAATA--AAGAAAGATAT----CCTA-CGGCCT--
ClpR2 C----------T
ClpR3 CATTTC-------ACTAGTA--AAGAGTGTTAC----CAAA-T-GAGAGA
ClpR4 AACGCTCCTTTTAAT--CTA--CAGATTGCCTCGAACTATA-T-TAGAGG
ClpP3 CCTACT-------G--AATATGA-----GATGT----CGTCTT-GAGGGT
ClpP4 A---CCCTATGAAAT--T-------TTT-----GAACC----------
ClpP5 CCTGCT-------GCCAGGA--A-----GAAAA----TGTA-T-GCCA--
ClpP6 AATCTC-------GCCAG-----AAAGT-CGAC----AAAA-T-GTATGC


ClpR1 AAAT-ATTTCAGGGC-----GCAAG-AG-GCCA----------
ClpR2 TGGCT----------GCAAG-TGTTGT--TCTGCAAGAAAATTG-
ClpR3 AAAT-TCTGGTTTGT-----GCAAG-TCTTGAA--ATGTACGCACTCGC-
ClpR4 C----CACAGTT-GG-----GACAGCTATTATA--CTTGTTTTATACAGA
ClpP3 TCATTGTAAGATTATTAACAGGAAT-TTTTATATTATGGTCGACGTCAG-
ClpP4 -------CAG----------ATATC--CCTGAT-GA------
ClpP5 AAATTTTTA-CTTGTT-G--GGAAA-GAGTGTA--ATGTACCTGCCCAG-
ClpP6 TGCT-TTTAC----------TGGC-
ClpR1 ----------TTGACTAT--GG----CCTTGCAG-ATAAGAT
ClpR2 T-TTAA---TCTGC-AT---ATTGAACG-------CTT-TTG-ATC---T
ClpR3 T-GTAGC--TCTC----CAAGATTATACAA----GTATCATG-ATGAGAT
ClpR4 TCCTAG---TCAC----TTAGATTCTGCATT---CTGTGTTGGCTCA-AC
ClpP3 T-TGAGCCTTCTGTTGTATCAATGTCTCCTCTTAGTAT-TTG-AACTGGT
ClpP4 ----------TGAGAT----------A---
ClpP5 ------A--TCT--TATATAGATGTTTCCTC-----AT-ATC-AGCA-AT
ClpP6 ----------CA--ATCA----------ATTGAG-ATGATAC
ClpR1 AAT-TAG-TTCA-AGTGACGAT--------GC---AT---------TTGA
ClpR2 ACT-TATT--CA------A-----AAATTTGC---AT-TGCTGTTG--AA
ClpR3 ACT-TAC-TACATAGTAACCAAG--AA-TAGG---AT-TTTCGCTTTGTA
ClpR4 GAAGTAG-CTTATAG--AACACG--T-GTG-----AA-GTTTGCACTAT-
ClpP3 CCTTTATCAACAAAGAGAACATTTGAAATGGT---AT-TTTTGTTGGGGA
ClpP4 -TATTAG-CTGGTGC--AACAGG--T----------
ClpP5 TCTTTAC-CCCATGTTG----------T-TCATGTTGT--G
ClpP6 AA-------AC----ATACACTG--AA-AGGGATCGTTTTATGTCTTCCG
ClpR1 CAA--ACGGAAC----------TAT--GAAGAGA--TGCTCA
ClpR2 GTA--AAAGAATTGAA-----GCTT----------A----
ClpR3 TTA--AAAGCATTGTA-----CA----------
ClpR4 --TTT--AGAATGTTATG--GTCT----------TAAGA--T-----
ClpP3 TTTATATAGCATATCACATCCTTTTAGGTCTATTAGTAGAGACTCACTCA
ClpP4 ----------AGGGA--T-----
ClpP5 TTTC--TTGAAGAGCACG--ATATT----------A----
ClpP6 CTG--AGGCCAT-GGA----------
ClpR1 T--CCAA----TC----------TAG--A-ATGTCGAGACCAGGTGCTC
ClpR2 ------ATCTTTCAT----------ATTATTT---TAT-TTTTC
ClpR3 ---CAAATTGTTG----TTGGTTTCTG--AATTTGTGA-GTGAGTCGAAC
ClpR4 --------GGTTC----CAATATTCAGTAAAATATTC---TAACTGCAAG
ClpP3 TGTCAAACCAATGATAATTGGTAGC-----AATTATGA---CAT-TGCTG
ClpP4 --------GGCTC----TTGG-CTCAG--AAATATCG---C-AT------
ClpP5 ------ATGTTTCG------AGTGC-----AATAATGT---CAGTTGAAG
ClpP6 ------GT---------TTGGTCTC-----ATTGACGG----GGTGCTAG
*
ClpR1 -AAGCTGCT---CCCTC--CGGGT--T---CA-GGTGA
ClpR2 --ACAA---------AA--AAAAT---GT-----TCTG
ClpR3 -AATTATCAGCTCATGGGCAAATT--TTTTCTCTCTCT
ClpR4 -TCTTTACACCA-ATTTGTTAAGTGGAGATCTCAGAAA
ClpP3 TAACAACTA-T--AAACTAAAAAT--TGG---TTAGTA
ClpP4 -ACCTAACA-------TGCAGCGT--TGTCCTCATCGC
ClpP5 -AAGAAACA-C--ACACAC-ACAC--AGA-----GGAG
ClpP6 -AA---A----------CAGAG-----T----ACTAG

Publications

Methods in Molecular Biology 1153

Springer Protocols

Manuel Rodríguez-Concepción *Editor*

Plant Isoprenoids

Methods and Protocols

Humana Press

Chapter 16

Confocal Laser Scanning Microscopy Detection of Chlorophylls and Carotenoids in Chloroplasts and Chromoplasts of Tomato Fruit

Lucio D'Andrea, Montse Amenós, and Manuel Rodríguez-Concepción

Abstract

Plant cells are unique among eukaryotic cells because of the presence of plastids, including chloroplasts and chromoplasts. Chloroplasts are found in green tissues and harbor the photosynthetic machinery (including chlorophyll molecules), while chromoplasts are present in non-photosynthetic tissues and accumulate large amounts of carotenoids. During tomato fruit development, chloroplasts are converted into chromoplasts that accumulate high levels of lycopene, a linear carotenoid responsible for the characteristic red color of ripe fruit. Here, we describe a simple and fast method to detect both types of fully differentiated plastids (chloroplasts and chromoplasts), as well as intermediate stages, in fresh tomato fruits. The method is based on the differential autofluorescence of chlorophylls and carotenoids (lycopene) detected by Confocal Laser Scanning Microscopy.

Key words Chloroplast, Chlorophylls, Chromoplast, Carotenoids, Lycopene, Confocal microscopy, Tomato fruit, Fluorescence

1 Introduction

Plastids are organelles ubiquitously found in plant cells but absent from animal or fungal cells. Based on their color, structure, and metabolic profile, plastids can be categorized into different types [1]. Proplastids, the progenitors of other plastid types, are colorless plastids with limited internal membrane vesicles which are typically found in meristematic cells. Etioplasts, the plastids of dark-grown (etiolated) seedlings, are yellow plastids that contain low levels of carotenoids associated to prolamellar bodies and prothylakoid membranes. Chloroplasts are green, chlorophyll-accumulating photosynthetic organelles with distinctive internal thylakoid membranes and grana. Chromoplasts are plastids specialized in the production and accumulation of carotenoids in many flowers and fruits. Other plastids found in non-photosynthetic tissues are leucoplasts, a general term for colorless plastids that

Manuel Rodríguez-Concepción (ed.), *Plant Isoprenoids: Methods and Protocols*, Methods in Molecular Biology, vol. 1153, DOI 10.1007/978-1-4939-0606-2_16,

include elaioplasts (those accumulating oil) and amyloplasts (those accumulating starch granules) [1, 2].

Plastids fulfill different functions, serving as the main sites for photosynthesis (chloroplasts) and other important primary and secondary pathways [2, 3]. Among non-photosynthetic plastids, chromoplasts have been best studied due to their capacity to store massive levels of health-promoting carotenoid pigments and the derived effect on the coloration of plant-derived foods with red (lycopene), orange (carotenes), and yellow (xanthophylls) colors [4–6]. A well-characterized system for the study of chromoplast biogenesis is fruit ripening in tomato (*Solanum lycopersicum*), when the chloroplasts present in mature (i.e., full-size) green fruit differentiate into lycopene-accumulating chromoplasts [7–9]. The chloroplast to chromoplast transition during tomato ripening can be visualized by the change in fruit color from green to orange and red. Color changes are due to the degradation of chlorophylls and the accumulation of carotenoids (particularly lycopene) as ripening progresses. Both types of isoprenoid metabolites are autofluorescent but have different emission spectra, and this property has been exploited to monitor the presence of chloroplasts (chlorophyll-rich), chromoplasts (carotenoid-rich), and intermediate plastids in tomato fruit by Confocal Laser Scanning Microscopy (CLSM) [9, 10]. Here, we present an optimized CLSM-based protocol that virtually eliminates interference between chlorophyll and carotenoid (lycopene) fluorescence signals (Fig. 1). This protocol allows to record and quantify

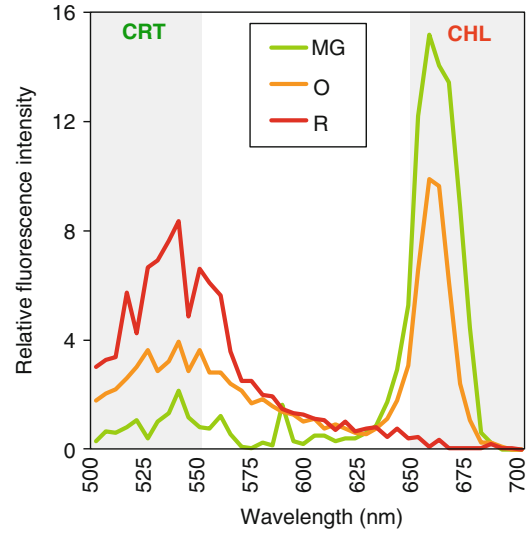

Fig. 1 Fluorescence emission spectra of tomato fruit samples at three stages of fruit development. Pericarp tissue obtained from tomatoes at the *mature green* (MG), *orange* (O), and *red ripe* (R) stages was analyzed by CLSM to generate fluorescence emission spectra after excitation at 488 nm. Representative spectra were obtained from single plastids. Fluorescence intensity is represented relative to the total fluorescence of the sample. The fluorescence emission range used to detect carotenoids (CRT, 500–550 nm) and chlorophylls (CHL, 650–700 nm) is marked

the levels of these isoprenoid pigments in the plastids present in fresh hand-cut sections of tomato fruit pericarp at different developmental stages (Fig. 2). At the mature green stage, all plastids are chloroplasts, which emit red fluorescence due to the presence of chlorophylls (Figs. 1 and 2). At the ripe stage, only fully developed chromoplasts devoid of chlorophylls and rich in lycopene are present. These chromoplasts only emit green fluorescence (Figs. 1 and 2). By contrast, a heterogeneous population of chloroplasts (red fluorescence), chromoplasts (green fluorescence), and intermediate plastids that contain high levels of both chlorophylls and lycopene (yellowish color due to the merging of red and green fluorescence) is found at the breaker and orange stages (Figs. 1 and 2). Although we describe the method for tomato fruit, it can be used (with some optimization) with any other plant material.

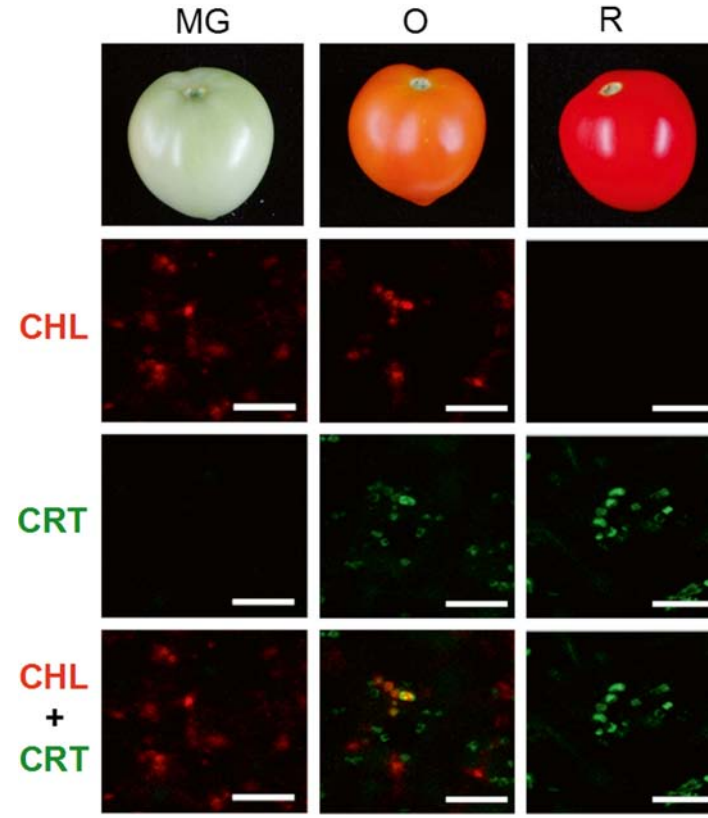

Fig. 2 Images of tomato fruit development stages and the corresponding chlorophyll and carotenoid (lycopene) autofluorescence. Fresh pericarp tissue from tomatoes at the *mature green* (MG), *orange* (O), and *red ripe* (R) stages (*upper panels*) was analyzed by CLSM. Overlay images of autofluorescence emitted at 650–700 nm (chlorophylls, CHL) or 500–550 nm (carotenoids, CRT) after excitation with the 488 nm ray line of an argon laser were obtained. Lower panels correspond to merged images (CHL + CRT). Plastids containing chlorophylls appear *red*, those containing carotenoids appear *green*, and those containing both isoprenoid pigments appear *orange*/*yellow*. Scale bars, 10 μm

2 Materials

1. Greenhouse or plant growth chambers at 22–24 °C at night, and 26–28 °C during the day.
2. Tomato seeds.
3. Soil (vermiculite).
4. Trays and pots.
5. Plastic wrap.
6. Microscope slides and coverslips.
7. Surgical blades and tweezers.
8. Olympus FV 1000 Confocal Laser Scanning Microscope or a similar equipment.

3 Methods

Chlorophylls and carotenoids can be excited with blue light at 488 nm, giving rise to different emission spectra (Fig. 1). The method described here takes advantage of the differences in such spectra to distinguish between organelles that accumulate chlorophyll (chloroplasts), lycopene (chromoplasts), or both in fresh tomato fruit tissue. To improve resolution and avoid overlapping of fluorescence signals, we restricted the detection window to 650–700 nm for chlorophyll and 500–550 nm for lycopene (Fig. 1). For other plant tissues, emission spectra of the target plastids should be constructed as described in **steps 7** and **8** below and, based on these data, appropriate fluorescence emission windows should be selected for signal detection. **Steps 7** and **8** can be skipped when analyzing tomato fruit samples.

1. Sow tomato seeds in pots filled with wet vermiculite and transfer them to appropriate trays in the greenhouse or plant growth chamber. Cover the pots with plastic wrap until true leaves appear. Grow the plants until fruits develop.
2. Sample tomato fruits at different developmental stages: mature green, orange, and red ripe (Fig. 2).
3. Cut a thin layer of tomato pericarp tissue using a surgical blade (*see* **Note 1**).
4. Using appropriate tweezers transfer the tissue to a glass slide (*see* **Note 2**) with a drop of water (*see* **Note 3**).
5. Cover the sample with a coverslip (*see* **Note 4**).
6. Place the sample on the microscope stage and focus progressively with the different objectives. Once the region of interest has been selected, use a water-immersion 60× objective (such as U-PlanSApo AN:1,2) to focus the plastids (*see* **Note 5**).

7. Using a zoom factor of 2.5 and the 488 nm ray line of an argon laser for excitation, scan the region of interest in lambda mode to generate emission spectra. Record the emitted fluorescence from 500 to 700 nm using a bandwidth of 10 nm and a stepsize of 5 nm (*see* **Note 6**).
8. Select representative plastids in the scanned region and plot their corresponding emission spectra data using Olympus FV10-ASW or the corresponding CLSM software (Fig. 1).
9. Based on the fluorescence emission spectra obtained, select appropriate fluorescence emission windows for signal detection. For tomato fruit, set the channel for carotenoid (lycopene) detection between 500 and 550 nm and the channel for chlorophyll detection between 650 and 700 nm (*see* **Note 7**).
10. For signal detection, fix the photomultiplier (PMT) settings as follows: PMT High Voltage (HV) ca. 720 V for carotenoids (channel 1) and 770 V for chlorophylls (channel 2); PMT Offset 12 in both channels (*see* **Note 8**).
11. Scan the region of interest taking a *z*-stack of images composed of 8–13 optical sections separated 1 μm. We recommend a resolution of 512×512 pixels for digital images. To reduce background noise, we suggest to use a Kalman filter to average the signal over four frames. Set the scanning speed at 4 μs/pixel.
12. Overlay the images of the *z*-stack on a maximum projection to form a single image using the CLSM software (Fig. 2).

4 Notes

1. It is important to minimize tissue damage as much as possible. Damaged cells/tissues can produce false positive signals due to autofluorescence, which typically displays a yellowish color.
2. Although the pericarp sample can be placed on the microscopy slide in any orientation, we recommend laying the sample with the internal (pulp) side facing the slide and put the coverslip on the external (cuticle) side for optimal observation in the bright field.
3. Do not allow the sample to dry. If that occurs, it is recommended to discard it and use a new sample.
4. Pay attention to not generate bubbles, as they can interfere during the focusing process.
5. Focusing can be done directly with the 60× water-immersion objective.
6. An emission wavelength range from 500 to 700 nm includes autofluorescence from chlorophylls and carotenoids in tomato fruit pericarp (Fig. 1) and it should also work for other plant

tissues. If the signal is weak, laser power or bandwidth settings can be increased.

7. It is recommended to first compare samples harboring only one type of plastid (green and red fruit pericarp, in the case of tomato) to make sure that there is no emission fluorescence overlap.
8. The pinhole aperture can be increased if photodamage is observed due to laser illumination or if electronic noise occurs when the photomultiplier HV is increased.

Acknowledgements

Our work is funded by grants from the Catalan AGAUR (2009SGR-26 and XRB), Spanish DGI (BIO2011-23680 and PIM2010IPO-00660), and European Union FP7 (TiMet, contract 245143). We are members of the IBERCAROT network funded by CYTED (112RT0445). L.D. received a predoctoral fellowship of the Spanish Ministerio de Educación FPU program.

References

1. López-Juez E, Pike K (2005) Plastids unleashed: their development and their integration in plant development. Int J Dev Biol 410:557–577
2. Neuhaus HE, Emes MJ (2000) Nonphotosynthetic metabolism in plastids. Annu Rev Plant Physiol Plant Mol Biol 51:111–140
3. López-Juez E (2007) Plastid biogenesis, between light and shadows. J Exp Bot 58: 11–26
4. Lu S, Li L (2008) Carotenoid metabolism: biosynthesis, regulation, and beyond. J Integ Plant Biol 50:778–785
5. Cazzonelli C, Pogson B (2010) Source to sink: regulation of carotenoid biosynthesis in plants. Trends Plant Sci 15:1360–1385
6. Ruiz-Sola MA, Rodriguez-Concepción M (2012) Carotenoid biosynthesis in arabidopsis: a colorful pathway. Arabidopsis Book 10:e0158
7. Waters M, Pyke K (2005) Plastid development and differentiation. Annu Plant Rev Plastids 13:30–59
8. Bian W, Barsan C, Egea I, Purgatto E, Chervin C, Zouine M, Latché A, Bouzayen M, Pech JC (2011) Metabolic and molecular events occurring during chromoplast biogenesis. J Bot 2011:289859
9. Egea I, Barsan C, Bian W, Purgatto E, Latche A, Chervin C, Bouzayen M, Pech JC (2010) Chromoplast differentiation: current status and perspectives. Plant Cell Physiol 51:1601–1611
10. Egea I, Bian W, Barsan C, Jauneau A, Pech JC, Latche A, Li Z, Chervin C (2011) Chloroplast to chromoplast transition in tomato fruit spectral confocal microscopy analyses of carotenoid and chlorophylls in isolated plastids and time lapse recording on intact live tissue. Ann Bot 108:2101–2107

the plant journal

SEB Society for Experimental Biology

The Plant Journal (2016) **85,** 107–119 doi: 10.1111/tpj.13094

Tomato fruit carotenoid biosynthesis is adjusted to actual ripening progression by a light-dependent mechanism

Briardo Llorente[1,*], Lucio D'Andrea[1], M. Aguila Ruiz-Sola[1,†], Esther Botterweg[1,‡], Pablo Pulido[1,‡], Jordi Andilla[2], Pablo Loza-Alvarez[2] and Manuel Rodriguez-Concepcion[1,*]

[1]*Centre for Research in Agricultural Genomics, (CRAG) CSIC-IRTA-UAB-UB, Campus UAB Bellaterra, 08193 Cerdanyola del Valles (Barcelona), Spain, and*

[2]*Institut de Ciencies Fotoniques (ICFO), Barcelona Institute of Science and Technology, 08860 Castelldefels (Barcelona), Spain*

Received 27 October 2015; accepted 23 November 2015; published online 9 December 2015.

*For correspondence (e-mails briardo.llorente@cragenomica.es; manuel.rodriguez@cragenomica.es).

†Present address: Department of Biology, ETH Zürich, Universitätsstraße 2, 8092 Zürich, Switzerland.

‡Present address: Copenhagen Plant Science Centre, Department of Plant and Enviromental Sciences, University of Copenhagen, Frederiksberg C, Copenhagen, Denmark.

SUMMARY

Carotenoids are isoprenoid compounds that are essential for plants to protect the photosynthetic apparatus against excess light. They also function as health-promoting natural pigments that provide colors to ripe fruit, promoting seed dispersal by animals. Work in *Arabidopsis thaliana* unveiled that transcription factors of the phytochrome-interacting factor (PIF) family regulate carotenoid gene expression in response to environmental signals (i.e. light and temperature), including those created when sunlight reflects from or passes though nearby vegetation or canopy (referred to as shade). Here we show that PIFs use a virtually identical mechanism to modulate carotenoid biosynthesis during fruit ripening in tomato (*Solanum lycopersicum*). However, instead of integrating environmental information, PIF-mediated signaling pathways appear to fulfill a completely new function in the fruit. As tomatoes ripen, they turn from green to red due to chlorophyll breakdown and carotenoid accumulation. When sunlight passes through the flesh of green fruit, a self-shading effect within the tissue maintains high levels of PIFs that directly repress the master gene of the fruit carotenoid pathway, preventing undue production of carotenoids. This effect is attenuated as chlorophyll degrades, causing degradation of PIF proteins and boosting carotenoid biosynthesis as ripening progresses. Thus, shade signaling components may have been co-opted in tomato fruit to provide information on the actual stage of ripening (based on the pigment profile of the fruit at each moment) and thus finely coordinate fruit color change. We show how this mechanism may be manipulated to obtain carotenoid-enriched fruits.

Keywords: carotenoid, fruit, ripening, shade, tomato, phytochrome-interacting factor.

INTRODUCTION

Fleshy fruits typically lose their green color during ripening and accumulate pigments that provide a distinctive color to the ripe fruit. It is assumed that these pigment changes evolved as an adaptive characteristic that attracts seed-dispersing animals once seeds have matured and are therefore able to germinate (Klee and Giovannoni, 2011; Seymour *et al.*, 2013; Zhong *et al.*, 2013). Of the three major groups of plant pigments other than chlorophylls (anthocyanins, betalains and carotenoids), only carotenoids are essential for plant life as photoprotectants of the photosynthetic apparatus against excess light and as hormone precursors (Fraser and Bramley, 2004; Ruiz-Sola and Rodriguez-Concepcion, 2012). In tomato (*Solanum lycopersicum*), a leading vegetable crop and the main model system for fleshy fruits, enhanced production of carotenoids contributes to visual changes in color during ripening. Thus, the green color of mature (full-sized) tomato fruits changes to orange and red when ripe due to breakdown of chlorophylls and accumulation of the orange carotenoid β–carotene and the red carotenoid lycopene in the fruit flesh (i.e. the pericarp) (Tomato Genome Consortium, 2012; Fantini *et al.*, 2013; Seymour *et al.*, 2013) (Figure S1). In addition to conferring attractive colors, carotenoids increase the nutritional quality of the fruit as they serve as precursors for the production of retinoids (including vitamin A) and provide many other health-related

benefits (Fraser and Bramley, 2004; Ruiz-Sola and Rodriguez-Concepcion, 2012).

Previous studies have shown that, in addition to endogenous developmental, hormonal and epigenetic regulation, environmental factors such as light have a profound influence on fruit ripening (Azari *et al.*, 2010). In particular, fruit-localized phytochromes have been found to control various aspects of tomato ripening, including carotenoid accumulation (Alba *et al.*, 2000; Schofield and Paliyath, 2005; Gupta *et al.*, 2014). Phytochromes are photoreceptors of red light (R; wavelength 660 nm) and far-red light (FR; wavelength 730 nm) that exist in a dynamic photoequilibrium between the inactive R-absorbing Pr form and the active FR-absorbing Pfr form (Neff *et al.*, 2000; Azari *et al.*, 2010). Low R/FR ratios shift the equilibrium to the inactive Pr form, while high R/FR ratios shift it to the active Pfr form. Work in *Arabidopsis thaliana* has shown that Pfr translocates to the nucleus upon photoactivation to interact with transcription factors of the bHLH phytochrome-interacting factor (PIF) family, causing their inactivation, mainly by proteasome-mediated degradation, and hence regulating gene expression (Bae and Choi, 2008; Leivar and Monte, 2014). Our previous results (Toledo-Ortiz *et al.*, 2010, 2014; Bou-Torrent *et al.*, 2015) demonstrated that Arabidopsis PIF1 and other members of the so-called PIF quartet (collectively referred to as PIFq) repress carotenoid biosynthesis both in the dark and in response to a reduction in the R/FR ratio, a plant proximity signal referred to as 'shade' that is generated due to the preferential absorbance of R by leaves of neighboring or canopy plants (Martínez-García *et al.*, 2010; Casal, 2013). Phytochrome-mediated degradation of PIFq proteins de-represses carotenogenesis during seedling de-etiolation under R or high R/FR ratio light (e.g. white light or direct sunlight). Specifically, PIF1 was shown to repress carotenoid biosynthesis mainly by binding to a G–box motif in the promoter of the single Arabidopsis gene encoding phytoene synthase (PSY), the first and main rate-determining enzyme of the carotenoid pathway (Fraser *et al.*, 2002; Toledo-Ortiz *et al.*, 2010; Ruiz-Sola and Rodriguez-Concepcion, 2012). The role of PIF1 as a direct negative regulator of *PSY* expression is antagonized by the bZIP transcription factor LONG HYPOCOTYL 5 (HY5). In contrast to PIFq proteins, HY5 is degraded in the dark but accumulates in the light and induces *PSY* expression upon binding to the same promoter motif bound by PIF1 (Toledo-Ortiz *et al.*, 2014). The repression/activation module formed by PIF1 and HY5 also provides robustness to the control of *PSY* expression by temperature cues (Toledo-Ortiz *et al.*, 2014). By contrast, HY5 appears not to be relevant in regulating *PSY* expression after perception of a low R/FR signal (i.e. shade) (Bou-Torrent *et al.*, 2015). PIF1 and other PIFq proteins are not required to control *PSY* gene expression in Arabidopsis roots (Ruiz-Sola *et al.*, 2014a).

Arabidopsis and tomato diverged some 100 million years ago (Ku *et al.*, 2000), and their different histories of polyploidization and subsequent gene loss have resulted in different numbers of paralogs for carotenoid biosynthesis enzymes, including PSY (Ruiz-Sola and Rodriguez-Concepcion, 2012; Tomato Genome Consortium 2012). Three genes encode PSY in tomato, but only one (*PSY1*) contributes to carotenoid biosynthesis during fruit ripening (Fray and Grierson, 1993; Giorio *et al.*, 2008; Tomato Genome Consortium 2012; Fantini *et al.*, 2013). Transcriptional induction of the *PSY1* gene actually fuels the burst in carotenoid biosynthesis that takes place at the onset of ripening (Fray and Grierson, 1993; Giorio *et al.*, 2008; Tomato Genome Consortium 2012; Fantini *et al.*, 2013). Transcription factors of the MADS box family, such as RIPENING INHIBITOR (RIN) and FRUITFULL 1 (FUL1/TDR4), which are positive regulators of ripening, were found to stimulate carotenoid biosynthesis by directly binding to the promoter of the *PSY1* gene to induce its expression (Martel *et al.*, 2011; Fujisawa *et al.*, 2013, 2014; Shima *et al.*, 2013). HY5 is also known to positively regulate carotenoid accumulation in tomato fruit (Liu *et al.*, 2004), whereas other components of light signaling pathways have been described as negative regulators of ripening and carotenoid biosynthesis (Azari *et al.*, 2010). However, the molecular pathways connecting the perception of light signals with the regulation of carotenoid gene expression remain unknown. Here we demonstrate that a tomato ripening-induced PIF1 homolog (PIF1a) directly binds to the promoter of the *PSY1* gene to repress fruit carotenoid biosynthesis, indicating that basic molecular mechanisms for the light-dependent control of carotenogenesis are conserved in Arabidopsis leaves and tomato fruits. Most strikingly, we propose that this PIF-dependent core mechanism plays a different biological function during fruit development, i.e. to continuously monitor the progression of ripening based on the perception of fruit pigment composition changes.

RESULTS

The ripening-induced tomato PIF1 homolog PIF1a is a true PIF

Phytochromes have been proposed to control PSY activity and carotenoid biosynthesis in tomato fruit (Alba *et al.*, 2000; Schofield and Paliyath, 2005; Gupta *et al.*, 2014). While the changes in *PSY1* transcript levels observed when fruits are irradiated with R or exposed to simulated shade (i.e. FR-enriched white light) support a positive role for phytochrome signaling in modulating *PSY1* gene expression (Figure S2), the precise molecular mechanism awaits investigation. Because PIF1 is directly involved in phytochrome-dependent regulation of the single Arabidopsis *PSY* gene (Toledo-Ortiz *et al.*, 2010, 2014; Bou-Torrent *et al.*, 2015), we first evaluated whether tomato PIF1 homo-

logs are present in the fruit to regulate *PSY1* expression during ripening. A survey of the tomato genome (Tomato Genome Consortium 2012) for PIF sequences found six genes, including two with homology to Arabidopsis PIF1 (Figure 1a). The tomato gene encoding the PIF-like protein most closely related to Arabidopsis PIF1 (Figure 1a) was named *PIF1a* (Solyc09 g063010). Analysis of the Tomato Functional Genomics Database (http://ted.bti.cornell.edu/) and quantitative PCR analysis of transcript levels (Figure 1b) showed that, unlike the close homolog *PIF1b* (Solyc06g008030), *PIF1a* is expressed in the fruit and induced during ripening. The level of transcripts encoding PIF1a remained virtually constant during the maturation process, i.e. when immature green fruit grow to achieve their final size at the mature green (MG) stage. However, upon induction of ripening, *PIF1a* transcript levels increased approximately twofold at the orange (OR) stage and approximately fivefold in red ripe (RR) fruit compared to MG samples (Figure 1b). We therefore selected PIF1a for further studies.

To confirm whether PIF1a functions as a PIF, we evaluated its subcellular localization (Figure 1c), its light-dependent stability (Figure 1d), and its *in vivo* activity (Figure 1e). Transient expression assays in *Nicotiana benthamiana* leaves confirmed localization of a GFP-tagged PIF1a protein (PIF1a–GFP) in nuclear bodies (Figure 1c), as expected for a true PIF transcription factor (Al–Sady *et al.*, 2006; Shen *et al.*, 2008; Trupkin *et al.*, 2014). Also as expected, the PIF1a–GFP protein was degraded when nuclei were irradiated with R (i.e. upon activation of phytochromes) but not

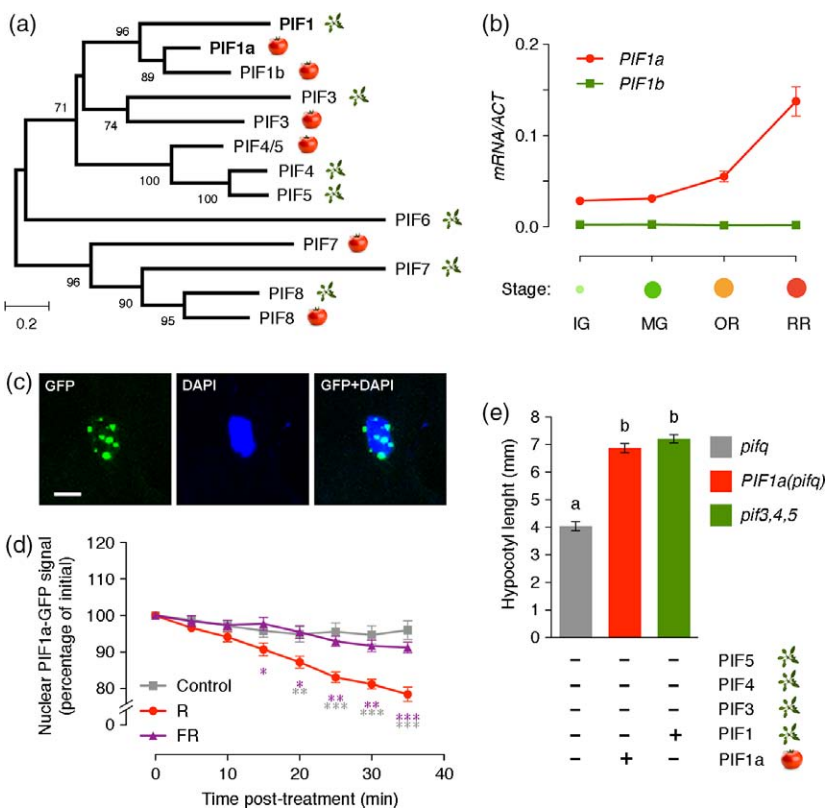

Figure 1. Tomato PIF homologs.
(a) Maximum-likelihood tree constructed using Arabidopsis and putative tomato PIF sequences. The percentage of trees in which the associated sequences clustered together with >70% reliability is shown next to the branches. The scale bar represents the mean number of substitutions per site. Images indicate the species.
(b) Quantitative PCR analysis of transcript levels for tomato PIF1 homologs during fruit ripening. IG, immature green; MG, mature green; OR, orange; RR, red ripe. Values are means ± SEM of $n \geq 5$ independent samples.
(c) Confocal microscopy images of GFP and DAPI fluorescence in the nucleus of a *N. benthamiana* leaf cell transiently expressing a GFP-tagged tomato PIF1a protein. Scale bar = 5 μm.
(d) Quantification of PIF1a–GFP fluorescence in nuclei such as those shown in (c) for samples kept in the dim light of the microscope room (control) or illuminated with supplemental R or FR light for the indicated times ($n \geq 11$). Values are means ± SEM, and significant differences (according to ANOVA followed by Newman–Keuls) compared with the symbols of corresponding color are indicated by asterisks (*$P < 0.05$, **$P < 0.01$, ***$P < 0.001$).
(e) Hypocotyl length of etiolated Arabidopsis seedlings defective in PIF1, PIF3, PIF4 and PIF5 (*pifq*) compared to triple mutants expressing wild-type PIF1 (*pif3,4,5*) and quadruple mutants expressing the tomato *PIF1a* sequence ($n = 25$). Values are means ± SEM, and significant differences (according to ANOVA followed by Newman–Keuls) are indicated by different letters ($P < 0.0001$).

when irradiated with FR or when kept under dim light (Figure 1d). As shown in Figure 1(e), expression of the tomato *PIF1a* gene under the control of the constitutive CaMV 35S promoter in an Arabidopsis quadruple mutant defective in PIF1, PIF3, PIF4 and PIF5 (*pifq*) resulted in a phenotype identical to that of the triple mutant lacking PIF3, PIF4 and PIF5 (Leivar *et al.*, 2009; Shin *et al.*, 2009; Leivar and Quail, 2011). We therefore conclude that the tomato PIF1a protein complements the loss of Arabidopsis PIF1 activity, and hence that it functions as a true PIF *in vivo*.

PIF1a represses *PSY1* expression by binding to a PBE box in its promoter

We next explored the putative role of PIF1a in the control of tomato *PSY1* expression and fruit carotenoid biosynthesis during ripening (Figure 2). Transient over-expression of the PIF1a–GFP protein in tomato pericarp tissue by agroinjection of MG fruit resulted in the eventual development of carotenoid-lacking sections as the fruit reached the RR stage (Figure 2a). This phenotype is consistent with a loss of PSY1 activity in these sections, which phenocopied the PSY1-defective mutant *yellow flesh* (*r*) (Fray and Grierson, 1993). To confirm whether PIF1a functions as a repressor of carotenoid biosynthesis in tomato fruit by down-regulating *PSY1* gene expression (similar to that reported for PIF1 and *PSY* in Arabidopsis), we next reduced *PIF1a* transcript levels and analyzed the concomitant changes in *PSY1* expression. Using a virus-induced gene silencing (VIGS) approach (Orzaez *et al.*, 2009; Fantini *et al.*, 2013), up-regulation of *PSY1* transcripts was indeed detected in *PIF1a*-silenced pericarp tissue compared with neighboring non-silenced tissue (Figure 2b). To further corroborate this observation, we generated stably transformed tomato plants harboring an artificial microRNA (Ossowski *et al.*, 2008) designed to specifically silence the *PIF1a* gene under the control of the 35S promoter (amiPIF1a lines). Consistent with the VIGS results, transgenic RR fruits showed increased levels of *PSY1* transcripts that inversely correlated with the extent of *PIF1a* silencing in various lines (Pearson correlation coefficient $r = -0.9725$; $P = 0.0054$) (Figure 2c). The expression of other tomato *PIF* genes in the fruit, including *PIF1b*, was found to be unaltered in these samples (Figure S3), confirming the specificity of the amiPIF1a construct. In agreement with the conclusion that higher *PSY1* transcript levels in amiPIF1a fruits resulted in increased PSY activity, metabolite profiling of transgenic OR and RR fruit showed higher amounts of phytoene, the direct product of PSY activity (Figure 2d). Also consistent with the rate-limiting role demonstrated for PSY activity by metabolic flux control analysis (Fraser *et al.*, 2002), levels of total carotenoids in amiPIF1 fruits were significantly higher than those in untransformed controls (Figure 2d).

Examination of the genomic sequence upstream of the translation start codon of *PSY1* revealed the existence of two conserved PIF-binding motifs (Toledo-Ortiz *et al.*, 2003; Zhang *et al.*, 2013): a G–box (CACGTG) and a PBE box (CACATG) (Figure 2e). Chromatin immunoprecipitation assays with tomato pericarp sections transiently over-expressing PIF1a–GFP (Figure 2a) indicated that PIF1a specifically binds to the PBE box of the *PSY1* promoter *in vivo* (Figure 2e). Based on these data, we conclude that PIF1a binds to the promoter of the *PSY1* gene to repress its expression and hence reduce PSY activity to eventually inhibit carotenoid biosynthesis.

Tomato fruit chlorophyll reduces the R/FR ratio of sunlight as it penetrates the fruit flesh

The ripening-associated accumulation of *PIF1a* transcripts (Figure 1b) may function as a mechanism to repress *PSY1* expression and hence antagonistically balance the effect of other ripening-induced transcription factors such as RIN and FUL1, which are direct activators of *PSY1* expression (Martel *et al.*, 2011; Fujisawa *et al.*, 2013, 2014; Shima *et al.*, 2013). However, we decided to explore new regulatory roles for PIF1a based on its properties as a PIF, specifically its phytochrome-mediated degradation response when the proportion of R increases (Figure 1d). It has been shown that the amount of R that passes through the pericarp of tomato fruit exposed to sunlight is much lower in green stages compared to orange/red stages, but the amount of FR changes very little (Alba *et al.*, 2000). However, the dynamics of light quality changes within the tissues of tomato fruits, and their potential biological relevance, remain unknown. To address the first point, we measured both the quantity (transmittance) and quality (R/FR ratio) of artificial white light (W) at increasing depths in the tomato pericarp (Figure 3 and Figure S4). Whereas transmittance showed a similar decrease in MG and OR fruit, the R/FR ratio only decreased in MG fruit. We tentatively conclude that the preferential absorbance of R (but not FR) by the chlorophyll present in fruit pericarp chloroplasts may be responsible for the observed decrease in the R/FR ratio within the cells of MG fruit, whereas this ratio was virtually unaffected by the presence of increasing amounts of carotenoids in OR fruit.

To next confirm whether the pigment composition of the fruit was responsible for the observed changes, we set up an experimental system to mimic the natural filter provided by these pigments. Total pigments were extracted from MG, OR and RR fruit, and used to characterize their chlorophyll and carotenoid composition (Figure S1) and absorbance spectra (Figure 4a). Pigment extracts from MG fruit showed an absorbance profile almost identical to that observed in leaves, with a characteristic peak at 660 nm due to the presence of chlorophylls. By contrast, this peak is almost completely absent in extracts from OR and RR fruits (Figure 4a). As a consequence, sunlight or artificial white (W) light passing

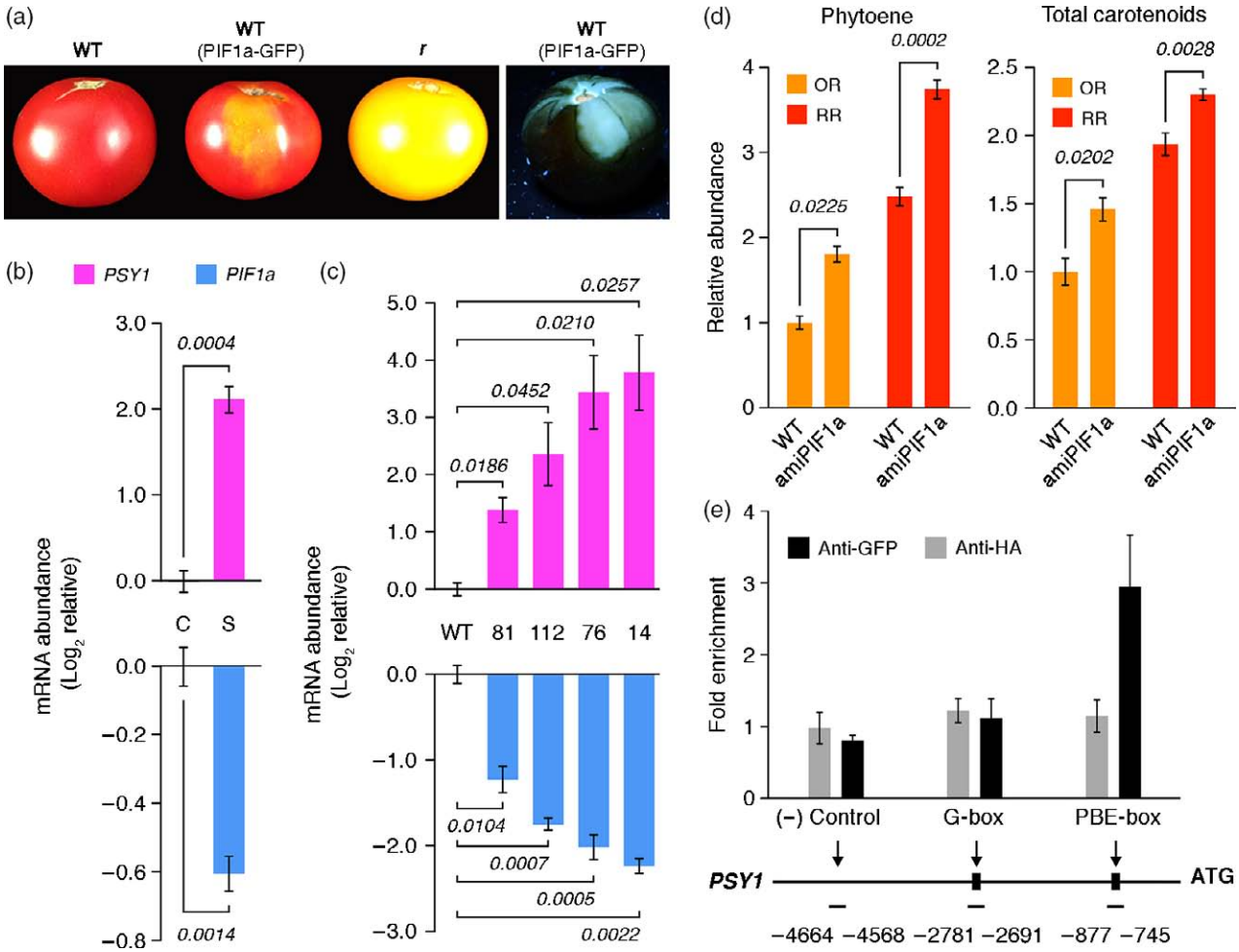

Figure 2. PIF1a directly represses *PSY1* expression in tomato fruit.
(a) Transient over-production of PIF1a in tomato fruits. Wild-type (WT) fruits at the MG stage were agroinjected with a construct to over-express the PIF1a–GFP protein, and left attached to the plant until they reached the RR stage. The fruit sections where the PIF1a–GFP protein was present (as deduced from GFP fluorescence detected by illumination with UV light, as shown on the right) showed a reduced accumulation of carotenoids, resulting in a yellow color (due to flavonoids) identical to that observed in ripe fruit of the PSY1-defective mutant *yellow ripe* (*r*).
(b) Quantitative PCR data show that VIGS-mediated down-regulation of *PIF1a* transcripts in silenced (S) sectors of tomato fruit causes an up-regulation of *PSY1* transcripts compared to non-silenced (C) sectors of the same fruits.
(c) Constitutive silencing of *PIF1a* in fruit from various transgenic tomato lines expressing a specific artificial microRNA (amiPIF1a) leads to a concomitant induction in *PSY1* transcript levels compared to untransformed (WT) controls.
(d) HPLC analysis of carotenoid levels in transgenic amiPIF1a fruits (line 112) shows an increased accumulation of phytoene (the direct product of PSY activity) and total carotenoids relative to untransformed (WT) controls at both OR and RR stages.
(e) ChIP/quantitative PCR analysis performed using tomato fruit sections transiently expressing the PIF1a–GFP protein using anti-GFP antibodies. Control reactions were processed in parallel using anti-HA serum or no antibodies. The location of *PSY1* promoter amplicons used in quantitative PCR quantification of ChIP-enriched DNA regions corresponding to control (–) and PIF-binding domains (G–box and PBE box) are indicated in the map.
Values in (b)–(d) are means ± SEM ($n \geq 3$). Italic numbers above the bars indicate *P* values (Student's *t* test). Values in (e) are means ± SEM from two independent experiments. Values are reported relative to non-silenced sectors (b), WT (c), OR (d) or blank samples (e).

through extracts from OR or RR fruit maintained a high R/FR ratio whereas the light passing through extracts from MG fruit showed a low R/FR ratio (Figure 4b and Figure S5). Almost identical results were obtained when whole hand-cut sections of pericarp tissue were used instead of extracts (Figure S5), confirming that the observed effects on light quality were due to the presence of photosynthetic pigments (chlorophylls and carotenoids) in the samples.

Fruit pigmentation-dependent changes in the R/FR ratio specifically influence *PSY1* expression

Once we had established that the pigment composition of MG fruit resulted in a reduction in the R/FR ratio of the light reaching the inner layers of pericarp cells, but the pigment composition of OR or RR fruit (rich in carotenoids but almost completely lacking chlorophylls) had little or no effect on this ratio, we assessed whether this has

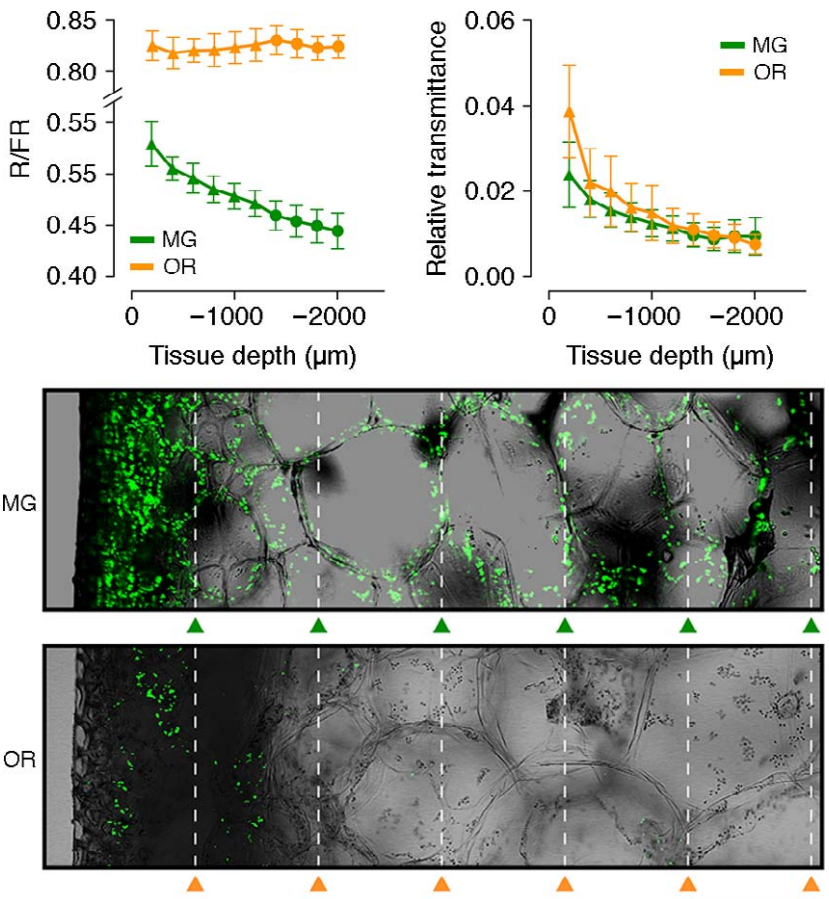

Figure 3. The R/FR ratio inside the fruit pericarp changes during ripening.
Serial sections of the outer pericarp of MG and OR fruit were obtained using a vibratome. Starting with 2000 μm thick samples, 200 μm layers were sequentially removed from the internal side of the pericarp to obtain samples of decreasing thickness until only a thin section of the fruit surface was left. After removing each 200 μm layer, the remaining section was illuminated with artificial white light, and both the R/FR ratio and the intensity (transmittance) of the light that passed through it were determined. Bright-field images of MG and OR fruit pericarp tissue merged with chlorophyll autofluorescence (corresponding to chloroplasts, green) are also shown. Dashed lines indicate the depths at which the last six light measurements were performed (represented by the triangles in the graphs). Values are means ± SEM (n = 3) relative to blank controls.

biological relevance. We designed a filter system that involved placing a glass plate containing MG and RR fruit pigment extracts between the source of light (W) and the experimental samples (Figure S6). To test whether the change in the R/FR ratio obtained after filtering of light through MG or RR filters affected gene expression, we used Arabidopsis as a well-known model for the molecular response to low R/FR signals (i.e. shade). W-grown Arabidopsis seedlings were exposed to W filtered through MG or RR filters, and the expression of known shade-regulated genes was analyzed. As shown in Figure S7, transcripts of shade-induced genes accumulated at higher levels in samples exposed to W+MG. By contrast, *PSY* expression was lower in samples illuminated with W+MG (Figure 4c), consistent with the reported down-regulation of the gene in response to shade (Bou-Torrent *et al.*, 2015). Altogether, these results demonstrate that the fruit pigments effectively alter the quality of the light that penetrates the tomato pericarp, generating signals that eventually modulate the expression of shade-responsive genes.

To confirm whether fruit pigment composition also has an effect on the regulation of tomato carotenoid biosynthetic genes, we used pigment-lacking (white) tomato fruits obtained by preventing exposure to light from the very early stages of fruit set and development (Cheung *et al.*, 1993). To avoid developmental variability among visually similar fruits, we compared the effects of illuminating the same fruit with either W+MG or W+RR. To do so, individual white fruits were longitudinally cut into two halves in the dark, and each of the halves was then treated with the corresponding light for 2 h (Figure 4d). Expression analysis of genes encoding enzymes of the carotenoid biosynthesis pathway, including *DXS1*, *PSY1*, *PSY2*, *PSY3*, *PDS*, *LCY–E*, *LCY–B* and *CYC–B* (Figure 4e), revealed that only *PSY1* exhibited significant changes, showing levels that were approximately twofold higher in the halves placed under the RR filter compared to those illuminated with W+MG (Figure 4f). Higher levels of *PSY1* transcripts in samples exposed to light with a higher R/FR ratio were expected as a consequence of the instability of the PIF1a repressor under such conditions (Figure 1d).

Changes in the R/FR ratio of the light sensed in pericarp cells probably adjust carotenoid biosynthesis to the actual progress of ripening

We next tested whether the differential light-filtering properties of fruit pigments also affect carotenoid metabolism during fruit ripening (Figure 5). Because this experiment

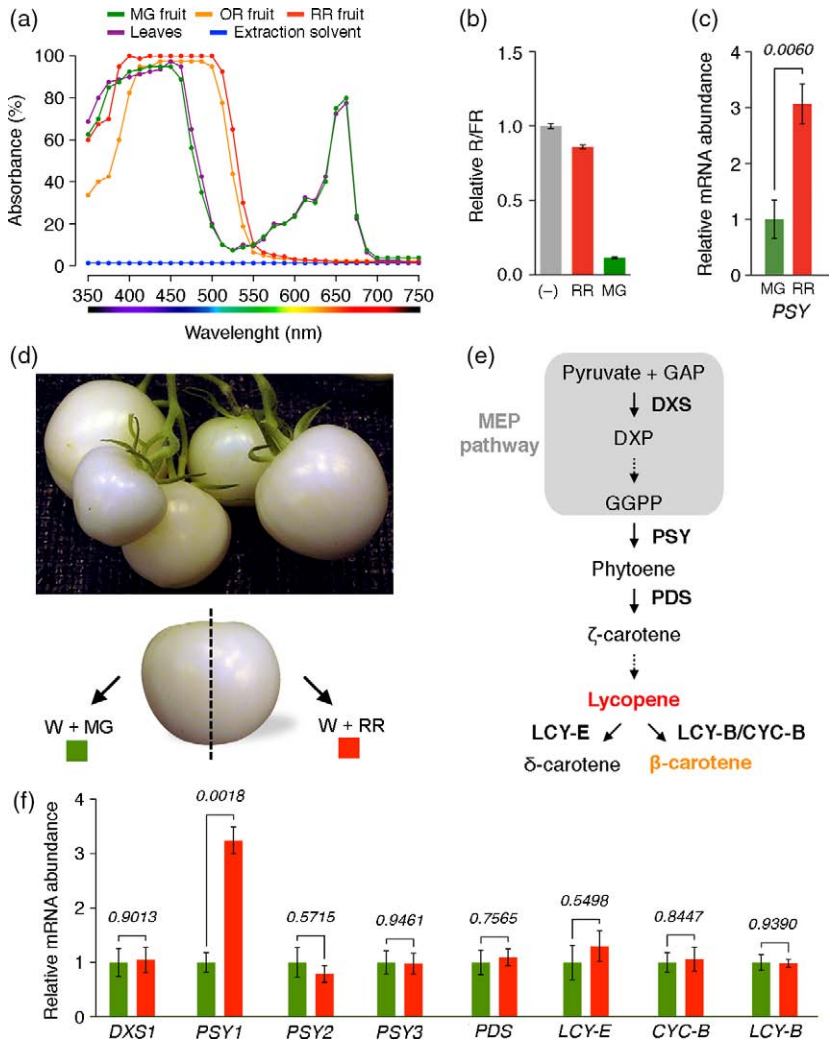

Figure 4. Light filtered through tomato fruit photosynthetic pigments specifically affects the expression of PSY-encoding genes.
(a) Absorption spectra of organic extracts of photosynthetic pigments (chlorophylls and carotenoids) isolated from tomato leaves and fruits at various developmental stages.
(b) R/FR ratio of artificial white light (W) filtered through pigment extracts prepared from red (RR) or green (MG) fruits relative to that of unfiltered light (–). Values are means ± SEM ($n \geq 6$).
(c) Effect of light filtered through tomato MG or RR extracts on expression of the Arabidopsis *PSY* gene. Arabidopsis seedlings germinated and grown in the dark for 3 days were exposed for 1 h to W filtered through MG or RR filters. Transcript abundance was assessed by quantitative PCR, Values are means ± SEM ($n = 4$) relative to the MG filter condition. The number above the bars indicates the *P* value (Student's *t* test).
(d) Tomato fruits lacking any kind of endogenous pigments were obtained approximately 40 days after covering whole inflorescences with light-proof bags. The resulting white fruits were collected in the bags and then cut in two halves in the dark. Each of the halves was immediately exposed for 2 h to W light filtered through MG or RR filters.
(e) Enzymes of the carotenoid biosynthesis pathway in tomato. The methylerythritol 4–phosphate (MEP) pathway provides substrates for the carotenoid pathway, while PSY leads to downstream accumulation of carotenoids. GAP, glyceraldehyde-3–phosphate; DXP, deoxyxylulose-5–phosphate; GGPP, geranylgeranyl diphosphate. Solid and dashed arrows represent single or multiple enzymatic steps, respectively. Enzymes are shown in bold: DXS, DXP synthase; PSY, phytoene synthase; PDS, phytoene desaturase; LCY–E, lycopene ε–cyclase; LCY–B, lycopene β–cyclase; CYC–B, chromoplast-specific lycopene β–cyclase.
(f) Quantitative PCR analysis of samples treated as described in (d) to estimate the abundance of transcripts for tomato genes encoding the enzymes indicated in (e). Values are means ± SEM from $n = 3$ biological replicates relative to the W+MG condition. The numbers above the bars indicate *P* values (Student's *t* test).

required irradiating fruit at a pre-ripening stage and visually identifying the developmental stage was not possible in the case of white fruit, we used MG fruit. Individual fruits were split in two halves immediately before exposing each half to either W+MG or W+RR. Exposure was maintained for a few days until both halves had entered the breaker stage (i.e. started losing chlorophylls and turning orange/red). Reaching this stage typically took longer for fruit halves illuminated with W+MG (Figure 5a). Consistent with this visual observation, W+RR-exposed halves showed a higher accumulation of the major carotenoids lycopene and β–carotene compared with their

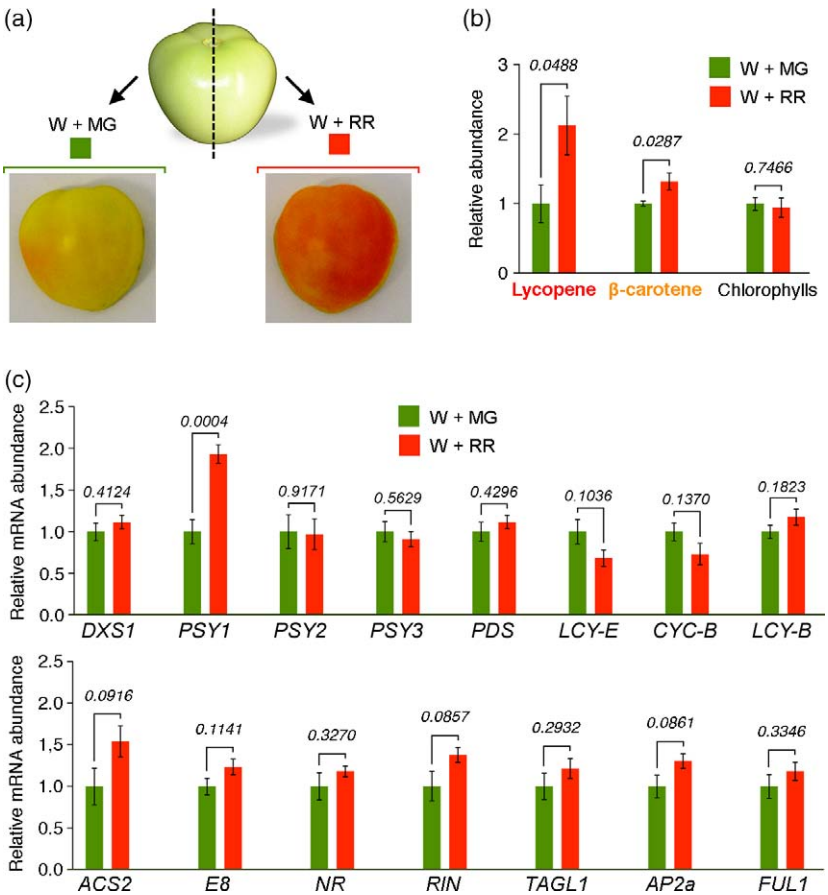

Figure 5. The light-absorbing properties of fruit photosynthetic pigments influence carotenoid biosynthesis but not ripening.
(a) Fruits at the MG stage were cut in two and exposed to W light filtered through MG or RR filters until pigmentation changes were visually observed in both halves.
(b) HPLC analysis of major photosynthetic pigments in fruit halves treated as described in (a).
(c) Quantitative PCR analysis of transcript abundance of the indicated tomato genes in fruit halves treated as described in (a). The upper graph includes genes for carotenoid biosynthetic enzymes, and the lower graph corresponds to ripening-related genes. Values are means ± SEM from $n = 6$ biological replicates relative to the W+MG condition. The numbers above the bars indicate *P* values (Student's *t* test).

W+MG-exposed counterparts, while chlorophylls were not affected by the light filters (Figure 5b). Similar to the results obtained with white fruits, the halves illuminated with W+RR also showed a significantly increased accumulation of *PSY1* transcripts, but no changes were observed in other carotenoid-related genes (Figure 5c). We also analyzed the expression of several well-characterized ripening-related genes in the same samples. We included the genes encoding RIN and FUL1/TDR4, which are positive regulators of ripening that directly induce *PSY1* expression (Martel *et al.*, 2011; Fujisawa *et al.*, 2013, 2014; Shima *et al.*, 2013). Notably, no statistical differences were found between halves exposed to W+MG or W+RR filters (Figure 5c), suggesting that the light treatments did not have a significant influence on ripening but specifically affected fruit carotenoid biosynthesis by modulating *PSY1* expression.

In agreement with the conclusion that the R/FR ratio of the light reaching the pericarp cells affects carotenoid biosynthesis by specifically modulating *PSY1* gene expression, breaker fruits showed higher levels of *PSY1* transcripts and derived carotenoids such as phytoene (the immediate PSY product) and lycopene in the outer side of the pericarp tissue (Figure 6a), which experiences a higher R/FR ratio than the internal section (Figure 3). Furthermore, PIF1a appears to be the main factor regulating *PSY1* expression in response to this signal, as the difference in *PSY1* transcript levels observed in fruit halves exposed to W+MG or W+RR (Figure 5) is strongly attenuated in transgenic amiPIF1a fruits (Figure 6b). These results confirm that the low R/FR ratio of the light reaching the inner pericarp cells of MG fruit due to the presence of chlorophylls (referred to as a self-shading effect) represses carotenoid biosynthesis by specifically down-regulating *PSY1* gene expression via PIF1a. This effect progressively decreases as soon as chlorophylls start to disappear at the onset of ripening, thus boosting (i.e. de-repressing) *PSY1* expression and carotenoid accumulation in breaker fruits.

DISCUSSION

Carotenoids are lipophilic isoprenoid pigments that are synthesized by all photosynthetic organisms, including plants. Because they are essential to protect the photosynthetic apparatus against excess light, it is not surprising that their production is tightly regulated by light (Fraser and Bramley, 2004; Azari *et al.*, 2010; Ruiz-Sola and Rodriguez-Concepcion, 2012). Carotenoids also provide colors to fruits as a signal of ripeness, so that animals disperse the

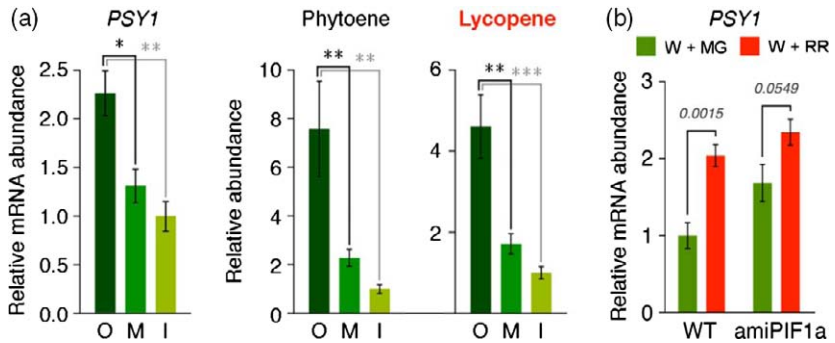

Figure 6. PIF1a regulates *PSY1* expression in response to changes in R/FR ratio.
(a) *PSY1* expression and carotenoid levels in various regions of the pericarp. The graphs represent quantitative PCR analysis of *PSY1* transcript levels and HPLC analysis of phytoene and lycopene accumulation in the outer section, i.e. that most exposed to sunlight (O), the middle section (M) and the inner section (I) (approximately 1 mm) of the pericarp of fruits at the breaker stage ($n \geq 5$). Values are means ± SEM relative to inner pericarp samples. Significant differences (according to ANOVA followed by Newman–Keuls) are indicated by asterisks (*$P < 0.05$, **$P < 0.01$, ***$P < 0.001$).
(b) Quantitative PCR analysis of *PSY1* transcript abundance in untransformed (WT) and transgenic amiPIF1a fruit halves treated as described in Figure 5(a). Values are means ± SEM from $n = 5$ biological replicates relative to the W+MG condition. The numbers above the bars indicate *P* values (Student's *t* test).

enclosed seeds only when their development has been completed. Thus, carotenoids give yellow color to bananas, orange color to peaches and oranges, and red color to tomatoes. Here we show that carotenoid biosynthesis in ripening tomato fruit is regulated by a PIF-based molecular mechanism that is identical to that regulating carotenogenesis in Arabidopsis leaves in response to light signals. A striking difference, however, is that this mechanism appears to fulfill a completely different function in tomato fruit, as it uses shade signaling components not to gather environmental information (e.g. the presence of plant neighbors that may eventually compete for resources) but to provide information on the progression of ripening based on the pigment profile of the fruit at any given moment. A model summarizing the proposed mechanism is presented in Figure 7. A self-shading effect due to the presence of high chlorophyll levels and low carotenoid levels in green fruit alters the spectral composition of the light that penetrates the pericarp (Figure 3), maintaining a relatively high proportion of phytochromes in their inactive Pr form. In this context, PIF1a accumulates (Figure 1), repressing *PSY1* gene expression by directly binding to its promoter (Figure 2). When the ripening developmental program starts, chlorophylls begin to degrade, progressively reducing the self-shading effect and consequently shifting the photoequilibrium of phytochromes to their active Pfr form. This promotes PIF1a degradation, resulting in *PSY1* de-repression and a subsequent increase in carotenoid biosynthesis (Figure 7).

It is striking that the described self-shade signaling pathway specifically targets *PSY1*, the main gene controlling the metabolic flux into the carotenoid pathway during tomato ripening (Figures 4 and 5). These findings parallel those previously described in Arabidopsis, where PIF1 specifically targets the *PSY* gene for control of carotenoid biosynthesis during de-etiolation (Toledo-Ortiz *et al.*,

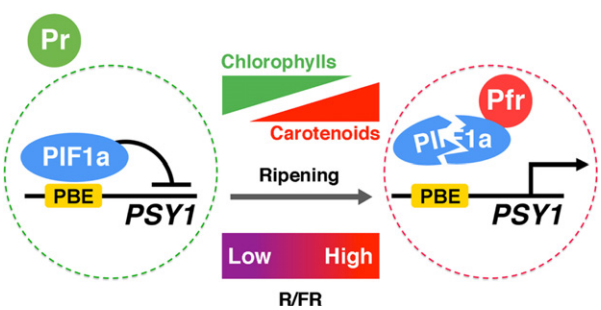

Figure 7. Self-shading model of carotenoid biosynthesis control.
Chlorophylls in green fruit generate a self-shading effect that maintains phytochromes predominantly in the inactive Pr form and high PIF1a levels that repress *PSY1* expression. Chlorophyll breakdown at the onset of ripening reduces the self-shading effect, shifting phytochromes to the active Pfr form and promoting PIF1a degradation. Consequently, *PSY1* is de-repressed and carotenoid biosynthesis is boosted. The dashed circles represent nuclei.

2010). It remains unknown whether the same mechanism is also active in tomato leaves or de-etiolating seedlings (probably involving other PIF homologs and PSY-encoding genes, as PIF1a and PSY1 appear to be mostly restricted to the fruit). While it is likely that direct transcriptional control of genes encoding PSY by PIF transcription factors may be a conserved mechanism in nature for light-mediated regulation of the carotenoid pathway, PIFs are not required to regulate *PSY* expression in Arabidopsis roots either under normal conditions or in response to abscisic acid or salt signals that promote root-specific up-regulation of the gene (Ruiz-Sola *et al.*, 2014a,b). These results suggest that PIFs may only be relevant for the control of *PSY* gene expression and carotenoid biosynthesis in organs that are normally exposed to light.

Similar to the general mechanisms involved in PIF-mediated control of carotenoid biosynthesis in Arabidopsis shoot tissues, tomato PIF1a may be part of an antagonistic

module to regulate expression of the *PSY1* gene in tomato fruit. Thus, the levels of transcripts encoding direct negative regulators of the gene such as PIF1a (Figure 1b) but also direct positive regulators such as RIN and FUL1 (Martel *et al.*, 2011; Fujisawa *et al.*, 2013, 2014; Shima *et al.*, 2013) increase during ripening. This may function as a 'gas-and-brake' mechanism to provide a more robust control of tomato *PSY1* expression during ripening, similar to that proposed to regulate Arabidopsis *PSY* expression and carotenoid biosynthesis in response to light and temperature cues (Toledo-Ortiz *et al.*, 2014; Bou-Torrent *et al.*, 2015). However, we speculate that the main function of PIF1a during ripening is to modulate the developmental control of *PSY1* expression and hence carotenoid biosynthesis by finely adjusting the transcription rate of the gene to the actual progression of ripening (Figure 7). Based on the described data, we propose that the developmental induction of *PSY1* expression directly mediated by general ripening activators such as RIN is additionally promoted by reduced PIF1a activity when chlorophylls degrade at the onset of ripening (due to the pigmentation-derived increase in the R/FR ratio). However, as ripening progresses, increasing levels of *PIF1a* transcripts may produce more protein as a buffering mechanism to counterbalance the positive effects of transcriptional activators on *PSY1* expression.

Based on the widespread occurrence of ripening-associated fruit pigmentation changes as an adaptive characteristic for attracting animals that disperse viable seeds, we propose that similar PIF-mediated mechanisms may operate in other plant species bearing fleshy fruits that lose their green color and accumulate carotenoids when ripe. Furthermore, the pigmentation-based dynamic regulation unveiled here may have implications that go beyond evolution and ecology to affect fruit biotechnology. Thus, constitutive down-regulation of PIF levels in tomato plants was shown here to be effective at increasing accumulation of carotenoids in the fruit (Figure 2d). It is predicted that more targeted manipulations of PIF levels (i.e. using fruit-specific and ripening-induced promoters) may further improve the carotenoid profile of tomato and a number of other fruits, and hence lead to successful creation of healthier, carotenoid-rich foods.

EXPERIMENTAL PROCEDURES

Plant material and growth conditions

Tomato (*Solanum lycopersicum*) and tobacco (*Nicothiana benthamiana*) plants were grown under standard greenhouse conditions (14 h light at 27 ± 1°C and 10 h dark at 22 ± 1°C). The tomato varieties MicroTom and Moneymaker were used for most experiments. White tomatoes were obtained from Moneymaker plants as described previously (Cheung *et al.*, 1993). VIGS experiments were performed using a Del/Ros1 line N in the Moneymaker background (Orzaez *et al.*, 2009). All *Arabidopsis thaliana* lines used in this work were in the Col–0 background. Arabidopsis seeds were surface-sterilized and sown on sterile Murashige and Skoog medium containing 1% agar and no sucrose. Seeds were stratified for 3 days at 4°C before use. Hypocotyl length was quantified using ImageJ (http://rsb.info.nih.gov/) as described previously (Sorin *et al.*, 2009).

Unless otherwise stated, light-filtering experiments with fruit pigment filters were performed in climate-controlled growth chambers equipped with fluorescent tubes providing continuous white light (22°C; 90 μmol m^{-2} sec^{-1} PAR). Fluence rates were measured using a SpectroSense2 meter associated with a four-channel sensor (Skye Instruments, http://www.skyeinstruments.com/), which measures PAR (400–700 nm) and 10 nm windows in the R (664–674 nm) and FR (725–735 nm) regions. Fruit pigment filters were freshly prepared for each experiment. Pericarp samples were homogenized at a 1:2 w/v ratio of tissue (fresh weight) to cold extraction solvent (hexane/acetone/methanol, 2:1:1) using a stainless steel blender. The homogenate was incubated in the dark at 4°C with agitation (320 rpm) for 2 h, and then centrifuged at 5000 ***g*** for 30 min at 4°C. The organic phase enriched in chlorophylls and carotenoids was recovered and directly transferred to glass plates to create the filters (Figure S6). When required, pigment concentration was adjusted by adding extraction solvent to the extracts in the plate until the PAR value of the light passing through the filters was approximately 40–50 μmol m^{-2} sec^{-1}.

Biophotonics

The quantity (transmittance) and quality (R/FR ratio) of white light (400–800 nm) filtered through pericarp sections of tomato fruit was determined using a Lambda 950 UV/VIS/NIR spectrophotometer (Perkin-Elmer, http://www.perkinelmer.com/). Data were sequentially acquired after removing successive layers (200 μm thick) of inner pericarp tissue using a VT12000 S vibrating-blade microtome (Leica, http://www.leika.com/).

Metabolite analysis

Chlorophylls and carotenoids were purified from 15 mg lyophilized tomato pericarp tissue using 1 ml cold extraction solvent as described previously (Saladie *et al.*, 2014), and profiled by HPLC using an Agilent 1200 series HPLC system (Agilent Technologies, http://www.agilent.com) as described previously (Fraser *et al.*, 2000). Absorbance spectra were measured using a quartz cuvette and a SpectraMax M3 multi-mode microplate reader (Molecular Devices, http://www.moleculardevices.com/).

Gene expression analysis

RNA was isolated using PureLink™ RNA Mini and TRIzol Kit (Life Technologies, https://www.thermofisher.com/) and TRIzol (Invitrogen, https://www.thermofisher.com/) according to the manufacturer's instructions, quantified using a NanoDrop 1000 spectrophotometer (Thermo Scientific, http://www.nanodrop.com/), and checked for integrity by agarose gel electrophoresis. A first-strand cDNA synthesis kit (Roche, http://www.roche.com/) was used to generate cDNA according to the manufacturer's instructions. Relative mRNA abundance was evaluated via quantitative PCR using LightCycler 480 SYBR Green I Master Mix (Roche) on a LightCycler 480 real-time PCR system (Roche). At least two technical replicates of each biological replicate were performed, and the mean values were used for further calculations. Normalized transcript abundances were calculated as described previously (Simon, 2003) using tomato *ACT* (Solyc04g011500.2.1) and Arabidopsis *UBC* (At5g25760) as endogenous reference genes. Gene accession numbers and primers used are listed in Table S1.

Phylogenetic analysis

Arabidopsis PIF sequences (Leivar and Quail, 2011) were used as queries to search for putative tomato homologs using BLAST on the National Center for Biotechnology Information website (www.ncbi.nlm.nih.gov/) and the SolGenomics Network website (http://solgenomics.net/). Alignments were performed using MUSCLE (Edgar, 2004a,b) and an unrooted tree was constructed using MEGA5 (Tamura *et al.*, 2011) as described previously (Hall, 2013). Evolutionary relationships were inferred by using the maximum-likelihood method based on the JTT matrix-based model (Jones *et al.*, 1992). The tree with the highest log likelihood (−5298.8282) was selected. Initial tree(s) for the heuristic search were obtained automatically by applying the Neighbor-Joining (NJ) and BioNJ algorithms to a matrix of pairwise distances estimated using a JTT model, and then selecting the topology with superior log likelihood value. A discrete gamma distribution was used to model evolutionary rate differences among sites (five categories (+G, parameter = 0.9307)). The analysis involved 13 amino acid sequences. All positions with less than 95% site coverage were eliminated. A total of 215 positions remained in the final dataset. Analyzed proteins are described in Table S2.

Constructs and plant transformation

Full-length cDNAs encoding PIF1a were amplified from RR fruit and cloned into pDONR207 using Gateway technology (Invitrogen). The sequence was then sub-cloned into pGWB405 (Nakagawa *et al.*, 2007) and into a version of pCAMBIA1301 (Hajdukiewicz *et al.*, 1994) modified for Gateway-compatible cloning using the Gateway vector conversion system (Life Technologies). The pCAMBIA1301-PIF1a construct (35S:PIF1a) was used for *Agrobacterium tumefaciens*-mediated transformation (Bechtold and Pelletier, 1998) of the Arabidopsis *pifq* mutant (Leivar *et al.*, 2009). The pGWB405-PIF1a construct (35S:PIF1a–GFP) was used for transient expression in *N. benthamiana* leaves (Sparkes *et al.*, 2006) and tomato fruit (Orzaez *et al.*, 2006). For VIGS, a 180 bp fragment of the *PIF1a* cDNA was PCR-amplified and cloned into pDONR207 prior to sub-cloning into pTRV2/DR/Gateway (Orzaez *et al.*, 2009). The fragment was designed to minimize off-target silencing. Fruit VIGS was performed as described previously (Orzaez *et al.*, 2009; Fantini *et al.*, 2013). An artificial microRNA (amiRNA) was designed as described previously (Ossowski *et al.*, 2008) to specifically silence *PIF1a* in stably transformed tomato lines. Briefly, plasmid pRS300 was used as template to introduce an anti-*PIF1a* amiRNA sequence into the *miR319a* precursor by site-directed mutagenesis (Schwab *et al.*, 2006). The overlapping PCR amplification steps were performed as described previously (Fernandez *et al.*, 2009), with the exception that primers A and B were re-designed (primers miR A and miR B in Table S3). The resulting PCR product was cloned into pDONR221P4r-P3r to generate plasmid pEF4r-PIF1a-3r. Then plasmids pEF1-2x35S-4, pEF4r-PIF1a-3r and pEF3-Tnos-2 were recombined (Estornell *et al.*, 2009), and the resulted triple recombination was sub-cloned into binary vector pKGW (Karimi *et al.*, 2005) to obtain plasmid pKGW-PIF1a. Tomato MicroTom plants were transformed with pKGW-PIF1a as previously described (Fernandez *et al.*, 2009). All constructs were confirmed by restriction mapping and DNA sequence analysis. Primers are listed in Table S3.

Confocal microscopy

After agroinfiltration of *N. benthamiana* leaves with pGWB405-PIF1a as described previously (Sparkes *et al.*, 2006), PIF1a–GFP fluorescence was detected using a Leica TCS SP5 confocal laser-scanning microscope. Nuclei were identified by directly incubating the leaf samples with 4′,6–diamidino-2–phenylindole (DAPI) (1 mg ml^{-1}). Excitation filters of 450–490 nm and 410–420 nm were used for detection of GFP fluorescence and DAPI signal, respectively. PIF1a–GFP levels in individual nuclei were estimated by quantifying the GFP fluorescence signal in *z*–stacks of optical sections separated by 0.5 μm using the integrated microscope software. To estimate PIF1a–GFP stability in response to light, GFP fluorescence in the nuclei found in a given field was quantified in the dim light of the microscope room and then the microscope stage was moved down to expose the sample to either R (30 μmol m^{-2} sec^{-1}) or FR (30 μmol m^{-2} sec^{-1}) using a portable QBEAM 2200 LED lamp (Quantum Devices, http://www.quantum-dev.com/). After illumination for 5 min, the microscope stage was moved up to quantify the GFP signals in the same field. GFP excitation was limited to image acquisition steps to minimize photobleaching. Control samples were treated similarly except that they were not irradiated. Tomato pericarp sections were obtained using a Vibratome series 1000 sectioning system (Vibratome, http://www.vibratome.com/). Chloroplasts were identified using excitation at 488 nm and a 610–700 nm filter to detect chlorophyll autofluorescence.

ChIP analysis

Tomato Moneymaker fruit at the MG stage were agroinjected with pGWB405-PIF1a as described previously (Orzaez *et al.*, 2006) to produce the PIF1a–GFP protein. GFP fluorescence in pericarp sections was monitored using a Blak-Ray B–100AP high-intensity UV lamp (Ultra-Violet Products, http://www.uvp.com/). Pericarp sections showing fluorescence were then excised using a scalpel, fixed with 1% formaldehyde for 15 min under vacuum, and then ground to fine powder under liquid nitrogen. ChIP assays were performed as described previously (Osnato *et al.*, 2012) using a commercial anti-GFP antibody (Life Technologies). An anti-HA antibody (Santa Cruz Biotechnology, http://www.scbt.com/) was used in parallel control reactions. Primers for quantitative PCR reactions are listed in Table S4.

Statistical analysis

Student's *t* test, ANOVA followed by the Newman–Keuls multiple comparison post hoc test and Pearson correlation coefficients (*r* values) were calculated using GraphPad Prism 5.0a (GraphPad Software, http://www.graphpad.com/).

ACCESSION NUMBERS

Accession numbers for genes analyzed by quantitative RT–PCR and for protein sequences used for molecular phylogenetic analysis are listed in Tables S1 and S2, respectively.

ACKNOWLEDGMENTS

We thank Cathie Martin (Department of Metabolic Biology, John Innes Centre, Norwich Research Park, Norwich NR4 7UH, UK) and José Luis Riechmann for critical reading of the manuscript, Jaime F. Martínez-García for valuable discussion, and César Alonso-Ortega for providing some of the equipment used in this work. We gratefully acknowledge the experimental advice of Luis Matías-Hernández and technical assistance of María Rosa Rodríguez-Goberna and core facilities staff of the Centre for Research in Agricultural Genomics. Work at the Centre for Research in Agricultural Genomics was funded by the following grants: CarotenActors (FP7-PEOPLE-2011-IIF 300862), TiMet

(FP7-KBBE-2009-3 245143), Ibercarot (CYTED-112RT0445), Spanish Ministerio de Economia y Competitividad (BIO2011-23680) and Generalitat de Catalunya (2014SGR-1434) to MRC. Work by researchers at the Institut de Ciencies Fotoniques was partially performed at the super-resolution light nanoscopy facility and supported by Fundació Cellex Barcelona.

SUPPORTING INFORMATION

Additional Supporting Information may be found in the online version of this article.

Figure S1. Tomato fruit ripening stages and photosynthetic pigment composition.

Figure S2. *PSY1* response to R and FR.

Figure S3. Specificity of the amiRNA against PIF1a.

Figure S4. Light spectra at various depths of the pericarp.

Figure S5. R/FR ratio of sunlight filtered through the pericarp of tomato fruit.

Figure S6. Set-up for experiments with tomato fruit pigment extracts.

Figure S7. Effect of light filtered through tomato fruit pigment extracts on Arabidopsis shade-responsive gene expression.

Table S1. Accession IDs and primers for genes analyzed by quantitaive RT–PCR.

Table S2. Accession IDs for protein sequences used for molecular phylogenetic analysis.

Table S3. Primers used in cloning.

Table S4. Primers used for ChIP/quantitative PCR analysis.

REFERENCES

Alba, R., Cordonnier-Pratt, M.M. and Pratt, L.H. (2000) Fruit-localized phytochromes regulate lycopene accumulation independently of ethylene production in tomato. *Plant Physiol.* **123**, 363–370.

Al–Sady, B., Ni, W., Kircher, S., Schafer, E. and Quail, P.H. (2006) Photoactivated phytochrome induces rapid PIF3 phosphorylation prior to proteasome-mediated degradation. *Mol. Cell*, **23**, 439–446.

Azari, R., Reuveni, M., Evenor, D., Nahon, S., Shlomo, H., Chen, L. and Levin, I. (2010) Overexpression of UV-DAMAGED DNA BINDING PROTEIN 1 links plant development and phytonutrient accumulation in *high pigment–1* tomato. *J. Exp. Bot.* **61**, 3627–3637.

Bae, G. and Choi, G. (2008) Decoding of light signals by plant phytochromes and their interacting proteins. *Annu. Rev. Plant Biol.* **59**, 281–311.

Bechtold, N. and Pelletier, G. (1998) *In planta Agrobacterium*-mediated transformation of adult *Arabidopsis thaliana* plants by vacuum infiltration. *Methods Mol. Biol.* **82**, 259–266.

Bou-Torrent, J., Toledo-Ortiz, G., Ortiz-Alcaide, M., Cifuentes-Esquivel, N., Halliday, K.J., Martinez-Garcia, J.F. and Rodriguez-Concepcion, M. (2015) Regulation of carotenoid biosynthesis by shade relies on specific subsets of antagonistic transcription factors and co-factors. *Plant Physiol.* **169**, 1584–1594.

Casal, J.J. (2013) Photoreceptor signaling networks in plant responses to shade. *Annu. Rev. Plant Biol.* **64**, 403–427.

Cheung, A.Y., McNellis, T. and Piekos, B. (1993) Maintenance of chloroplast components during chromoplast differentiation in the tomato mutant green flesh. *Plant Physiol.* **101**, 1223–1229.

Edgar, R.C. (2004a) MUSCLE: a multiple sequence alignment method with reduced time and space complexity. *BMC Bioinformatics*, **5**, 113.

Edgar, R.C. (2004b) MUSCLE: multiple sequence alignment with high accuracy and high throughput. *Nucleic Acids Res.* **32**, 1792–1797.

Estornell, L.H., Orzaez, D., Lopez-Pena, L., Pineda, B., Anton, M.T., Moreno, V. and Granell, A. (2009) A multisite Gateway-based toolkit for targeted gene expression and hairpin RNA silencing in tomato fruits. *Plant Biotechnol. J.* **7**, 298–309.

Fantini, E., Falcone, G., Frusciante, S., Giliberto, L. and Giuliano, G. (2013) Dissection of tomato lycopene biosynthesis through virus-induced gene silencing. *Plant Physiol.* **163**, 986–998.

Fernandez, A.I., Viron, N., Alhagdow, M. *et al.* (2009) Flexible tools for gene expression and silencing in tomato. *Plant Physiol.* **151**, 1729–1740.

Fraser, P.D. and Bramley, P.M. (2004) The biosynthesis and nutritional uses of carotenoids. *Prog. Lipid Res.* **43**, 228–265.

Fraser, P.D., Pinto, M.E., Holloway, D.E. and Bramley, P.M. (2000) Application of high-performance liquid chromatography with photodiode array detection to the metabolic profiling of plant isoprenoids. *Plant J.* **24**, 551–558.

Fraser, P.D., Romer, S., Shipton, C.A., Mills, P.B., Kiano, J.W., Misawa, N., Drake, R.G., Schuch, W. and Bramley, P.M. (2002) Evaluation of transgenic tomato plants expressing an additional phytoene synthase in a fruit-specific manner. *Proc. Natl Acad. Sci. USA*, **99**, 1092–1097.

Fray, R.G. and Grierson, D. (1993) Identification and genetic analysis of normal and mutant phytoene synthase genes of tomato by sequencing, complementation and co-suppression. *Plant Mol. Biol.* **22**, 589–602.

Fujisawa, M., Nakano, T., Shima, Y. and Ito, Y. (2013) A large-scale identification of direct targets of the tomato MADS box transcription factor RIPENING INHIBITOR reveals the regulation of fruit ripening. *Plant Cell*, **25**, 371–386.

Fujisawa, M., Shima, Y., Nakagawa, H., Kitagawa, M., Kimbara, J., Nakano, T., Kasumi, T. and Ito, Y. (2014) Transcriptional regulation of fruit ripening by tomato FRUITFULL homologs and associated MADS box proteins. *Plant Cell*, **26**, 89–101.

Giorio, G., Stigliani, A.L. and D'Ambrosio, C. (2008) Phytoene synthase genes in tomato (*Solanum lycopersicum* L.) – new data on the structures, the deduced amino acid sequences and the expression patterns. *FEBS J.* **275**, 527–535.

Gupta, S.K., Sharma, S., Santisree, P., Kilambi, H.V., Appenroth, K., Sreelakshmi, Y. and Sharma, R. (2014) Complex and shifting interactions of phytochromes regulate fruit development in tomato. *Plant, Cell Environ.* **37**, 1688–1702.

Hajdukiewicz, P., Svab, Z. and Maliga, P. (1994) The small, versatile pPZP family of *Agrobacterium* binary vectors for plant transformation. *Plant Mol. Biol.* **25**, 989–994.

Hall, B.G. (2013) Building phylogenetic trees from molecular data with MEGA. *Mol. Biol. Evol.* **30**, 1229–1235.

Jones, D.T., Taylor, W.R. and Thornton, J.M. (1992) The rapid generation of mutation data matrices from protein sequences. *Comput. Appl. Biosci.* **8**, 275–282.

Karimi, M., De Meyer, B. and Hilson, P. (2005) Modular cloning in plant cells. *Trends Plant Sci.* **10**, 103–105.

Klee, H.J. and Giovannoni, J.J. (2011) Genetics and control of tomato fruit ripening and quality attributes. *Annu. Rev. Genet.* **45**, 41–59.

Ku, H., Vision, T., Liu, J., and Tranksley, S.D. (2000) Comparing sequenced segments of the tomato and Arabidopsis genomes: Large-scale duplication followed by selective gene loss creates a network of synteny. *Proc. Natl Acad. Sci. USA*, **97**, 9121–9126.

Leivar, P. and Monte, E. (2014) PIFs: systems integrators in plant development. *Plant Cell*, **26**, 56–78.

Leivar, P. and Quail, P.H. (2011) PIFs: pivotal components in a cellular signaling hub. *Trends Plant Sci.* **16**, 19–28.

Leivar, P., Tepperman, J.M., Monte, E., Calderon, R.H., Liu, T.L. and Quail, P.H. (2009) Definition of early transcriptional circuitry involved in light-induced reversal of PIF-imposed repression of photomorphogenesis in young *Arabidopsis* seedlings. *Plant Cell*, **21**, 3535–3553.

Liu, Y., Roof, S., Ye, Z., Barry, C., van Tuinen, A., Vrebalov, J., Bowler, C. and Giovannoni, J. (2004) Manipulation of light signal transduction as a means of modifying fruit nutritional quality in tomato. *Proc. Natl Acad. Sci. USA*, **101**, 9897–9902.

Martel, C., Vrebalov, J., Tafelmeyer, P. and Giovannoni, J.J. (2011) The tomato MADS-box transcription factor RIPENING INHIBITOR interacts with promoters involved in numerous ripening processes in a COLORLESS NONRIPENING-dependent manner. *Plant Physiol.* **157**, 1568–1579.

Martínez-García, J.F., Galstyan, A., Salla-Martret, M., Cifuentes-Esquivel, N., Gallemí, M. and Bou-Torrent, J. (2010) Regulatory components of shade avoidance syndrome. *Adv. Bot. Res.* **53**, 65–116.

Nakagawa, T., Suzuki, T., Murata, S. *et al.* (2007) Improved Gateway binary vectors: high-performance vectors for creation of fusion constructs in transgenic analysis of plants. *Biosci. Biotechnol. Biochem.* **71**, 2095–2100.

Neff, M.M., Fankhauser, C. and Chory, J. (2000) Light: an indicator of time and place. *Genes Dev.* **14**, 257–271.

Orzaez, D., Mirabel, S., Wieland, W.H. and Granell, A. (2006) Agroinjection of tomato fruits. A tool for rapid functional analysis of transgenes directly in fruit. *Plant Physiol.* **140**, 3–11.

Orzaez, D., Medina, A., Torre, S., Fernandez-Moreno, J.P., Rambla, J.L., Fernandez-Del-Carmen, A., Butelli, E., Martin, C. and Granell, A. (2009) A visual reporter system for virus-induced gene silencing in tomato fruit based on anthocyanin accumulation. *Plant Physiol.* **150**, 1122–1134.

Osnato, M., Castillejo, C., Matias-Hernandez, L. and Pelaz, S. (2012) TEMPRANILLO genes link photoperiod and gibberellin pathways to control flowering in *Arabidopsis*. *Nat. Commun.* **3**, 808.

Ossowski, S., Schwab, R. and Weigel, D. (2008) Gene silencing in plants using artificial microRNAs and other small RNAs. *Plant J.* **53**, 674–690.

Ruiz-Sola, M.A. and Rodriguez-Concepcion, M. (2012) Carotenoid biosynthesis in Arabidopsis: a colorful pathway. *Arabidopsis Book*, **10**, e0158.

Ruiz-Sola, M.A., Arbona, V., Gomez-Cadenas, A., Rodriguez-Concepcion, M. and Rodriguez-Villalon, A. (2014a) A root specific induction of carotenoid biosynthesis contributes to ABA production upon salt stress in arabidopsis. *PLoS ONE*, **9**, e90765.

Ruiz-Sola, M.A., Rodriguez-Villalon, A. and Rodriguez-Concepcion, M. (2014b) Light-sensitive phytochrome-interacting factors (PIFs) are not required to regulate phytoene synthase gene expression in the root. *Plant Signal Behav.* **9**, e29248.

Saladie, M., Wright, L.P., Garcia-Mas, J., Rodriguez-Concepcion, M. and Phillips, M.A. (2014) The 2-C-methylerythritol 4-phosphate pathway in melon is regulated by specialized isoforms for the first and last steps. *J. Exp. Bot.* **65**, 5077–5092.

Schofield, A. and Paliyath, G. (2005) Modulation of carotenoid biosynthesis during tomato fruit ripening through phytochrome regulation of phytoene synthase activity. *Plant Physiol. Biochem.* **43**, 1052–1060.

Schwab, R., Ossowski, S., Riester, M., Warthmann, N. and Weigel, D. (2006) Highly specific gene silencing by artificial microRNAs in *Arabidopsis*. *Plant Cell*, **18**, 1121–1133.

Seymour, G.B., Ostergaard, L., Chapman, N.H., Knapp, S. and Martin, C. (2013) Fruit development and ripening. *Annu. Rev. Plant Biol.* **64**, 219–241.

Shen, H., Zhu, L., Castillon, A., Majee, M., Downie, B. and Huq, E. (2008) Light-induced phosphorylation and degradation of the negative regulator PHYTOCHROME-INTERACTING FACTOR1 from *Arabidopsis* depend upon its direct physical interactions with photoactivated phytochromes. *Plant Cell*, **20**, 1586–1602.

Shima, Y., Kitagawa, M., Fujisawa, M., Nakano, T., Kato, H., Kimbara, J., Kasumi, T. and Ito, Y. (2013) Tomato FRUITFULL homologues act in fruit ripening via forming MADS-box transcription factor complexes with RIN. *Plant Mol. Biol.* **82**, 427–438.

Shin, J., Kim, K., Kang, H., Zulfugarov, I.S., Bae, G., Lee, C.H., Lee, D. and Choi, G. (2009) Phytochromes promote seedling light responses by inhibiting four negatively-acting phytochrome-interacting factors. *Proc. Natl Acad. Sci. USA*, **106**, 7660–7665.

Simon, P. (2003) Q-Gene: processing quantitative real-time RT–PCR data. *Bioinformatics*, **19**, 1439–1440.

Sorin, C., Salla-Martret, M., Bou-Torrent, J., Roig-Villanova, I. and Martinez-Garcia, J.F. (2009) ATHB4, a regulator of shade avoidance, modulates hormone response in Arabidopsis seedlings. *Plant J.* **59**, 266–277.

Sparkes, I.A., Runions, J., Kearns, A. and Hawes, C. (2006) Rapid, transient expression of fluorescent fusion proteins in tobacco plants and generation of stably transformed plants. *Nat. Protoc.* **1**, 2019–2025.

Tamura, K., Peterson, D., Peterson, N., Stecher, G., Nei, M. and Kumar, S. (2011) MEGA5: molecular evolutionary genetics analysis using maximum likelihood, evolutionary distance, and maximum parsimony methods. *Mol. Biol. Evol.* **28**, 2731–2739.

Toledo-Ortiz, G., Huq, E. and Quail, P.H. (2003) The Arabidopsis basic/helix-loop-helix transcription factor family. *Plant Cell*, **15**, 1749–1770.

Toledo-Ortiz, G., Huq, E. and Rodriguez-Concepcion, M. (2010) Direct regulation of phytoene synthase gene expression and carotenoid biosynthesis by phytochrome-interacting factors. *Proc. Natl Acad. Sci. USA*, **107**, 11626–11631.

Toledo-Ortiz, G., Johansson, H., Lee, K.P., Bou-Torrent, J., Stewart, K., Steel, G., Rodriguez-Concepcion, M. and Halliday, K.J. (2014) The HY5–PIF regulatory module coordinates light and temperature control of photosynthetic gene transcription. *PLoS Genet.* **10**, e1004416.

Tomato Genome Consortium. (2012) The tomato genome sequence provides insights into fleshy fruit evolution. *Nature*, **485**, 635–641.

Trupkin, S.A., Legris, M., Buchovsky, A.S., Tolava Rivero, M.B. and Casal, J.J. (2014) Phytochrome B nuclear bodies respond to the low red to far-red ratio and to the reduced irradiance of canopy shade in Arabidopsis. *Plant Physiol.* **165**, 1698–1708.

Zhang, Y., Mayba, O., Pfeiffer, A., Shi, H., Tepperman, J.M., Speed, T.P. and Quail, P.H. (2013) A quartet of PIF bHLH factors provides a transcriptionally centered signaling hub that regulates seedling morphogenesis through differential expression-patterning of shared target genes in *Arabidopsis*. *PLoS Genet.* **9**, e1003244.

Zhong, S., Fei, Z., Chen, Y.R. *et al.* (2013) Single-base resolution methylomes of tomato fruit development reveal epigenome modifications associated with ripening. *Nat. Biotechnol.* **31**, 154–159.

Supplemental Figures S1-S7 and Tables S1-S4

Supplemental Figures

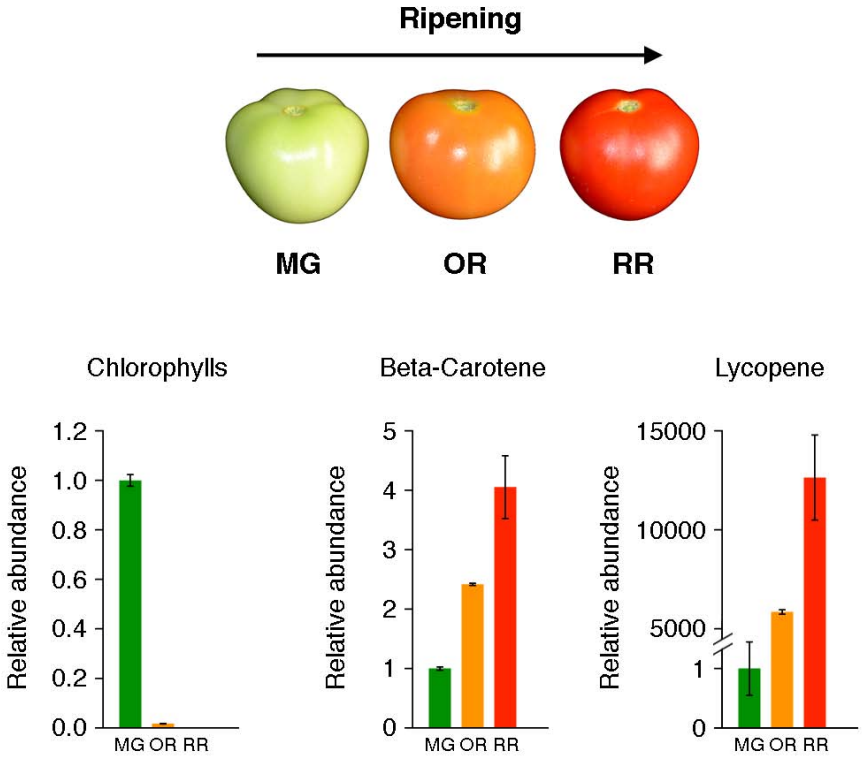

Supplemental Figure S1. Tomato fruit ripening stages and photosynthetic pigment composition. Representative images of tomato fruit at the mature green (MG), orange (OR) and red ripe (RR) stages are shown in the upper panel. Graphs show representative HPLC-determined profiles of chlorophylls and carotenoids at these stages. The values and bars represent the mean ± SEM from *n* = 3 biological replicates and they are shown relative to those in MG samples.

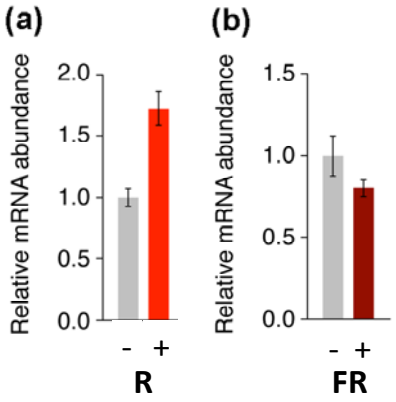

Supplemental Figure S2. *PSY1* response to R and FR. Quantitative PCR analysis of *PSY1* transcript levels in fruits halves irradiated with R or FR-enriched light. (**a**) Tomato fruits at the MG stage were cut in two halves. One of the halves was incubated in the dark (-) for 2h, whereas the other half was irradiated (+) with R light (30 µmol m^{-2} s^{-1} PAR) for the same time period. (**b**) Tomato fruits at the OR stage were cut in two halves and each of them was illuminated either with (-) white light (25 µmol m^{-2} s^{-1} PAR, R/FR ratio of 0.05) or with (+) white light supplemented with FR (25 µmol m^{-2} s^{-1} PAR, R/FR ratio of 3) for 4h. Data correspond to mean ± SEM from n=3 (**a**) or n=4 (**b**) fruits.

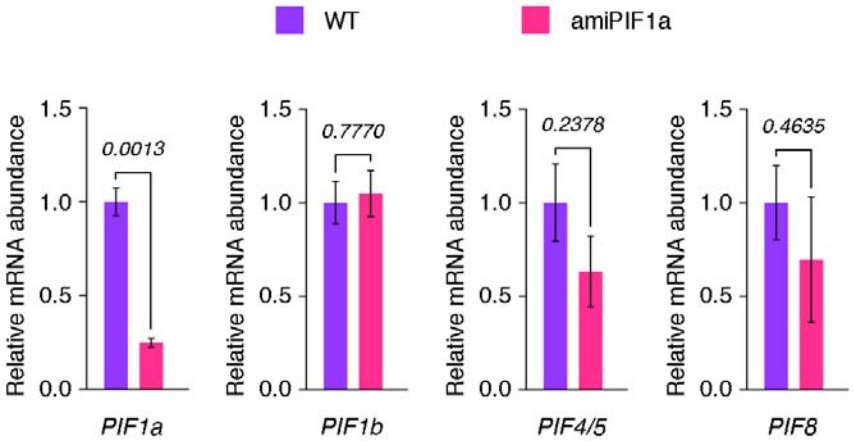

Supplemental Figure S3. Specificity of the amiRNA against *PIF1a*. Transcript abundance was assessed by quantitative PCR. Data correspond to amiPIF1a line 14. Accessions and primers used are listed in Supplemental Table S1. The values and bars represent the mean ± SEM from *n* ≥ 3 biological replicates. Values are reported relative to the non-transformed WT controls.

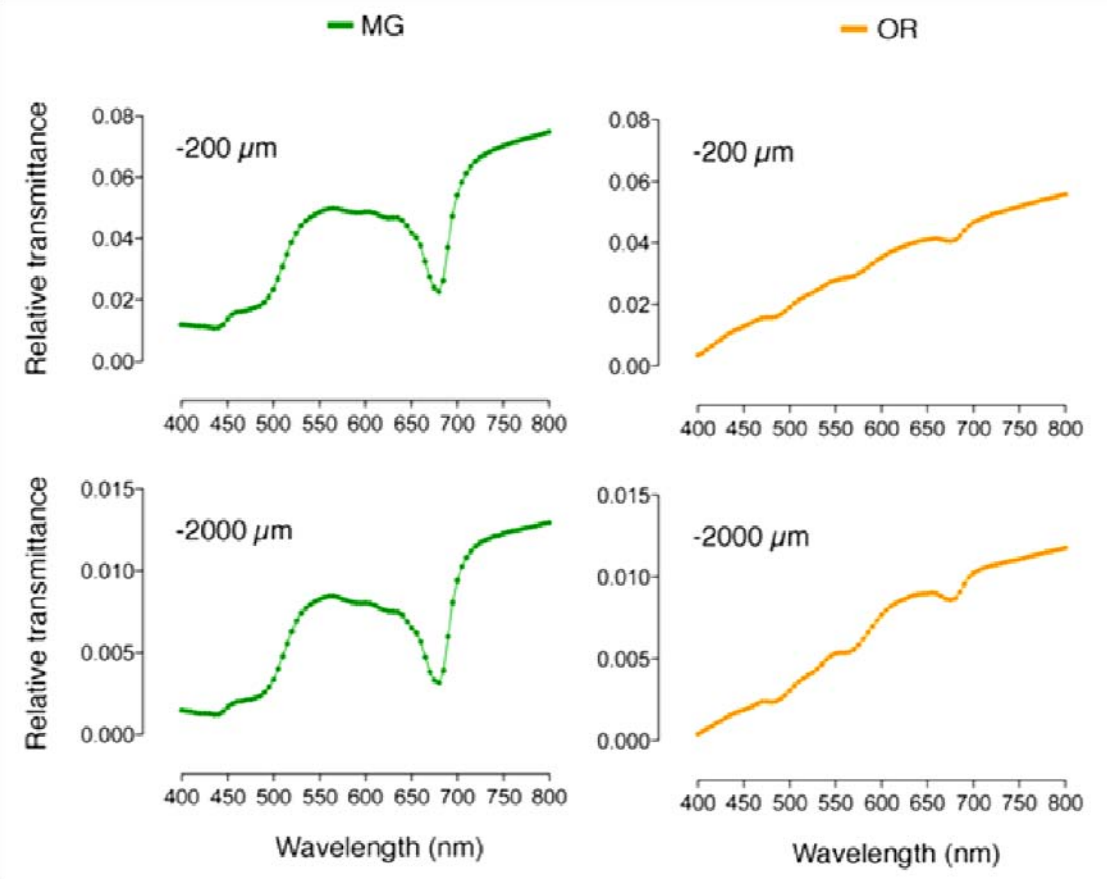

Supplemental Figure S4. Light spectra at different depths of the pericarp. Measurements correspond to tissue depths of 200 and 2000 μm from the surface of MG and OR fruit (see Figure 3 for experimental details). Data are represented relative to blank controls with no fruit samples.

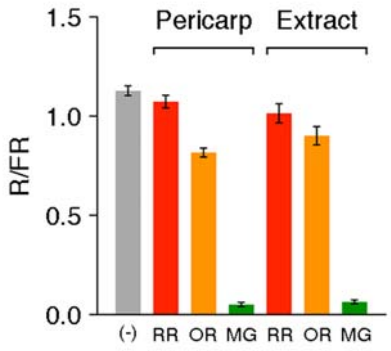

Supplemental Figure S5. R/FR ratio of sunlight filtered through the pericarp of tomato fruit. Measurements were performed in the greenhouse (GPS coordinates: 41°49'82"N 2°10'80"E) and correspond to R/FR ratio values of direct sunlight before (-) and after passing through fresh hand-cut pericarp sections or pigment extracts from MG, OR or RR fruit ($n \geq 6$).

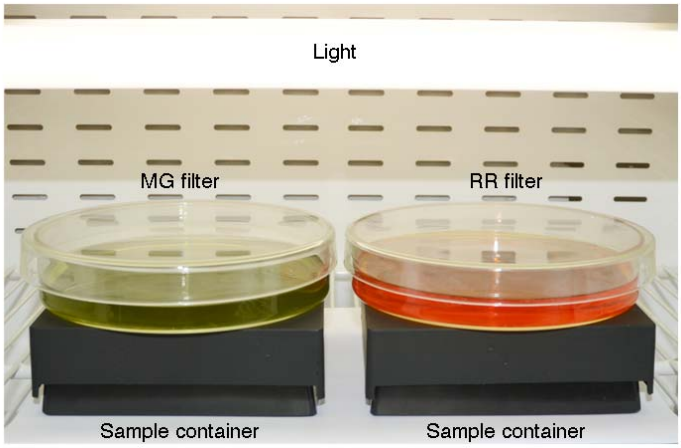

Supplemental Figure S6. Setup for experiments with tomato fruit pigment extracts. Glass plates containing extracts of photosynthetic pigments (chlorophylls and carotenoids) isolated from tomato fruit pericarp tissue were placed on top of light-proof boxes with an opening in the lid so that all the light coming into the box passed through the corresponding pigment filter. Light sensors and biological samples were placed inside the corresponding box. When comparing different fruit extracts, the same climate controlled chamber and source of artificial white light (fluorescent tubes providing 90 µmol m^{-2} s^{-1} PAR) was used and the pigment concentration in the extracts was adjusted so that the filtered light showed similar PAR values (40-50 µmol m^{-2} s^{-1}).

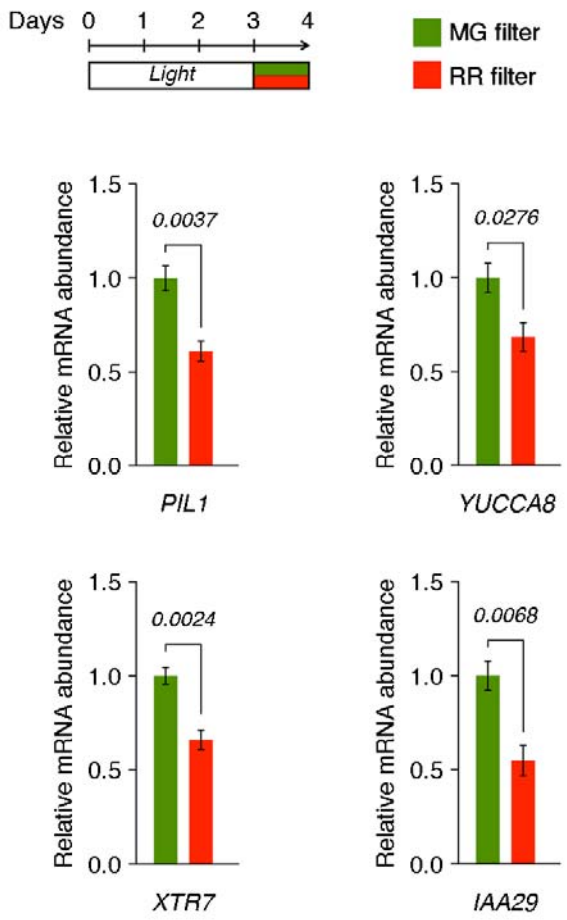

Supplemental Figure S7. Effect of light filtered through tomato fruit pigment extracts on Arabidopsis shade-responsive gene expression. Arabidopsis wild-type seedlings germinated and grown under continuous light for 3 days were exposed for 24 h to light filtered through MG or RR filters (see Supplemental Figure S4). Transcript abundance of the indicated genes was assessed by quantitative PCR. Accessions and primers used are listed in Supplemental Table S1. The values and bars represent the mean ± SEM from *n* = 4 biological replicates. Numbers above the bars show statistical *P* values according to the *t*-test. Values are reported relative to the MG filter condition.

Supplemental Tables

Supplemental Table S1. Accession IDs and primers for genes analyzed by RT-qPCR in this study

Organism	Gene name	Accession number	qPCR primers
S. lycopersicum	*PSY1*	Solyc03g031860	F: GCCATTGTTGAAAGAGAGGGTG R: AGGCAAACCAACTTTTCCTCAC
S. lycopersicum	*PSY2*	Solyc02g081330	F: CTCTAGTGCCCCCTAAGTCAAC R: TTTAGAAACTTCATTCATGTCTTTGC
S. lycopersicum	*PSY3*	Solyc01g005940	F: TTGGATGCAATAGAGGAGAATG R: ATTGAATGGCTAAACTAGGCAAAG
S. lycopersicum	*DXS1*	Solyc01g067890	F: TGACCATGGATCTCCTGTTG R: GCCTCTCTGGTTTGTCCAAG
S. lycopersicum	*PDS*	Solyc03g123760	F: AGCAACGCTTTTTCCTGATG R: TCGGAGTTTTGACAACATGG
S. lycopersicum	*LCY-E*	Solyc12g008980	F: GCCACAAGAACGAAAACGAC R: CGCGGAAAAATGACCTTATC
S. lycopersicum	*LCY-B*	Solyc10g079480	F: TTGTGGCCCATAGAAAGGAG R: GGCATCGAAAAACCTTCTTG
S. lycopersicum	*CYC-B*	Solyc06g074240	F: TGGCAAGGGTTCCTTTCTTC R: AGTCATGTTTGAGCCATGTCC
S. lycopersicum	*ACS2*	Solyc01g095080	F: CGTTTGAATGTCAAGAGCCAGG R: TCGCGAGCGCAATATCAAC
S. lycopersicum	*E8*	Solyc09g089580	F: AGCTGCAAGTTGGAGAGACACG R: CCGCATGGAGTTGGAAATTC
S. lycopersicum	*NR*	Solyc09g075440	F: CTCCCAGAGGCAGATTGAAC R: TTCACAGACATCCCACCATC
S. lycopersicum	*RIN*	Solyc05g012020	F: GCTAGGTGAGGATTTGGGACAA R: AATTTGCCTCAATGATGAATCCA
S. lycopersicum	*TAGL1*	Solyc07g055920	F: GCCATTGGTAGAGTCCGTTC R: GATACATGTTGGCGTTCTGC
S. lycopersicum	*AP2a*	Solyc03g044300	F: AACGGACCACAATCTTGAC R: CTGCTCGGAGTCTGAACC
S. lycopersicum	*FUL1*	Solyc06g069430	F: CAACAACTGGACTCTCCTCACCTT R: TCCTTCCACTTCCCCATTATCTATT
S. lycopersicum	*PIF1a*	Solyc09g063010	F: TCGAACCAGCCAAGACTTCC R: CGGTAATGCAACTTGCGC
S. lycopersicum	*PIF1b*	Solyc06g008030	F: TCAGGAAGTGGAACAGCTGAG R: TTGATGATTCCCTCTACTTCCTTC
S. lycopersicum	*ACT*	Solyc04g011500	F: CCTTCCACATGCCATTCTCC R: CCACGCTCGGTCAGGATCT
A. thaliana	*PIL1*	At2g46970	F: GGAAGCAAAACCCTTAGCATCAT R: TCCATATAATCTTCATCTTTTAATTTTGGTTTA
A. thaliana	*YUCCA8*	At4g28720	F: AATGGACGCGGTTAAGATCG R: CCCCTTGAGCGTTTCGTG
A. thaliana	*XTR7*	At4g14130	F: CGGCTTGCACAGCCTCTT R: TCGGTTGCCACTTGCAATT
A. thaliana	*IAA29*	At4g32280	F: CTTCCAAGGGAAAGAGGGTGA R: TTCCGCAAAGATCTTCCATGTAAC
A. thaliana	*PSY*	At5g17230	F: GACACCCGAAAGGCGAAAGG R: CAGCGAGAGCAGCATCAAGC
A. thaliana	*UBC*	At5g25760	F: TCAAATGGACCGCTCTTATC R: CACAGACTGAAGCGTCCAAG

Supplemental Table S2. Accession IDs for protein sequences used for molecular phylogenetic analysis

Organism	Protein name	Accession number
A. thaliana	PIF1	NP_179608.2
A. thaliana	PIF3	NP_172424.1
A. thaliana	PIF4	NP_565991.2
A. thaliana	PIF5	NP_191465.3
A. thaliana	PIF6	NP_191768.2
A. thaliana	PIF7	NP_200935.2
A. thaliana	PIF8	NP_191916.3
S. lycopersicum	PIF1a	XP_004247109.1
S. lycopersicum	PIF1b	XP_004240467.1
S. lycopersicum	PIF3	XP_010313958.1
S. lycopersicum	PIF4/5	XP_004243631.1
S. lycopersicum	PIF7	XP_004242180.1
S. lycopersicum	PIF8	XP_004229781.1

Supplemental Table S3. Primers used in cloning approaches in this study

Primer name	Sequence
PIF1a F	GGGGACAAGTTTGTACAAAAAAGCAGGCTATGAATCATTCTGTTCCTGATTTTG
PIF1a R	GGGGACCACTTTGTACAAGAAAGCTGGGTTTAACCAGATTGATGATTGCCTG
PIF1a C-tag R	GGGGACCACTTTGTACAAGAAAGCTGGGTACCAGATTGATGATTGCCTGG
PIF1a VIGS F	GGGGACAAGTTTGTACAAAAAAGCAGGCTGCTCCTCGACCGCCTATAC
PIF1a VIGS R	GGGGACCACTTTGTACAAGAAAGCTGGGTCCCTGTAATTGGAGTTACGTTTG
PIF1a ImiR-s	GATATGTAGTCGTCGGTTCGCTACTCTCTTTTGTATTCC
PIF1a IImiR-a	AGTAGCGAACCGACGACTACATATCAAAGAGAATCAATGA
PIF1a IIImiR*s	AGTAACGAACCGACGTCTACATTTCACAGGTCGTGATATG
PIF1a IVmiR*a	GAAATGTAGACGTCGGTTCGTTACTACATATATATTCCTA
miR A	GGGGACAACTTTTCTATACAAAGTTGCTCCCCAAACACACGCTCGGA
miR B	GGGGACAACTTTATTATACAAAGTTGTCCCCATGGCGATGCCTTAA

Supplemental Table S4. Primers used for ChIP-qPCR analysis

Region analyzed	qPCR primers
(-) Control	F: CGGACAGAGACGAATCCAAG R: TTTTGTGCGGAATTGAAACC
G-box	F: AGTACCCAATTTTCCCAAAAC R: ATTTGAAGTGCCGTCATTGG
PBE-box	F: TGATTCCACTGTCATAGGAGG R: CCCAAAACTACAACAAAATCAGC

frontiers in Plant Science

MINI REVIEW
published: 07 March 2016
doi: 10.3389/fpls.2016.00263

Evolutionary Recycling of Light Signaling Components in Fleshy Fruits: New Insights on the Role of Pigments to Monitor Ripening

Briardo Llorente, Lucio D'Andrea and Manuel Rodríguez-Concepción**

Centre for Research in Agricultural Genomics (CRAG) CSIC-IRTA-UAB-UB, Barcelona, Spain

Besides an essential source of energy, light provides environmental information to plants. Photosensory pathways are thought to have occurred early in plant evolution, probably at the time of the Archaeplastida ancestor, or perhaps even earlier. Manipulation of individual components of light perception and signaling networks in tomato (*Solanum lycopersicum*) affects the metabolism of ripening fruit at several levels. Most strikingly, recent experiments have shown that some of the molecular mechanisms originally devoted to sense and respond to environmental light cues have been re-adapted during evolution to provide plants with useful information on fruit ripening progression. In particular, the presence of chlorophylls in green fruit can strongly influence the spectral composition of the light filtered through the fruit pericarp. The concomitant changes in light quality can be perceived and transduced by phytochromes (PHYs) and PHY-interacting factors, respectively, to regulate gene expression and in turn modulate the production of carotenoids, a family of metabolites that are relevant for the final pigmentation of ripe fruits. We raise the hypothesis that the evolutionary recycling of light-signaling components to finely adjust pigmentation to the actual ripening stage of the fruit may have represented a selective advantage for primeval fleshy-fruited plants even before the extinction of dinosaurs.

Keywords: photosensory pathways, light, fleshy fruits, ripening, evolution

OPEN ACCESS

Edited by:
Antonio Granell, Consejo Superior de Investigaciones Científicas, Spain

Reviewed by:
Cornelius Barry, Michigan State University, USA
Maria Jesus Rodrigo, Instituto de Agroquímica y Tecnología de Alimentos – Consejo Superior de Investigaciones Científicas, Spain

****Correspondence:***
Briardo Llorente
briardo.llorente@cragenomica.es;
Manuel Rodríguez-Concepción
manuel.rodriguez@cragenomica.es

Specialty section:
This article was submitted to Plant Physiology, a section of the journal Frontiers in Plant Science

Received: *26 November 2015*
Accepted: *19 February 2016*
Published: *07 March 2016*

Citation:
Llorente B, D'Andrea L and Rodríguez-Concepción M (2016) Evolutionary Recycling of Light Signaling Components in Fleshy Fruits: New Insights on the Role of Pigments to Monitor Ripening. Front. Plant Sci. 7:263. doi: 10.3389/fpls.2016.00263

INTRODUCTION

Light has a dual role in plants as an essential source of energy for driving photosynthesis and, on the other hand, as an environmental cue that modulates many aspects of plant biology such as photomorphogenesis, germination, phototropism, and entrainment of circadian rhythms (Chen et al., 2004; Jiao et al., 2007). The ability to perceive and respond to light changes is mediated by a set of sophisticated photosensory pathways capable of discriminating the quality (spectral composition), intensity (irradiance), duration (including day length), and direction of light (Moglich et al., 2010). In particular, plants perceive light through at least five types of sensory photoreceptors that are distinct from photosynthetic components and detect specific regions of the electromagnetic spectrum. Cryptochromes (CRYs), phototropins, and Zeitlupe family members function in the blue (390–500 nm) and ultraviolet-A (320–390 nm) wavelengths, while the

photoreceptor UVR-8 operates in the ultraviolet-B (280–315 nm) region. Phytochromes (PHYs), which are probably the best studied photoreceptors, function in a dynamic photoequilibrium determined by the red (R, ca. 660 nm) to far-red (FR, ca. 730 nm) ratio in land plants and throughout the visible spectrum (blue, green, orange, red, and far-red) in different algae (Moglich et al., 2010; Rizzini et al., 2011; Rockwell et al., 2014). The photonic information gathered by these photoreceptors is then transduced into changes in gene expression that ultimately promote optimal growth, development, survival and reproduction (Jiao et al., 2007).

Photosensory pathways are thought to have occurred early in plant evolution, probably at the time of the Archaeplastida ancestor (i.e., the last common ancestor of glaucophyte, red algae, green algae and land plants) or perhaps even earlier, before the occurrence of the endosymbiotic event that gave rise to photosynthetic eukaryotes over more than a billion years ago (Duanmu et al., 2014; Mathews, 2014; Fortunato et al., 2015). Through the ages, these mechanisms diverged to play particular roles in different branches of the plant lineage, ranging from presumably acclimative roles in algae (Duanmu et al., 2014; Rockwell et al., 2014) to resource competition functions in land plants (Jiao et al., 2007). In particular, the ability of PHYs to detect changes in the R/FR ratio allows land plants to detect the presence of nearby vegetation that could potentially compete for light. Light filtered or reflected by neighboring leaves (i.e., shade) has a distinctive spectral composition that is characterized by a decreased R/FR ratio due to a preferential absorption of R light by chlorophyll (Casal, 2013). Low R/FR ratios reduce PHY activity, allowing PHY-interacting transcription factors (PIFs) to bind to genomic regulatory elements that tune the expression of numerous genes (Casal, 2013; Leivar and Monte, 2014). Oppositely, high R/FR ratios enhance PHY activity, causing the inactivation of PIF proteins mainly by proteasome-mediated degradation (Bae and Choi, 2008; Leivar and Monte, 2014). Carotenoid biosynthesis represents a rather well characterized example of this regulation. In *Arabidopsis thaliana*, shade decreases the production of carotenoids in photosynthetic tissues (Roig-Villanova et al., 2007; Bou-Torrent et al., 2015) in part by promoting the accumulation of PIF proteins that repress the expression of the gene encoding phytoene synthase (PSY), the main rate-determining enzyme of the carotenoid pathway (Roig-Villanova et al., 2007; Toledo-Ortiz et al., 2010; Bou-Torrent et al., 2015). De-repression of *PSY* under sunlight induces carotenoid biosynthesis, which in turn maximizes light harvesting and protects the photosynthetic machinery from harmful oxidative photodamage caused by intense light (Sundstrom, 2008).

Light signals in general and PHYs in particular also modulate the genetic programs associated to fruit development and ripening. Here we will revise current and emerging knowledge on this area based on work carried out in tomato (*Solanum lycopersicum*), which is the main model system for fleshy fruits, that is, fruits containing a juicy fruit pulp. Further, we will discuss potential selection pressures that might account for the evolutionary recycling of light-signaling components in fleshy fruits.

FLESHY FRUIT RIPENING: THE CASE OF TOMATO

Fleshy fruits are differentiated floral tissues that evolved 80–90 million years ago (Ma), i.e., relatively recently in the history of plants (Givnish et al., 2005; Eriksson, 2014), as an adaptive characteristic promoting the animal-assisted dissemination of viable seeds (Tiffney, 2004; Seymour et al., 2013; Duan et al., 2014). After seed maturation, fleshy fruits typically undergo a ripening process that involves irreversible changes in organoleptic characteristics such as color, texture, and flavor, all of which result in the production of an appealing food to frugivorous animals. In this manner, the ripening process orchestrates the mutualistic relationship between fleshy-fruited plants and seed-disperser animals (Tiffney, 2004; Seymour et al., 2013; Duan et al., 2014).

Upon fertilization, the development of fleshy fruits such as tomato can be divided into three distinct phases: cell division, cell expansion, and ripening (Gillaspy et al., 1993; Seymour et al., 2013). These different stages are characterized by hormonal, genetic, and metabolic shifts that have been reviewed in great detail elsewhere (Carrari and Fernie, 2006; Klee and Giovannoni, 2011; Seymour et al., 2013; Tohge et al., 2014). Before ripening occurs, tomato fruits have a green appearance due to the presence of chloroplasts that contain the whole photosynthetic machinery. The transition to ripening is characterized by a loss of chlorophylls, cell wall softening, accumulation of sugars, and drastic alterations in the profile of volatiles and pigments. Most distinctly, chlorophyll degradation is accompanied by a conversion of chloroplasts into chromoplasts that progressively accumulate high levels of the health-promoting carotenoids β-carotene (pro-vitamin A) and lycopene (Tomato Genome Consortium, 2012; Fantini et al., 2013; Seymour et al., 2013). These carotenoid pigments give the characteristic orange and red colors to ripe tomatoes. A large number of other fruits (including bananas, oranges, or peppers) also lose chlorophylls and accumulate carotenoids during ripening, resulting in a characteristic pigmentation change (from green to yellow, orange or red) that acts as a visual signal informing animals when the fruit is ripe and healthy (Klee and Giovannoni, 2011).

THE EFFECT OF LIGHT SIGNALING COMPONENTS ON FRUIT RIPENING

Multiple lines of evidence have exposed the relevance of fruit-localized photosensory pathways as important players in the regulation of fruit ripening and the potential of their manipulation to improve the nutritional quality of tomatoes (Azari et al., 2010). Among many light-signaling mutants displaying altered fruit phenotypes, the tomato high pigment (*hp*) mutants *hp1* and *hp2* are two of the best characterized. These mutants owe their name to a deep fruit pigmentation derived from an increment in the number and size of plastids, which in turn result in elevated levels of carotenoids such as lycopene (Yen et al., 1997; Mustilli et al., 1999; Levin

et al., 2003). Detailed characterization of the *hp1* and *hp2* mutants, which also show increased levels of extraplastidial metabolites such as flavonoids, revealed that the mutated genes encode tomato homologs of the previously described light signal transduction proteins DAMAGED DNA BINDING PROTEIN 1 (DDB1) and DEETIOLATED1 (DET1), respectively (Mustilli et al., 1999; Schroeder et al., 2002; Levin et al., 2003; Liu et al., 2004) (**Figure 1**). Other components that participate in the same light-signaling pathway that HP1 and HP2 have also been shown to impact tomato fruit metabolism. For instance, silencing the tomato E3 ubiquitin-ligase CUL4, which directly interacts with HP1, also produces highly pigmented fruits (Wang et al., 2008). Another example is the E3 ubiquitin-ligase CONSTITUTIVELY PHOTOMORPHOGENIC 1 (COP1), which specifically promotes the degradation of the light-signaling effector ELONGATED HYPOCOTYL 5 (HY5) (Schwechheimer and Deng, 2000) (**Figure 1**). Transgenic plants with downregulated transcripts of COP1 and HY5 produce tomato fruits with increased and reduced levels of carotenoids, respectively (Liu et al., 2004).

Work with photoreceptors (**Figure 1**) has also shed light on the subject. Tomato plants overexpressing the blue light photoreceptor cryptochrome 2 (CRY2) produce fruits with increased levels of flavonoids and carotenoids (Giliberto et al., 2005). PHYs have been found to control different aspects of tomato fruit ripening as well. Activation of fruit-localized PHYs with R light treatments promotes carotenoid biosynthesis, while subsequent PHY inactivation by irradiation with FR light reverts it (Alba et al., 2000; Schofield and Paliyath, 2005). Furthermore, preventing light exposure from the very early stages of fruit set and development results in white fruits completely devoid of pigments (Cheung et al., 1993), a phenotype that resembles that of *phyA phyB1 phyB2* PHY triple mutant plants (Weller et al., 2000). In addition to regulating carotenoid levels in tomato fruits, PHYs seem to regulate the timing of phase transition during ripening (Gupta et al., 2014).

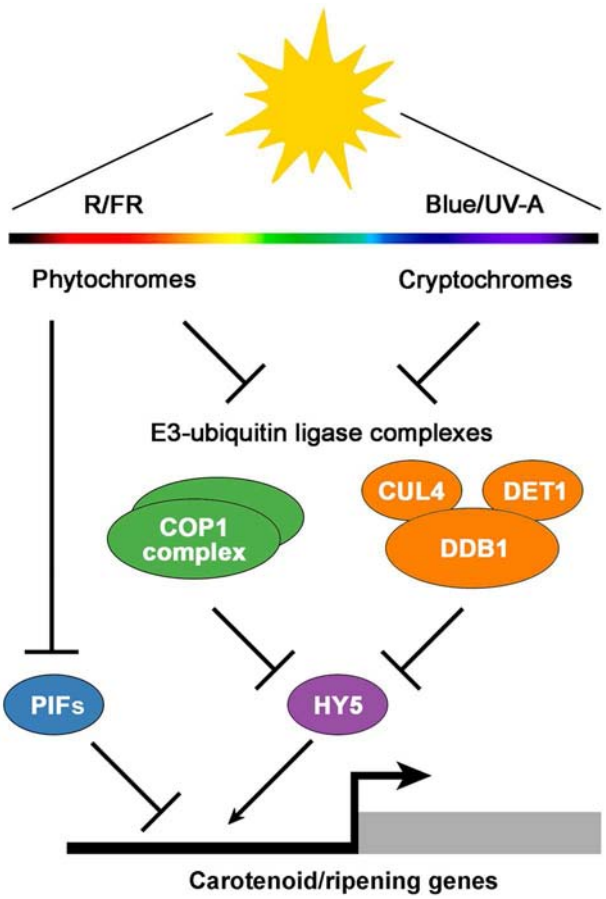

FIGURE 1 | A simplified model of light signaling components involved in the regulation of tomato fruit pigmentation and ripening. Fruit-localized phytochrome and cryptochrome photoreceptors regulate the activity of the downstream E3-ubiquitin ligase COP1 and CUL4-DDB1-DET1 complexes, which in turn mediate the degradation of the transcriptional activator HY5. In addition, active phytochromes reduce the activity of transcriptional repressors such as PIFs. The balance between activators and repressors finally modulates the expression of carotenoid and ripening-associated genes. R, red light; FR, far-red light; Blue, blue light; UV-A, ultraviolet-A light.

A MECHANISM TO MONITOR RIPENING BASED ON SELF-SHADING AND LIGHT SIGNALING

Although light signaling components have long been known to modulate fruit ripening, another important piece of the puzzle was revealed recently. In tomato, fruit pericarp cells are morphologically similar to leaf palisade cells (Gillaspy et al., 1993). Thus, fruits can be viewed as modified leaves that, besides enclosing the seeds, have suffered a change in organ geometry, namely, a shift from a nearly planate conformation to an expanded three-dimensional anatomy. This anatomy imposes spatial constrains coercing light to pass through successive cell layers, so that the quality of the light that reaches inner sections of the fruit is influenced by the cells of outer pericarp sections (**Figure 2**). Another key difference between tomato leaves and fruits is the cuticle, which is far more pronounced in the fruit. While a potential role of the cuticle in altering the spectral properties of the light that reaches the pericarp cells remains to be investigated, it is now well established that the occurrence of chlorophyll in fruit chloroplasts significantly reduces the R/FR ratio of the light filtered through the fruit fresh (Alba et al., 2000; Llorente et al., 2015). A reduction in R/FR ratio (also referred to as shade) normally informs plants about the proximity of surrounding vegetation (Casal, 2013). In tomato fruit, however, changes in R/FR ratio can inform of the ripening status. As a consequence of self-shading, it is proposed that a relatively high proportion of PHYs remain inactive in green fruit. This condition stabilizes the tomato PIF1a transcription factor, that binds to a PBE-box located in the promoter of the gene encoding the PSY isoform that controls the metabolic flux to the carotenoid pathway during fruit ripening, *PSY1*. PIF1a binding directly represses *PSY1* expression (**Figure 2**). Chlorophyll breakdown at the onset of ripening reduces the self-shading effect, consequently

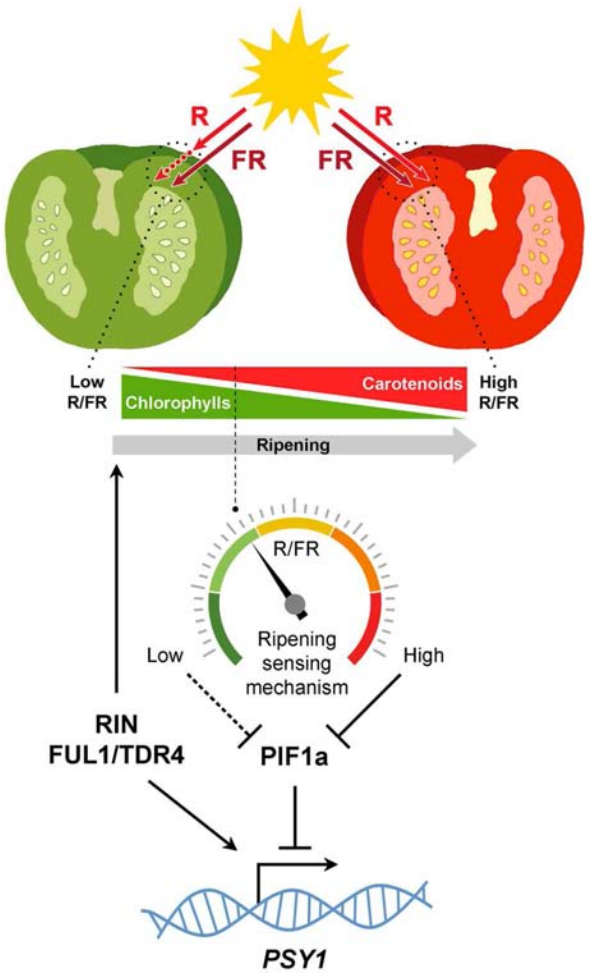

FIGURE 2 | Self-shading model for the light mediated modulation of carotenoid biosynthesis in tomato fruits. Chlorophylls in green fruits preferentially absorb red (R, ca. 660 nm) wavelengths of the light spectrum, generating a self-shading effect characterized by low R to far-red (FR, ca. 730 nm) ratios that maintain PHYs predominantly in the inactive form and relatively high levels of PIF1a repressing *PSY1*. Once seeds mature, the developmental program induces the expression of genes encoding master activators of the ripening process. Some of them, like RIN and FUL1/TDR4, also induce *PSY1* gene expression directly. Chlorophyll breakdown reduces the self-shading effect so that the R/FR ratio within the cells gradually increase, consequently displacing PHYs to their active form, reducing PIF1a levels and derepressing *PSY1* expression. By sensing the spectral composition of the light filtered through the fruit pericarp, this mechanism diagnoses actual ripening progression to finely adjust fruit carotenoid biosynthesis.

promoting PHY activation, degradation of PIF1a, derepression of *PSY1*, and eventually carotenoid biosynthesis (**Figure 2**). In this manner, the genetically controlled expression of *PSY1* (and hence the production of carotenoid pigments) is fine-tuned to the actual progression of ripening (Llorente et al., 2015).

Translation of molecular insights from tomato to other fleshy-fruited plants has indicated that many regulatory networks are conserved across a wide range of species (Seymour et al., 2013). Thus, given the ubiquitous nature of PHYs in land plants and the widespread occurrence of ripening-associated fruit pigmentation changes that typically involve the substitution of an initially chlorophyll-based green color with distinctive non-green (i.e., non-R-absorbing) eye-catching colors, it is possible that similar self-shading regulatory mechanisms might operate in other plant species to inform on the actual stage of ripening (based on the pigment profile of the fruit at every moment) and thus finely coordinate fruit color change. However, the composition of the cuticle or even the anatomy of the most external layer of the pericarp (i.e., the exocarp) might also impact the quality and quantity of light that penetrates the fruit flesh. The self-shading mechanism is expected to be irrelevant in fleshy fruits with a thick skin or exocarp that prevents light to pass through and reach more internal fruit layers.

FRUIT COLORS AS RIPENING SIGNALS IN AN EVOLUTIONARY CONTEXT

Fleshy fruits are considered to have first appeared in the Late Cretaceous (circa 90 Ma) (Givnish et al., 2005; Eriksson, 2014), at a time when the Earth's vegetation was dense and exuberant, and where most ecological niches were taken over by angiosperms (Lidgard and Crane, 1988; Berendse and Scheffer, 2009). The plentiful surplus of nutritious food gave rise to a huge explosion in the Cretaceous fauna, bringing about the coexistence of numerous herbivorous and omnivorous reptiles (dinosaurs, pterosaurs, lizards), birds and mammals (Lloyd et al., 2008; Prentice et al., 2011; Vullo et al., 2012; Wilson et al., 2012; Jones et al., 2013; Jarvis et al., 2014). With such an abundance of plant-eating animals, being able to display a change in fruit color when ripe probably represented a valuable trait among early fleshy-fruited plants to call the attention of these various potential seed dispersers.

Although deep time co-evolutionary scenarios may be difficult to support, this idea gains plausibility if we consider that the same strategy had been successfully implemented beforehand by gymnosperms, which had already evolved fleshy fruit-like structures by the Early Cretaceous, at least some 20-30 million years before the first fleshy fruits (Yang and Wang, 2013). Several gymnosperms (e.g., *Ginkgo biloba*, *Taxus baccata*, and *Ephedra distachya*) produce fleshy colorful tissues around their seeds and, similar to that occurring in angiosperms, these fruit-like structures undergo a ripening process that also serves as a visual advertisement for animals to eat them and disperse their seeds. Recent evidence supports the hypothesis that the main molecular networks underlying the formation of the fleshy fruit were originally established in gymnosperms (Lovisetto et al., 2012, 2015), thus suggesting that the ripening phenomenon was first selected as an ecological adaptation in gymnosperms and that angiosperms merely exploited it afterwards. If correct, this would imply that Cretaceous plant-eater animals would have already been used to feeding on color-changing fleshy fruit-like tissues by the time that angiosperm fleshy-fruited plants evolved, something that may have facilitated the establishment of the latter.

Another relevant fact is that the dominant land animals during the Cretaceous period, the dinosaurs, as well as pterosaurs, lizards, and birds, had highly differentiated color vision, much superior to that of most mammals (Rowe, 2000; Chang et al., 2002; Bowmaker, 2008). Differentiated color vision, or tetrachromacy, is a basal characteristic of land vertebrates derived from the presence of four spectrally distinct retinal cone cells that allow discriminating hues ranging from ultraviolet to red (Bowmaker, 2008; Koschowitz et al., 2014). Turtles, alligators, lizards and birds, are all known to have tetrachromatic color vision, a shared trait inherited from their common reptilian ancestry (Rowe, 2000; Bowmaker, 2008). We have recently come to know that some dinosaurs even sported plumage color patterns and flamboyant cranial crests that may have served for visual display purposes (Li et al., 2010, 2012; Zhang et al., 2010; Bell et al., 2014; Foth et al., 2014; Koschowitz et al., 2014). Altogether, these insights suggest that color cues were likely an important means of signaling among dinosaurs. Although purely speculative at the moment, it is reasonable to assume that there could have also been dinosaurs that, analogously to several birds and reptiles nowadays (Svensson and Wong, 2011), consumed fleshy fruits within their diet as a source of carotenoid pigments used for ornamental coloration. Even though the relevance of, now extinct, Cretaceous megafauna as biological vectors involved in the seed dispersal of primeval fleshy-fruited plants remains speculative and controversial (Tiffney, 2004; Butler et al., 2009; Seymour et al., 2013), it is clear that they certainly had fleshy fruit available to eat during the last 25–35 million years of their existence, until the occurrence of the Cretaceous-Paleogene mass extinction event (65 Ma).

Fruit color change meets the criteria of a classical signal, which can be defined as a cue that increases the fitness of the sender (i.e., fleshy-fruited plants) by altering the behavior of the receivers (i.e., seed-disperser animals) (Maynard Smith and Harper, 1995). Importantly, besides visibility conditions and the visual aptitude of the receiver, the detectability of a visual signal is determined by its contrast against the background, that is, the conspicuousness of the signal (Schmidt et al., 2004). Ripe fruits displaying a distinct coloration against the foliage leaves are more conspicuous for animals than green fruits and there is no evidence to consider that it was any different to Cretaceous animals. In fact, the invention of fruit fleshiness took place along with expanding tropical forests, suggesting it may have evolved as an advantageous trait related to changes in vegetation from open to more closed environments (Seymour et al., 2013; Eriksson, 2014). In this context, light signaling pathways already established in land plants may have had the chance to evolutionary explore novel phenotypic space in fleshy fruits. Subsequent adaptations under selection in the fruit may have then integrated these pathways as modulatory components of the pigmentation process during ripening. For instance, the self-shading regulation of the tomato fruit carotenoid pathway (Llorente et al., 2015) (**Figure 2**) might have evolved by co-option of components from the preexisting shade-avoidance responses (Mathews, 2006; Casal, 2013). This evolutionary recycling of light-signaling components in fleshy fruits might therefore be a legacy from the time when dinosaurs walked the earth.

AUTHOR CONTRIBUTIONS

BL, LA, and MR-C searched and discussed the literature and wrote the article.

ACKNOWLEDGMENTS

We acknowledge the support of grants from EC (CarotenActors, 300862), CYTED (Ibercarot, 112RT0445), MINECO (FPDI-2013-018882, BIO2011-23680, BIO2014-59092-P), MEC (AP2012-0189), and AGAUR (2014SGR-1434).

REFERENCES

Alba, R., Cordonnier-Pratt, M. M., and Pratt, L. H. (2000). Fruit-localized phytochromes regulate lycopene accumulation independently of ethylene production in tomato. *Plant Physiol.* 123, 363–370. doi: 10.1104/pp.123.1.363

Azari, R., Tadmor, Y., Meir, A., Reuveni, M., Evenor, D., Nahon, S., et al. (2010). Light signaling genes and their manipulation towards modulation of phytonutrient content in tomato fruits. *Biotechnol. Adv.* 28, 108–118. doi: 10.1016/j.biotechadv.2009.10.003

Bae, G., and Choi, G. (2008). Decoding of light signals by plant phytochromes and their interacting proteins. *Annu. Rev. Plant Biol.* 59, 281–311. doi: 10.1146/annurev.arplant.59.032607.092859

Bell, P. R., Fanti, F., Currie, P. J., and Arbour, V. M. (2014). A mummified duck-billed dinosaur with a soft-tissue cock's comb. *Curr. Biol.* 24, 70–75. doi: 10.1016/j.cub.2013.11.008

Berendse, F., and Scheffer, M. (2009). The angiosperm radiation revisited, an ecological explanation for Darwin's 'abominable mystery'. *Ecol. Lett.* 12, 865–872. doi: 10.1111/j.1461-0248.2009.01342.x

Bou-Torrent, J., Toledo-Ortiz, G., Ortiz-Alcaide, M., Cifuentes-Esquivel, N., Halliday, K. J., Martinez-García, J. F., et al. (2015). Regulation of carotenoid biosynthesis by shade relies on specific subsets of antagonistic transcription factors and cofactors. *Plant Physiol.* 169, 1584–1594. doi: 10.1104/pp.15.00552

Bowmaker, J. K. (2008). Evolution of vertebrate visual pigments. *Vis. Res.* 48, 2022–2041. doi: 10.1016/j.visres.2008.03.025

Butler, R. J., Barrett, P. M., Kenrick, P., and Penn, M. G. (2009). Diversity patterns amongst herbivorous dinosaurs and plants during the Cretaceous: implications for hypotheses of dinosaur/angiosperm co-evolution. *J. Evol. Biol.* 22, 446–459. doi: 10.1111/j.1420-9101.2008.01680.x

Carrari, F., and Fernie, A. R. (2006). Metabolic regulation underlying tomato fruit development. *J. Exp. Bot.* 57, 1883–1897. doi: 10.1093/jxb/erj020

Casal, J. J. (2013). Photoreceptor signaling networks in plant responses to shade. *Annu. Rev. Plant Biol.* 64, 403–427. doi: 10.1146/annurev-arplant-050312-120221

Chang, B. S., Jonsson, K., Kazmi, M. A., Donoghue, M. J., and Sakmar, T. P. (2002). Recreating a functional ancestral archosaur visual pigment. *Mol. Biol. Evol.* 19, 1483–1489. doi: 10.1093/oxfordjournals.molbev.a004211

Chen, M., Chory, J., and Fankhauser, C. (2004). Light signal transduction in higher plants. *Annu. Rev. Genet.* 38, 87–117. doi: 10.1146/annurev.genet.38.072902.092259

Cheung, A. Y., McNellis, T., and Piekos, B. (1993). Maintenance of chloroplast Components during chromoplast differentiation in the tomato mutant green flesh. *Plant Physiol.* 101, 1223–1229.

Consortium. (2012). The tomato genome sequence provides insights into fleshy fruit evolution. *Nature* 485, 635–641. doi: 10.1038/nature 11119

Duan, Q., Goodale, E., and Quan, R. C. (2014). Bird fruit preferences match the frequency of fruit colours in tropical Asia. *Sci. Rep.* 4:5627. doi: 10.1038/srep05627

Duanmu, D., Bachy, C., Sudek, S., Wong, C. H., Jimenez, V., Rockwell, N. C., et al. (2014). Marine algae and land plants share conserved phytochrome signaling systems. *Proc. Natl. Acad. Sci. U.S.A.* 111, 15827–15832. doi: 10.1073/pnas.1416751111

Eriksson, O. (2014). Evolution of angiosperm seed disperser mutualisms: the timing of origins and their consequences for coevolutionary interactions between angiosperms and frugivores. *Biol. Rev. Camb. Philos. Soc.* 91, 168–186. doi: 10.1111/brv.12164

Fantini, E., Falcone, G., Frusciante, S., Giliberto, L., and Giuliano, G. (2013). Dissection of tomato lycopene biosynthesis through virus-induced gene silencing. *Plant Physiol.* 163, 986–998. doi: 10.1104/pp.113.224733

Fortunato, A. E., Annunziata, R., Jaubert, M., Bouly, J. P., and Falciatore, A. (2015). Dealing with light: the widespread and multitasking cryptochrome/photolyase family in photosynthetic organisms. *J. Plant Physiol.* 172, 42–54. doi: 10.1016/j.jplph.2014.06.011

Foth, C., Tischlinger, H., and Rauhut, O. W. (2014). New specimen of Archaeopteryx provides insights into the evolution of pennaceous feathers. *Nature* 511, 79–82. doi: 10.1038/nature13467

Giliberto, L., Perrotta, G., Pallara, P., Weller, J. L., Fraser, P. D., Bramley, P. M., et al. (2005). Manipulation of the blue light photoreceptor cryptochrome 2 in tomato affects vegetative development, flowering time, and fruit antioxidant content. *Plant Physiol.* 137, 199–208. doi: 10.1104/pp.104.051987

Gillaspy, G., Ben-David, H., and Gruissem, W. (1993). Fruits: a developmental perspective. *Plant Cell* 5, 1439–1451. doi: 10.1105/tpc.5.10.1439

Givnish, T. J., Pires, J. C., Graham, S. W., McPherson, M. A., Prince, L. M., Patterson, T. B., et al. (2005). Repeated evolution of net venation and fleshy fruits among monocots in shaded habitats confirms a priori predictions: evidence from an ndhF phylogeny. *Proc. R. Soc. B.* 272, 1481–1490. doi: 10.1098/rspb.2005.3067

Gupta, S. K., Sharma, S., Santisree, P., Kilambi, H. V., Appenroth, K., Sreelakshmi, Y., et al. (2014). Complex and shifting interactions of phytochromes regulate fruit development in tomato. *Plant Cell Environ.* 37, 1688–1702. doi: 10.1111/pce.12279

Jarvis, E. D., Mirarab, S., Aberer, A. J., Li, B., Houde, P., Li, C., et al. (2014). Whole-genome analyses resolve early branches in the tree of life of modern birds. *Science* 346, 1320–1331. doi: 10.1126/science.1253451

Jiao, Y., Lau, O. S., and Deng, X. W. (2007). Light-regulated transcriptional networks in higher plants. *Nat. Rev. Genet.* 8, 217–230. doi: 10.1038/nrg2049

Jones, M. E., Anderson, C. L., Hipsley, C. A., Muller, J., Evans, S. E., and Schoch, R. R. (2013). Integration of molecules and new fossils supports a Triassic origin for Lepidosauria (lizards, snakes, and tuatara). *BMC Evol. Biol.* 13:208. doi: 10.1186/1471-2148-13-208

Klee, H. J., and Giovannoni, J. J. (2011). Genetics and control of tomato fruit ripening and quality attributes. *Annu. Rev. Genet.* 45, 41–59. doi: 10.1146/annurev-genet-110410-132507

Koschowitz, M. C., Fischer, C., and Sander, M. (2014). Beyond the rainbow. *Science* 346, 416–418. doi: 10.1126/science.1258957

Leivar, P., and Monte, E. (2014). PIFs: systems integrators in plant development. *Plant Cell* 26, 56–78. doi: 10.1105/tpc.113.120857

Levin, I., Frankel, P., Gilboa, N., Tanny, S., and Lalazar, A. (2003). The tomato dark green mutation is a novel allele of the tomato homolog of the DEETIOLATED1 gene. *Theor. Appl. Genet.* 106, 454–460.

Li, Q., Gao, K. Q., Meng, Q., Clarke, J. A., Shawkey, M. D., D'Alba, L., et al. (2012). Reconstruction of Microraptor and the evolution of iridescent plumage. *Science* 335, 1215–1219. doi: 10.1126/science.1213780

Li, Q., Gao, K. Q., Vinther, J., Shawkey, M. D., Clarke, J. A., D'Alba, L., et al. (2010). Plumage color patterns of an extinct dinosaur. *Science* 327, 1369–1372. doi: 10.1126/science.1186290

Lidgard, S., and Crane, P. R. (1988). Quantitative-analyses of the early angiosperm radiation. *Nature* 331, 344–346. doi: 10.1038/331344a0

Liu, Y., Roof, S., Ye, Z., Barry, C., van Tuinen, A., Vrebalov, J., et al. (2004). Manipulation of light signal transduction as a means of modifying fruit nutritional quality in tomato. *Proc. Natl. Acad. Sci. U.S.A.* 101, 9897–9902. doi: 10.1073/pnas.0400935101

Llorente, B., D'Andrea, L., Ruiz-Sola, M. A., Botterweg, E., Pulido, P., Andilla, J., et al. (2015). Tomato fruit carotenoid biosynthesis is adjusted to actual ripening progression by a light-dependent mechanism. *Plant J.* 85, 107–119. doi: 10.1111/tpj.13094

Lloyd, G. T., Davis, K. E., Pisani, D., Tarver, J. E., Ruta, M., Sakamoto, M., et al. (2008). Dinosaurs and the Cretaceous terrestrial revolution. *Proc. R. Soc. B* 275, 2483–2490. doi: 10.1098/rspb.2008.0715

Lovisetto, A., Baldan, B., Pavanello, A., and Casadoro, G. (2015). Characterization of an AGAMOUS gene expressed throughout development of the fleshy fruit-like structure produced by Ginkgo biloba around its seeds. *BMC Evol. Biol.* 15:139. doi: 10.1186/s12862-015-0418-x

Lovisetto, A., Guzzo, F., Tadiello, A., Toffali, K., Favretto, A., and Casadoro, G. (2012). Molecular analyses of MADS-box genes trace back to Gymnosperms the invention of fleshy fruits. *Mol. Biol. Evol.* 29, 409–419. doi: 10.1093/molbev/msr244

Mathews, S. (2006). Phytochrome-mediated development in land plants: red light sensing evolves to meet the challenges of changing light environments. *Mol. Ecol.* 15, 3483–3503. doi: 10.1111/j.1365-294X.2006.03051.x

Mathews, S. (2014). Algae hold clues to eukaryotic origins of plant phytochromes. *Proc. Natl. Acad. Sci. U.S.A.* 111, 15608–15609. doi: 10.1073/pnas.1417990111

Maynard Smith, J., and Harper, D. G. C. (1995). Animal signals: models and terminology. *J. Theor. Biol.* 177, 305–311. doi: 10.1006/jtbi.1995.0248

Moglich, A., Yang, X., Ayers, R. A., and Moffat, K. (2010). Structure and function of plant photoreceptors. *Annu. Rev. Plant Biol.* 61, 21–47. doi: 10.1146/annurev-arplant-042809-112259

Mustilli, A. C., Fenzi, F., Ciliento, R., Alfano, F., and Bowler, C. (1999). Phenotype of the tomato high pigment-2 mutant is caused by a mutation in the tomato homolog of DEETIOLATED1. *Plant Cell* 11, 145–157. doi: 10.1105/tpc.11.2.145

Prentice, K. C., Ruta, M., and Benton, M. J. (2011). Evolution of morphological disparity in pterosaurs. *J. Syst. Palaeontol.* 9, 337–353. doi: 10.1080/14772019.2011.565081

Rizzini, L., Favory, J. J., Cloix, C., Faggionato, D., O'Hara, A., Kaiserli, E., et al. (2011). Perception of UV-B by the Arabidopsis UVR8 protein. *Science* 332, 103–106. doi: 10.1126/science.1200660

Rockwell, N. C., Duanmu, D., Martin, S. S., Bachy, C., Price, D. C., Bhattacharya, D., et al. (2014). Eukaryotic algal phytochromes span the visible spectrum. *Proc. Natl. Acad. Sci. U.S.A.* 111, 3871–3876. doi: 10.1073/pnas.1401871111

Roig-Villanova, I., Bou-Torrent, J., Galstyan, A., Carretero-Paulet, L., Portoles, S., Rodriguez-Concepcion, M., et al. (2007). Interaction of shade avoidance and auxin responses: a role for two novel atypical bHLH proteins. *EMBO J.* 26, 4756–4767. doi: 10.1038/sj.emboj.7601890

Rowe, M. P. (2000). Inferring the retinal anatomy and visual capacities of extinct vertebrates. *Palaeontol. Electron.* 3, 3–43.

Schmidt, V., Schaefer, H. M., and Winkler, H. (2004). Conspicuousness, not colour as foraging cue in plant–animal signalling. *Oikos* 106, 551–557. doi: 10.1111/j.0030-1299.2004.12769.x

Schofield, A., and Paliyath, G. (2005). Modulation of carotenoid biosynthesis during tomato fruit ripening through phytochrome regulation of phytoene synthase activity. *Plant Phys. Biochem.* 43, 1052–1060. doi: 10.1016/j.plaphy.2005.10.006

Schroeder, D. F., Gahrtz, M., Maxwell, B. B., Cook, R. K., Kan, J. M., Alonso, J. M., et al. (2002). De-etiolated 1 and damaged DNA binding protein 1 interact to regulate *Arabidopsis* photomorphogenesis. *Curr. Biol.* 12, 1462–1472. doi: 10.1016/S0960-9822(02)01106-5

Schwechheimer, C., and Deng, X. W. (2000). The COP/DET/FUS proteins-regulators of eukaryotic growth and development. *Semin. Cell Dev. Biol.* 11, 495–503. doi: 10.1006/scdb.2000.0203

Seymour, G. B., Ostergaard, L., Chapman, N. H., Knapp, S., and Martin, C. (2013). Fruit development and ripening. *Annu. Rev. Plant Biol.* 64, 219–241. doi: 10.1146/annurev-arplant-050312-120057

Sundstrom, V. (2008). Femtobiology. *Annu. Rev. Phys. Chem.* 59, 53–77. doi: 10.1146/annurev.physchem.59.032607.093615

Svensson, P. A., and Wong, B. B. M. (2011). Carotenoid-based signals in behavioural ecology: a review. *Behaviour* 148, 131–189. doi: 10.1163/000579510X548673

Tiffney, B. H. (2004). Vertebrate dispersal of seed plants through time. *Annu. Rev. Ecol. Evol. S* 35, 1–29. doi: 10.1146/annurev.ecolsys.34.011802.132535

Tohge, T., Alseekh, S., and Fernie, A. R. (2014). On the regulation and function of secondary metabolism during fruit development and ripening. *J. Exp. Bot.* 65, 4599–4611. doi: 10.1093/jxb/ert443

Toledo-Ortiz, G., Huq, E., and Rodriguez-Concepcion, M. (2010). Direct regulation of phytoene synthase gene expression and carotenoid biosynthesis by phytochrome-interacting factors. *Proc. Natl. Acad. Sci. U.S.A.* 107, 11626–11631. doi: 10.1073/pnas.0914428107

Vullo, R., Marugan-Lobon, J., Kellner, A. W., Buscalioni, A. D., Gomez, B., de la Fuente, M., et al. (2012). A new crested pterosaur from the Early Cretaceous of Spain: the first European tapejarid (Pterodactyloidea: Azhdarchoidea). *PLoS ONE* 7:e38900. doi: 10.1371/journal.pone.0038900

Wang, S., Liu, J., Feng, Y., Niu, X., Giovannoni, J., and Liu, Y. (2008). Altered plastid levels and potential for improved fruit nutrient content by downregulation of the tomato DDB1-interacting protein CUL4. *Plant J.* 55, 89–103. doi: 10.1111/j.1365-313X.2008.03489.x

Weller, J. L., Schreuder, M. E., Smith, H., Koornneef, M., and Kendrick, R. E. (2000). Physiological interactions of phytochromes A, B1 and B2 in the control of development in tomato. *Plant J.* 24, 345–356. doi: 10.1046/j.1365-313x.2000.00879.x

Wilson, G. P., Evans, A. R., Corfe, I. J., Smits, P. D., Fortelius, M., and Jernvall, J. (2012). Adaptive radiation of multituberculate mammals before the extinction of dinosaurs. *Nature* 483, 457–460. doi: 10.1038/nature10880

Yang, Y., and Wang, Q. (2013). The earliest fleshy cone of Ephedra from the early cretaceous Yixian Formation of northeast China. *PLoS ONE* 8:e53652. doi: 10.1371/journal.pone.0053652

Yen, H. C., Shelton, B. A., Howard, L. R., Lee, S., Vrebalov, J., and Giovannoni, J. J. (1997). The tomato high-pigment (hp) locus maps to chromosome 2 and influences plastome copy number and fruit quality. *Theor. Appl. Genet.* 95, 1069–1079. doi: 10.1007/s001220050664

Zhang, F., Kearns, S. L., Orr, P. J., Benton, M. J., Zhou, Z., Johnson, D., et al. (2010). Fossilized melanosomes and the colour of Cretaceous dinosaurs and birds. *Nature* 463, 1075–1078. doi: 10.1038/nature08740

Conflict of Interest Statement: The authors declare that the research was conducted in the absence of any commercial or financial relationships that could be construed as a potential conflict of interest.